ROBUST ADAPTIVE CONTROL OF MANIPULATORS WITH APPLICATION TO JOINT FLEXIBILITY

Thesis by
Ho-Hoon Lee

In Partial Fulfillment of the Requirements
for the Degree of
Doctor of Philosophy

California Institute of Technology
Pasadena, California 91125

1992

(Submitted September 19, 1991)

ACKNOWLEDGEMENTS

I wish to express my deep gratitude to my advisor, Professor Fred E. C. Culick for his most valuable guidance, encouragement, and patience during my stay at Caltech. I would also like to thank Professors Joel Burdick, Thomas Caughey, and Athanasios Sideris, and Dr. Homayoun Seraji for their review and constructive criticisms of this research. I am thankful to Professor James Knowles for his excellent class and helpful discussions.

I am grateful to my colleagues Albert Moser, Eliot Fried, Mark Lusk, Carl Ruoff, Beth McKenney, Wen-Jean Hsueh, Ralph Aldredge, and I-Ming Chen for their friendship and helpful discussions. In addition, I am indebted to Min-Kun Chung at JPL for his help on innumerable occasions with computers. My thanks also go to Dorothy Eckerman for her support and help.

The research described in this thesis has been funded by JPL/Caltech Director's Discretionary Funds. This support is gratefully acknowledged. I would also like to thank Caltech for the teaching assistantships and POSCO for its financial support, which have facilitated my stay.

Finally, I thank all my family members for steadfast loving support and encouragement for higher education in the face of repeated family tragedies. I dedicate this thesis to the memories of my mother, Jai-Ok Park, and my brother, Kwan-Hoon Lee. Their invaluable love and sacrifice have made completion of this research possible.

ABSTRACT

This thesis discusses the model-based adaptive trajectory control of commercial manipulators whose dynamics are well known with uncertainties confined to parameters.

This thesis emphasizes the importance of the transient behavior as well as robust stability of a system and takes it into account in the design of adaptive control laws. The basic idea is to search for compensators in the direction of minimizing a quadratic performance index, and then analyze the stability and robustness of the selected compensators in the presence of bounded disturbances, sensor noises, and unmodelled dynamics. With this idea, centralized and decentralized adaptive control schemes are proposed for rigid-joint manipulators. Stability bounds for disturbances, control and adaptation gains, and desired trajectories and their time-derivatives are derived for the proposed schemes. These bounds are sufficient conditions for robust stability of the proposed schemes in the presence of unmodelled dynamics such as feedback delays in the digital control systems and the coupled dynamics in the decentralized scheme.

A flexibility compensator is designed to treat the problem of joint flexibility. With the flexibility compensator, a manipulator having flexible joints is transformed to that having rigid joints with high-frequency dynamics of joint couplings representing unmodelled dynamics. In this way, control of flexible-joint manipulators is converted to that of the corresponding rigid-joint manipulators. Accordingly, the robust adaptive control schemes proposed for rigid-joint manipulators are applied. Then, through stability analysis, stability bounds for disturbances, control and adaptation gains, and desired trajectories and their time-derivatives are derived for the scheme with the flexibility compensator, in the presence of the unmodelled dynamics. Under the constraint of these bounds, the proposed

adaptive scheme is not only almost independent of the gear-reduction ratios, flexibilities of joint couplings, and characteristics of actuators, but also free from the requirements of measuring angular accelerations and jerks of links.

TABLE OF CONTENTS

LIST OF FIGURES

Chapter 1

INTRODUCTION

1.1 Overview

Through science-fiction and cartoon films, robots have been recognized as fancy mechanical super-humans in our deep dream and imagination. Our ability and desire to do research have been continuously stimulated by this dream and the grand expectation of constructing mechanical counterparts of ourselves. However, our dream is far beyond reality. Our technology is still in its infancy. Today's robots are only numerically controlled mechanical manipulators with simple hands or end-effectors for grasping objects.

The first commercial robots were produced by Unimation Inc. in 1959. Since then, various commercial robots have been manufactured. Research and developments in robotics have been led mainly by social and industrial needs. Demand for high wages and necessity for cost reduction have motivated application of robots. Needs for improvement in quality and productivity have led to investment in robots. Indeed, robots are closely related to industry. In most applications, they are installed firmly to one place and commanded by computers to do some useful work. This may range from simple pick and place operations to motions such as welding along predetermined paths. Hence, robots can be defined as reprogrammable multifunctional manipulators, designed to perform some physical tasks on the environment through some preprogrammed motions.

Today's robots are far from the wonderful machines of science-fiction. However, our dream will eventually come into reality while we try to improve each function of robots little by little. Since our ultimate goal is to fabricate mechanical super humans, robotics has diverse related fields: kinematics, dynamics, de-

sign, path planning, trajectory control, force control, control language, redundant robots, mobile robots, computer vision, neural network, etc.

Among these fields, this thesis addresses trajectory control. The objective of this is to make a robot to follow as closely as possible any desired trajectory through space in spite of uncertain payloads and highly nonlinear and coupled dynamics. This objective is always limited by various factors: inertia of links, mass of payloads, torque and power capacity of actuators, amplifier capacity, sensor accuracy, characteristics of the control law, sampling time, computation speed, and so on. The characteristics of the control law may in particular be dominant factors for control performance. The desired trajectories are always planned within the capacities of actuators and amplifiers. Nowadays, reasonably good position, velocity, and torque sensors are also available. Recently, computers have become enormously more powerful, and progress continues. New DSP chips have already provided 20 MFLOPS (Million Floating Point Operations Per Second). Hence it is quite feasible to use a full dynamic model in the controller.

This thesis focuses on the model-based trajectory control of commercial manipulators whose dynamics are well known with uncertainties confined to parameters. This thesis deals mainly with these classes of practical problems: (1), the design of high performance control laws for rigid-joint manipulators; (2), trajectory control of manipulators having flexible joint couplings and possibly high gear-reduction ratios between the links and the actuators; and (3), the robustness of proposed adaptive schemes in the presence of bounded disturbances and unmodelled dynamics such as high-frequency dynamics of flexible joints, feedback delays in the digital control systems, and the coupled dynamics for the decoupled joint control laws. In our discussion we will use the terms "joint flexibility" and "flexible joint" for the flexibility which exists in power transmission mechanism.

1.2 Background and Motivation of This Thesis

1.2.1 Control of Rigid-Joint Manipulators

The productivity of a robot may be measured in connection with the envi-

ronment on which it works. A robot very often operates in a dynamic environment such as assembly lines. Sometimes several robots join to accomplish a complex task. In these circumstances, coordinated motion is critical. As a result, the productivity of a robot may be evaluated by how fast it can move and how accurately it can follow a given trajectory. Industrial robots run with very simple controllers such as PD or PID feedback compensators. The performance of these systems are not always satisfactory for applications which require precise tracking of fast trajectories. As the motion of a robot becomes faster, the performance gets worse. A major reason is that the simple feedback compensators cannot take care of all the high nonlinearities and coupling effects contained in robot dynamics. Consequently, these expensive machines have probably not been utilized to their full potential in terms of speed and accuracy of tracking.

To improve performance, the computed torque method[1.1-1.4] was proposed. This is based on a well-established dynamic model for rigid-link rigid-joint manipulators. Theoretically, this method allows us to compensate for complicated coupling effects and nonlinearities such as centrifugal forces, Coriolis forces, gravity, and friction damping. However, this method was found to be sensitive to the uncertainties in the parameters associated with the dynamics. In other words, this method is not robust.

As a way of improving robustness, adaptive control has been practiced in various fields. In general, there are two basic approaches in adaptive control[1.5]: STR (Self-Tuning Regulator[1.6-1.8]) and MRAC (Model Reference Adaptive Control[1.9-1.14]). The design procedure of the STR consists of (i) system linearization, (ii) parameter estimation for the linearized system, (iii) and design of a control law based on the estimated parameters. The MRAC is based principally on Lyapunov's second method[1.10-1.12] or Popov's hyperstability theory[1.12-1.14]. The objective is to force outputs of a plant to follow asymptotically those of a reference model using any of these stability theories. We will review both approaches in detail in Chapter 2.

Dubowsky and DesForges[1.15,1.16] were apparently the first to introduce

this technique to the control of robots. They used the steepest descent method[1.9] to derive their MRAC adaptation rule. This method requires separate stability analysis. Since they use a linear decoupled model, their scheme is valid under the assumption that nonlinearities and coupling effects in the robot dynamics are quasi-time-invariant. Therefore, stability and desired performance are guaranteed only when a robot moves slowly. Consequently, one of the primary objectives in this field is to remove this assumption from adaptive control laws.

The design procedure of the STR is more explicit and straightforward than that of the MRAC. Basically, this method is restricted to linear time-invariant systems. Therefore, all the STR schemes in trajectory control of robots are standardized. Koivo et al.[1.17-1.20] employed linear time-invariant decoupled models. They applied recursive least-square parameter estimators, and devised one-step-ahead optimal control laws. Walters[1.21], Leininger[1.22-1.24], Backes[1.25,1.26], and their colleagues applied the least-square estimators and pole-placement to linear decoupled time-invariant models. After estimating the parameters using the least square method, Sundareshen and Koenig[1.27] designed a control law with a constraint that velocity and position tracking errors must decay to zero as time goes to infinity. Since the STR is developed based on linear time-invariant decoupled models and linear control theory, all the STR schemes require the assumption of quasi-time-invariance, and they are not so satisfactory for robot control.

The design of the MRAC is more indirect and specialized than that of the STR. This usually requires experience and intuition. The MRAC is not limited to linear systems. It can be applied to nonlinear coupled systems and hence has great potential. Therefore, the control community in robotics seems to favor the MRAC techniques. Takegaki and Arimoto[1.28] applied Lyapunov's second method to their linear model to derive their adaptation rule. Seraji[1.29,1.30] proposed some adaptive schemes and demonstrated some potential in adaptive control of robots through experimentations. Oh[1.31], Gavel[1.32,1.33], and their colleagues developed decoupled feedback adaptive control laws. All these schemes use no dynamic model of a robot in their control laws. Hence, to prove stability, they all rely on the

assumption of quasi-time-invariance or on very high control gains. In general, high control gains cause excitation of high-frequency unmodelled dynamics. Instead of this assumption, Lim[1.34-1.36], Nicosia[1.37], Balestrino[1.38], Ozguner[1.39], Pandian[1.40], and their colleagues used large chattering control signals which switch at infinite frequency to guarantee asymptotic stability of their systems. However, infinite-frequency signals can not be physically implemented.

Horowitz and Tomizuka[1.41] included a part of the robot dynamics in their control law. A variant of this scheme was implemented by Anex and Hubbard[1.42]. They still need the assumption of quasi-time-invariance. Craig et al.[1.43,1.44] used a full dynamic model in their control law so that they removed the assumption. However, their adaptation rule contains angular acceleration which is difficult to access. Kabtab[1.45] made the problem even more difficult. He modified Craig's by adding the inverse of some non-square function matrix. Slotine and Li[1.46-1.48] combined ideas of Craig and Arimoto[1.49] and their colleagues so that they improved Craig's scheme by deleting the requirement of measuring the angular acceleration.

Lee[1.51-1.54], Choi[1.55,1.56], deSilva[1.57], and their colleagues tried a little different approach. They compute a nominal torque along a desired trajectory using Newton-Euler formulation with nominal values of parameters of the links. They used the STR or the MRAC techniques only to compensate perturbed torques. In this case, the assumption of quasi-time-invariance is also indispensable to their derivations of adaptation rules.

Slotine's scheme may be the best of the control schemes described above. However, convergence of parameters to the true values can be guaranteed only if a trajectory that a manipulator must follow is persistently excited. Practical trajectories usually do not satisfy the condition of persistent excitation. Moreover, whenever a manipulator picks up different payloads, the parameters associated with the dynamics change. As a consequence, it is almost impossible to obtain the true values of the parameters, causing deterioration of transient behavior, a factor that can not be emphasized too strongly in tracking control. In fact, there

is no analytical way of estimating the transient response in adaptive control. We can use higher gains for this scheme to enhance the transient behavior. However, in general, as the gain of any feedback compensator increases, the tracking error decreases, but stability also decreases due to unmodelled dynamics.

Hence, in this thesis, we will focus on improving the transient response without reducing the asymptotic stability of the combined system (robot dynamics plus control compensator).

1.2.2 Control of Flexible-Joint Manipulators

In the previous section, we have discussed control of an ideal robot having rigid links and rigid joints. In reality, there always exist a certain degree of flexibility in the robot structure. Depending on the degree of flexibility, the discussion in the previous section can be invalid, or a different control strategy may be required. The links of most commercial robots are well approximated by rigid bodies. According to Rivin[1.60], 80 to 95% of the flexibility in several robot manipulators was due to joint flexibility. We may easily stiffen the links with added structural mass. Here we restrict our discussion to the joint flexibility. We can minimize the flexibility in the joints by mounting high torque actuators directly in the joints (direct-drive mechanism). In this case, the mass of bulky actuators and their housing are very often a significant fraction of the total mass of the structure. The mass and its position in a robot is one of the crucial factors for commercial robots, as well as space robots, since the required actuator power is approximately proportional to the speed and the mass moment of inertia of the structure. Accordingly, increased mass due to the direct-drive mechanism may offset the benefits of the mechanism. There should be a trade-off between stiffness and weights.

We can reduce the weights of actuators with appropriate gearing. This allows use of smaller actuators. There are two kinds of gearing mechanisms: harmonic drive, and ordinary pinion and gear. The latter is much stiffer but carries considerable backlash. The former exhibits negligible backlash and their compact

size makes it easier to integrate them into practical designs. As an alternative, we can mount the actuators on or close to the stationary base of the structure so that we can substantially reduce the mass moment of inertia in the overall configuration. Sometimes it is possible to install all the actuators far from the links. Belts, cables, drive shafts, or combinations of these are then used for power transmission.

One unavoidable characteristic of these mechanisms is that they are flexible: belts and cables stretch, drive shafts and harmonic drives twist, and gear teeth bend. Their compliance may be advantageous for force control or for the protection of the mechanical components of manipulators from the impacts of collisions. However, joint flexibility causes difficulties in control. Link and actuator angles may be different. Hence, the equations of motion of a flexible-joint robot are much more complicated than those of the rigid-joint counterpart. In commercial robots, actuator angles are controlled. Hence, flexibility causes positional errors and undesirable vibrations. Consequently, joint flexibility is one of the sources of reduced productivity in commercial robots[1.61]. One might try to control link angles instead of actuator angles. Then, the problem becomes even worse. The gains of compensators must be kept small[1.62] to avoid instabilities of the flexible dynamics which are inside the feedback loop. There have been many efforts to find an alternate solution to this problem.

De Luca[1.63,1.64], Spong[1.65], and their colleagues treated this problem with the concept of feedback linearization and inverse dynamics. Then, the problem comes down to solving a set of fourth-order decoupled differential equations. As a result, these schemes require measurements of angular accelerations and jerks of the links. Moreover, the complexity of the dynamic equations goes beyond our imagination. In other words, it is nearly impossible to implement the schemes in real time.

Chen and Fu[1.66] proposed an adaptive scheme for the structure of Spong's scheme[1.65], based on the assumptions that the inertia and friction coefficients of actuators are precisely known and that the angular accelerations of links are

measurable. This assumption is too ideal. The computational burden of Chen and Fu's method is much heavier than that of Spong's.

Khorasani[1.67] and Spong[1.68] applied the concept of integral manifolds. In this approach, the dynamics of a manipulator with flexible joints is restricted to an integral manifold. Then, a reduced model is derived which has the same order as the model of the corresponding rigid-joint manipulator. This model is used for feedback linearization. Lack of robustness to parametric uncertainties, however, makes these methods impractical.

To treat the problem of parameter uncertainties in schemes[1.67,1.68], Khorasani[1.69] proposed an adaptive regulation scheme. Derivation of this scheme is based on an unrealistic assumption that the flexible-joint system restricted to an integral manifold is linear in the uncertain parameters. Furthermore, its integration adaptation rule may cause parameter drift in the presence of bounded disturbances and unmodelled dynamics.

Ghorbel et al.[1.70] attacked this problem using singular perturbation theory. This approach may avoid the aforementioned problems for some applications. It appears that this method may work if the stiffness of the joint couplings is sufficiently high. Stability of this scheme is not proved. Instead, a simple experimental demonstration is provided.

Hollars et al.[1.71-1.73] linearized the dynamics around an operating point, and then estimated the states of the system using an extended Kalman filter. Then they designed a full state feedback control law using LQR (Linear Quadratic Regulator). They scheduled the gains of their control law for several different payload conditions. Since the extended Kalman filter requires complete knowledge of the system, this scheme is sensitive to parameter variations. Uhlik[1.74] extended Hollars' scheme by scheduling the gains for some additional configurations. He also added feedforward compensators based on perfect knowledge of the parameters contained in dynamics. Effects of payloads are compensated using his estimation scheme based on the assumption that values of the parameters of the link dynamics are accurately known.

In this work, we will focus on the design of a control law for flexible-joint robots whose performance is independent of the stiffness of the joint, the inertia and damping of the actuators, and the gear-reduction ratios. We also avoid the requirement of measuring angular accelerations and jerks.

1.2.3 The Issue of Robustness in Adaptive Control of Robots

In the 1960s and 1970s, the adaptive control community focused on obtaining asymptotic stability of systems having parameter uncertainties under the ideal assumption that there exists no disturbance, sensor noise, and unmodelled dynamics. In the early 1980s, research in adaptive control had to treat a new problem: lack of **robustness** in adaptive schemes. Several researchers showed instability of asymptotically stable adaptive schemes for linear time-invariant systems when the assumption is not satisfied[1.75], and proposed some modified adaptation laws[1.76-1.83]. Instability is caused by drift of parameters (or control gains) to large (possibly unbounded) values due to integrators in the adaptation loop in the presence of bounded disturbances, sensor noises, or unmodelled dynamics. Accordingly, the basic idea of all the modifications in adaptation laws is to prevent the parameter drift by eliminating integration in the adaptation loop. Examples of these are "use of dead zone," "use of bounds on parameters," "σ-modification," and "e_1-modification," described below. Robustness in adaptive control does not mean the robustness with respect to parameter uncertainties but rather means the robustness with respect to parameter drift in the presence of bounded disturbances, sensor noises, and unmodelled dynamics.

The "dead-zone"[1.76,1.77] overcomes the parameter drift by stopping adaptation when the magnitudes of tracking errors become smaller than prescribed values. Bounds of parameters can be positively used in adaptation laws[1.78-1.80]. When estimated parameters are smaller than preset values (usually larger than the nominal values), the regular integration adaptation law is used. When the estimated parameters grow larger than the preset values, some nonlinear memory components are used instead of the integrators. The "σ-modification"[1.81,1.82]

replaces the integrators in adaptation laws with first-order filters whose break frequencies are constant. The drawback of this modification is that the tracking errors do not converge to zero even when the bounded disturbances are removed. The "e_1-modification"[1.83] is the same as the "σ-modification" except that the break frequencies of the first-order filters are proportional to the magnitudes of the tracking errors. Accordingly, this modification causes zero tracking errors when no disturbances exist.

Robustness of adaptive control of robots was discussed in [1.84] with some artificial unmodelled dynamics. With sensor noises in simulations, instability due to parameter drift was observed in some adaptive control laws for robots which are asymptotically stable under a certain ideal condition[1.85].

In this thesis, we use the σ-modification to prevent parameter drift. In addition, we propose some robust adaptation laws based on the bounds of the parameters. We investigate the robustness of adaptive control schemes in the presence of bounded disturbances and unmodelled dynamics such as high-frequency dynamics of flexible joints, feedback delays in the digital control systems, and coupled dynamics in the decentralized scheme. We derive a sufficient condition on the bounds of disturbances, control and adaptation gains, and desired trajectories and their time-derivatives, which guarantees robust stability of the proposed schemes in the presence of unmodelled dynamics.

1.3 Contribution of This Thesis

This thesis deals with the design of high performance adaptive trajectory control laws for manipulators which guarantee not only robust stability of the system but also a reasonable transient response.

The main contributions of this work are as follows.

(i) The importance of the transient behavior as well as robust stability of a system is emphasized and taken into account in the design of adaptive control laws, whereas in previous work only the stability of the system has been treated. As a result, with the present schemes, tracking errors are considerably reduced.

(ii) A new 2-norm approach to the design of adaptive control laws has been developed. This method provides sufficient conditions for (asymptotic) stability of a given (nonlinear coupled time-varying) system. This method involves search for compensators in the direction of minimizing a quadratic performance index. In other words, it contains a feature of optimal control. This method also takes the loop shaping method of linear control theory into adaptive control. As a result, advantages from the optimal control and loop shaping method are maximized in adaptive control.

(iii) A robust decentralized adaptive control scheme is proposed for manipulators. The scheme adopts feedforward adaptive compensators, feedback adaptive compensators, and an improved PD feedback law. Stability of the proposed scheme is proved under the reasonable assumption that the structure of the coupled dynamics is known. Under some moderate constraints, the proposed scheme is stable and robust in the presence of bounded disturbances and unmodelled dynamics due to feedback delays in the digital control systems. In previous work, the stability proof required an additional assumption that the coupled dynamics is bounded and quasi-time-invariant, if the feedforward adaptive compensator is included in the decoupled adaptive schemes.

(iv) A robust control scheme for trajectory control of manipulators having flexible joints is developed. The control law is unique in that this scheme is not only almost independent of the gear-reduction ratios, flexibilities of the joint couplings, and characteristics of the actuators, but also free from the requirements of measuring accelerations and jerks of link angles.

(v) Stability bounds for disturbances, control and adaptation gains, and desired trajectories and their time-derivatives are obtained for the proposed adaptive schemes. These bounds are sufficient conditions for robust stability of the proposed schemes in the presence of bounded disturbances and unmodelled dynamics such as high-frequency dynamics of flexible joints, feedback delays in the digital control systems, or the coupled dynamics in the decoupled control scheme.

1.4 Preview of This Thesis

The remaining chapters of this thesis are briefly outlined here.

In Chapter 2, we briefly review the essence of various methods in the design of adaptive control laws. With a prototype example, we discuss the design procedure in the self-tuning method. We summarize Lyapunov's and Popov's stability theories, and explain with examples how they can be applied to the design of adaptive control laws.

In Chapter 3, we first model a system to control as a linear decoupled system with bounded disturbances under some reasonable assumptions. Then we apply the loop shaping method to design non-adaptive feedback compensators. Secondly, we develop a 2-norm approach to the design of adaptive control laws. The new method can handle both linear decoupled and nonlinear coupled systems. Finally, based on the original nonlinear dynamics, we add adaptive compensators via the 2-norm approach to the non-adaptive counterparts so that we can achieve asymptotic stability of the system. Two kinds of adaptive compensators are adopted: model-based parameter-adaptive compensators and decoupled robust feedback compensators. The importance of the transient behavior of the control law is addressed and taken into account in the design procedures.

In Chapter 4, we investigate the robustness of the scheme developed in Chapter 3 in the presence of bounded disturbances. We show that the integration adaptation law in the previous chapter may cause parameter drift even in adaptive control of robots. We add to the model of the system bounded disturbances, sensor noises, and unmodelled dynamics due to feedback delays in the digital control systems in order to investigate the effects of these on the stability and robustness of adaptive control systems. To design a control law, we first define an appropriate quadratic performance index. Secondly, we search for compensators toward minimizing the quadratic performance index so as to improve tracking performance. In this search, we select the compensators used in Chapter 3, and redesign their adaptation laws to prevent parameter drift. Finally, we analyze the stability of the

proposed adaptive scheme in the presence of bounded disturbances and unmodelled dynamics due to feedback delays. As a result, we find some stability bounds for disturbances, control and adaptation gains, and desired trajectories and their time-derivatives, in the presence of feedback delays.

In Chapter 5, we deal with the design of a robust decoupled adaptive scheme. The coupled dynamics of manipulators in this case become additional unmodelled dynamics. The design procedure in this chapter is basically the same as that in the previous chapter except that only the decoupled compensators are selected in the search. We show that there exists a region of attraction of the proposed decentralized scheme for the nonlinear coupled dynamics of robots, under some moderate constraints on desired trajectories, bounded disturbances, and control and adaptation gains, if the sampling period is sufficiently small.

In Chapter 6, we examine joint flexibility. We view the actuator dynamics and joint couplings as prefilters to the link dynamics. We investigate how to optimize the characteristics of the prefilters by adding some flexibility compensators. With the compensators we transform a manipulator having flexible joints into that having almost rigid joints. This means that we make the flexible joint couplings artificially rigid by adding the flexibility compensators. In this way, we convert the control of flexible-joint manipulators to that of the corresponding rigid-joint manipulators, which has been already treated in the previous chapters. However, the transformed system (almost rigid-joint robot) still contains some degree of high-frequency unmodelled dynamics. Through additional stability analysis, we impose some constraints on the proposed scheme so that the scheme stabilizes the original flexible-joint system. Finally, we focus on attenuation of high-frequency sensor noises for the flexibility compensation loop.

In Chapter 7, we summarize this thesis and point out possible areas of extension.

In this thesis, the proposed adaptive schemes do not have any reference model. This implies that trackable desired trajectories are provided by trajectory generators. This approach in robot control is superior to the usual model-following

adaptive control since the latter drives the output of the system not to the desired trajectory but to the output of a reference model. When we do not have a trajectory generator, we filter a given trajectory through a stable second-order differential equation, so that the filtered trajectory becomes the desired trajectory to the system. In this case, the stable second-order filter can be considered as a reference model in the regular model reference adaptive schemes.

Throughout this thesis, the theories are illustrated by realistic computer simulations.

Finally, we note that symbols are defined independently in each chapter. Also, each chapter contains its own lists of references and appendices.

References

[1.1] Markiewicz, B. R., *Analysis of the Computed Torque Drive Method and Comparison with Conventional Position Servo for a Computer-Controlled Manipulator,* Technical Memorandum 33-601, Jet Propulsion Laboratory, California Institute of Technology, Mar. 1973.

[1.2] Bejczy, A. K., *Robot Arm Dynamics and Control,* JPL NASA Technical Memorandum 33-669, February 1974.

[1.3] Lewis, R. A., *Autonomous Manipulation on a Robot: Summary of Manipulator Software Functions,* JPL Technical Memorandum 33-679, March 1974.

[1.4] Tourassis, V. D. and Neuman, C. P., *Robust Nonlinear Feedback Control for Robotic Manipulators,* IEE Proc., Vol. 132, Part D, No. 4, pp. 134-143, July 1985.

[1.5] Astrom, K. J., *Theory and Applications of Adaptive Control- Survey,* Automatica, Vol. 19, No. 5, pp. 471-486, 1983.

[1.6] Kalman, R. E., *Design of a Self-Optimizing Control System,* Trans. ASME, p. 486, 1958.

[1.7] Goodwin, G. C. and Sin, K. S., *Adaptive Filtering, Prediction, and Control,* Prentice-Hall, Reading, 1984.

[1.8] Harris, C. J. and Billings, S. A., *Self-Tuning and Adaptive Control: Theory and Application,* Peter Peregrinus Ltd., Reading, 1981.

[1.9] Donalson, D. D. and Leondes, C. T., *A Model Referenced Parameter Tracking Technique for Adaptive Control Systems: Part I The Principle of Adaptation, and Part II Stability Analysis by the Second Method of Lyapunov,* Trans of IEEE on Applications and Industry, Vol. 82, No. 68, pp. 240-262, Sep. 1963.

[1.10] Kalman, R. E. and Bertram, J. E., *Control System Analysis and Design Via the Second Method of Lyapunov: Part I Continuous-Time Systems, and Part II Discrete-Time Systems,* Journal of Basic Engineering, Trans of ASME, pp. 371-400, June 1960.

[1.11] Narendra, K. S. and Kudva, P., *Stable Adaptive Schemes for System Identification and Control,* IEEE Trans. Man and Cybernetics, Vol. SMC- 4, No. 6, pp. 542-551, November 1974.

[1.12] Landau, Y. D., *Adaptive Control: The Model Reference Approach,* Marcel Dekker Inc., Reading, 1979.

[1.13] Landau, Y. D. and Courtial, B., *Design of Multivariable Adaptive Model Following Control Systems,* Automatica, Vol. 10, pp. 483-494, 1974.

[1.14] Popov, V. M., *Hyperstability of Control Systems,* New York: Springer-Verlay, Reading, 1983.

[1.15] Dubowsky, S. and DesForges, D. F., *The Application of Model-Reference Adaptive Control to Robotic Manipulators,* ASME J. of DSMC, Vol. 101, pp. 193-200, 1979.

[1.16] Dubowsky, S. and Kornbluh, R., *On the Development of High Performance Adaptive Control Algorithms for Robotic Manipulators,* Robotics Research edited by Inoue Hanafusa, pp. 119-126, 1984.

[1.17] Koivo, A. J. and Guo, T. M., *Adaptive Linear Controller for Robotic Manipulators,* IEEE Trans. on Aut. Contr., Vol. AC-28, No. 2, pp. 162-172, 1983.

[1.18] Koivo, A. J., Lewczyk, R. and Chiu, T. H., *Adaptive Path Control of a Manipulator with Visual Information,* IEEE Conference on Robotics, Atlanta, March 1984.

[1.19] Koivo, A. J., *Adaptive Position-Velocity-Force Control of Two Manipulators,* 24th IEEE Conf. on Decision and Control, Fort Lauderdale, Fla., 1985.

[1.20] Koivo, A. J., *Force-Velocity Control with Self-Tuning for Robotic Manipulators,* IEEE Conference on Robotics and Automation, San Francisco, April 1986.

[1.21] Walters, R. G. and Bayoumi, M. M., *Application of a Self-Tuning Pole Placement Regulator to an Industrial Manipulator,* IEEE, Conference on Decision and Control, pp. 323-329, 1982.

[1.22] Leininger, G. G. and Wang , S., *Pole Placement Self-Tuning Control of*

Manipulators, IFAC Symposium on Computer Aided Design of Multivariable Technological Systems, West Lafayette, Ind., September 15-17, 1982.

[1.23] Leininger, G. G., *Self-Tuning Control of Manipulators,* International Symposium on Advanced Software in Robotics, Liege, Belgium, May 1983.

[1.24] Leininger, G. G., *Adaptive Control of Manipulators Using Self-Tuning Methods,* Robotics Research, Chap.9 edited by M. Brady and R. Pall, 1984.

[1.25] Backes, P., *Real Time Control with Adaptive Manipulator Control Schemes,* M.S. Thesis, Purdue University, School of Mechanical Engineering, West Lafayette, Ind., December 1984.

[1.26] Backes, P., Leininger, G. G., *Real Time Cartesian Coordinate Hybrid Control of a Puma 560 Manipulator,* IEEE Conference on Robotics and Automation, St. Louis, March 1985.

[1.27] Sundareshan, M. K. and Koenig, M. A., *Decentralized Model Reference Adaptive Control of Robotic Manipulators,* Proceedings, Automatic Control Conference, pp. 44-49, 1985.

[1.28] Takegaki, M. and Arimoto, S., *An Adaptive Trajectory Control of Manipulators,* Int. J. of Control, Vol. 34, No. 2, pp. 219-230, 1981.

[1.29] Seraji, H., *Direct Adaptive Control of Manipulators in Cartesian Space,* J. of Robotic Systems, Vol. 4, No. 1, pp. 157-178, 1987.

[1.30] Seraji, H., *Decentralized Adaptive Control of Manipulators: Theory, Simulation, and Experimentation,* IEEE Trans. on Robotics and Automation, Vol. 5, No. 2, pp. 183-201, April 1989.

[1.31] Oh, B. J., Jamshidi, M. and Seraji, H., *Decentralized Adaptive Control,* Proc. of IEEE Int. Conf. on Robotics and Automation, pp. 1016-1021, 1988.

[1.32] Gavel, D. T. and Hsia, T. C., *Decentralized Adaptive Control of Robotic Manipulators,* Proc. of IEEE Int. Conf. on Robotics and Automation, pp. 1230-1235, April 1987.

[1.33] Gavel, D. T. and Hsia, T. C., *Decentralized Adaptive Control Experiments with the PUMA Robot Arm,* Proc. of IEEE Int. Conf. on Robotics and Automation, pp. 1022-1027, 1988.

[1.34] Lim, K. Y. and Eslami, M., *New Controller Design for Robot Manipulator Systems,* Proc., Amer. Contr. Conf., pp. 38-43, June 1985.

[1.35] Lim, K. Y. and Eslami, M., *Adaptive Controller Designs for Robot Manipulator Systems Yielding Reduced Cartesian Error,* IEEE Trans. on Automatic Control, Vol. AC-32, No. 2, pp. 184-187, Feb. 1987.

[1.36] Lim, K. Y. and Eslami, M., *Robust Adaptive Controller Designs for Robot Manipulator Systems,* IEEE J. of Robotics and Automation, Vol. RA-3, No. 1, pp. 54-66, Feb. 1987.

[1.37] Nicosia, S. and Tomei, P., *Model Reference Adaptive Control Algorithms for Industrial Robots,* Automatica, Vol. 20, No. 5, pp. 635-644, 1984.

[1.38] Balestrino, A., De Maria, G. and Sciavicco, L., *An Adaptive Model Following Control for Robotic Manipulators,* ASME J. of DSMC, Vol. 105, pp. 143-151, 1983.

[1.39] Ozguner, U., Yurkovich, S. and Al-Abbass, F, *Decentralized Variable Structure Control of Two-Arm Robotic System,* Proc. of IEEE Int. Conf. on Robotics and Automation, pp. 1248-1254, 1987

[1.40] Pandian, S. R., Hanmandlu, M. and Gopal, M., *A Decentralized Variable Structure Model Following Controller for Robot Manipulators,* Proc. of IEEE Int. Conf. on Robotics and Automation, pp. 1324-1328, 1988.

[1.41] Horowitz, R. and Tomizuka, M., *An Adaptive Control Scheme for Mechanical Manipulators - Compensation of Nonlinearity and Decoupling Control,* ASME J. of DSMC, Vol. 108, pp. 127-135, June 1986.

[1.42] Anex, Jr., R. P. and Hubbard, M., *Modeling and Adaptive Control of a Mechanical Manipulator,* ASME. J. of DSMC, Vol. 106, pp. 211-217, Sep. 1984.

[1.43] Craig, J. J., *Adaptive Control of Mechanical Manipulators,* Ph.D. thesis, Stanford University, Department of Electrical Engineering, Stanford, CA 94305, June 1986; Also published by Addison-Wesley

[1.44] Craig, J. J., Hsu, P. and Sastry, S. S., *Adaptive Control of Mechanical Manipulators,* Proc. IEEE Conf. on Robotics and Automation, pp. 190-

195, 1986.

[1.45] Kabtab, A., *Nonlinear Control of Robotic Manipulators-Hyperstability Approach,* Robotics and Autonomous Systems, Vol. 4, No. 3, pp. 265-274, 1988.

[1.46] Slotine, J. J. E. and Li, W., *On the Adaptive Control of Robot Manipulators,* Proc. ASME Winter Annual Meeting, 1986.

[1.47] Slotine, J. J. E. and Li, W., *Adaptive Manipulator Control: Parameter Convergence and Task-Space Strategies,* Proc. of the 1987 American Control Conference, pp. 828-835, 1987.

[1.48] Slotine, J. J. E. and Li, W., *Adaptive Manipulator Control: A Case Study,* Proc. of the 1987 Int. Conf. on Robotics and Automation, pp. 1392-1400, 1987.

[1.49] Arimoto, A. and Miyazaki, F., *Stability and Robustness of PID Feedback Controller for Robot Manipulators of Sensory Capability,* Robotics Research: The First International Symposium edited by Brady, M. and Paul, R., pp. 783-799, 1984.

[1.50] Lee, C. G. S. and Chung, M. J., *An Adaptive Control Strategy for Computer-Based Manipulator,* 21st Conf. on Decision and Control, Orlando, Fla., pp. 95-100, 1982.

[1.51] Lee, C. G. S., Chung, M. J. and Lee, B. H., *An Adaptive Control for Robotic Manipulators in Joint and Cartesian Coordinates,* IEEE Conf. on Robotics, Atlanta, March 1984.

[1.52] Lee, C. G. S., Chung, M. J. and Lee, B. H., *An Approach of Adaptive Control for Robotic Manipulators,* J. of Robotic System, p1, 1984.

[1.53] Lee, C. G. S. and Lee, B. H., *Resolved Motion Adaptive Control for Mechanical Manipulators,* ASME Trans., Vol. 106, pp. 134-142, June 1984.

[1.54] Lee, C. G. S. and Chung, M. J., *An Adaptive Control Strategy for Mechanical Manipulators,* IEEE Trans. Auto. Control, Vol. AC-29, No. 9, pp. 837-840, 1984.

[1.55] Choi, Y. K., Chung, M. J. and Bien, Z., *An Adaptive Control Scheme for Robot Manipulators,* Int. J. Control, Vol. 44, No. 4, pp. 1185-1191, 1986.

[1.56] Choi, Y. K. and Bien, Z., *Decentralized Adaptive Control Scheme for Control of a Multi-Arm Type Robot,* Int. J. Control, Vol. 48, No. 4, pp. 1715-1722, 1988.

[1.57] deSilva, C. W. and Winssen, J.,V., *Least Squares Adaptive Control for Trajectory Following Robots,* ASME Trans., Vol. 109, pp. 104-110, June 1987.

[1.58] Hsia, T. C., *Adaptive Control of Robot Manipulator- A Review,* IEEE Conf. on Robotics and Automation, pp. 190-195, 1986.

[1.59] Kreisselmeier, G., *Adaptive Observers with Exponential Rate of Convergence,* IEEE Trans. on Automatic Control, Vol. AC-22, 1977.

[1.60] Rivin, E. R., *Effective Rigidity of Robot Structures: Analysis and Enhancement,* Proc. American Control Conf., pp. 381-382, Boston, June 1985.

[1.61] Sweet, L. M. and Good, M. C., *Redefinition of the Robot Motion Control Problem: Effects of Plant Dynamics, Drive System Constraints, and User Requirements,* Proc. 23^{rd} IEEE CDC, Las Vegas, NV, 1984.

[1.62] Stepien, T. M., Sweet, L. M, Good, M. C. and Tomizuka, M., *Control of Tool/Working Piece Contact Force with Application to Robotic Deburring,* IEEE J. of Robotics and Automation, Vol. RA-3, pp. 7-18, 1987.

[1.63] De Luca, A., *Control Properties of Robot Arms with Joint Elasticities,* Proc. MTNS, Phoenix, AZ, June, 1987.

[1.64] De Luca, A., Isadori, A. and Nicolo, F., *An Application of Nonlinear Model Matching to the Control of Robot Arms with Elastic Joints,* 1^{st} IFAC Symp. Robot Control, Barcelona, 1985.

[1.65] Spong, M. W., *Modelling and Control of Elastic Joint Manipulators,* J. of Dyn. Sys. Meas. and Control, Vol. 109, pp. 310-319, 1987.

[1.66] Chen, K. and Fu, L., *Nonlinear Adaptive Motion Control for a Manipulator with Flexible Joints*, Proc. of IEEE Int. Conf. on Robotics and Automation, pp. 1201-1206, 1989.

[1.67] Khorasani, K. and Spong, M. W., *Invariant Manifolds and Their Application to Robot Manipulators with Flexible Joints,* Proc. IEEE Int'l Conf. on Robotics and Automation, St. Louis, Mar. 1985.

[1.68] Spong, M. W., Khorasani, K. and Kokotovic, P. V., *An Integral Manifold Approach to the Feedback Control of Flexible Joint Robots,* IEEE J. of Robotics and Automation, Vol. RA-3, No. 4, pp. 291-300, Aug. 1987.

[1.69] Khorasani, K., *Robust Adaptive Stabilization of Flexible Joint Manipulators,* Proc. of IEEE Int. Conf. on Robotics and Automation, pp. 1194-1199, 1989.

[1.70] Ghorbel, F., Hung, J. Y. and Spong, M. W., *Adaptive Control of Flexible Joint Manipulators,* IEEE Conf. on Robotics and Automation, pp. 1188-1193, 1989.

[1.71] Hollars, M. G. and Cannon, Jr. R. H., *Initial Experiments on End-Point Control of a Two-Link Manipulator with Flexible Tendons,* Prec. of ASME Winter Annual Meeting, Fl, November 1985.

[1.72] Hollars, M. G. and Cannon, Jr., R. H., *Experiments on End-Point Control of a Two-Link Robot with Elastic Drive,* Proc of AIAA Guidance, Navigation and Control Conf., pp. 19-27, August 1986.

[1.73] Hollars, M. G., *Experiments in End-Point Control of Manipulators with Elastic Drive,* Ph.D. thesis, Stanford University, Department of Aeronautics and Astronautics, Stanford, CA 94305, May 1988.

[1.74] Uhlik, C. R., *Experiments in High-Performance Nonlinear and Adaptive Control of a Two-Link, Flexible-Drive-Train Manipulator,* Ph.D. thesis, Stanford University, Department of Aeronautics and Astronautics, Stanford, CA 94305, May 1990.

[1.75] Rohrs, C. E., Valavani, L., Atheans, M. and Stein, G., *Robustness of Adaptive Control Algorithms in the Presence of Unmodelled Dynamics,* IEEE Conf. on Decision and Control, Proc., pp. 3-11, 1982.

[1.76] Peterson, B. B. and Narendra, K. S., *Bounded Error Adaptive Control,* IEEE Trans. on Auto. Contr., Vol. AC-27, pp. 1161-1168, Dec. 1982.

[1.77] Samson, C., *Stability Analysis of Adaptively Controlled Systems Subject to Bounded Disturbances,* Automatica, Vol. 19, pp. 81-86, 1983.

[1.78] Kreisselmeier, G. and Narendra, K. S., *Stable Model Reference Adaptive Control in the Presence of Bounded Disturbances,* IEEE Trans. on Auto. Contr., Vol. AC-27, No. 6, pp. 1169-1175, Dec. 1982.

[1.79] Ioannou, P. A. and Tsakalis, K. S., *A Robust Direct Adaptive Controller,* IEEE Trans. on Auto. Contr., Vol. AC-31, No. 11, pp. 1033-1043, Nov. 1986.

[1.80] Ioannou, P. A., *Robust Adaptive Control with Zero Residual Tracking Errors,* IEEE Trans. on Auto. Contr., Vol. AC-31, No. 8, pp. 773-776, Aug. 1986.

[1.81] Ioannou, P. A. and Kokotovic, P. V., *Instability Analysis and Improvement of Robustness of Adaptive Control,* Automatica, Vol. 20, No. 5, pp. 583-594, 1984.

[1.82] Ioannou, P. A. and Kokotovic, P. V., *Robust Redesign of Adaptive Control,* IEEE Trans. on Auto. Contr., Vol. AC-29, No. 3, pp. 202-211, March 1984.

[1.83] Narendra, K. S. and Annaswamy, A. M., *A New Adaptive Law for Robust Adaptation Without Persistent Excitation,* IEEE Trans. on Auto. Contr., Vol. AC-32, No. 2, pp. 134-145, Feb. 1987.

[1.84] Reed, J. S. and Ioannou, P. A., *Instability Analysis and Robust Adaptive Control of Robotic Manipulators,* Conf. on Decision and Control, Proc., pp. 1607-1612, Dec. 1988.

[1.85] Schwartz, H. M., Warshaw. G. and Janabi, T., *Issues in Adaptive Robot Control,* American Control Conf., Vol. 3, pp. 2797-2805, 1990.

Chapter 2

REVIEW OF ADAPTIVE CONTROL

2.1 Introduction

As a way of compensating parameter uncertainties in a system to control, adaptive control strategies have been applied in various fields. Adaptive control can be classified as a special branch of nonlinear feedback control. There are two fundamental approaches: self-tuning and model reference methods. Sometimes gain scheduling is also classified as a form of adaptive control[2.1]. Schematic diagrams of these methods are given in Figure 2.1. There is nothing new in this chapter; this material is included to provide background and for convenient reference in the remainder of this thesis.

Gain scheduling has been used mainly in flight control systems. The basic idea of this method is to preset the controller gains for all possible situations in the whole operating range of a plant. Thus, the method is based on precise knowledge of the physics of the plant or on the results of extensive experiments with the plant. This is a kind of table-look-up method. During operation, the state of the plant is measured and the results are used to determine the values of gains chosen according to the predetermined schedule. One drawback of this method is that it is based on open-loop compensation. There is no feedback which compensates for an incorrect scheduling of the gains. Thus, this method can be viewed as a feedback control system in which the feedback gains are adjusted by feedforward compensation. Another drawback of this method is that its design is a time consuming process. This method has been highly successful for control of aircrafts. This method has been also tested for trajectory control of a flexible-joint robot[2.2-2.5]. However, gain scheduling is not practical for robot control

since the dynamics of a robot is affected by too many factors: trajectories and their time-derivatives, weight and shape of payloads, weight and size of the robot itself, etc.

The self-tuning method was originally proposed by Kalman[2.6]. The theory of this method[2.7,2.8] is based on linearization of the plant behavior around operating points; parameter estimation; and linear control theory. The dynamics of the discretized plant at the sampling points is parameterized as a linear combination of the discretized sequences of the applied inputs and measured outputs of the plant with time-varying parameters (the coefficients of the sequence). The parameters are estimated recursively. For recursive estimation of parameters, many different schemes have been developed: least squares, extended and generalized least squares, stochastic approximation, extended Kalman filtering, and the maximum likelihood method. Linear control theory is then applied with the estimated parameters characterizing the plant. Examples of the controller design strategy include pole-placement and optimal control theory. This method has also been applied to problems of robot control[2.9-2.19]. One drawback of this method is that there are always parameter estimation errors since the convergence of the estimation is generally not fast enough, especially for time-varying systems. Furthermore, convergence of the estimation to the true values of the parameters is guaranteed only if the input of the system is persistently excited. Thus, the self-tuning control schemes are designed with errors in the estimation of the plant. As a consequence, this method has not been so successful for robot control.

In the model reference method[2.20-2.53], the objective is to drive the output of a system asymptotically to that of a reference model; the difference between the output of the model and that of the system is called "model-following error." To achieve the objective, the steepest descent method[2.25-2.27], Lyapunov's direct method[2.20-2.22], and Popov's hyperstability theory[2.22-2.24] have been employed. The steepest descent method minimizes the model-following error by reducing an objective function in the steepest descent direction of the function. One of the drawbacks of this method is that separate stability analysis has to be

worked out. Design of control laws[2.28-2.53] using Lyapunov's or Popov's theories offers alternative possibilities. Thus, extensive research has been carried out for applications of those stability theories.

In this chapter we will briefly review "self-tuning" and "model reference" methods along with design examples of some adaptive control laws for a spring-mass-damper system to illustrate applications of the theories. We assume that there exist no disturbance, sensor noise, and unmodelled dynamics, so that we do not consider the problem of parameter drift in adaptation.

2.2 Self-tuning Method

In this section, we briefly discuss the essential parts of a design procedure for the self-tuning method with a simple spring-mass-damper system. However, the technique here can be readily extended to more complicated systems. For more information about the self-tuning method, see references [2.7] and [2.8].

Let us model a spring-mass-damper system as

$$m\ddot{y} + d\dot{y} + ky = u, \tag{2.2.1}$$

where u and y are the input (force) and the output (position) of the system respectively; m, d, and k are the mass, damping coefficient, and spring constant of the system.

2.2.1 System Representation (Linearization)

The self-tuning method has been developed in the discrete time domain so that we need to represent the plant (2.2.1) using the sequences of applied inputs and measured outputs. Conversion of a continuous time system to the discrete time counterpart is not unique. Here we apply the zero-hold-equivalence approximation[2.54] to the system (2.2.1) under the assumption of time-invariant coefficients. Then, we have the following form of the discrete system:

$$y_i = \alpha_1 y_{i-1} + \alpha_2 y_{i-2} + \alpha_3 u_{i-1} + \alpha_4 u_{i-2}, \tag{2.2.2}$$

where α_j for j=1, 2, 3, 4 is the parameter of the discretized dynamics; y_i and u_i are the output and the input at time i respectively. We can also express the system (2.2.2) in the following vector form:

$$y_i = \phi_{i-1}^T \theta, \tag{2.2.3}$$

where

$$\begin{aligned} \phi_{i-1} &= [y_{i-1}, y_{i-2}, u_{i-1}, u_{i-2}]^T, \\ \theta &= [\alpha_1, \alpha_2, \alpha_3, \alpha_4]^T. \end{aligned} \tag{2.2.4}$$

This model is called the ARMA (Auto-Regressive Moving-Average) model[2.7].

2.2.2 Parameter Estimation.

Numerical values of the parameter θ for a given system are estimated in such a way that these minimize the difference between the actual output of the plant and the value predicted by the model (2.2.3) with estimated values of the parameter θ. Hence, estimation of parameters involves minimization of some quadratic cost function (usually subject to some constraints). Since the choice of the cost function is not unique, there are many estimation schemes. Examples of these are the "projection scheme," "least square method," and their variants. Here we consider the least square method[2.7].

We define the following quadratic cost function:

$$J_i(\theta) = \frac{1}{2}(\underline{y}_i - \Phi_{i-1}\theta)^T(\underline{y}_i - \Phi_{i-1}\theta) + \frac{1}{2}(\theta - \hat{\theta}_0)^T \Psi_0^{-1}(\theta - \hat{\theta}_0), \tag{2.2.5}$$

where

$$\begin{aligned} \underline{y}_i &= [y_1, y_2, \cdots, y_i]^T, \\ \Phi_{i-1} &= [\phi_0, \phi_1, \cdots, \phi_{i-1}]^T; \end{aligned} \tag{2.2.6}$$

Ψ_0 is the 4×4 positive-definite matrix; and $\hat{\theta}_0$ is the initial value of the estimated parameter vector. The first term of the cost function (2.2.5) represents the sum of squares of the difference between the actual output and the value predicted by the model with the parameter vector θ. The second term is included to account for the initial condition. Hence, minimizing this cost function leads to a least square estimator.

To minimize the cost function, we differentiate it with respect to θ and set the result to zero, then we have

$$(\Phi_{i-1}^T\Phi_{i-1} + \Psi_0^{-1})\theta = \Psi_0^{-1}\hat{\theta}_0 + \Phi_{i-1}^T\underline{y}_i. \tag{2.2.7}$$

Let us denote the value of θ satisfying this equation as $\hat{\theta}_i$. Then,

$$\hat{\theta}_i = \Psi_{i-1}(\Psi_0^{-1}\hat{\theta}_0 + \Phi_{i-1}^T\underline{y}_i), \tag{2.2.8}$$

where

$$\Psi_{i-1}^{-1} = \Phi_{i-1}^T\Phi_{i-1} + \Psi_0^{-1}. \tag{2.2.9}$$

Then, using (2.2.6), we have

$$\Psi_{i-1}^{-1} = \Psi_{i-2}^{-1} + \phi_{i-1}\phi_{i-1}^T. \tag{2.2.10}$$

From (2.2.8)

$$\begin{aligned}
\hat{\theta}_i &= \Psi_{i-1}(\Psi_0^{-1}\hat{\theta}_0 + \Phi_{i-2}^T\underline{y}_{i-1} + \phi_{i-1}y_i) \\
&= \Psi_{i-1}(\Psi_{i-2}^{-1}\hat{\theta}_{i-1} + \phi_{i-1}y_i) \qquad \text{using (2.2.8)} \\
&= \Psi_{i-1}(\Psi_{i-1}^{-1} - \phi_{i-1}\phi_{i-1}^T)\hat{\theta}_{i-1} + \Psi_{i-1}\phi_{i-1}y_i \qquad \text{using (2.2.10)} \\
&= \hat{\theta}_{i-1} + \Psi_{i-1}\phi_{i-1}(y_i - \phi_{i-1}^T\hat{\theta}_{i-1}).
\end{aligned} \tag{2.2.11}$$

By applying the "matrix inversion lemma" to (2.2.10), we have the following recursive equation:

$$\Psi_{i-1} = \Psi_{i-2} - \frac{\Psi_{i-2}\phi_{i-1}\phi_{i-1}^T\Psi_{i-2}}{1 + \phi_{i-1}^T\Psi_{i-2}\phi_{i-1}}. \tag{2.2.12}$$

This can be proved by direct verification. In this equation we set Ψ_{-2}, the initial value of Ψ_i, to be Ψ_0. By using (2.2.12), we write (2.2.11) in the form

$$\hat{\theta}_i = \hat{\theta}_{i-1} + \frac{\Psi_{i-2}\phi_{i-1}}{1 + \phi_{i-1}^T \Psi_{i-2}\phi_{i-1}}(y_i - \phi_{i-1}^T \hat{\theta}_{i-1}), \quad i \geq 1. \tag{2.2.13}$$

With (2.2.12) and (2.2.13), we can recursively estimate the parameter $\hat{\theta}_i$ at time i. Note that $(\hat{\theta}_i - \hat{\theta}_{i-1})$, the increment of the estimated parameter at time i, is proportional to $(y_i - \phi_{i-1}^T \hat{\theta}_{i-1})$, the difference between the actual output at time i and the value predicted by the model (2.2.3) with estimated parameters at time $i-1$.

2.2.3 Design of A Control law

In the self-tuning method, control laws are designed based on the estimated values of parameters. The underlying assumption is that the parameter estimators are perfect, i.e., the estimated parameters are assumed to be true values. Accordingly, hereafter we assume we have a discrete linear time-invariant system without uncertainty. To design a control law, we can minimize some quadratic cost function (possibly with some constraints). We can also apply "closed-loop pole assignment." In the following, we design a simple control law, and examine the characteristics of this law.

For simplicity, we rewrite the discrete system (2.2.2) in the following form:

$$\underline{a}(q^{-1})y_i = q^{-1}\underline{b}(q^{-1})u_i, \tag{2.2.14}$$

with

$$\begin{aligned} \underline{a}(q^{-1}) &= 1 - \alpha_1 q^{-1} - \alpha_2 q^{-2}, \\ \underline{b}(q^{-1}) &= \alpha_3 + \alpha_4 q^{-1}, \end{aligned} \tag{2.2.15}$$

where q^{-1} is a delay operator such that

$$q^{-1}y_i = y_{i-2}. \tag{2.2.16}$$

The constants α_1, α_2, α_3, and α_4 are given by the on-line parameter estimator (2.2.12) and (2.2.13).

Alternatively, we express the system in a 1-step-ahead predictor form:

$$y_{i+1} = \underline{a}_*(q^{-1})y_i + \underline{b}(q^{-1})u_i, \tag{2.2.17}$$

where

$$\underline{a}_*(q^{-1}) = \alpha_1 + \alpha_2 q^{-1}. \tag{2.2.18}$$

Now we define a quadratic cost function as

$$\begin{aligned} J_{i+1} &= \frac{1}{2}\Big[(r_{i+1} - y_{i+1})^2 + \lambda u_i^2\Big] \\ &= \frac{1}{2}\Big[[r_{i+1} - \underline{a}_*(q^{-1})y_i - \underline{b}(q^{-1})u_i]^2 + \lambda u_i^2\Big], \end{aligned} \tag{2.2.19}$$

where λ is a positive constant. The cost function consists of the predicted squared error at the future time $i+1$ and squared input at the current time i. Hence, minimizing the cost function leads to minimizing the error at the future time $i+1$ with a minimum control input.

To minimize J_{i+1}, we differentiate with respect to u_i and set the result to zero:

$$\alpha_3[\underline{a}_*(q^{-1})y_i + \underline{b}(q^{-1})u_i - r_{i+1}] + \lambda u_i^2 = 0. \tag{2.2.20}$$

From this, we have the following control law:

$$u_i = \frac{\alpha_3[r_{i+1} - \underline{a}_*(q^{-1})y_i - \alpha_4(q^{-1})u_{i-1}]}{\alpha_3^2 + \lambda}. \tag{2.2.21}$$

Now, let us examine the closed loop system associated with the control law (2.2.21). With (2.2.17), (2.2.20) can be rewritten as

$$\alpha_3[y_{i+1} - r_{i+1}] + \lambda u_i = 0. \tag{2.2.22}$$

Multiply this by $\underline{b}(q^{-1})$. Then,

$$\alpha_3[\underline{b}(q^{-1})y_{i+1} - \underline{b}(q^{-1})r_{i+1}] + \lambda \underline{b}(q^{-1})u_i = 0. \tag{2.2.23}$$

With (2.2.14), (2.2.23) becomes

$$[\underline{b}(q^{-1}) + \frac{\lambda}{\alpha_3}\underline{a}(q^{-1})]y_{i+1} = \underline{b}(q^{-1})r_{i+1}. \tag{2.2.24}$$

Therefore, the characteristics of the control law depend on the zeros of $[\underline{b}(q^{-1}) + \frac{\lambda}{\alpha_3}\underline{a}(q^{-1})]$, the poles of the closed loop system. The positions of the zeros dominate stability and performance such as the transient response and steady state error. We can stabilize the system when the zeros of $\underline{b}(q^{-1})$ lie within unit circle around the origin. This means that sometimes we cannot obtain stability partly because we have only one free parameter λ. We may have some additional free parameters by replacing the input u_i with a filtered input in the cost function (2.2.19). Even in this case, to guarantee stability there should be no common unstable zeros between $\underline{a}(q^{-1})$ and $\underline{b}(q^{-1})$. When we apply the closed loop pole assignment, we can also lift the limitation in the number of free parameters. However, $\underline{a}(q^{-1})$ and $\underline{b}(q^{-1})$ should satisfy a certain condition to place poles in desired locations. For more information, read reference[2.7].

2.2.4 Concluding Remarks

We have derived an on-line parameter estimator. The underlying assumption for derivation of the estimator is that the true values of parameters are constant. This assumption is also required to derive other parameter estimators. Moreover, the sequences of applied inputs must be persistently excited to guarantee convergence of estimated parameters to the true values. In robot dynamics, the parameters are time-varying since the nonlinear dynamics is linearized around operating points. Hence, to apply a parameter estimator to robot control, we need to assume that the parameters are quasi-time-invariant. This implies "very slow motion." Hence, in reality, a parameter estimator can not keep up with rapid changes in time-varying parameter values. Faster motion causes larger parameter estimation errors. Furthermore, "slow motion" of a robot would be contradictory to the condition of persistent excitation. Therefore, estimated values of parameters always carry estimation errors. Since we design a control law based on these

estimated values of parameters, the performance obtained with the "Self-Tuning" method in robot control could be unsatisfactory.

2.3 Model Reference Method

The steepest descent method is rarely applied to adaptive control because a separate stability analysis is required. Hence in this section, we focus on Lyapunov's second method and Popov's hyperstability theory. Application of these stability theories is not limited to linear time-invariant systems: they can be applied to nonlinear coupled time-varying systems. These theories provide some sufficient conditions for stability of a given system. The main idea is to use the sufficient condition to stabilize the error dynamics associated with the system. Then as a by-product of stabilization, a control law is produced. Since the sufficient condition is not unique, there may exist many stabilizing control laws for a given system, the performances of which vary widely. Since these stability theories deal with only stability, there is no standard way of judging the performance such as the transient behavior of a control law.

Here we briefly review these stability theories, and their use in the design of new control laws for a spring-mass-damper system having a single degree of freedom.

2.3.1 Stability Theories

2.3.1.1 Lyapunov's Second Method[2.55]

Consider a nonlinear time-varying differential equation representing the behavior of a system having $\hat{m}$ degrees of freedom,

$$\dot{x} = f(t, x(t)), \quad \forall\, t \geq 0, \tag{2.3.1}$$

where x is the $\hat{m}\times 1$ vector, assuming that the origin is an equilibrium point at time t_0, i.e., $f(t,0) = 0, \quad \forall\, t \geq t_0$.

Definition: The equilibrium point 0 at time t_0 of (2.3.1) is said to be *stable*

at time t_0 if, for each finite $\epsilon > 0$, there exists a $\delta(t_0, \epsilon) > 0$ such that

$$\|x(t_0)\| < \delta(t_0, \epsilon) \quad \Longrightarrow \quad \|x(t)\| < \epsilon, \quad \forall\, t \geq t_0,$$

where $\|x\| = \sqrt{x^T x}$.

Definition: The equilibrium point 0 at time t_0 is *asymptotically stable* at time t_0 if (i) it is stable at time t_0, and (ii) there exists a positive number $\delta_1(t_0)$ such that

$$\|x(t_0)\| < \delta_1(t_0) \quad \Longrightarrow \quad \lim_{t \to \infty} \|x(t)\| = 0.$$

That is, the system eventually reaches its equilibrium condition.

Theorem: The equilibrium point 0 at time t_0 of (2.3.1) is *stable* if there exists a continuous differentiable function v for (2.3.1) such that

(i) $v(x) \geq 0$,

(ii) $\dot{v}(x) \leq 0, \quad \forall\, t \geq t_0$.

Theorem: The equilibrium point 0 at time t_0 of (2.3.1) is *asymptotically stable* over the interval $[t_0, \infty)$ if there exists a continuous differentiable function v for (2.3.1) such that

(i) $v(x) > 0, \quad \forall\, x \neq 0$ and $v(0) = 0$,

(ii) $\dot{v}(x) < 0, \quad \forall\, x \neq 0$.

The function $v(x)$ satisfying the requirements in these two theorems is called a *Lyapunov function.* The Lyapunov function is not unique for a given system. Lyapunov's direct method gives only a sufficient condition for the stability of a given system. That is, one's inability to find a satisfactory Lyapunov function *does not mean* that the system is *unstable.*

Theorem: Consider a linear system

$$\dot{x} = Ax, \qquad x(0) = x_0,$$

where A is a $\hat{m} \times \hat{m}$ system matrix. The necessary and sufficient conditions that

the linear system is *asymptotically stable* are that there exist $P = P^T > 0$ and $Q = Q^T > 0$ such that

$$A^T P + PA = -Q. \tag{2.3.2}$$

For proofs of these theorems, see references [2.55] and [2.56].

2.3.1.2 Popov's Hyperstability Theory[2.22]

Consider a nonlinear time-varying feedback system which consists of (i) a linear part described by the following state equations:

$$\begin{aligned} \dot{x} &= Ax + Bu = Ax - Bw, \\ z &= Cx, \end{aligned} \tag{2.3.3}$$

and (ii) a nonlinear time-varying part described by

$$u = -w, \tag{2.3.4}$$

$$w = g(z(\tau), t), \quad 0 < \tau \leq t, \tag{2.3.5}$$

where x is the $\hat{m}\times 1$ state vector; $u{=}{-}w$ and z are the $\check{m}\times 1$ input and output vectors respectively; $g(z(\tau), t)$ is the $\check{m}\times 1$ nonlinear time-varying vector function which is bounded for bounded z and t; A, B, and C are the $\hat{m}\times\hat{m}$ system matrix, the $\hat{m}\times\check{m}$ input matrix, and the $\check{m}\times\hat{m}$ output matrix respectively; (A,B) is completely controllable; and (C,A) is completely observable. Note that the nonlinear time-varying part is confined in w. The schematic diagram for this system is shown in Figure 2.2.

Definition: The feedback system represented by (2.3.3), (2.3.4) and (2.3.5) is *hyperstable* if there exist finite constants $\delta \geq 0$ and $\gamma \geq 0$ such that

$$\|x(t)\| < \delta\|x(0)\| + \gamma, \qquad \forall\, t \geq 0, \quad \delta > 0, \quad \gamma \geq 0.$$

That is, $x(t)$ is bounded for all $t \geq 0$.

Definition: The feedback system (2.3.3), (2.3.4) and (2.3.5) is *asymptotically hyperstable* if it is hyperstable and in addition

$$\lim_{t\to\infty} \|x(t)\| = 0.$$

That is, the state $x(t)$ not only is bounded but also converges asymptotically to zero.

Theorem: The feedback system (2.3.3), (2.3.4) and (2.3.5) is *asymptotically hyperstable* if

(i) the system (2.3.3) is strictly positive real; the necessary and sufficient condition for this is given by the Kalman-Yakubovitch-Popov lemma.

(ii) the feedback block satisfies the following inequality

$$\eta(0,t) = \int_0^t w^T z d\tau \geq -\gamma_0^2, \qquad \forall\, t \geq 0, \quad \text{and} \quad \infty > \gamma_0 \geq 0. \tag{2.3.6}$$

Kalman-Yakubovitch-Popov lemma: The system (2.3.3) is strictly positive real if and only if there exist Q and P such that

$$A^T P + PA = -Q, \qquad P = P^T > 0, \quad Q = Q^T > 0, \tag{2.3.7}$$

and

$$B^T P = C. \tag{2.3.8}$$

For a proof, see reference[2.22].

2.3.2 Application of Stability Theories to Design of Adaptive Control Laws

The stability theories due to Lyapunov and Popov can be used to determine whether a given system is (asymptotically) stable or not. Conversely, with these stability theories a given system can be stabilized by selecting appropriate compensators which can be freely set to meet the stability criteria.

Here we will discuss a prototype problem as an example of the procedure. With the stability theories we will design new model-based parameter-adaptive

control laws which guarantee that the output of the spring-mass-damper system follows that of a reference model. In other words, we will stabilize the "model-following error."

2.3.2.1 Design of Control Laws Using Lyapunov's Second Method

Design Procedure:

(i) Define an appropriate lower-bounded Lyapunov function v for a given system which contains some free parameters.

(ii) Take the time-derivative of the Lyapunov function v along the trajectories of the system.

(iii) Enforce $\dot{v} \leq 0$ using the free parameters.

Consider the same system we have worked with in the previous section:

$$m\ddot{y} + c\dot{y} + ky = u, \tag{2.3.9}$$

where y is the output and u is the input.

Define a reference model which has desirable characteristics such as guaranteed stability and moderate transient behavior. The dynamic equation for this model is

$$\ddot{y}_m + \kappa_1 \dot{y}_m + \kappa_2 y_m = r, \tag{2.3.10}$$

where r and y_m are the reference input and output of the reference model respectively; κ_1 and κ_2 are the positive constants whose values are chosen to give the desired characteristics.

The objective in this section is to select a control input u such that y, the actual output of the plant, is driven asymptotically to y_m, the output of the reference model.

Let us select a control law for the system (2.3.9) as

$$u = k_a \ddot{y}_m + k_v \dot{e} + k_p e + \bar{u}, \tag{2.3.11}$$

where the model-following error e is defined as

$$e = y_m - y; \tag{2.3.12}$$

$\bar{u}$ is a dynamics compensator to be chosen later; $k_a (m > k_a > 0)$, $k_v > 0$, and $k_p > 0$ are the acceleration, velocity, and position gains respectively.

Note that the reference input r is not fed into the plant. That is, the reference model is serially connected to the plant, while usually in the literature of adaptive control, the model is collaterally connected. However, the objective is the same: to drive the model following error asymptotically to zero. In our case, we do not need to use a reference model at all if a tractable trajectory (reference input) is provided, as in robot control. The block diagram for the control system is given in Figure 2.3.

From (2.3.9), and (2.3.11) we have

$$k_a \ddot{e} + k_v \dot{e} + k_p e = (m - k_a)\ddot{y} + d\dot{y} + ky - \bar{u}. \tag{2.3.13}$$

We rewrite this in the following state space form:

$$\dot{\underline{x}} = A\underline{x} + b_* \Big((m - k_a)\ddot{y} + d\dot{y} + ky - \bar{u} \Big), \tag{2.3.14}$$

where $\underline{x}$ is the state vector of the following form:

$$\underline{x}^T = (e,\ \dot{e}); \tag{2.3.15}$$

$$A = \begin{pmatrix} 0 & 1 \\ -k_p/k_a & -k_v/k_a \end{pmatrix}; \tag{2.3.16}$$

and

$$b_*^T = (0,\ 1/k_a). \tag{2.3.17}$$

Now define a Lyapunov function which is lower bounded as

$$v = \frac{1}{2}\Big(\underline{x}^T P \underline{x} + \frac{1}{\beta_1}(m - k_a)\zeta^2 + \frac{1}{\beta_2}(m - k_a - m_e)^2 + \frac{1}{\beta_3}(d - d_e)^2 + \frac{1}{\beta_4}(k - k_e)^2 \Big), \tag{2.3.18}$$

where β_i $(i = 1,2,3,4)$ is the positive constant; $(m - k_a) > 0$; m_e, d_e, and k_e respectively denote the estimated values of m, d, and k computed with an adaptation rule to be selected later; ζ is an auxiliary signal to be used if necessary; according to the theorem (2.3.2), P is to be chosen such that

$$A^T P + PA = -Q, \qquad P = P^T > 0, \quad Q = Q^T > 0. \tag{2.3.19}$$

In equation (2.3.19) we need to choose Q and solve for P.

Note that m_e, d_e, k_e and ζ are the free parameters in the Lyapunov function v, which will be used to enforce $\dot{v} \leq 0$. We include the estimated parameters m_e, d_e, and k_e in v so as to derive an adaptation rule for these parameters, which will be used for dynamics compensation.

To stabilize the system (2.3.14), we will make $\dot{v}$, the time-derivative of the Lyapunov function, non-positive by using the free parameters in the Lyapunov function. Differentiate (2.3.18) with respect to time to find the time-derivative of v along the trajectories of (2.3.14):

$$\begin{aligned}\dot{v} = &- \underline{x}^T Q \underline{x} + z\Big((m - k_a)\ddot{y} + d\dot{y} + ky - \bar{u}\Big) + \frac{1}{\beta_1}(m - k_a)\zeta\dot{\zeta} \\ &- \frac{1}{\beta_2}(m - k_a - m_e)\dot{m}_e - \frac{1}{\beta_3}(d - d_e)\dot{d}_e - \frac{1}{\beta_4}(k - k_e)\dot{k}_e,\end{aligned} \tag{2.3.20}$$

where

$$z \equiv (p_2 e + p_3 \dot{e})/k_a \equiv \rho_1(\dot{e} + \rho_2 e) \tag{2.3.21}$$

with

$$P = \begin{pmatrix} p_1 & p_2 \\ p_2 & p_3 \end{pmatrix} > 0.$$

Hence $\rho_1 = p_3/k_a$ and $\rho_2 = p_2/p_3$. Here we have assumed that m, d, and k, the parameters of the dynamics, are constant. Now try two strategies.

(i) Design of a control law without the auxiliary signal ζ (i.e., $\frac{1}{\beta_1} = 0$)

The first term of (2.3.20) is negative definite and the rest of them are sign-indefinite. Hence one of the ways of guaranteeing $\dot{v} \leq 0$ is to cancel out all

the sign-indefinite terms. Since we have free parameter $\bar{u}$, we can create some common factors to cancel out the sign-indefinite β_i terms. Therefore, we choose the dynamics compensator $\bar{u}$ as

$$\bar{u} = m_e\ddot{y} + d_e\dot{y} + k_e y. \tag{2.3.22}$$

Then,

$$\begin{aligned}
\dot{v} = & - \underline{x}^T Q \underline{x} + z\Big((m - k_a - m_e)\ddot{y} + (d - d_e)\dot{y} + (k - k_e)y\Big) \\
& - \frac{1}{\beta_2}(m - k_a - m_e)\dot{m}_e - \frac{1}{\beta_3}(d - d_e)\dot{d}_e - \frac{1}{\beta_4}(k - k_e)\dot{k}_e \\
= & - x^T Q x + (z\ddot{y} - \frac{1}{\beta_2}\dot{m}_e)(m - k_a - m_e) \\
& + (z\dot{y} - \frac{1}{\beta_3}\dot{d}_e)(d - d_e) + (zy - \frac{1}{\beta_4}\dot{k}_e)(k - k_e).
\end{aligned} \tag{2.3.23}$$

The first term of (2.3.23) is negative, because Q is positive definite. Then, to guarantee $\dot{v} \leq 0$, we choose

$$\begin{aligned}
\dot{m}_e &= \beta_2 z\ddot{y}, \\
\dot{d}_e &= \beta_3 z\dot{y}, \\
\dot{k}_e &= \beta_4 zy.
\end{aligned} \tag{2.3.24}$$

From (2.3.11), (2.3.22), and (2.3.24), we have the following adaptive control law:

$$u = k_a\ddot{y}_m + k_v\dot{e} + k_p e + m_e\ddot{y} + d_e\dot{y} + k_e y; \tag{2.3.25}$$

with the adaptation rule:

$$\begin{aligned}
m_e &= \beta_2 \int_0^t z\ddot{y}d\tau + m_e(0), \\
d_e &= \beta_3 \int_0^t z\dot{y}d\tau + d_e(0),
\end{aligned}$$

$$k_e = \beta_4 \int_0^t zyd\tau + k_e(0). \tag{2.3.26}$$

Choice of (2.3.24) ensures $\dot{v} \leq 0$. Hence Lyapunov's second method guarantees that the system (2.3.14) is stable. Since $\dot{v} = 0 \Rightarrow \dot{e} = e = 0$, the system is asymptotically stable.

Note that this control law requires measurement of $\ddot{y}$. This causes no serious problem in this case since we can use linear accelerometers. However, sometimes in practice we need to avoid measuring acceleration signal. For example, measuring angular acceleration causes difficulties. We can avoid this problem using the auxiliary signal ζ.

(ii) Design of a control law using the auxiliary signal ζ

Note that $\ddot{y}$ and $\dot{\zeta}$ in (2.3.20) have the common coefficient $(m - k_a)$, and that from (2.3.21)

$$\dot{z}/\rho_1 = \ddot{y}_m - \ddot{y} + \rho_2\dot{e}. \tag{2.3.27}$$

Hence, to remove $\ddot{y}$ in (2.3.20), we set $\zeta = z$ and $\beta_1 = \rho_1$. Then, (2.3.20) becomes

$$\begin{aligned}\dot{v} = &- \underline{x}^T Q \underline{x} + z\Big((m - k_a)(\ddot{y}_m + \rho_2\dot{e}) + d\dot{y} + ky - \bar{u}\Big) \\ &- \frac{1}{\beta_2}(m - k_a - m_e)\dot{m}_e - \frac{1}{\beta_3}(d - d_e)\dot{d}_e - \frac{1}{\beta_4}(k - k_e)\dot{k}_e.\end{aligned} \tag{2.3.28}$$

Similar to (2.3.22), let us choose the dynamics compensator as

$$\bar{u} = m_e(\ddot{y}_m + \rho_2\dot{e}) + d_e\dot{y} + k_e y. \tag{2.3.29}$$

Then,

$$\begin{aligned}\dot{v} = &- \underline{x}^T Q \underline{x} + z\Big((m - k_a - m_e)(\ddot{y}_m + \rho_2\dot{e}) + (d - d_e)\dot{y} + (k - k_e)y\Big) \\ &- \frac{1}{\beta_2}(m - k_a - m_e)\dot{m}_e - \frac{1}{\beta_3}(d - d_e)\dot{d}_e - \frac{1}{\beta_4}(k - k_e)\dot{k}_e \\ = &- \underline{x}^T Q \underline{x} + \Big(z(\ddot{y}_m + \rho_2\dot{e}) - \frac{1}{\beta_2}\dot{m}_e\Big)(m - k_a - m_e)\end{aligned}$$

$$+ (z\dot{y} - \frac{1}{\beta_3}\dot{d}_e)(d - d_e) + (zy - \frac{1}{\beta_4}\dot{k}_e)(k - k_e). \tag{2.3.30}$$

Therefore, to enforce the requirement $\dot{v} \leq 0$, we choose

$$\begin{aligned} \dot{m}_e &= \beta_2 z(\ddot{y}_m + \rho_2 \dot{e}), \\ \dot{d}_e &= \beta_3 z\dot{y}, \\ \dot{k}_e &= \beta_4 zy. \end{aligned} \tag{2.3.31}$$

From (2.3.11), (2.3.29), and (2.3.31), we have the following adaptive control law:

$$u = k_a\ddot{y}_m + k_v\dot{e} + k_p e + m_e(\ddot{y}_m + \rho_2\dot{e}) + d_e\dot{y} + k_e y, \tag{2.3.32}$$

with the adaptation rule:

$$\begin{aligned} m_e &= \beta_2 \int_0^t z(\ddot{y}_m + \rho_2\dot{e})d\tau + m_e(0), \\ d_e &= \beta_3 \int_0^t z\dot{y}d\tau + d_e(0), \\ k_e &= \beta_4 \int_0^t zyd\tau + k_e(0). \end{aligned} \tag{2.3.33}$$

Choice of (2.3.31) ensures $\dot{v} \leq 0$. Hence Lyapunov's second method guarantees that the system (2.3.14) is stable. Since $\dot{v} = 0 \Rightarrow \dot{e} = e = 0$, the system is asymptotically stable. Note that the adaptation law is a by-product of the procedure followed to guarantee stability.

The Lyapunov function is not unique for a given system. Hence the choices of control laws to guarantee $\dot{v} \leq 0$ are not unique. The forms of the control and adaptation laws depend on what Lyapunov function v is used and on how the time-derivative of the Lyapunov function $\dot{v}$ is constructed to guarantee $\dot{v} \leq 0$. Therefore, there could be many stabilizing control laws for a given system.

The schematic diagram for the proposed control and adaptation laws is given in Figure 2.3.

2.3.2.2 Design of Control Laws using Hyperstability Theory

Design Procedure:

(i) Separate the system to be controlled so that the nonlinear time-varying part becomes an input to the linear part. See equations (2.3.3), (2.3.4), and (2.3.5).

(ii) Define a new output z such that the linear part of the system becomes strictly positive real. Use the Kalman-Yakubovitch-Popov lemma in (2.3.8).

(iii) Close the loop of the system by assuming $u = g(z)$.

(iv) Choose plausible control and adaptation laws, and check whether these satisfy the inequality condition (2.3.6).

Therefore, this method involves "search" for appropriate control and adaptation laws. Here, however, we need not go through the search since we have already designed two control and adaptation laws. We have only to show the adaptive control laws designed with Lyapunov's second method satisfy the hyperstability theory.

Here we consider the same system to control (spring-mass-damper system).

First, we separate the system. This has been done already in (2.3.14):

$$\dot{\underline{x}} = A\underline{x} + b_* u, \tag{2.3.34}$$

where $b_*^T = (0,\ 1/k_a)$, and

$$u \equiv -w = (m - k_a)\ddot{y} + d\dot{y} + ky - \bar{u}. \tag{2.3.35}$$

Secondly, let us define z, a new output of (2.3.34), such that the linear part becomes strictly positive real. We can guarantee this by using the Kalman-Yakubovitch-Popov lemma in (2.3.8). That is, we choose

$$z \equiv c^T \underline{x} = p_2 e + p_3 \dot{e} \equiv \rho_1(\dot{e} + \rho_2 e), \tag{2.3.36}$$

where $c^T = b_*^T P$ with $A^T P + PA = -Q,\ \ P = P^T > 0,\ \ Q = Q^T > 0$; $\rho_1 = p_3/k_a$ and $\rho_2 = p_2/p_3$.

Thirdly, we close the loop:

$$u = -w = -f(z). \tag{2.3.37}$$

This means that $\bar{u}$ in (2.3.35) must be functions of z.

Finally, we need to select control and adaptation laws, and test whether the selected control law with the corresponding adaptation law satisfies the inequality condition (2.3.6). For this system (2.3.6) becomes

$$\eta(0,t_1) = \int_0^{t_1} z\Big(\bar{u} - (m-k_a)\ddot{y} - d\dot{y} - ky\Big)dt. \tag{2.3.38}$$

(i) We will show that the first adaptive control law designed with Lyapunov's method satisfies the inequality (2.3.6). The control and adaptation laws (2.3.22) and (2.3.26) are rewritten as

$$\bar{u} = m_e\ddot{y} + d_e\dot{y} + k_e y, \tag{2.3.39}$$

where

$$\begin{aligned} m_e &= \beta_2 \int_0^t z\ddot{y}d\tau + m_e(0), \\ d_e &= \beta_3 \int_0^t z\dot{y}d\tau + d_e(0), \\ k_e &= \beta_4 \int_0^t zyd\tau + k_e(0). \end{aligned} \tag{2.3.40}$$

With (2.3.38), (2.3.39), and (2.3.40), we check the inequality condition (2.3.6):

$$\begin{aligned} \eta(0,t_1) = \int_0^{t_1} z\Big(&\beta_2\Big(\int_0^t z\ddot{y}d\tau + m_e(0) - m + k_a\Big)\ddot{y} \\ &+ \Big(\beta_3\int_0^t z\dot{y}d\tau + d_e(0) - d\Big)\dot{y} + \Big(\beta_4\int_0^t zyd\tau + k_e(0) - k\Big)y\Big)dt. \end{aligned} \tag{2.3.41}$$

For simplicity, we define

$$m_o = (m_e(0) - m + k_a)/\beta_2,$$
$$d_o = (d_e(0) - d)/\beta_3,$$
$$k_o = (k_e(0) - k)/\beta_4. \tag{2.3.42}$$

Then,

$$\begin{aligned}\eta(0,t_1) = &\int_0^{t_1} \Big(\beta_2 z(\int_0^t z\ddot{y}d\tau - m_o)\ddot{y} + \beta_3 z(\int_0^t z\dot{y}d\tau - d_o)\dot{y} \\ &+ \beta_4 z(\int_0^t zyd\tau - k_o)y\Big)dt \\ =&\frac{1}{2}\Big(\beta_2(\int_0^{t_1} z\ddot{y}dt - m_o)^2 + \beta_3(\int_0^{t_1} z\dot{y}dt - d_o)^2 \\ &+ \beta_4(\int_0^{t_1} zydt - k_o)^2 - \beta_2 m_o^2 - \beta_3 d_o^2 - \beta_4 k_o^2\Big) \\ \geq &-\frac{1}{2}(\beta_2 m_o^2 + \beta_3 d_o^2 + \beta_4 k_o^2),\end{aligned} \tag{2.3.43}$$

where we have used the following identity:

$$\int_0^{t_1} \xi \int_0^t \xi d\tau dt = \frac{1}{2}(\int_0^{t_1} \xi dt)^2, \qquad \forall\, t_1 \geq 0 \quad \& \quad \text{integrable } \xi. \tag{2.3.44}$$

Since $\bar{u}$ given by (2.3.39) and (2.3.40) satisfies the inequality condition, these constitute an adaptive control law which guarantees the asymptotic stability of the model-following error e.

(ii) To show that the second control law satisfies the inequality condition, we modify the equation (2.3.38) using the fact:

$$\dot{z}/\rho_1 = (\ddot{e} + \rho_2\dot{e}) = (\ddot{y}_m - \ddot{y} + \rho_2\dot{e}). \tag{2.3.45}$$

Then, (2.3.38) becomes

$$\eta(0,t_1) = \int_0^{t_1} z\Big(\bar{u} - (m-k_a)(\ddot{y}_m + \rho_2\dot{e} - \dot{z}/\rho_1) - d\dot{y} - ky\Big)dt$$
$$= \int_0^{t_1} z\Big(\bar{u} - (m-k_a)(\ddot{y}_m + \rho_2\dot{e}) - d\dot{y} - ky\Big)dt + \frac{m-k_a}{2\rho_1}z^2\Big|_0^{t_1}. \tag{2.3.46}$$

Now, consider the second control law (2.3.29):

$$\bar{u} = m_e(\ddot{y}_m + \rho_2\dot{e}) + d_e\dot{y} + k_e y \tag{2.3.47}$$

with the following adaptation law (2.3.33):

$$m_e = \beta_2 \int_0^t z(\ddot{y}_m + \rho_2\dot{e})d\tau + m_e(0),$$
$$d_e = \beta_3 \int_0^t z\dot{y}d\tau + d_e(0),$$
$$k_e = \beta_4 \int_0^t zyd\tau + k_e(0). \tag{2.3.48}$$

Then, with (2.3.46), (2.3.47), and (2.3.48), we check the inequality condition (2.3.6):

$$\eta(0,t_1) = \int_0^{t_1} z\Big(\beta_2(\int_0^t z(\ddot{y}_m + \rho_2\dot{e})d\tau + m_e(0) - m + k_a)(\ddot{y}_m + \rho_2\dot{e})$$
$$+ \beta_3(\int_0^t z\dot{y}d\tau + d_e(0) - d)\dot{y} + \beta_4(\int_0^t zyd\tau + k_e(0) - k)y\Big)dt$$
$$+ \frac{m-k_a}{2\rho_1}z^2\Big|_0^{t_1}. \tag{2.3.49}$$

Using the definition (2.3.42), we have

$$\eta(0,t_1) = \int_0^{t_1} \Big(\beta_2 z(\int_0^t z(\ddot{y}_m + \rho_2\dot{e})d\tau - m_o)(\ddot{y}_m + \rho_2\dot{e})$$
$$+ \beta_3 z(\int_0^t z\dot{y}d\tau - d_o)\dot{y} + \beta_4 z(\int_0^t zyd\tau - k_o)y\Big)dt + \frac{m-k_a}{2\rho_1}z^2\Big|_0^{t_1}$$

$$
\begin{aligned}
=&\frac{1}{2}\Big(\beta_2(\int_0^{t_1} z(\ddot{y}_m+\rho_2\dot{e})dt-m_o)^2+\beta_3(\int_0^{t_1} z\dot{y}dt-d_o)^2 \\
&+\beta_4(\int_0^{t_1} zydt-k_o)^2-\beta_2 m_o^2-\beta_3 d_o^2-\beta_4 k_o^2\Big)+\frac{m-k_a}{2\rho_1}z^2\Big|_0^{t_1} \\
\geq&-\frac{1}{2}(\beta_2 m_o^2+\beta_3 d_o^2+\beta_4 k_o^2)+\frac{m-k_a}{2\rho_1}z^2\Big|_0^{t_1} \\
\geq&-\frac{1}{2}(\beta_2 m_o^2+\beta_3 d_o^2+\beta_4 k_o^2)-\frac{m-k_a}{2\rho_1}z^2(0), \qquad (2.3.50)
\end{aligned}
$$

where we have used that fact that $(m-k_a)>0$. If the initial model-following errors $\dot{e}$ and e are bounded, $z(0)$ is bounded. Therefore, (2.3.50) shows that the second adaptive control law satisfies the inequality (2.3.6) and asymptotic stability as well.

As we pointed out at the beginning, the hyperstability theory provides only sufficient conditions. Hence a stabilizing control law for a given system is not unique.

2.3.3 Concluding Remarks

We have described how Lyapunov's and Popov's stability theories can be used to design two new adaptive control laws. For simplicity, we have considered a linear SISO (single-input single-output) system. Extension to nonlinear MIMO (multi-input multi-output) systems can be readily achieved as long as the mass (matrix) m is positive definite.

It must be emphasized that convergence of the estimated parameters to the true values is not required to guarantee asymptotic stability in the model reference method. This result is in contrast to that obtained with the "self-tuning" method. Of course, the convergence is guaranteed if the input is persistently exited. Furthermore, the self-tuning method uses a linearized system around its operating points. Therefore, the parameters of the system in the self-tuning method must be time-varying if the plant is nonlinear. However, in the (parameter-adaptive) model reference method the parameters are time-invariant if the corresponding nonlinear plant is linear in the time-invariant parameters. This is because this

method can be directly applied to a nonlinear plant without linearization.

Lyapunov's and Popov's stability theories provide only sufficient conditions for stability. Therefore, there may exist many different model reference adaptive control schemes for a given system. The design procedure of a self-tuning scheme consists of system discretization, parameter estimation, and application of linear control theory. None of these are unique. Hence, there may also exist many different self-tuning adaptive control schemes for a given system. However, the underlying principle and the design procedure remain the same.

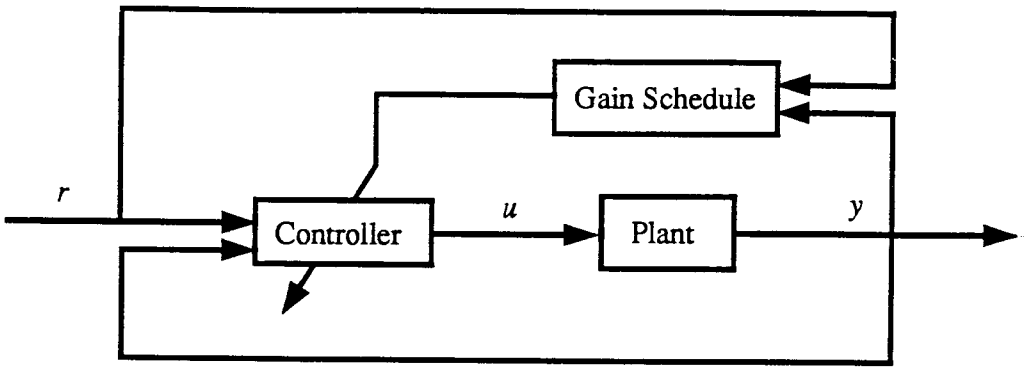

Gain Scheduling Method

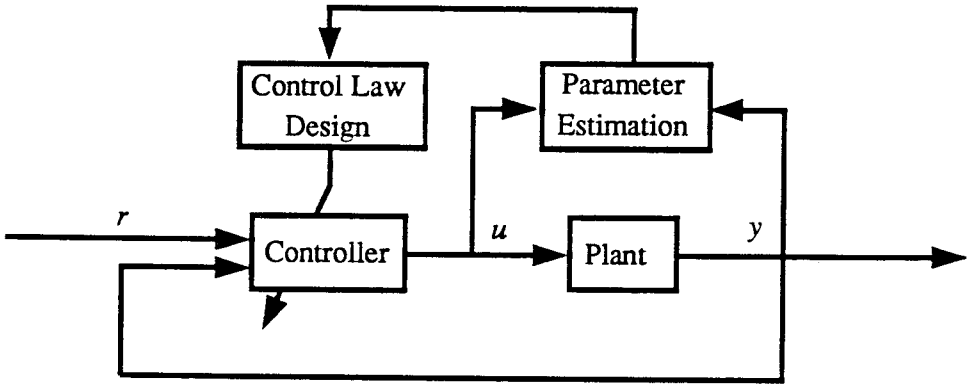

Self-Tuning Method

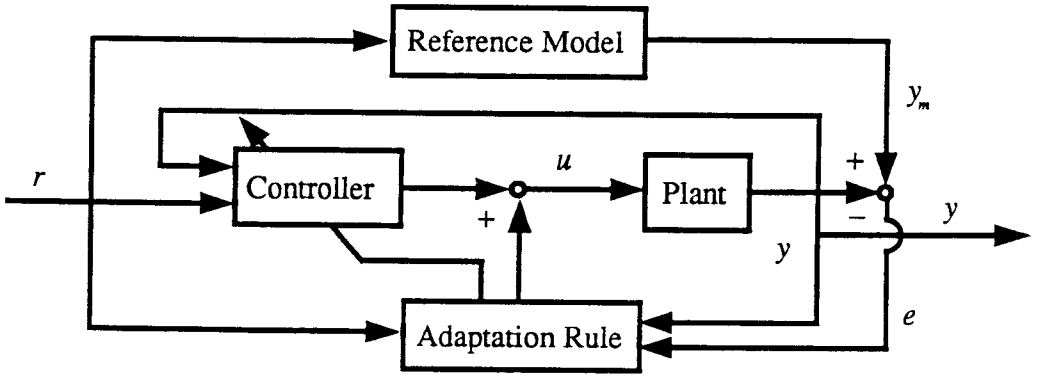

Model Reference Method

Figure 2.1 Block diagrams of various kinds of adaptive control

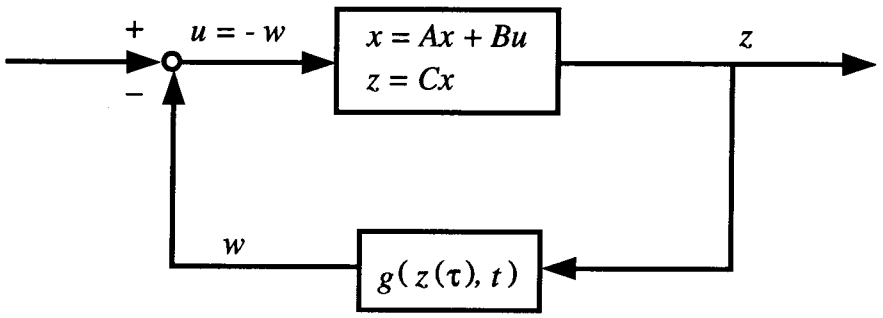

Figure 2.2 A nonlinear time-varying feedback system

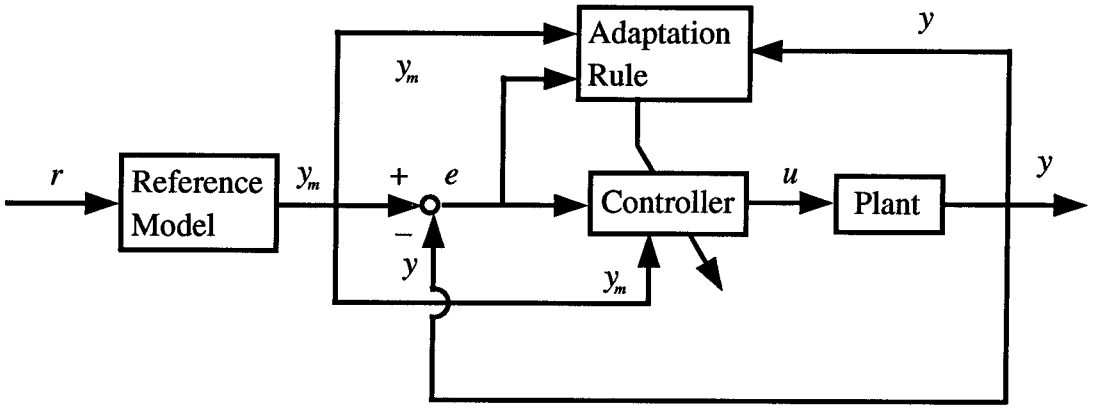

Figure 2.3 Block diagram of a model reference adaptive control system

References

[2.1] Astrom, K. J., *Theory and Applications of Adaptive Control- Survey,* Automatica, Vol. 19, No. 5, pp. 471-486, 1983.

[2.2] Hollars, M. G. and Cannon, Jr. R. H., *Initial Experiments on End-Point Control of a Two-Link Manipulator with Flexible Tendons,* Prec. of ASME Winter Annual Meeting, Fl, November 1985.

[2.3] Hollars, M. G. and Cannon, Jr., R. H., *Experiments on End-Point Control of a Two-Link Robot with Elastic Drive,* Proc of AIAA Guidance, Navigation and Control Conf., pp. 19-27, August 1986.

[2.4] Hollars, M. G., *Experiments in End-Point Control of Manipulators with Elastic Drive,* Ph.D. thesis, Stanford University, Department of Aeronautics and Astronautics, Stanford, CA 94305, May 1988.

[2.5] Uhlik, C. R., *Experiments in High-Performance Nonlinear and Adaptive Control of a Two-Link, Flexible-Drive-Train Manipulator,* Ph.D. thesis, Stanford University, Department of Aeronautics and Astronautics, Stanford, CA 94305, May 1990.

[2.6] Kalman, R. E., *Design of a Self-Optimizing Control System,* Trans. ASME, p. 486, 1958.

[2.7] Goodwin, G. C. and Sin, K. S., *Adaptive Filtering, Prediction, and Control,* Prentice-Hall, Reading, 1984.

[2.8] Harris, C. J. and Billings, S. A., *Self-Tuning and Adaptive Control: Theory and Application,* Peter Peregrinus Ltd., Reading, 1981.

[2.9] Koivo, A. J. and Guo, T. M., *Adaptive Linear Controller for Robotic Manipulators,* IEEE Trans. on Aut. Contr., Vol. AC-28, No. 2, pp. 162-172, 1983.

[2.10] Koivo, A. J., Lewczyk, R. and Chiu, T. H., *Adaptive Path Control of a Manipulator with Visual Information,* IEEE Conference on Robotics, Atlanta, March 1984.

[2.11] Koivo, A. J., *Adaptive Position-Velocity-Force Control of Two Manipulators,*

24th IEEE Conf. on Decision and Control, Fort Lauderdale, Fla., 1985.

[2.12] Koivo, A. J., *Force-Velocity Control with Self-Tuning for Robotic Manipulators,* IEEE Conference on Robotics and Automation, San Francisco, April 1986.

[2.13] Walters, R. G. and Bayoumi, M. M., *Application of a Self-Tuning Pole Placement Regulator to an Industrial Manipulator,* IEEE, Conference on Decision and Control, pp. 323-329, 1982.

[2.14] Leininger, G. G. and Wang , S., *Pole Placement Self-Tuning Control of Manipulators,* IFAC Symposium on Computer Aided Design of Multivariable Technological Systems, West Lafayette, Ind., September 15-17, 1982.

[2.15] Leininger, G. G., *Self-Tuning Control of Manipulators,* International Symposium on Advanced Software in Robotics, Liege, Belgium, May 1983.

[2.16] Leininger, G. G., *Adaptive Control of Manipulators Using Self-Tuning Methods,* Robotics Research, Chap.9 edited by M. Brady and R. Pall, 1984.

[2.17] Backes, P., *Real Time Control with Adaptive Manipulator Control Schemes,* M.S. Thesis, Purdue University, School of Mechanical Engineering, West Lafayette, Ind., December 1984.

[2.18] Backes, P., Leininger, G. G., *Real Time Cartesian Coordinate Hybrid Control of a Puma 560 Manipulator,* IEEE Conference on Robotics and Automation, St. Louis, March 1985.

[2.19] Sundareshan, M. K. and Koenig, M. A., *Decentralized Model Reference Adaptive Control of Robotic Manipulators,* Proceedings, Automatic Control Conference, pp. 44-49, 1985.

[2.20] Kalman, R. E. and Bertram, J. E., *Control System Analysis and Design Via the Second Method of Lyapunov: Part I Continuous-Time Systems, and Part II Discrete-Time Systems,* Journal of Basic Engineering, Trans of ASME, pp. 371-400, June 1960.

[2.21] Narendra, K. S. and Kudva, P., *Stable Adaptive Schemes for System Identification and Control,* IEEE Trans. Man and Cybernetics, Vol. SMC- 4, No. 6, pp. 542-551, November 1974.

[2.22] Landau, Y. D., *Adaptive Control: The Model Reference Approach,* Marcel Dekker Inc., Reading, 1979.

[2.23] Landau, Y. D. and Courtial, B., *Design of Multivariable Adaptive Model Following Control Systems,* Automatica, Vol. 10, pp. 483-494, 1974.

[2.24] Popov, V. M., *Hyperstability of Control Systems,* New York: Springer-Verlay, Reading, 1983.

[2.25] Donalson, D. D. and Leondes, C. T., *A Model Referenced Parameter Tracking Technique for Adaptive Control Systems: Part I The Principle of Adaptation, and Part II Stability Analysis by the Second Method of Lyapunov,* Trans of IEEE on Applications and Industry, Vol. 82, No. 68, pp. 240-262, Sep. 1963.

[2.26] Dubowsky, S. and DesForges, D. F., *The Application of Model-Reference Adaptive Control to Robotic Manipulators,* ASME J. of DSMC, Vol. 101, pp. 193-200, 1979.

[2.27] Dubowsky, S. and Kornbluh, R., *On the Development of High Performance Adaptive Control Algorithms for Robotic Manipulators,* Robotics Research edited by Inoue Hanafusa, pp. 119-126, 1984.

[2.28] Takegaki, M. and Arimoto, S., *An Adaptive Trajectory Control of Manipulators,* Int. J. of Control, Vol. 34, No. 2, pp. 219-230, 1981.

[2.29] Seraji, H., *Direct Adaptive Control of Manipulators in Cartesian Space,* J. of Robotic Systems, Vol. 4, No. 1, pp. 157-178, 1987.

[2.30] Seraji, H., *Decentralized Adaptive Control of Manipulators: Theory, Simulation, and Experimentation,* IEEE Trans. on Robotics and Automation, Vol. 5, No. 2, pp. 183-201, April 1989.

[2.31] Oh, B. J., Jamshidi, M. and Seraji, H., *Decentralized Adaptive Control,* Proc. of IEEE Int. Conf. on Robotics and Automation, pp. 1016-1021, 1988.

[2.32] Gavel, D. T. and Hsia, T. C., *Decentralized Adaptive Control of Robotic Manipulators,* Proc. of IEEE Int. Conf. on Robotics and Automation, pp. 1230-1235, April 1987.

[2.33] Gavel, D. T. and Hsia, T. C., *Decentralized Adaptive Control Experiments*

with the PUMA Robot Arm, Proc. of IEEE Int. Conf. on Robotics and Automation, pp. 1022-1027, 1988.

[2.34] Lim, K. Y. and Eslami, M., *New Controller Design for Robot Manipulator Systems,* Proc., Amer. Contr. Conf., pp. 38-43, June 1985.

[2.35] Lim, K. Y. and Eslami, M., *Adaptive Controller Designs for Robot Manipulator Systems Yielding Reduced Cartesian Error,* IEEE Trans. on Automatic Control, Vol. AC-32, No. 2, pp. 184-187, Feb. 1987.

[2.36] Lim, K. Y. and Eslami, M., *Robust Adaptive Controller Designs for Robot Manipulator Systems,* IEEE J. of Robotics and Automation, Vol. RA-3, No. 1, pp. 54-66, Feb. 1987.

[2.37] Nicosia, S. and Tomei, P., *Model Reference Adaptive Control Algorithms for Industrial Robots,* Automatica, Vol. 20, No. 5, pp. 635-644, 1984.

[2.38] Balestrino, A., De Maria, G. and Sciavicco, L., *An Adaptive Model Following Control for Robotic Manipulators,* ASME J. of DSMC, Vol. 105, pp. 143-151, 1983.

[2.39] Horowitz, R. and Tomizuka, M., *An Adaptive Control Scheme for Mechanical Manipulators - Compensation of Nonlinearity and Decoupling Control,* ASME J. of DSMC, Vol. 108, pp. 127-135, June 1986.

[2.40] Anex, Jr., R. P. and Hubbard, M., *Modeling and Adaptive Control of a Mechanical Manipulator,* ASME. J. of DSMC, Vol. 106, pp. 211-217, Sep. 1984.

[2.41] Craig, J. J., *Adaptive Control of Mechanical Manipulators,* Ph.D. thesis, Stanford University, Department of Electrical Engineering, Stanford, CA 94305, June 1986; Also published by Addison-Wesley

[2.42] Craig, J. J., Hsu, P. and Sastry, S. S., *Adaptive Control of Mechanical Manipulators,* Proc. IEEE Conf. on Robotics and Automation, pp. 190-195, 1986.

[2.43] Kabtab, A., *Nonlinear Control of Robotic Manipulators-Hyperstability Approach,* Robotics and Autonomous Systems, Vol. 4, No. 3, pp. 265-274, 1988.

[2.44] Slotine, J. J. E. and Li, W., *On the Adaptive Control of Robot Manipulators,* Proc. ASME Winter Annual Meeting, 1986.

[2.45] Slotine, J. J. E. and Li, W., *Adaptive Manipulator Control: Parameter Convergence and Task-Space Strategies,* Proc. of the 1987 American Control Conference, pp. 828-835, 1987.

[2.46] Slotine, J. J. E. and Li, W., *Adaptive Manipulator Control: A Case Study,* Proc. of the 1987 Int. Conf. on Robotics and Automation, pp. 1392-1400, 1987.

[2.47] Arimoto, A. and Miyazaki, F., *Stability and Robustness of PID Feedback Controller for Robot Manipulators of Sensory Capability,* Robotics Research: The First International Symposium edited by Brady, M. and Paul, R., pp. 783-799, 1984.

[2.48] Peterson, B. B. and Narendra, K. S., *Bounded Error Adaptive Control,* IEEE Trans. on Auto. Contr., Vol. AC-27, pp. 1161-1168, Dec. 1982.

[2.49] Kreisselmeier, G. and Narendra, K. S., *Stable Model Reference Adaptive Control in the Presence of Bounded Disturbances,* IEEE Trans. on Auto. Contr., Vol. AC-27, No. 6, pp. 1169-1175, Dec. 1982.

[2.50] Ioannou, P. A. and Tsakalis, K. S., *A Robust Direct Adaptive Controller,* IEEE Trans. on Auto. Contr., Vol. AC-31, No. 11, pp. 1033-1043, Nov. 1986.

[2.51] Ioannou, P. A. and Kokotovic, P. V., *Instability Analysis and Improvement of Robustness of Adaptive Control,* Automatica, Vol. 20, No. 5, pp. 583-594, 1984.

[2.52] Ioannou, P. A. and Kokotovic, P. V., *Robust Redesign of Adaptive Control,* IEEE Trans. on Auto. Contr., Vol. AC-29, No. 3, pp. 202-211, March 1984.

[2.53] Narendra, K. S. and Annaswamy, A. M., *A New Adaptive Law for Robust Adaptation Without Persistent Excitation,* IEEE Trans. on Auto. Contr., Vol. AC-32, No. 2, pp. 134-145, Feb. 1987.

[2.54] Franklin, G., F. and Powell, J., D., *Digital Control of Dynamic Systems,* Addison-Wesley, Reading, 1980.

[2.55] Vidyasaga, M., *Nonlinear Systems Analysis,* Prentice-Hall, Inc., 1987

[2.56] Caughey, T. K., *Lecture Notes for AM151,* Caltech, 1986.

Chapter 3

A 2-NORM APPROACH TO ADAPTIVE CONTROL OF ROBOTS

3.1 Introduction

In the previous chapter, we have reviewed the essence of adaptive control with prototype applications to a spring-mass-damper system having one degree of freedom. Now, we are ready to extend our discussion to a more practical problem of parameter-adaptive control of manipulators. The dynamics of a manipulator is nonlinear, coupled, and trajectory dependent. Hence, control of manipulators is one of the most challenging control problems, and has attracted a great deal of attention from the adaptive control community.

In 1979, adaptive control was first applied to trajectory control of manipulators by Dubowsky and DesForges[3.1]. Since then, extensive research has been performed. Earlier applications[3.1-3.11] were simply to apply adaptive schemes developed for linear time-invariant systems to robot control with the assumption that the nonlinear part of the robot dynamics is quasi-time-invariant. Some schemes[3.12-3.15] could obtain stability without this assumption by using chattering signals. However, these signals may excite high-frequency unmodelled dynamics. Adaptive control of robots has gradually progressed up to compensation for the full nonlinear dynamics of robots, so that some recent schemes[3.16-3.18] can guarantee asymptotic stability under some ideal conditions.

In this chapter, the objective is not only to obtain the asymptotic stability but also to improve the transient behavior. To achieve the objective, we combine the loop shaping method, the adaptive control strategy, and the concept of optimal control in harmony to extract the best result; in contrast, each method has been

independently applied to the design of control laws in the existing literature.

In Section 2, we model the system to control from the standard result of the manipulator dynamics. In Section 3, via the loop shaping method, we improve the decoupled PD or PID feedback laws which are the bases for existing adaptive control laws and for controllers for industrial robots, including direct drive arms.

In Section 4, we derive a new stability criterion to integrate the methods of loop shaping, optimal control, and adaptive control into controller design. To improve the transient response we search for compensators in the direction of minimizing a certain quadratic performance index. Then, to guarantee asymptotic stability of the system, we show that the compensators selected through the loop shaping method and the performance index satisfy the new stability criterion. The adaptive compensator consists of two parts: adaptive feedforward compensators (parameter-adaptive compensators) and decoupled feedback adaptive compensators.

3.2 Modelling of A Manipulator to Control

Consider a general robot manipulator having n joints. The dynamic equations including the actuator dynamics are well known in the literature of robot dynamics (e.g., reference[3.19]) and can be written in the following vector form:

$$M(q)\ddot{q} + C(q,\dot{q})\dot{q} + D\dot{q} + D_c\mathrm{sgn}(\dot{q}) + g(q) = u, \qquad (3.2.1)$$

where the following definitions apply:

u : $n\times 1$ input vector;

$q, \dot{q}, \ddot{q}$: $n\times 1$ joint displacement, velocity, and acceleration vector respectively;

M : $n\times n$ effective coupling inertia matrix including payload;

$C\dot{q}$: $n\times 1$ centrifugal and Coriolis force vector;

g : $n\times 1$ gravitational loading vector;

D : $n\times n$ diagonal matrix for viscous damping coefficient;

D_c : $n\times n$ diagonal matrix for friction damping coefficient.

Hereafter, the arguments of the variables will be omitted whenever these are clearly understood.

3.3 Application of Loop Shaping Design

Existing (adaptive) control laws have simply adopted the PD or PID feedback laws as a part of their compensators. The control objective in this section is to reduce tracking errors as much as possible by improving the PD or PID feedback laws via the loop shaping method. Since this method has been established for linear systems in the frequency domain, we need to model the plant as a linear decoupled system; we modify the system (3.2.1) to

$$M_d\ddot{q} + D\dot{q} + d_s = u, \tag{3.3.1}$$

with

$$\begin{aligned} M_d &= \mathrm{diag}(m_1,\ m_2, \cdots, m_n), \\ d_s &= (M - M_d)\ddot{q} + C\dot{q} + D_c\mathrm{sgn}(\dot{q}) + g, \end{aligned} \tag{3.3.2}$$

where m_i is the constant diagonal component of the inertia matrix for the i^{th} joint. Note that the constant decoupled inertia and viscous damping terms of the link and actuator dynamics are modelled as the system to control. Nonlinear or off-diagonal dynamics of the links are considered as disturbances to the system, which are deterministic if all the parameters of the dynamics are known.

We perform the Laplace transformation on the linear decoupled system (3.3.1). Here we define $G_i(s)$, the nominal transfer function of the plant, for each joint as

$$G_i(s) \equiv \frac{Q_i(s)}{U_i(s)} = \frac{1}{m_i s^2 + d_i s}, \tag{3.3.3}$$

where m_i is the i^{th} diagonal component of M_d, d_i is the i^{th} diagonal component of D, and $Q_i(s)$ and $U_i(s)$ are the Laplace transformations of q_i and u_i respectively.

Equation (3.3.1) is a linear decoupled system with the bounded disturbance d_s. Therefore, we can construct a feedback system for each joint as shown in Figure

3.1, where $D_{si}(s)$ is the Laplace transformation of d_{si}, the i^{th} component of d_s; $N_i(s)$ represents the Laplace transformation of the sensor noise; $E_i(s) = R_i(s) - Q_i(s) - N_i(s)$; and $K_i(s)$ is the transfer function of the feedback compensator to be determined later.

3.3.1 Applying Performance Criteria

The purpose of the loop shaping method[3.20] is to optimize the open loop transfer function $L_i(s)$ based on robust stability, disturbance rejection, and sensor noise attenuation, where

$$L_i(s) \equiv K_i(s)G_i(s). \tag{3.3.4}$$

Then, the feedback compensator $K_i(s)$ is readily obtained using equation (3.3.4) since $G_i(s)$ is given. The standard results from the loop shaping method can be summarized as follows:

(a) To reject low-frequency disturbances, increase the low-frequency gain of $L_i(s)$ as much as possible. To attenuate high-frequency sensor noise and to obtain robust stability, reduce the high-frequency gain of $L_i(s)$ as much as possible.

(b) To stabilize the system, increase the phase margin of $L_i(s)$ as much as possible, based on the Nyquist stability criterion. Since a greater slope of $|L_i(s)|$ near the crossover frequency provides a smaller phase margin of $L_i(s)$, the slope of $|L_i(s)|$ around the crossover frequency should not be less than that of $(\omega_c/s)^2$, which has zero phase margin, where ω_c is the crossover frequency. Thus, a rule of thumb is that $L_i(s)$ is selected to be approximately ω_c/s near the crossover frequency.

In a sampled data system, computations for the control can not be achieved instantaneously. Therefore, information acquired at one sampling time is used to compute the input to the system at the next sampling time. This causes one sampling delay, which can be converted to an additional phase lag. Therefore, we include this additional lag in the phase margin above. From the geometry of a sinusoidal wave and the sampling action sketched in Figure 3.2, $\arg L_s$, the maximum additional phase lag due to the sampling, is ωt_s radians, where t_s is the

sampling time in seconds. In other words,

$$0 \leq \arg L_s \leq \omega t_s \quad \text{(rad)}, \qquad \omega \leq \frac{\omega_s}{2} = \pi/t_s. \tag{3.3.5}$$

Hence, the crossover frequency must be limited by the sampling frequency.

Based on the arguments above, a general procedure for optimizing $L_i(s)$ can be visualized in Figure 3.3.

3.3.2 Design of The Feedback Controller

With an optimally designed $L_i(s)$, $K_i(s)$, the controller, can be obtained by

$$K_i(s) = G_i(s)^{-1} L_i(s), \tag{3.3.6}$$

where the plant $G_i(s)$ is stable and minimum phase.

When we carry out the procedures and considerations above, we have the following form for the feedback compensators:

$$K_i(s) = \alpha_i \delta_i \frac{(s+\beta_i)(s+\kappa_i)}{(s+\gamma_i)(s+\delta_i)}, \tag{3.3.7}$$

where constants are chosen so that $\alpha_i > 0$ and $\delta_i > \beta_i > \kappa_i > \gamma_i \geq 0$.

Note that $K_i(s)$ includes an integrator when γ_i is chosen to be zero. It is expected that the performance of the feedback law (3.3.7) designed here is better than those of PD, PI, or PID control laws.

3.4 New Approach to the Design of Adaptive Control Laws

In this section, we derive a stability criterion with which we can absorb the improved feedback law in the previous section into adaptive control. This stability criterion is applicable not only to linear systems but also to nonlinear coupled systems. Via the stability criterion, we add dynamics compensators to the improved feedback law in order to compensate for both the link and actuator dynamics so that the total control system achieves asymptotic stability of tracking error. The design procedure with the new stability criterion includes search for

compensators in the direction of minimizing a quadratic performance index to improve the transient behavior.

Since we want to compensate for the system dynamics, in this section, we will use the original nonlinear coupled system (3.2.1) throughout our discussion. For the stability analysis, we assume that (1) uncertainties in (3.2.1) are confined in the parameters of the dynamics; and (2) there exist no sensor noise, disturbances, and unmodelled dynamics. In the next chapter, we will remove the second assumption, and treat some problems arising as a result.

3.4.1 Control Objectives

Our control objective in this section is

(1) to find a control input which guarantees

$$\lim_{t\to\infty} \dot{e}(t) = \lim_{t\to\infty} e(t) = 0, \tag{3.4.1}$$

where

$$e = r - q, \tag{3.4.2}$$

r is the $n\times 1$ desired trajectory vector; and

(2) to reduce the transient tracking error as much as possible with bounded control inputs.

3.4.2 Some Useful Stability Lemmas

To derive a stability criterion, we use the known fact: If the 2-norm of any differentiable signal is bounded, the signal approaches zero as time goes to infinity. Mathematically this can be formulated as

Lemma 1:

$$\lim_{t\to\infty} y(t) = 0, \quad \text{if } \int_0^t y(\tau)^T y(\tau) d\tau < \infty, \quad \forall\, t \geq 0, \tag{3.4.3}$$

where $y(t)$ is any finite-dimensional differentiable vector. This lemma has been proved by several researchers, but the original work was attributed to Barbalat by Popov[3.21].

We extend the Lemma 1 to apply to later derivation of a stability criterion.

Lemma 2:

$$\lim_{t\to\infty} y(t) = 0, \quad \text{if } \int_0^t y(\tau)^T S(\tau) y(\tau) d\tau < \infty, \quad \forall\, t \geq 0, \tag{3.4.4}$$

where $y(t)$ is any $\tilde{n}\times 1$ differentiable vector; $S(t)$ is any $\tilde{n}\times\tilde{n}$ bounded differentiable positive-definite symmetric matrix. A proof of Lemma 2 is given in Appendix 3.A. Lemma 2 can be interpreted as: any differentiable signal approaches zero as time goes to infinity, if a 2-norm of the signal weighted with a bounded differentiable positive-definite symmetric matrix is bounded.

3.4.3 Developing A New Stability Criterion

With the Lemma 2, we develop a stability criterion, a sufficient condition on the control input u, for the objective (3.4.1) of achieving zero tracking error. The underlying principle for the derivation of the new stability criterion is as follows:

(1) To achieve $e(t) \to 0$ and $\dot{e}(t) \to 0$ as $t \to \infty$ simultaneously, we enforce $y(t) \to 0$ as $t \to \infty$, where the filtered tracking error $y(t)$ is defined as

$$y \equiv \dot{e} + \underline{K} e, \tag{3.4.5}$$

and $\underline{K} = \text{diag}(\kappa_1, \kappa_2, \cdots, \kappa_n) > 0$; κ_i is already defined in Section 3, equation (3.3.7).

(2) To impose $y(t) \to 0$ as $t \to \infty$, we obtain a weighted 2-norm of y from the system dynamics, and make it bounded, in order to apply the Lemma 2. Then, as a part of the procedure, we deduce a sufficient condition on the control input u for asymptotic stability of tracking error e.

The first step of deriving a stability criterion is to obtain a weighted 2-norm of y. To obtain this norm from the system dynamics, we modify the system equation (3.2.1) to

$$M(\ddot{q} + \rho\dot{y}) + C\dot{q} + D\dot{\sigma} + D_c \text{sgn}(\dot{q}) + g - u = \rho M y + D y, \tag{3.4.6}$$

where ρ is some non-negative scalar to be selected; and $\dot{\sigma}$ is defined as

$$\dot{\sigma} \equiv \dot{r} + \underline{K}e. \tag{3.4.7}$$

Premultiply both sides of (3.4.6) by y^T and integrate from 0 to t to find the norm:

$$\int_0^t y^T(\rho M + D)y d\tau = \int_0^t y^T\Big(M(\ddot{q}+\rho y)+C\dot{q}+D\dot{\sigma}+D_c\mathrm{sgn}(\dot{q})+g-u\Big)d\tau. \tag{3.4.8}$$

Note that it is very difficult to measure angular accelerations. Hence, it is crucially important to avoid using these signals in a control law. Since differentiation of (3.4.5) and (3.4.7) with respect to time gives $\ddot{q} = \ddot{\sigma} - \dot{y}$, we replace $\ddot{q}$ in (3.2.8) with $[\ddot{\sigma} - \dot{y}]$. Then, the system equation (3.2.8) becomes

$$\begin{aligned}&\int_0^t y^T(\rho M + D)y d\tau \\ &\quad = -\frac{1}{2}y^T My\Big|_0^t + \int_0^t y^T\Big(M(\ddot{\sigma}+\rho y) + C\dot{\sigma} + D\dot{\sigma} + D_c\mathrm{sgn}(\dot{q}) + g - u\Big)d\tau,\end{aligned} \tag{3.4.9}$$

which can be written

$$\int_0^t y^T(\rho M+D)y d\tau = \frac{1}{2}y(0)^T M(0)y(0) - \frac{1}{2}y^T My + \int_0^t y^T\Big(Wx-u\Big)d\tau, \tag{3.4.10}$$

where the $m\times 1$ true parameter vector x and the $n\times m$ function matrix W are defined such that

$$Wx \equiv M(\ddot{\sigma}+\rho y) + C\dot{\sigma} + D\dot{\sigma} + D_c\mathrm{sgn}(\dot{q}) + g. \tag{3.4.11}$$

We have used the fact that

$$\int_0^t y^T M\dot{y} d\tau = \frac{1}{2}y^T My\Big|_0^t - \frac{1}{2}\int_0^t y^T\dot{M}y d\tau; \tag{3.4.12}$$

and that $(\dot{M}-2C)$ is skew-symmetric ($y^T(\dot{M}-2C)y = 0$) if the non-unique matrix C is chosen properly[3.22].

Since we have obtained a weighted 2-norm of y in (3.4.10), we are ready to apply the Lemma 2 to form:

Lemma 3: When $|\ddot{r}(t)| < \infty$ for all $t \geq 0$, we can guarantee that $e \to 0$ and $\dot{e} \to 0$ as $t \to \infty$ if we find a control input u such that

$$\eta(t) \equiv \int_0^t y^T(Wx - u)d\tau < \infty, \qquad \forall t \geq 0. \tag{3.4.13}$$

Proof:

$$(3.4.10) \quad \text{and} \quad (3.4.13) \qquad \Longrightarrow \qquad \int_0^t y^T(\rho M + D)y d\tau < \infty, \quad \forall\, t \geq 0, \tag{3.4.14}$$

if the initial error is bounded, that is, if $y^T(0)y(0) < \infty$.

Since M and D are differentiable, symmetric, and positive-definite, by the Lemma 2, asymptotic stability is established. Q.E.D.

We have used M and D for the weight of the 2-norm of y in (3.4.10). However, we can use any combination of any differentiable positive-definite symmetric matrices with appropriate dimensions (e.g., any of M and D). Then, the definition of Wx changes accordingly.

3.4.4 Design of Adaptive Control Laws Using A Performance Index

In this section, we design adaptive control laws based on the Lemma 3. The design procedure involves **search**: we select a plausible candidate for control (and adaptation) law, and then check whether or not this candidate satisfies the Lemma 3.

To make the search easy and to improve the transient response, we apply the basic principle of optimal control: we search for the control input which minimizes a quadratic performance index. From (3.4.10), we select the following performance index:

$$J = \int_0^t y^T(\rho M + D)y d\tau + \frac{1}{2}y^T M y. \tag{3.4.15}$$

Minimizing J minimizes the maximum magnitude of y, and consequently improves the transient response. According to the definition of $\eta(t)$ in (3.4.13),

$$\min_u J \iff \min_u \eta(t), \qquad \forall\, t \geq 0. \tag{3.4.16}$$

Hence, minimizing the performance index is equivalent to minimizing $\eta(t)$. Minimizing $\eta(t)$ and satisfying the stability criterion (the Lemma 3) impose almost the same requirements on the control input u. However, the former requires stricter constraints than the latter since the former requires $\eta(t)$ to be minimized and the latter requires it to be bounded. The former improves the transient response and the latter guarantees the asymptotic stability (i.e., performance for $t \to \infty$). Since there is no general solution for nonlinear systems, we relax the conditions of minimizing $\eta(t)$ to those of reducing $\eta(t)$, from which we deduce the following:

(a). Selecting Dynamics Compensators:

To minimize the non-positive $\eta(t)$ defined in (3.4.13), we need to cancel each components of Wx with a compensator u. We take advantage of the structure of Wx. That is, we choose

$$u = W\bar{x}, \tag{3.4.17}$$

where $\bar{x}$ is the parameter vector to be estimated. The best possible way is to update $\bar{x}$ such that $\bar{x}$ may approach asymptotically to the true parameter x.

With the choice (3.4.17), we have

$$\eta(t) = \int_0^t y^T W(x - \bar{x}) d\tau. \tag{3.4.18}$$

Note that when no uncertainties exist on the parameters of the system dynamics (i.e., $\bar{x} = x$), the choice (3.4.17) makes $\eta(t) = 0$.

To reduce $\eta(t)$ in (3.4.18), we choose $\bar{x}$ such that

$$\int_0^t y^T W\bar{x} d\tau \geq 0, \quad \forall\, t \geq 0. \tag{3.4.19}$$

The condition (3.4.19) can be satisfied only if $\bar{x}$ is a function of W and y.

(b). Selecting Feedback Compensators:

According to (3.4.13), to reduce $\eta(t)$, we need select a compensator u that satisfies

$$\int_0^t y^T u d\tau \geq 0, \quad \forall\, t \geq 0, \tag{3.4.20}$$

which is similar to the condition (3.4.19). To satisfy this condition, we need to select u as a function of y, the feedback component. Hence the requirement (3.4.20) leads to feedback compensators.

(c). Selecting A Candidate for The Control and Adaptation Laws:

There may exist many compensators which satisfy (3.4.17) and (3.4.19), or (3.4.20). Some or all of them are candidates for control and adaptation laws. Note that a dynamics compensator is indispensable for the **asymptotic** stability of the system. In general, higher gain produces smaller tracking errors at the expense of reduced stability. Hence, we need to find compensators whose characteristics are much different from one another.

In summary, the design procedure is **(i)** choose candidates (some compensators) based on (3.4.17), (3.4.19), and (3.4.20), the relaxed requirements for minimizing η; **(ii)** show that some of the compensators make $\eta(t)$ bounded, i.e., they satisfy the Lemma 3 for asymptotic stability; and **(iii)** show that the remaining compensators reduce $\eta(t)$ (the quadratic performance index) even further from the bound of $\eta(t)$ sufficient for asymptotic stability, so that these compensators improve the transient response.

Note that the proposed approach can be applied to the controller design of any system whose dynamics is linear in the parameters of the system, with appropriate modifications in the definition of y, if necessary, depending on the order of the system.

Based on the Lemma 3 (for asymptotic stability) and the constraints (3.4.17), (3.4.19), and (3.4.20), we have found the following control and adaptation laws:

Theorem 1: A control law which guarantees that $e \rightarrow 0$ and $\dot{e} \rightarrow 0$ as

$t \to \infty$ is given by

$$u = W\bar{x} + \mathcal{O}(t)y + \sum_{j=1}^{\infty}(\check{\mathcal{F}}_j Y)\hat{\mathcal{F}}_j(Y\check{\mathcal{F}}_j y) \tag{3.4.21}$$

with an adaptation law

$$\bar{x} = P\int_0^t W^T y d\tau + \sum_{j=1}^{\infty}\mathcal{F}_j(W^T y) + \bar{x}(0). \tag{3.4.22}$$

The memory component $\bar{x}$ is the $m\times 1$ estimated parameter vector such that

$$W\bar{x} \equiv \bar{M}(\ddot{\sigma} + \rho y) + \bar{C}\dot{\sigma} + \bar{D}\dot{\sigma} + \bar{D}_c \mathrm{sgn}(\dot{q}) + \bar{g}, \tag{3.4.23}$$

where $\bar{M}$, $\bar{C}$, $\bar{D}$, $\bar{D}_c$, and $\bar{g}$ correspond to the unbarred variables computed with the estimated parameters; the infinite sign ∞ in the summations indicates that we can use as many filters and hence free parameters as we wish. The various symbols appearing in (3.4.21) and (3.4.22) are defined as follows:

$$\begin{aligned} P &= \mathrm{diag}(p_1, p_2, \cdots, p_m) > 0, \\ Y &= \mathrm{diag}(y_1, y_2, \cdots, y_n). \end{aligned} \tag{3.4.24}$$

For simplicity, $\mathcal{O}$ is defined in the frequency domain as

$$\mathcal{O}(s) \equiv \mathrm{diag}(\mathcal{O}_1(s), \mathcal{O}_2(s), \mathcal{O}_3(s), \cdots, \mathcal{O}_n(s)), \tag{3.4.25}$$

with

$$\mathcal{O}_i(s) \equiv \frac{\alpha_i \delta_i (s + \beta_i)}{(s + \gamma_i)(s + \delta_i)}, \tag{3.4.26}$$

where $\alpha_i > 0$, $\delta_i > \beta_i \geq \gamma_i \geq 0$, but $\gamma_i \neq \delta_i$. For the definition of the operator $\mathcal{O}$ in the time domain, see Appendix 3.B.

The operators $\mathcal{F}_j$, $\check{\mathcal{F}}_j$, and $\hat{\mathcal{F}}_j$ are defined in the frequency domain as

$$\mathcal{F}_j \equiv \mathrm{diag}(\mathcal{F}_{1j}, \mathcal{F}_{2j}, \cdots, \mathcal{F}_{mj}),$$

$$\check{\mathcal{F}}_j \equiv \text{diag}(\check{\mathcal{F}}_{1j}, \check{\mathcal{F}}_{2j}, \cdots, \check{\mathcal{F}}_{nj}),$$

$$\hat{\mathcal{F}}_j \equiv \text{diag}(\hat{\mathcal{F}}_{1j}, \hat{\mathcal{F}}_{2j}, \cdots, \hat{\mathcal{F}}_{nj}), \tag{3.4.27}$$

with

$$\mathcal{F}_{ij}(s) = \left(\frac{a_{ij}b_{ij}}{s+b_{ij}}\right), \qquad a_{ij} \geq 0, \quad b_{ij} \geq 0,$$

$$\check{\mathcal{F}}_{ij}(s) = \left(\frac{\check{a}_{ij}\check{b}_{ij}}{s+\check{b}_{ij}}\right), \qquad \check{a}_{ij} \geq 0, \quad \check{b}_{ij} \geq 0,$$

$$\hat{\mathcal{F}}_{ij}(s) = \left(\frac{\hat{a}_{ij}\hat{b}_{ij}}{s+\hat{b}_{ij}}\right), \qquad \hat{a}_{ij} \geq 0, \quad \hat{b}_{ij} \geq 0. \tag{3.4.28}$$

For the definitions of these operators in the time domain, see Appendix 3.B. For simplicity, we have defined $\check{\mathcal{F}}_j(s)$ as a first-order filter. However, $\check{\mathcal{F}}_j(s)$ can be any kind of stable filters. This is shown in Appendix 3.C.

The proof of the Theorem 1 is given in Appendix 3.C. The block diagram of this control law is shown in Figure 3.4.

Theorem 2: $\sum_{j=1}^{\infty}\Big((\check{\mathcal{F}}_j\underline{\mathrm{E}})\hat{\mathcal{F}}_j(Y\check{\mathcal{F}}_j e) + (\check{\mathcal{F}}_j\dot{\underline{\mathrm{E}}})\hat{\mathcal{F}}_j(Y\check{\mathcal{F}}_j\dot{e})\Big)$ can replace or be added to $\sum_{j=1}^{\infty}(\check{\mathcal{F}}_j Y)\hat{\mathcal{F}}_j(Y\check{\mathcal{F}}_j y)$ in the Theorem 1. where

$$\underline{\mathrm{E}} = \text{diag}(e_1, e_2, \cdots, e_n),$$

$$\dot{\underline{\mathrm{E}}} = \text{diag}(\dot{e}_1, \dot{e}_2, \cdots, \dot{e}_n). \tag{3.4.29}$$

Theorem 2 is based on the condition (3.4.20) and can be proved with the following inequalities:

$$\int_0^t y^T(\check{\mathcal{F}}_j\underline{\mathrm{E}})\hat{\mathcal{F}}_j(Y\check{\mathcal{F}}_j e)d\tau \geq 0, \quad \forall\, j = 1, 2, \cdots, \infty, \ \forall\, t \geq 0,$$

$$\int_0^t y^T(\check{\mathcal{F}}_j\dot{\underline{\mathrm{E}}})\hat{\mathcal{F}}_j(Y\check{\mathcal{F}}_j\dot{e})d\tau \geq 0, \quad \forall\, j = 1, 2, \cdots, \infty, \ \forall\, t \geq 0. \tag{3.4.30}$$

Note that the control laws in the Theorem 2 require more computation time than that in the Theorem 1.

3.5 Remarks

1. From (3.3.7), (3.4.5), (3.4.25), and (3.4.26), we have $\mathcal{O}(s)Y(s) = K(s)E(s)$ where

$$K(s) = \text{diag}\Big(K_1(s), K_2(s), \cdots, K_n(s)\Big);$$
$$E(s) = \text{diag}\Big(E_1(s), E_2(s), \cdots, E_n(s)\Big);$$
$$Y(s) = \text{diag}\Big(Y_1(s), Y_2(s), \cdots, Y_n(s)\Big). \tag{3.5.1}$$

$Y_i(s)$ and $E_i(s)$ are the Laplace transforms of $y_i(t)$ and $e_i(t)$ respectively. Hence, the parameters in $\mathcal{O}_i(s)$ have been already chosen in (3.3.7) based on the loop shaping method.

2. The additional computations due to the ρy term in Wx, equation (3.4.11) and in $W\bar{x}$, equation (3.4.23), are only n (=number of joints) multiplications and n additions per one sampling period, the computation of which is almost negligible compared with the total computation time. The ρy term represents a feedback compensator whose gain is $\bar{M}$. The characteristics of this compensator are quite different from those of the other feedback compensators represented by the $\mathcal{O}y$ and $\hat{\mathcal{F}}_j$ terms.

3. According to the theorems, the filtered error y defined by (3.4.5), converges to zero. Hence, the adaptation rule (3.4.22) guarantees that $\bar{x}$, the parameter vector, converges to some constant values, but not necessarily to the true values. It may be shown that the updated parameters approach to the true parameters if trajectories are persistently excited. However, in practice, it is very difficult to meet the condition of persistent excitation. Hence, it may be almost meaningless to try to get the true parameters.

4. We have paid no attention to the sensor noise, disturbances, and unmodelled dynamics in the stability analysis. See the system equation (3.2.1). However, in reality, we can neglect none of these. Consequently, we may have some problems in physical implementations. In the next chapter, we will analyze the effects of

these on the stability of the system.

3.6 Computer Simulation

As an example, one of the schemes developed here has been applied to a two-link direct-drive arm shown in Figure 3.5. The masses of the actuators are included (modelled) in those of the link dynamics since the manipulator is a direct-drive arm. We used a 4^{th}-order Runge-Kutta method with adaptive step size[3.23] to guarantee accuracy in the solution of the manipulator dynamics. In this simulation, Coulomb friction is not used because this causes a problem with accuracy in the solution of the manipulator dynamic equation.

The dynamic equation of motion of the manipulator is that

$$M\ddot{q} + C\dot{q} + D\dot{q} + g = u, \tag{3.6.1}$$

where

$$\begin{aligned}
M &= \begin{bmatrix} x_1 + 2x_2\cos(q_2) + x_3 & x_1 + x_2\cos(q_2) \\ x_1 + x_2\cos(q_2) & x_1 \end{bmatrix}, \\
C &= \begin{bmatrix} -x_2\sin(q_2)\dot{q}_2 & -x_2\sin(q_2)\dot{q}_1 - x_2\sin(q_2)\dot{q}_2 \\ +x_2\sin(q_2)\dot{q}_1 & 0 \end{bmatrix}, \\
D &= \begin{bmatrix} x_4 & 0 \\ 0 & x_5 \end{bmatrix}, \\
g &= \begin{pmatrix} x_6\cos(q_1 + q_2) + x_7\cos(q_1) \\ x_6\cos(q_1 + q_2) \end{pmatrix},
\end{aligned} \tag{3.6.2}$$

with

$$\begin{aligned}
x_1 &= l_2^2 m_2, \\
x_2 &= l_1 l_2 m_2, \\
x_3 &= l_1^2(m_1 + m_2), \\
x_6 &= m_2 l_2 g, \\
x_7 &= (m_1 + m_2) l_1 g.
\end{aligned} \tag{3.6.3}$$

Matrix $D(x_4$ and $x_5)$ represents the damping coefficient of the links.

The numerical values used in this simulation are as follows; $m_1 = 15.91$ kg, $m_2 = 11.36$ kg, and $l_1 = l_2 = 0.432$ m. These values represent links 2 and 3 of the Unimation Puma 560 arm. We set $x_4 = 10.8$ Nm/sec and $x_5 = 3.2$ Nm/sec. As a disturbance, the mass 2 (m_2) was doubled after 2 seconds.

We have designed some adaptive control laws in the previous section. Among them, we use the following adaptive control law:

$$u = W\bar{x} + \mathcal{O}(t)y + \sum_{j=1}^{\infty}(\check{\mathcal{F}}_j Y)\hat{\mathcal{F}}_j(Y\check{\mathcal{F}}_j y), \tag{3.6.4}$$

$$W\bar{x} \equiv \bar{M}(\ddot{\sigma} + \rho y) + \bar{C}\dot{\sigma} + \bar{D}\dot{\sigma} + \bar{g}, \tag{3.6.5}$$

with an adaptation law

$$\bar{x} = P\int_0^t W^T y d\tau + \sum_{j=1}^{\infty}\mathcal{F}_j(W^T y) + \bar{x}(0), \tag{3.6.6}$$

where

$$\mathcal{O}(s) = \mathrm{diag}(\mathcal{O}_1(s), \mathcal{O}_2(s)), \tag{3.6.7}$$

with the following definitions from (3.B.1) and (3.4.28):

$$\mathcal{O}_i(s) = \alpha_i\delta_i(\frac{\gamma_i - \beta_i}{\gamma_i - \delta_i})\cdot(\frac{1}{s+\gamma_i}) + \alpha_i\delta_i(\frac{\beta_i - \delta_i}{\gamma_i - \delta_i})\cdot(\frac{1}{s+\delta_i}); \tag{3.6.8}$$

$$\begin{aligned}
\mathcal{F}_j &\equiv \mathrm{diag}\Big((\frac{a_{1j}b_{1j}}{s+b_{1j}}), (\frac{a_{2j}b_{2j}}{s+b_{2j}}), \cdots, (\frac{a_{mj}b_{mj}}{s+b_{mj}})\Big),\\
\check{\mathcal{F}}_j &\equiv \mathrm{diag}\Big((\frac{\check{a}_{1j}\check{b}_{1j}}{s+\check{b}_{1j}}), (\frac{\check{a}_{2j}\check{b}_{2j}}{s+\check{b}_{2j}})\Big),\\
\hat{\mathcal{F}}_j &\equiv \mathrm{diag}\Big((\frac{\hat{a}_{1j}\hat{b}_{1j}}{s+\hat{b}_{1j}}), (\frac{\hat{a}_{2j}\hat{b}_{2j}}{s+\hat{b}_{2j}})\Big).
\end{aligned} \tag{3.6.9}$$

W and x are defined as follows:

$$x = (x_1\ x_2\ x_3\ x_4\ x_5\ x_6\ x_7)^T,$$

$$W = \begin{bmatrix} w_{11} & w_{12} & w_{13} & w_{14} & 0 & w_{16} & w_{17} \\ w_{21} & w_{22} & 0 & 0 & w_{25} & w_{26} & 0 \end{bmatrix}, \tag{3.6.10}$$

with

$$\begin{aligned} w_{11} =& w_{21} = (\ddot{\sigma}_1 + \rho y_1) + (\ddot{\sigma}_2 + \rho y_2), \\ w_{12} =& \cos(q_2)\Big(2(\ddot{\sigma}_1 + \rho y_1) + (\ddot{\sigma}_2 + \rho y_2)\Big) \\ & - \sin(q_2)(\dot{q}_2\dot{\sigma}_1 + \dot{q}_1\dot{\sigma}_2 + \dot{q}_2\dot{\sigma}_2), \\ w_{13} =& \ddot{\sigma}_1 + \rho y_1, \\ w_{14} =& \dot{\sigma}_1, \\ w_{16} =& w_{26} = 10\cos(q_1 + q_2), \\ w_{17} =& 20\cos(q_1), \\ w_{22} =& \cos(q_2)(\ddot{\sigma}_1 + \rho y_1) + \sin(q_2)\dot{q}_1\dot{\sigma}_1, \\ w_{25} =& \dot{\sigma}_2. \end{aligned} \tag{3.6.11}$$

The update of the parameters is performed by (3.6.6) at predetermined sampling points. The true values of the parameters x_6 and x_7 are very large compared with the others. Therefore, when all the adaptation gains for the parameters are set to be the same, the adaptation rates of x_6 and x_7 are relatively small compared with those of the others. This means that convergence of these parameters is very slow. To fix this problem, we multiplied w_{16} and w_{17} by the factors 10 and 20 respectively; see equation (3.6.11).

The adaptive control law above is developed in the domain of continuous time (or s-domain). Therefore, when we implement the control law through the sampled data system, we need to discretize the control law; that is, we need to convert the domain of continuous time (or s-transformation) to that of discrete time (z-transformation). In our simulations, the integrations and the filterings associated with y in the control law have been performed using the following

trapezoid rule (Tustin's rule)[3.24]:

$$s \simeq \frac{2}{t_s}\frac{z-1}{z+1}. \tag{3.6.12}$$

To make our simulation realistic, we included a delay of one sampling time in our control inputs for computations, measurements, and conversion of signals. To relieve the computational burden, we use a dual-timing update rule: 2 msec for the feedback compensators, and 10 msec for the feedforward compensators. Hence, there are two different delays (2,10 msec) in our control inputs.

To see the importance of the transient behavior, we compare the proposed scheme with Slotine's scheme which focuses on asymptotic stability.

The desired trajectories are chosen as

$$\begin{aligned} r_1 &= \cos 5t, \\ r_2 &= \cos 3t, \end{aligned} \tag{3.6.13}$$

which are shown in Figure 3.6.

Figures 3.7 and 3.8 show the tracking errors 1 and 2 with the single-timing update rule ($t_s = 2$ msec), in which the dashed and the solid lines indicate the errors of Slotine's and present schemes respectively. The initial values for the parameter estimation are equal to 0 in Figure 3.7 and to the true values in Figure 3.8. The non-zero control and adaptation gains of both schemes for this simulation are as follows:

(1) Common numerical values for all simulations:

$\kappa_1 = \kappa_2 = 20$,

$\gamma_i = \beta_i < \infty$, $\delta_i = \infty$, $i = 1, 2$

$\alpha_1 = 360$, $\alpha_2 = 105$.

(2) Slotine's scheme (dashed lines):

$P = 20 I_{m\times m}$; where $I_{m\times m}$ is $m \times m$ identity matrix.

(3) Present scheme (solid lines):

$P = 20I_{m\times m}$, $\rho = 80$,

$\hat{a}_{i1} = 10 \times 10^6/3, \quad \check{a}_{i1} = \check{b}_{i1} = 20, \quad \hat{b}_{i1} = 3, \quad i = 1, 2.$

Note that in this simulation, we use only the first terms (j=1) of the adaptation law for the present scheme.

Figures 3.9 and 3.10 show the tracking errors 1 and 2 with the dual-timing update rule ($t_s = 2$ msec for the feedback laws and $t_s = 10$ msec for the dynamics compensator) in which the dashed and the solid lines indicate the errors of Slotine's and present schemes respectively. The initial values for the parameter estimation are set to be 0 and the true values in Figures 3.9 and 3.10 respectively. The non-zero control and adaptation gains of both schemes for this simulation are

(1) Slotine's scheme (dashed lines):

$P = 40I_{m\times m}$.

(2) Present scheme (solid lines):

$P = 40I_{m\times m}$, $\rho = 40$,

$\hat{a}_{i1} = 25 \times 10^5/3, \quad \check{a}_{i1} = \check{b}_{i1} = 20, \quad \hat{b}_{i1} = 3, \quad i = 1, 2.$

Note that we have not used any low-pass filter for $\mathcal{O}y$, because there is no sensor noise in this simulation.

In both sampling strategies, the present scheme reduces the tracking errors of Slotine's scheme by up to 2/3 in terms of the maximum magnitude. However, the increase in the computation time is less than 1/10 - 1/5 of the total computations. The gains for Slotine's scheme are thought to be optimum because the tracking errors can not be reduced further by increasing the gains of Slotine's scheme. The additional reduction of the tracking errors by the present scheme is much larger with the dual-timing sampling technique. This is because the delay of one sampling period of dynamics compensation becomes larger with the dual-timing sampling technique, and this is effectively compensated by additional computationally fast compensators in the present scheme.

We can also see the advantages of the present scheme from another point of view. Comparing Figures 3.7 with 3.9 and 3.8 with 3.10, we can see that the performances of the present scheme with dual-timing update are better than those

of the single-timing Slotine's scheme. This means that with the present scheme we can reduce the computation time of Slotine's scheme by up to 3/5 without sacrificing the performances.

In Figure 3.8, the tracking errors between 0 and 2 seconds are almost zero. This means that both schemes work perfectly when we have precise knowledge of the parameters. After 2 seconds when the mass 2 is doubled, the tracking errors become larger. A major reason is that the true values of the parameters are shifted due to mass change. The tracking errors do not subside within a couple of seconds. This means that a substantial amount of time is required for the parameters to converge. This result supports that the asymptotic stability guarantees nothing about the transient response other than stability, and that the transient response as well as the asymptotic stability need be considered in the design of adaptive control laws.

Through extensive simulations, we have found that larger adaptation gains of the dynamics compensator result in faster parameter convergence. We have also found that there exist upper bounds of these gains for stability in the simulated digital control systems. As the gains increase, the tracking errors decrease. When the gains reach certain values (i.e., optimum values), the decrease in tracking errors is saturated. As the gains increase above those optimum values, the response of the system gets noisier and noisier to instability. Noisier response (i.e., very high-frequency response) may hurt the mechanical parts of manipulators and excite unmodelled dynamics that cannot be avoided in the real world.

To make the comparisons fair, all the gains associated with the adaptation of Slotine's scheme are increased until the output becomes noisy, and then the other compensators ($\rho\bar{M}y$ and $\hat{\mathcal{F}}_j$ terms) are added.

The parameters are found never to converge to the true values, but remain in the bounded region around true values. This is because the parameter convergence is guaranteed only with zero tracking errors and persistently excited trajectories. Note that in the sampled data system we cannot achieve zero tracking errors for time-varying reference inputs due to the delay of one sampling period caused by

the computation time. When we use a trajectory whose final velocity is zero, the tracking errors approach approximately zero. As a result, the parameters converge to some constant values since the adaptation in (3.6.6) is proportional to the tracking errors. However, these values in general are not the true ones, because the condition of persistent excitation of the trajectory is not satisfied around the end point of the trajectory (when velocity is zero).

Similar results with the other trajectories and sampling periods have been obtained, but are not included here. Note that the integral controller is used mainly for suppression of the tracking errors due to static (or low-frequency) reference inputs (or disturbances). Since we used sinusoidal waves as the reference inputs, the integral controller helps little. Hence, in this simulation, we did not use the I-controller.

3.7 Conclusion

In this chapter, we have focused on improving the transient response of the system as well as obtaining the asymptotic stability of the system. We guarantee the asymptotic stability of the system by satisfying the new stability criterion, and improve the transient response by searching for compensators in the direction of minimizing a certain quadratic performance index.

A non-adaptive feedback compensator is designed independently by the loop shaping method. Then adaptive dynamics compensators and adaptive feedback compensators are added via our new stability criterion, combined with the principles of optimal control. Thus, our technique takes the maximum advantage of the loop shaping, optimal control, and adaptive methods; whereas each method has been independently applied to the design of control laws in the existing literature.

The computer simulations confirm that the proposed schemes emphasizing both the transient response and the asymptotic stability considerably outperform Slotine's scheme which focuses only on the latter, in terms of computation time and magnitudes of tracking errors. As a consequence, we conclude that it is important to take the transient response in addition to the asymptotic stability

into consideration in the design of adaptive control laws.

The proposed control laws are derived under the ideal condition of no sensor noise, disturbances, and unmodelled dynamics. Hence there may arise some problems when the ideal conditions are not met. In the next chapter, we will analyze the stability of the proposed control law in the presence of sensor noise, bounded disturbances, and unmodelled dynamics.

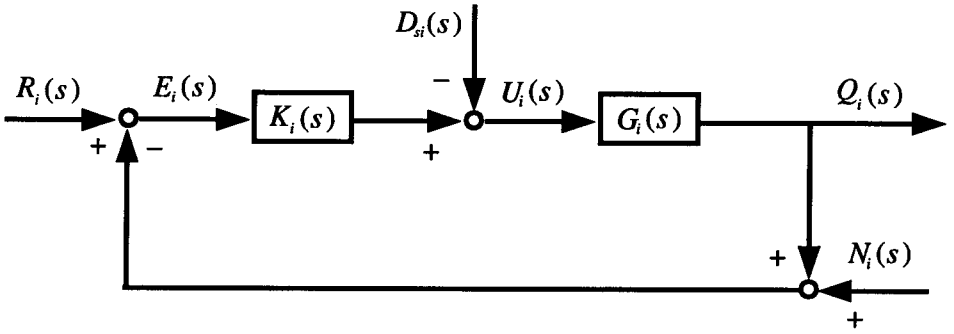

Figure 3.1 Joint control system

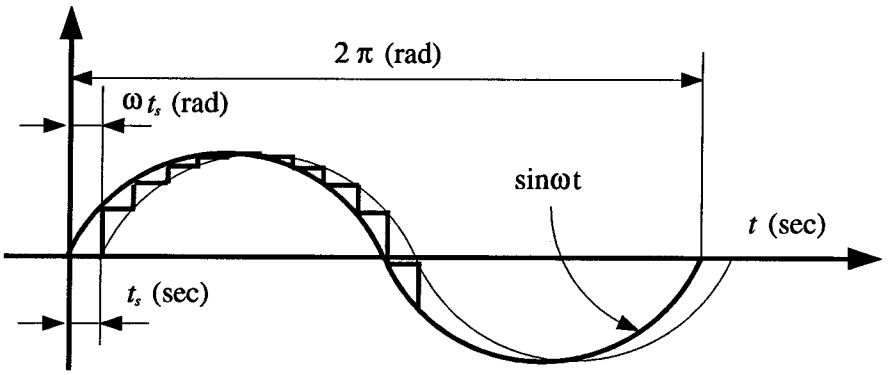

Figure 3.2 Phase lag due to sample-and-hold

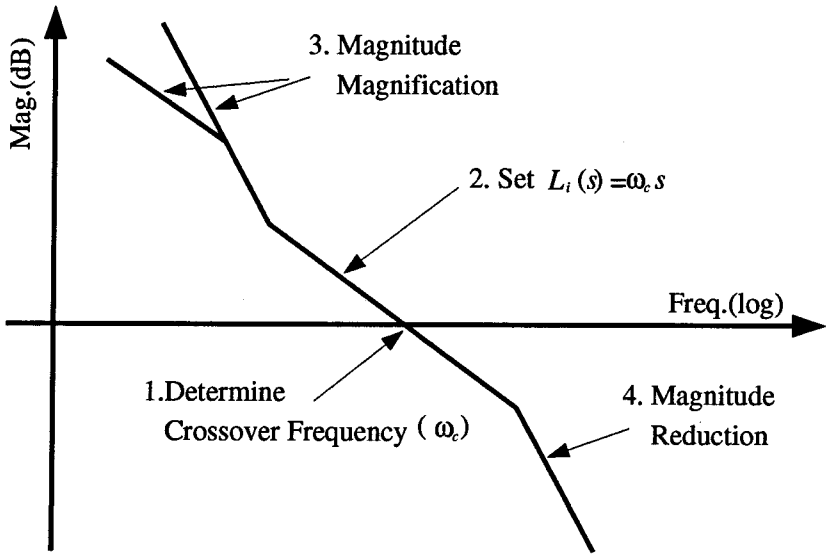

Figure 3.3 Design of the open loop transfer function

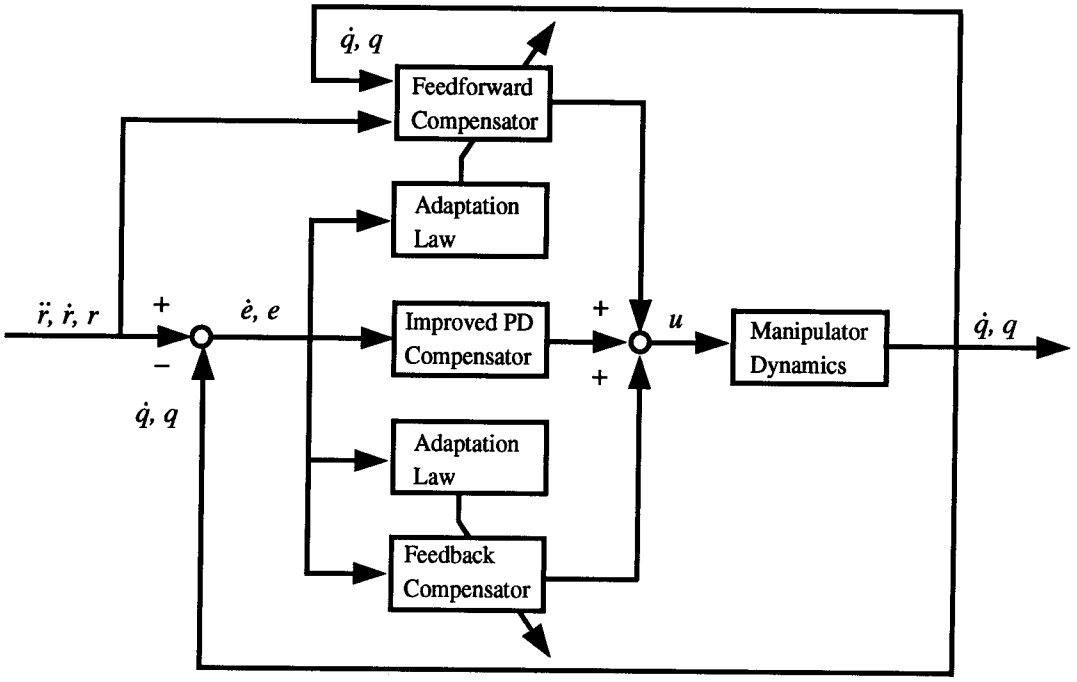

Figure 3.4 Schematic diagram of the proposed control law

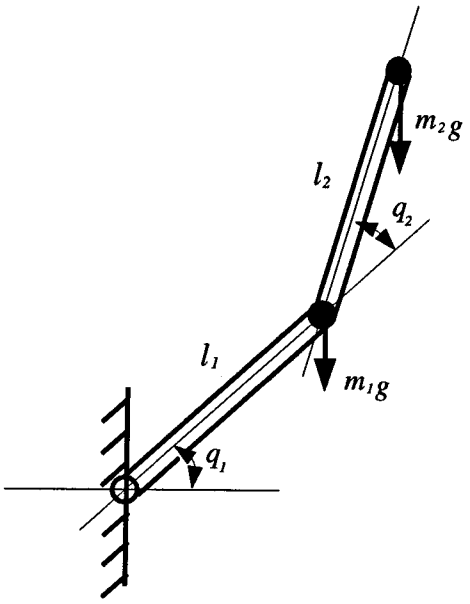

Figure 3.5 Modelling of links

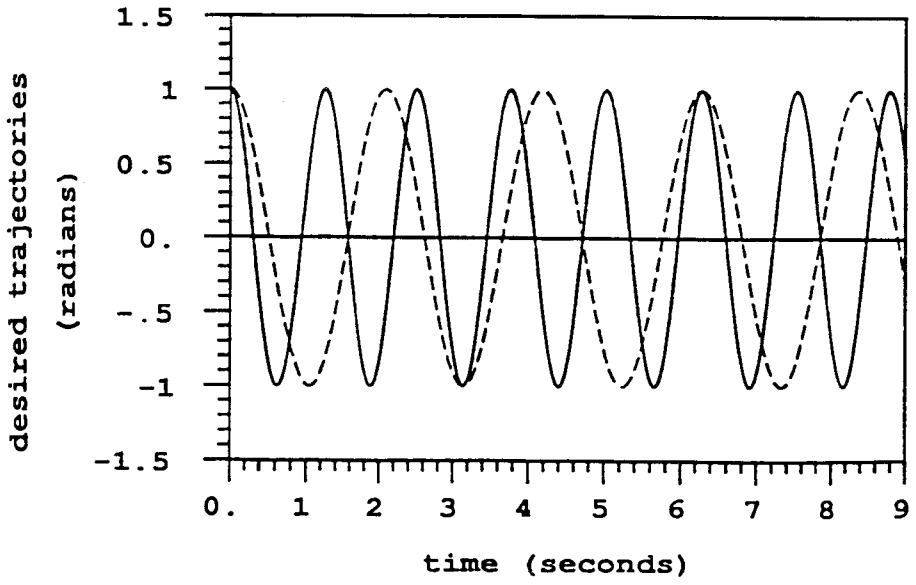

Figure 3.6 Desired trajectories: solid line for joint 1 and dotted line for joint 2

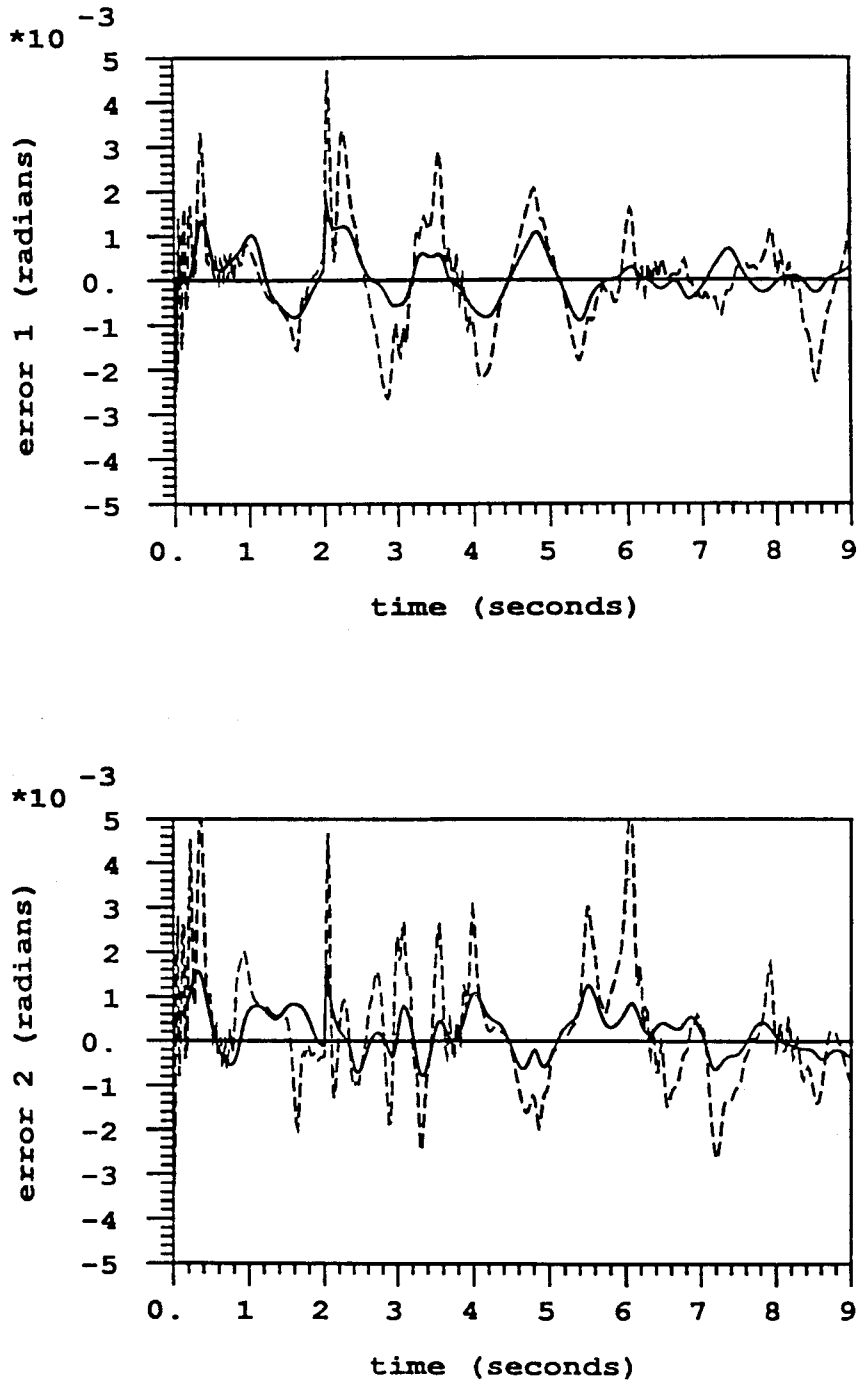

Figure 3.7 Tracking errors with single-timing update (2 msec) and zero initial parameters: solid lines for the present scheme and dotted lines for Slotine's scheme

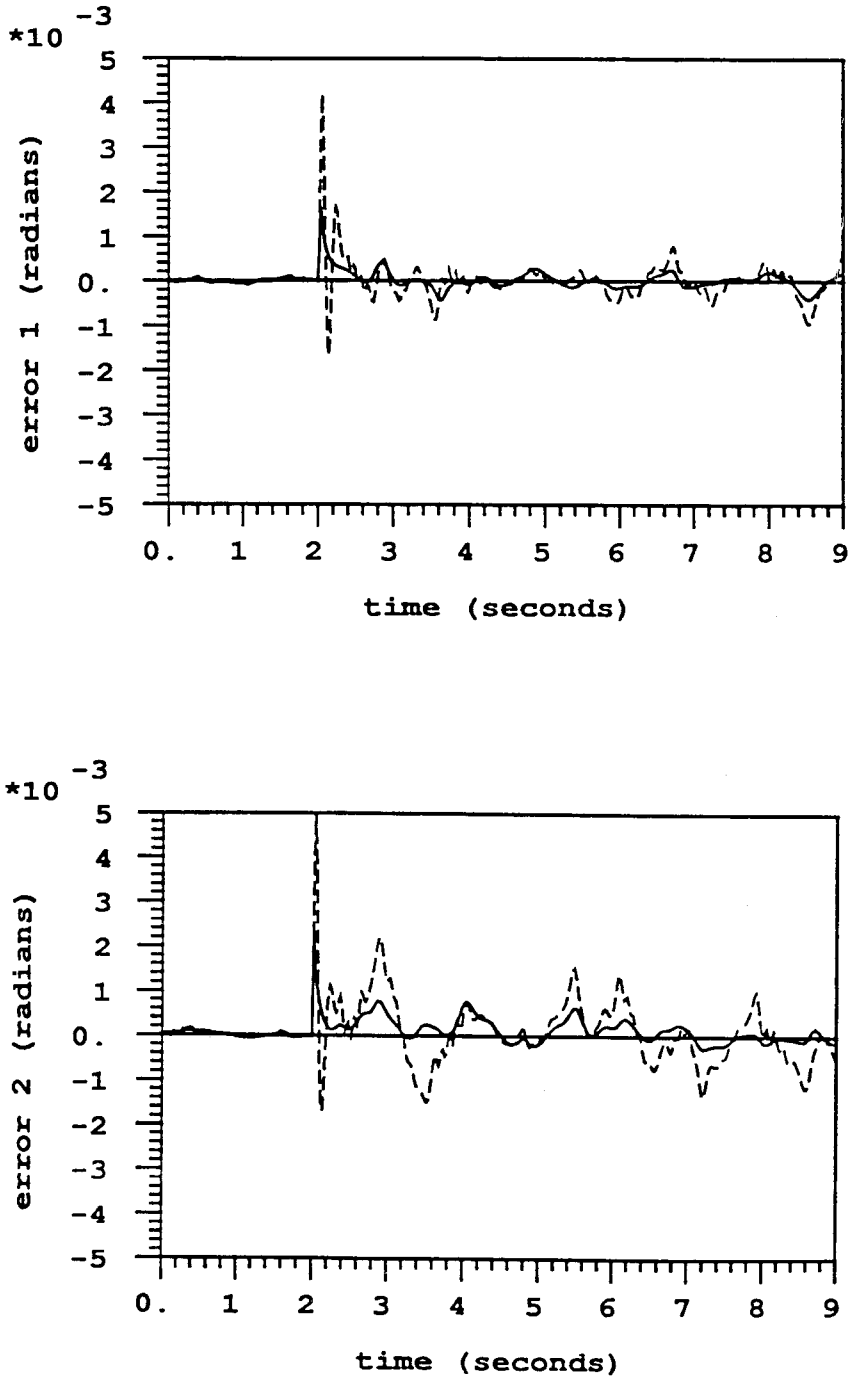

Figure 3.8 Tracking errors with single-timing update (2 msec) and exact initial parameters: solid lines for the present scheme and dotted lines for Slotine's scheme

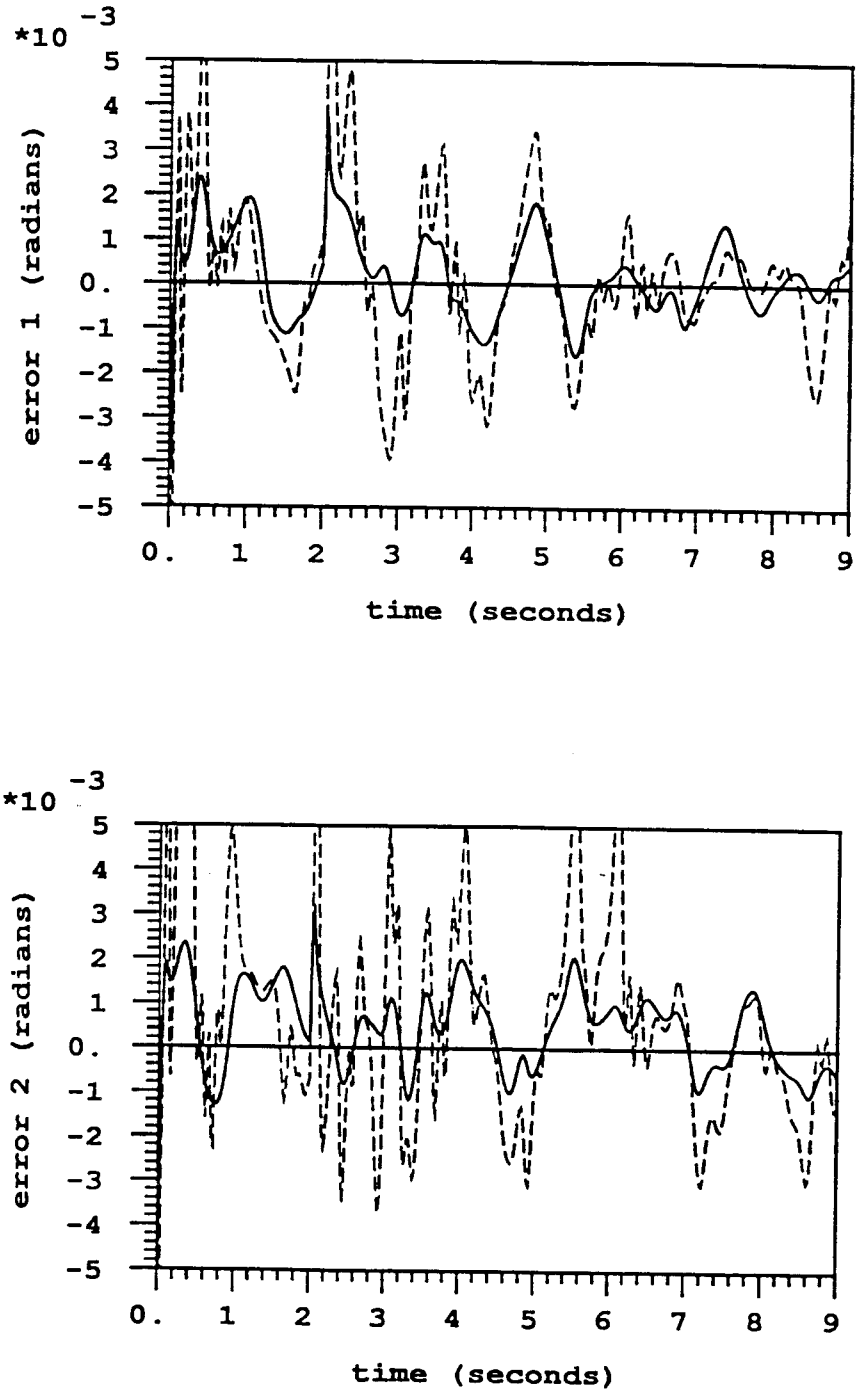

Figure 3.9 Tracking errors with dual-timing update (2 msec for feedback and 10 msec for feedforward compensators) and zero initial parameters: solid lines for the present scheme and dotted lines for Slotine's scheme

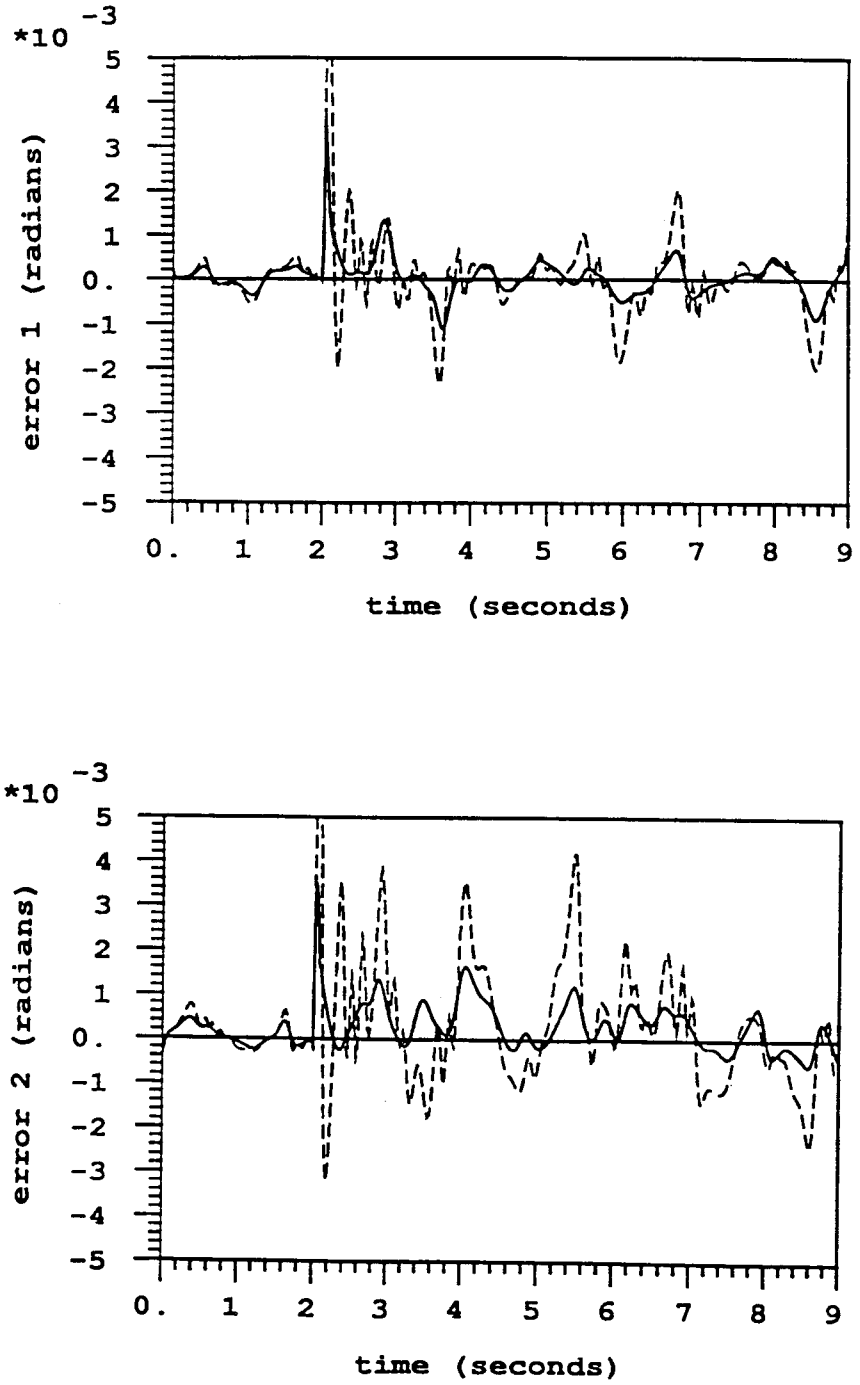

Figure 3.10 Tracking errors with dual-timing update (2 msec for feedback and 10 msec for feedforward compensators) and exact initial parameters: solid lines for the present scheme and dotted lines for Slotine's scheme

References

[3.1] Dubowsky, S. and DesForges, D. F., *The Application of Model-Reference Adaptive Control to Robotic Manipulators,* ASME J. of DSMC, Vol. 101, pp. 193-200, 1979.

[3.2] Koivo, A. J. and Guo, T. M., *Adaptive Linear Controller for Robotic Manipulators,* IEEE Trans. on Aut. Contr., Vol. AC-28, No. 2, pp. 162-172, 1983.

[3.3] Koivo, A. J., Lewczyk, R. and Chiu, T. H., *Adaptive Path Control of a Manipulator with Visual Information,* IEEE Conference on Robotics, Atlanta, March 1984.

[3.4] Walters, R. G. and Bayoumi, M. M., *Application of a Self-Tuning Pole Placement Regulator to an Industrial Manipulator,* IEEE, Conference on Decision and Control, pp. 323-329, 1982.

[3.5] Leininger, G. G. and Wang , S., *Pole Placement Self-Tuning Control of Manipulators,* IFAC Symposium on Computer Aided Design of Multivariable Technological Systems, West Lafayette, Ind., September 15-17, 1982.

[3.6] Leininger, G. G., *Adaptive Control of Manipulators Using Self-Tuning Methods,* Robotics Research, Chap.9 edited by M. Brady and R. Pall, 1984.

[3.7] Backes, P., Leininger, G. G., *Real Time Cartesian Coordinate Hybrid Control of a Puma 560 Manipulator,* IEEE Conference on Robotics and Automation, St. Louis, March 1985.

[3.8] Sundareshan, M. K. and Koenig, M. A., *Decentralized Model Reference Adaptive Control of Robotic Manipulators,* Proceedings, Automatic Control Conference, pp. 44-49, 1985.

[3.9] Takegaki, M. and Arimoto, S., *An Adaptive Trajectory Control of Manipulators,* Int. J. of Control, Vol. 34, No. 2, pp. 219-230, 1981.

[3.10] Seraji, H., *Direct Adaptive Control of Manipulators in Cartesian Space,* J. of Robotic Systems, Vol. 4, No. 1, pp. 157-178, 1987.

[3.11] Seraji, H., *Decentralized Adaptive Control of Manipulators: Theory, Simula-*

tion, and Experimentation, IEEE Trans. on Robotics and Automation, Vol. 5, No. 2, pp. 189-201, April 1989.

[3.12] Lim, K. Y. and Eslami, M., *New Controller Design for Robot Manipulator Systems,* Proc., Amer. Contr. Conf., pp. 38-43, Jun. 1985.

[3.13] Lim, K. Y. and Eslami, M., *Robust Adaptive Controller Designs for Robot Manipulator Systems,* IEEE J. of Robotics and Automation, Vol. RA-3, No. 1, pp. 54-66, Feb. 1987.

[3.14] Nicosia, S. and Tomei, P., *Model Reference Adaptive Control Algorithms for Industrial Robots,* Automatica, Vol. 20, No. 5, pp. 635-644, 1984.

[3.15] Balestrino, A., De Maria, G. and Sciavicco, L., *An Adaptive Model Following Control for Robotic Manipulators,* ASME J. of DSMC, Vol. 105, pp. 143-151, 1983.

[3.16] Craig, J. J., Hsu, P. and Sastry, S. S., *Adaptive Control of Mechanical Manipulators,* Proc. IEEE Conf. on Robotics and Automation, pp. 190-195, 1986.

[3.17] Slotine, J. J. E. and Li, W., *Adaptive Manipulator Control: Parameter Convergence and Task-Space Strategies,* Proc. of the 1987 American Control Conference, pp. 828-835, 1987.

[3.18] Slotine, J. J. E. and Li, W., *Adaptive Manipulator Control: A Case Study,* Proc. of the 1987 Int. conf. on Robotics and Automation, pp. 1392-1400, 1987.

[3.19] Coiffet, P. and Chirouze, M., *An Introduction to Robot Technology,* McGraw-Hill Book Co., 1983.

[3.20] Doyle, J., Francis, B. and Tansenbaum, A., *Feedback Control Theory,* MacMillan Publishing Co., New York, 1991.

[3.21] Popov, V. M., *Hyperstability of Control Systems,* New York: Springer-Verlay, 1983.

[3.22] Arimoto, A. and Miyazaki, F., *Stability and Robustness of PID Feedback Controller for Robot Manipulators of Sensory Capability,* Robotics Research: The First International Symposium edited by Brady, M. and Paul, R., pp.

783-799, 1984.

[3.23] Press, W. H., Flannery, B. P., Teukolsky, S. A. and Vetterting, W. T., *Numerical Recipes: The Art of Scientific Computing,* Cambridge, 1986.

[3.24] Franklin, G. F. and Powell, J. D., *Digital Control of Dynamic Systems,* Addison-Wesley, 1980.

Appendix 3.A: Proof of Lemma 2

Since $S(t)$ is an $\tilde{n}\times\tilde{n}$ symmetric matrix, bounded, differentiable, and positive definite, there always exist a bounded, differentiable, orthogonal matrix $\Theta(t)$ and a bounded, differentiable, positive-definite diagonal matrix $\tilde{P}(t)$ such that

$$S(t) = \Theta^T(t)\tilde{P}(t)\Theta(t), \quad \forall t \geq 0. \tag{3.A.1}$$

Then,

$$\int_0^t y(\tau)^T S(\tau)y(\tau)d\tau = \int_0^t (\Theta(\tau)y(\tau))^T \tilde{P}(\tau)(\Theta(\tau)y(\tau))d\tau < \infty, \quad \forall\, t \geq 0.$$

$$\Longrightarrow \qquad \int_0^t (\Theta(\tau)y(\tau))^T (\Theta(\tau)y(\tau))d\tau < \infty, \quad \forall\, t \geq 0,$$

since $\tilde{P}(t)$, $\forall t \geq 0$ is a bounded, differentiable, positive-definite diagonal matrix.

Then, by the Lemma 1 and the characteristics of $\Theta(t)$,

$$\lim_{t\to\infty} \Theta(t)y(t) = 0, \quad \text{hence, } \lim_{t\to\infty} y(t) = 0. \qquad \text{QED.}$$

Appendix 3.B: Computation of $\int_0^t y^T(\mathcal{O}y)d\tau$

Note that $\mathcal{O}_i(s)$ can be interpreted as

$$\begin{aligned}\mathcal{O}_i(s) &= \alpha_i\delta_i\left(\frac{s+\beta_i}{s+\gamma_i}\right)\cdot\left(\frac{1}{s+\delta_i}\right)\\ &= \alpha_i\delta_i\left(\frac{1}{s+\delta_i}\right)\cdot\left(\frac{s+\beta_i}{s+\gamma_i}\right)\\ &= \alpha_i\delta_i\left(\frac{1}{s+\gamma_i}\right)\cdot\left(\frac{s+\beta_i}{s+\delta_i}\right)\end{aligned}$$

$$= \alpha_i\delta_i(\frac{s+\beta_i}{s+\delta_i})\cdot(\frac{1}{s+\gamma_i})$$
$$= \alpha_i\delta_i(\frac{\gamma_i-\beta_i}{\gamma_i-\delta_i})\cdot(\frac{1}{s+\gamma_i}) + \alpha_i\delta_i(\frac{\beta_i-\delta_i}{\gamma_i-\delta_i})\cdot(\frac{1}{s+\delta_i}). \qquad (3.B.1)$$

Note that $(\frac{\gamma_i-\beta_i}{\gamma_i-\delta_i}) \geq 0$ and $(\frac{\beta_i-\delta_i}{\gamma_i-\delta_i}) \geq 0$.

Also note that $\mathcal{O}_i(s)$ may include an integrator when γ_i is chosen to be zero, and that the component $(s+\beta_i)/(s+\gamma_i)$ can be interpreted as a lag-lead compensator, i.e., a gain amplifier, in the low-frequency region.

Different interpretations of $\mathcal{O}_i(s)$ above lead to different realizations in the time domain. However, they are all equivalent. We can show the equivalences in the time domain. Here, we use the last realization in (3.B.1),

$$\mathcal{O}_i(s) = \mathcal{F}_{\gamma_i}(s) + \mathcal{F}_{\delta_i}(s), \qquad (3.B.2)$$

where the operators $\mathcal{F}_{\delta_i}$ and $\mathcal{F}_{\gamma_i}$ are defined as

$$\mathcal{F}_{\gamma_i}(s) \equiv \alpha_i\delta_i(\frac{\gamma_i-\beta_i}{\gamma_i-\delta_i})\cdot(\frac{1}{s+\gamma_i}),$$
$$\mathcal{F}_{\delta_i}(s) \equiv \alpha_i\delta_i(\frac{\beta_i-\delta_i}{\gamma_i-\delta_i})\cdot(\frac{1}{s+\delta_i}), \qquad (3.B.3)$$

such that in the time domain

$$\mathcal{F}_{\gamma_i}y(t) \equiv \alpha_i\delta_i(\frac{\gamma_i-\beta_i}{\gamma_i-\delta_i})e^{-\gamma_i t}\int_0^t ye^{\gamma_i\tau}d\tau,$$
$$\mathcal{F}_{\delta_i}y(t) \equiv \alpha_i\delta_i\frac{(\delta_i-\beta_i)}{(\delta_i-\gamma_i)}e^{-\delta_i t}\int_0^t ye^{\delta_i\tau}d\tau. \qquad (3.B.4)$$

When γ_i is chosen to be zero, $\mathcal{F}_{\gamma_i}$ includes an integrator. Hence, $\mathcal{O}_i$ can be an integrator, a low pass filter, or both, depending on γ_i, β_i, and δ_i.

The operators $\mathcal{F}_j$, $\check{\mathcal{F}}_j$, and $\hat{\mathcal{F}}_j$ can be defined in the time domain similar to (3.B.4).

$$\int_0^{t_1} z(t)(\mathcal{F}_{\delta_i}z(t))dt = \frac{(\delta_i-\gamma_i)}{\alpha_i\delta_i(\delta_i-\beta_i)}\Big(\frac{1}{2}(\mathcal{F}_i z(t_1))^2 + \delta_i\int_0^{t_1}(\mathcal{F}_i z(t))^2 dt\Big)$$

$$\geq 0, \qquad \forall\ \alpha_i \neq 0,\ \delta_i > \beta_i,\ \delta_i > \gamma_i,\ z, \text{ and } t_1 \geq 0. \qquad (3.B.5)$$

The computation of $\int_0^{t_1} z(t)\mathcal{F}_{\gamma_i} z(t)dt$ is similarly achieved.

Then,

$$\begin{aligned}\int_0^t y^T \mathcal{O} y d\tau = &\sum_{i=1}^{n}\Big(\frac{(\delta_i-\gamma_i)}{\alpha_i\delta_i(\delta_i-\beta_i)}\big(\frac{1}{2}(\mathcal{F}_{\delta_i}y_i(t))^2 + \delta_i\int_0^{t_1}(\mathcal{F}_{\delta_i}y_i(t))^2dt\big)\\ &+\frac{(\gamma_i-\delta_i)}{\alpha_i\delta_i(\gamma_i-\beta_i)}\big(\frac{1}{2}(\mathcal{F}_{\gamma_i}y_i(t))^2+\gamma_i\int_0^{t_1}(\mathcal{F}_{\gamma_i}y_i(t))^2dt\big)\Big)\\ \geq &0, \qquad \forall\ \alpha_i\neq 0,\ \delta_i>\beta_i,\ \delta_i>\gamma_i,\ y, \text{ and } t. \qquad (3.B.6)\end{aligned}$$

We can readily show that $\int_0^t y^T \mathcal{O} y d\tau \geq 0$ for the other realizations in (3.B.1).

Appendix 3.C: Proof of Theorem 1

Let us insert the chosen adaptation and control laws into $\eta(t)$ in (3.4.13):

$$\begin{aligned}\eta(t) &= \int_0^t y^T[W(x-\bar{x}) - \mathcal{O}y - \sum_{j=1}^{\infty}(\check{\mathcal{F}}_j Y)\hat{\mathcal{F}}_j(Y\check{\mathcal{F}}_j y)]d\tau\\ &= \int_0^t y^T[W\Big(x - P\int_0^\tau W^T y ds - \sum_{j=1}^{\infty}\mathcal{F}_j(W^T y) - \bar{x}(0)\Big)\\ &\quad - \mathcal{O}y - \sum_{j=1}^{\infty}(\check{\mathcal{F}}_j Y)\hat{\mathcal{F}}_j(Y\check{\mathcal{F}}_j y)]d\tau\\ &\leq \sum_{i=1}^{m}\Big((x_i-\bar{x}_i(0))\int_0^t(y^TW)_i d\tau - \frac{p_i}{2}(\int_0^t(y^TW)_i d\tau)^2\Big)\\ &\leq \sum_{i=1}^{m}\Big(-\frac{p_i}{2}(\int_0^t(y^TW)_i d\tau - \frac{(x_i-\bar{x}_i(0))}{p_i})^2 + \frac{1}{2p_i}(x_i-\bar{x}_i(0))^2\Big)\\ &\leq \frac{1}{2}\sum_{i=1}^{m}\frac{(x_i-\bar{x}_i(0))^2}{p_i} < \infty. \qquad (3.C.1)\end{aligned}$$

This shows that the control law (3.4.21) and the adaptation law (3.4.22) satisfy Lemma 3. Hence, this proves Theorem 1. Q.E.D.

In (3.C.1), it is assumed that x is the $m\times 1$ unknown but constant vector. The integral term of $\bar{x}$ is sufficient to make $\eta(t)$ bounded; see the first inequality in (3.C.1). Contributions from the $\mathcal{O}$, $\mathcal{F}_j$, and Y terms reduce $\eta(t)$ (the quadratic performance index) even further, since

$$\int_0^t y^T \mathcal{O} y d\tau \geq 0, \quad \forall\, t \geq 0,$$

$$\int_0^t (y^T W)\mathcal{F}_j(W^T y) d\tau \geq 0, \quad \forall\, j = 1, 2, \cdots, \infty,\ \forall\, t \geq 0,$$

$$\int_0^t y^T (\check{\mathcal{F}}_j Y)\hat{\mathcal{F}}_j(Y\check{\mathcal{F}}_j y) d\tau \geq 0, \quad \forall\, j = 1, 2, \cdots, \infty,\ \forall\, t \geq 0. \qquad (3.C.2)$$

These relations follow from (3.B.5) in Appendix 3.B. Hence, these three terms reduce the magnitude of the filtered tracking error y. Note that $\check{\mathcal{F}}_j$ can be any kind of stable filters since the Y term in (3.C.2) is always non-negative regardless of the type of $\check{\mathcal{F}}_j$.

Chapter 4

ROBUST REDESIGN OF ADAPTIVE CONTROL OF ROBOTS

4.1 Introduction

In the previous chapter, we have addressed the importance of the transient response as well as asymptotic stability of the system. To improve the transient behavior, we use compensators whose characteristics are much different from one another. Those compensators are found by search toward minimizing a certain quadratic performance index.

According to the analytical results in the previous chapter, larger control and adaptation gains result in smaller tracking errors since larger gains cause smaller values of the performance index. Computer simulations support this. However, the computer simulations also show instability when the gains become larger than some critical values. A major reason is that in the modelling and hence stability analysis of the system, we neglected the effects of feedback delays, signal holds, and quantization errors associated with the digital control systems, which can be interpreted as unmodelled dynamics. In fact, we have derived the adaptive schemes in the previous chapter under the assumption of no sensor noises, disturbances, and unmodelled dynamics. This assumption is far from reality. Hence, there arises a natural question of how these schemes will perform when the assumption is not met.

In the early 1980s, the adaptive control community began to deal with the robustness problem in adaptive control schemes for linear time-invariant systems. Several researchers observed instability[4.1] in some asymptotically stable adaptive schemes when the above assumption is not satisfied. As mentioned in Section

1.2.3 of Chapter 1, instability is caused by drift of parameters (or control gains) to large (possibly unbounded) values due to integrators in the adaptation loop in the presence of bounded disturbances, sensor noises, or unmodelled dynamics. Accordingly, those integrators were removed in several modified adaptation laws[4.2-4.9] to prevent parameter drift. Robustness in adaptive control does not mean the robustness with respect to parameter uncertainties but rather means the robustness with respect to parameter drift in the presence of bounded disturbances, sensor noises, and unmodelled dynamics.

Since Dubowsky and DesForges[4.10] first introduced an adaptive control strategy to the control of manipulators, extensive research has been performed toward obtaining asymptotic stability[4.10-4.35]. As a consequence, several recent schemes[4.36-4.40] and those proposed in the previous chapter come to guarantee the asymptotic stability under the assumption of no disturbances, sensor noises, and unmodelled dynamics. Robustness of adaptive control of robots was discussed in [4.41] with some artificial unmodelled dynamics and disturbance. With sensor noises in simulations, instability due to parameter drift was observed in some adaptive control laws for robots which are asymptotically stable under a certain ideal condition[4.42].

In this chapter, we show that the integration adaptation law used in the previous chapter may cause instability due to parameter drift in the presence of sensor noises or bounded disturbances. We redesign the adaptive scheme proposed in Chapter 3 by replacing its integration law with the σ-modification[4.7,4.8] to prevent parameter drift. We also propose new adaptation laws using the bounds of parameters. Then, we investigate the effects of bounded disturbances and feedback delays in the digital control systems on the stability of the adaptive scheme redesigned with the new adaptation laws. As a result, for the redesigned scheme, we derive stability bounds for disturbances, control and adaptation gains, and desired trajectories and their time-derivatives, in the presence of feedback delays. This result explains instability observed in the previous chapter when the control and adaptation gains are larger than certain critical values. In contrast, no

stability bounds have been provided in the literature of adaptive control of robots.

In Section 2, we examine the instability mechanism in relation to the integration adaptation law used in the previous chapter. In Section 3, we model feedback delays, signal holds, and quantization errors in signal conversions. In Section 4, we define an appropriate quadratic performance index. Then, we search for compensators which reduce the performance index as much as possible to improve the tracking performance. In the search, we select compensators from the Theorem 1 of Chapter 3, and modify them with the new adaptation laws. Then, in the Appendix, we analyze the stability of the selected adaptive scheme in the presence of bounded disturbances and unmodelled dynamics, and derive some stabilizing constraints.

4.2 Instability Mechanism

In this section, we examine why the integration adaptation law used in the Theorem 1 of Chapter 3 may cause parameter drift in the presence of bounded disturbances or sensor noises.

Consider a simple horizontal one degree of freedom robot under an ideal condition:

$$m_1 \ddot{q}_1 = u_1, \tag{4.2.1}$$

where m_1 is the mass moment of inertia of the link; u_1 is the control input; and q_1 is the angle of the link.

A basic adaptive control law for this robot is given by the Theorem 1 of Chapter 3:

$$u_1 = \bar{m}_1 \Big(\ddot{r}_1 + \kappa_1 \dot{e}_1 + \rho(\dot{e}_1 + \kappa_1 e_1) \Big) + \kappa_2 (\dot{e}_1 + \kappa_1 e_1) \tag{4.2.2}$$

with

$$\bar{m}_1 = \int_0^t \Big(\ddot{r}_1 + \kappa_1 \dot{e}_1 + \rho(\dot{e}_1 + \kappa_1 e_1) \Big) (\dot{e}_1 + \kappa_1 e_1) d\tau, \tag{4.2.3}$$

where $\rho \geq 0$; $\kappa_1 > 0$, $\kappa_2 > 0$; and $e_1 = r_1 - q_1$, $r_1(t)$ is the desired angle of the link.

Note that the adaptation law (4.2.3) also updates the constant inertia terms of a robot which has more than one degree of freedom.

Under the ideal condition, it is guaranteed that $e_1 \rightarrow 0$ and $\dot{e}_1 \rightarrow 0$ as $t \rightarrow \infty$, and that $\bar{m}_1 \rightarrow m_1$ as $t \rightarrow \infty$. In the presence of bounded disturbances, nothing is guaranteed unless the disturbances are completely compensated. Then, a question naturally arises as to whether it is still possible to guarantee $|e_1(t)| < \infty$ and $|\dot{e}_1(t)| < \infty$ for all $t \geq 0$. To answer this, we rewrite the adaptation law $\bar{m}_1$ as

$$\bar{m}_1 = \int_0^t \ddot{r}_1(\dot{e}_1 + \kappa_1 e_1)d\tau + \frac{\kappa_1}{2}e_1^2\Big|_0^t + \kappa_1 \int_0^t \dot{e}_1^2 d\tau + \rho \int_0^t (\dot{e}_1 + \kappa_1 e_1)^2 d\tau. \quad (4.2.4)$$

The third and fourth terms will grow unbounded since the tracking errors do not converge to zero as time goes to infinity due to lack of compensation for disturbances or sensor noises. Therefore $\bar{m}_1$ grows unbounded unless the first term exactly cancels the third and fourth terms, which is in general impossible. Hence, $\bar{m}_1$ grows unbounded and instability results. This supports the simulation result in the reference[4.42].

4.3 Modelling A System to Control

The dynamics of a rigid-joint robot is given[4.43] by

$$M\ddot{q} + C\dot{q} + D\dot{q} + g + \hat{d} = u_d, \quad (4.3.1)$$

where

$q, \dot{q}, \ddot{q}$: $n \times 1$ joint displacement, velocity, and acceleration vector for the links respectively;

$M(q)$: $n \times n$ effective coupling inertia matrix for the links including payloads;

$C(\dot{q}, q)\dot{q}$: $n \times 1$ centrifugal and Coriolis force vector;

D : $n \times n$ matrix for viscous damping coefficients of the links;

$g(q)$: $n \times 1$ gravitational loading vector;

$\underline{d}$: $n \times 1$ bounded disturbance vector;

u_d: $n \times 1$ actuator input vector;

$\hat{d}$: $n\times 1$ vector representing bounded disturbances;

n : number of joints.

In the digital control systems, feedback delays, signal holds, and quantization errors are inevitable. Here, we investigate the effects of these on the stability of adaptive control systems. We assume that the sampling time (t_s) and sensor resolution are sufficiently small. Then, the control input in the digital control systems can be represented by

$$\begin{aligned} u_d =&(1+\delta_1)u(t-t_s)+u_q \\ =&(1+\delta_1)u(t)+u_q-t_s\dot{u}(t)+\mathcal{O}(t_s^2), \end{aligned} \tag{4.3.2}$$

where u denotes the control input in the analogue systems; $t_s \ll 1$; $\delta_1(t)$ is some small scalar ($|\delta_1| \ll 1$), and $u_q(t)$ is the $n\times 1$ small vector ($u_q^T u_q \ll 1$), denoting the effects of the signal holds and quantization errors on the control input. $\mathcal{O}(\cdot)$ denotes the order of the argument.

From (4.3.1) and (4.3.2), we represent the dynamics of a robot in the digital control systems as

$$M\ddot{q}+C\dot{q}+D\dot{q}+g+\underline{\mathrm{d}}=u+u_e, \tag{4.3.3}$$

where

$$\begin{aligned} &\underline{\mathrm{d}}=\hat{d}-u_q-\mathcal{O}(t_s^2); \\ &u_e=\delta_1 u-t_s\dot{u}. \end{aligned} \tag{4.3.4}$$

4.4 Design of A Robust Adaptive Control Law

We cannot obtain asymptotic stability unless we completely compensate for disturbances and unmodelled dynamics. Accordingly, our control objective is to find a stable and robust adaptive control law which

(1) guarantees for some finite non-negative scalars $\tilde{\delta}_1$ and $\tilde{\delta}_2$ that

$$|\dot{e}(t)| \le \tilde{\delta}_1 \quad \text{and} \quad |e(t)| \le \tilde{\delta}_2, \qquad \forall\, t \ge 0, \tag{4.4.1}$$

where

$$e = r - q, \tag{4.4.2}$$

r is the $n \times 1$ desired trajectory vector; and

(2) reduces the maximum tracking error (e) as much as possible with bounded control inputs.

To achieve this objective, we first define an appropriate quadratic performance index for the system to control. Secondly, we search for compensators in the direction of minimizing the performance index to reduce the maximum tracking errors. Finally, through stability analysis, we derive some sufficient conditions on desired trajectories, disturbances, and control and adaptation gains, under which the proposed adaptive scheme stabilizes the system.

4.4.1 Defining A Quadratic Performance Index

To minimize both tracking error (e) and the derivative of the tracking error ($\dot{e}$), we minimize the following quadratic performance index in relation to the system dynamics:

$$J \equiv \int_0^t y^T(\rho M + D) y d\tau, \tag{4.4.3}$$

where we define the filtered tracking error y as

$$y \equiv \dot{e} + \underline{K} e; \tag{4.4.4}$$

$\underline{K} = \text{diag}(\kappa_1, \kappa_2, \cdots, \kappa_n) > 0$; ρ is some non-negative scalar to be selected.

To connect J to the system to control, we modify the system equation (4.3.3) and integrate from 0 to t:

$$\int_0^t y^T(\rho M + D) y d\tau = \int_0^t y^T \Big[M(\ddot{q} + \rho y) + C\dot{q} + D\dot{\sigma} + g + \underline{d} - u - u_e \Big] d\tau, \tag{4.4.5}$$

where σ is defined as

$$\dot{\sigma} \equiv \dot{r} + \underline{K} e. \tag{4.4.6}$$

Note that σ is a desired trajectory corrected with tracking error.

We replace $\ddot{q}$ in (4.4.5) with $(\ddot{\sigma} - \dot{y})$ to circumvent the requirement of measuring angular accelerations. Then, we can rewrite equation (4.4.5) as

$$\begin{aligned} J &= \int_0^t y^T(\rho M + D)y d\tau \\ &= -\frac{1}{2}y^T My\Big|_0^t + \int_0^t y^T\Big(M(\ddot{\sigma} + \rho y) + C\dot{\sigma} + D\dot{\sigma} + g + \underline{\mathrm{d}} - u - u_e\Big)d\tau, \end{aligned} \tag{4.4.7}$$

where we have used the fact that

$$\int_0^t y^T M\dot{y}d\tau = \frac{1}{2}y^T My\Big|_0^t - \frac{1}{2}\int_0^t y^T\dot{M}yd\tau; \tag{4.4.8}$$

and that $(\dot{M} - 2C)$ is skew-symmetric ($y^T(\dot{M} - 2C)y = 0$) if the non-unique matrix C is chosen properly[4.43].

We can rewrite (4.4.7) as

$$J = \frac{1}{2}y(0)^T M(0)y(0) - \frac{1}{2}y^T My + \int_0^t y^T\Big(Wx + \underline{\mathrm{d}} - u - u_e\Big)d\tau, \tag{4.4.9}$$

where the $m\times 1$ true parameter vector x and the $n\times m$ function matrix W are defined such that

$$Wx \equiv M(\ddot{\sigma} + \rho y) + C\dot{\sigma} + D\dot{\sigma} + g. \tag{4.4.10}$$

We have used M and D for the weight of the performance index. However, we can use any combination of any differentiable positive-definite symmetric matrices with appropriate dimensions (e.g., any of M and D). Then, the definition of Wx changes accordingly.

4.4.2 Design of A Robust Adaptive Control Law Using A Performance Index

The objective in this section is to find a control law which stabilizes the system and minimizes the performance index J. Minimizing J minimizes the maximum magnitude of y, and consequently improves the transient response.

Since there is no general solution for nonlinear systems, we relax the conditions of minimizing J to those of reducing J.

A control law reduces J if the control law (u) satisfies the following constraint:

$$\int_0^t y^T u d\tau \geq 0, \quad \forall\, t \geq 0. \tag{4.4.11}$$

See (4.4.9). This constraint requires that any compensator (u) be a function of y. The constraint also requires the compensator u to contain W to compensate for the dynamics. We search for compensators which satisfy the constraint (4.4.11). However, we need to analyze the stability of the chosen control law (the chosen compensators) for the given system since we relax the conditions of minimizing J to those of reducing J.

Larger magnitude of gains of a stable control law results in smaller performance index J and hence smaller maximum tracking errors. However, as in linear control theory, increasing the magnitude of gains above certain values may excite high-frequency unmodelled dynamics. Accordingly, we reduce J as much as possible, not by increasing the magnitudes of the gains but by employing various compensators whose characteristics are much different from one another.

Based on the constraint (4.4.11), we find the following robust control law:

Theorem : Consider the following control law

$$u = \sum_{j=1}^{k_1} W\bar{x}_j + K_1 y + K_2 f + \sum_{j=3}^{k_2} K_j Y_f h_j, \tag{4.4.12}$$

with an adaptation law

$$\begin{aligned}
&\dot{\bar{x}}_j + P_{2j}\bar{x}_j = P_{1j}W^T y, \qquad \bar{x}_1(0) = x_o, \quad \bar{x}_j(0) = 0,\ j = 2, 3, \cdots; \\
&\dot{f} + P_3 f = K_2 y, \qquad f(0) = 0; \\
&\dot{h}_j + P_{4j} h_j = K_j Y_f y, \qquad h_j(0) = 0,\ j = 3, 4, \cdots,
\end{aligned} \tag{4.4.13}$$

where

$$\dot{Y}_f + P_f Y_f = P_f Y,$$

$$Y = \mathrm{diag}(y_1, y_2, \cdots, y_n). \tag{4.4.14}$$

Then, these control and adaptation laws guarantee that

$$|\dot{e}_i(t)| < \infty, \quad |e_i(t)| < \infty, \quad \text{and} \quad |\bar{x}_j| < \infty,$$
$$\forall\, t \geq 0, \quad \forall\, i = 1, 2, \cdots, n, \quad \forall\, j = 1, 2, \cdots, m, \tag{4.4.15}$$

if desired trajectories, disturbances, and control and adaptation gains satisfy the following constraints:

$$\begin{aligned}
&(i) \quad \mathcal{O}(r) \leq \mathcal{O}(\mu), \ \ \mathcal{O}(\dot{r}) \leq \mathcal{O}(\mu), \ \ \mathcal{O}(\ddot{r}) \leq \mathcal{O}(\mu^2), \ \ \mathcal{O}(r^{III}) \leq \mathcal{O}(\mu^4), \\
&(ii) \quad \mathcal{O}(\underline{\mathrm{d}}) \leq \mu, \\
&(iii) \quad \mathcal{O}(\rho) \leq \mu, \ \ \mathcal{O}(P_f) \leq \mu^2, \ \ \mu \leq \mathcal{O}(K_1) \leq \mu^2, \ \ \mathcal{O}(K_2) \leq \mu^2, \\
&\qquad \mathcal{O}(K_j) \leq \mu \ (j \geq 3), \ \ \mathcal{O}(P_{1j}) \leq \mu^0, \ \ \mu^{-1} < \mathcal{O}(P_{21}) \leq \mathcal{O}(P_{2j}) \leq \mu^2, \\
&\qquad \mu^{-1} < \mathcal{O}(P_{21}) \leq \mathcal{O}(P_3) \leq \mu^2, \ \ \mu^{-1} < \mathcal{O}(P_{21}) \leq \mathcal{O}(P_{4j}) \leq \mu^2,
\end{aligned} \tag{4.4.16}$$

where $\mu = t_s^{-\frac{1}{4}}$ with $t_s \ll 1$ and μ^0 denotes unity consistent with the other orders of μ.

Note that the bounds (4.4.16) are derived for revolute-joint robots. The structure of the dynamics of robots is the same regardless of the type of joint. Hence, the corresponding bounds for prismatic-joint or prismatic-revolute-joint robots are similar to those in (4.4.16) and they can be readily derived.

The various symbols appearing in the Theorem are given as follows:

K_1 is the $n \times n$ positive-definite diagonal matrix; K_2 and K_j $(j = 3, 4, \cdots)$ are the $n \times n$ positive-semi-definite diagonal matrices; P_{11} and P_{21} are the $m \times m$ positive-definite diagonal matrices; P_{1j} and P_{2j} $(j = 2, 3, \cdots)$ are the $m \times m$ positive-semi-definite and positive-definite diagonal matrices respectively; P_3 and P_{4j} $(j = 3, 4, \cdots)$ are the $n \times n$ positive-semi-definite and positive-definite diagonal matrices respectively; P_f is the $n \times n$ positive-definite diagonal matrix; k_1 and k_2

are some positive integers such that $k_1 \geq 1$ and $k_2 \geq 3$; $\mathcal{O}(\cdot)$ denotes the order of the argument.

The memory component $\bar{x}$ is the $m \times 1$ estimated parameter vector such that

$$W\bar{x} \equiv \bar{M}(\ddot{\sigma} + \rho y) + \bar{C}\dot{\sigma} + \bar{D}\dot{\sigma} + \bar{g}, \tag{4.4.17}$$

where $\bar{M}$, $\bar{C}$, $\bar{D}$, and $\bar{g}$ correspond to the unbarred variables computed with the estimated parameters.

Proof of this Theorem is in Appendix 4.A.

The block diagram of the Theorem is shown in Figure 4.1.

Note that in this Theorem, we adopt compensators from the Theorem 1 of Chapter 3, and modify them with a new adaptation law (the σ-modification law). In addition, we specify the stability bounds (4.4.16).

4.4.3 Improved Adaptation Laws

As memory components in the adaptation law (4.4.13), we used first-order filters instead of integrators to prevent instability due to parameter drift [4.11]. Consequently, the parameter $\bar{x}$ estimated by this adaptation law becomes small when $\|W^T y\|$ is small for more than some finite duration. See (4.4.13). $\|\cdot\|$ denotes the Euclidean norm of the argument vector. Near an end point of a trajectory, $\|W^T y\|$ becomes very small since the desired angular accelerations ($\ddot{r}$) and velocities ($\dot{r}$) are almost zero and the actual velocities ($\dot{q}$) and the tracking errors (y) are also small for stable control laws. Hence, $\bar{x}$ becomes very small near end points of trajectories. As a result, $\bar{x}$ must be refreshed to the nominal values of the parameters for smooth transient response whenever a manipulator moves from the end points.

To fix this problem, we propose new adaptation laws. We use integrators for the adaptation law when the magnitude of $\bar{x}$ is smaller than the preset value (or the nominal value), and otherwise, we use first-order filters with variable break frequencies, as follows:

$$\dot{\bar{x}}_1 + P_{21}\bar{x}_1 = P_{11}W^T y, \tag{4.4.18}$$

with

$$p_{2ji} = \begin{cases} 0, & \text{for } |\bar{x}_{1i}| < x_i^*, \quad i = 1, 2 \cdots, n; \\ p_{5i}(|\bar{x}_{1i}| - x_i^*), & \text{for } |\bar{x}_{1i}| \geq x_i^*, \quad i = 1, 2, \cdots, n, \end{cases} \tag{4.4.19}$$

where p_{5i} and x_i^* are selected such that $p_{5i} > 0$ and $x_i^* > |x_i|$; the subscript i denotes the i^{th} component of the corresponding vectors (x, $\bar{x}_1$ and x^*) or the i^{th} diagonal component of the corresponding matrices (P_{2j} and P_5).

Without loss of generality, we can define x_i as a positive number. Then, we also have the following improved adaptation law:

$$p_{2ji} = \begin{cases} 0, & \text{for } 0 < \bar{x}_{1i} < x_i^*, \quad i = 1, 2 \cdots, n; \\ p_{5i}, & \text{otherwise.} \end{cases} \tag{4.4.20}$$

Then, in equation (4.A.11) in Appendix 4.A,

$$(x - \bar{x}_1)^T P_{11}^{-1} P_{21}(x - \bar{x}_1) + (\bar{x}_1^T P_{11}^{-1} P_{21} \bar{x}_1 - x^T P_{11}^{-1} P_{21} x) \geq 0, \quad \forall\, \bar{x}. \tag{4.4.21}$$

As a result, $V(t)$ and hence J exclude the x term so that the error bounds become smaller in (4.A.26). See the definition of α_3 in (4.A.20). In this case, we have the constraint of $\mu^{-1} < \mathcal{O}(P_5) \leq \mu$ when we go through the stability analysis.

4.5 Remarks

1. The design procedure presented in this chapter is the inverse of that of Lyapunov's second method in Section 2.3.2.1 of Chapter 2. The Lyapunov's method searches for an appropriate lower-bounded function $V(t)$ for a given system and enforces $\dot{V}(t) \leq 0$ in order to stabilize the system. Then, as a by-product of stabilization, desired compensators are produced. In contrast, the present method searches for compensators for a given system toward minimizing a certain performance index, and then shows that these compensators lead to a lower-bounded function $V(t)$ whose time-derivative ($\dot{V}(t)$) along the trajectory of the given system is non-positive outside a certain ball.

2. Constraints (4.4.16) requires that the spectral ranges of the reference inputs and disturbances be limited not to excite high-frequency unmodelled dy-

namics, and that the magnitudes of control and adaptation gains be also limited to avoid excitation of high-frequency unmodelled dynamics.

3. Constraint (4.A.14) with (4.A.17) means that $\mathcal{S}_2$, the region of attraction, is finite (local) for nonzero t_s, and that all the initial conditions (tracking errors and parameter errors) must belong to $\mathcal{S}_2$ for stability.

4. When the adaptation law (4.4.13) is used, larger P_{21} causes larger tracking errors. See the x term in (4.A.20) with (4.A.26). However, smaller P_{21} causes less robustness (higher possibility of parameter drift). The new adaptation laws (4.4.19) and (4.4.20) solve these contradictory problems. Furthermore, the new adaptation laws provide asymptotic stability when no unmodelled dynamics and disturbances exist.

5. When we set $P_3 = 0$, $K_2 f$ becomes a PI feedback compensator. $K_1 y$ is a PD feedback compensator. Therefore, we may select the gains K_1 and K_2 using a linearized model of robot dynamics.

4.6 Computer Simulation

As an example, the present scheme has been applied to a two-link direct-drive manipulator shown in Figure 4.2. We simulate the scheme on a Sun Microsystems Sparkstation 1. We used a 4^{th}-order Runge-Kutta method[4.44] with adaptive step size to guarantee accuracy in the solution of the manipulator dynamics. The dynamics of the manipulator and the numerical values of its parameters are given in (3.6.1) - (3.6.3) in Chapter 3.

As a bounded disturbance, the mass 2 is doubled between 2 and 4 seconds. In addition, we simulate sensor noises using "drand48()," the random number generator in the Sparkstation 1. We added the sensor noises to both angular velocities and positions of links. The maximum magnitude of the noises is 5×10^{-4}.

In this simulation, we use only the first terms of the summations in the control and adaptation laws:

$$u_{ta} = W\bar{x} + K_1 y + K_2 f + K_3 Y_f h, \tag{4.6.1}$$

where

$$\dot{Y}_f + P_f Y_f = P_f Y; \tag{4.6.2}$$

$$Y = \mathrm{diag}(y_1, y_2, \cdots, y_n). \tag{4.6.3}$$

One of the adaptation laws is given by

$$\begin{aligned} \dot{\tilde{x}} + P_2 \tilde{x} &= P_1 W^T y; \\ \dot{f} + P_3 f &= K_2 y; \\ \dot{h} + P_4 h &= K_3 Y_f y. \end{aligned} \tag{4.6.4}$$

W and x are defined as follows:

$$\begin{aligned} x &= (x_1\ x_2\ \cdots x_{10})^T, \\ W &= \begin{bmatrix} w_1 & w_2 & w_3 & w_4 & w_5 & w_6 & 0 & 0 & 0 & 0 \\ 0 & 0 & 0 & 0 & 0 & 0 & w_7 & w_8 & w_9 & w_{10} \end{bmatrix}, \end{aligned} \tag{4.6.5}$$

with

$$\begin{aligned} w_1 =& w_7 = (\ddot{\sigma}_1 + \rho y_1) + (\ddot{\sigma}_2 + \rho y_2), \\ w_2 =& [2(\ddot{\sigma}_1 + \rho y_1) + (\ddot{\sigma}_2 + \rho y_2)] \cos(q_2) \\ & - (\dot{q}_2 \dot{\sigma}_1 + \dot{q}_1 \dot{\sigma}_2 + \dot{q}_2 \dot{\sigma}_2) \sin(q_2), \\ w_3 =& \ddot{\sigma}_1 + \rho y_1, \\ w_4 =& \dot{q}_1, \\ w_5 =& w_{10} = 10 \cos(q_1 + q_2), \\ w_6 =& 20 \cos(q_1), \\ w_8 =& (\ddot{\sigma}_1 + \rho y_1) \cos(q_2) + \dot{q}_1 \dot{\sigma}_1 \sin(q_2), \\ w_9 =& \dot{q}_2. \end{aligned} \tag{4.6.6}$$

When P_2 is set to be zero, the adaptive control law (4.6.1) - (4.6.6) is the same as the scheme proposed in Theorem 1 of Chapter 3 which will be called the **previous scheme** hereafter.

As in Chapter 3, we have computed the filterings associated with y in the control law by using the following trapezoid rule (Tustin's rule)[4.45]:

$$s \simeq \frac{2}{t_s}\frac{z-1}{z+1}. \tag{4.6.7}$$

To relieve the computational burden we use a dual-time update rule: 2 msec for the feedback compensators ($K_1 y + K_2 f + K_3 Y_f h$) and 10 msec for the feedforward compensator ($W\bar{x}$). To make our simulations realistic, we include delays of one sampling period in our control inputs for measurements, computations, and DA and AD conversions. Since we use a dual-time update technique, there are two different delays in our control inputs.

The desired trajectories for the simulation are chosen as

$$\begin{aligned} r_1 &= -\cos t, \\ r_2 &= -\cos 2t, \end{aligned} \tag{4.6.8}$$

which are shown in Figure 4.3.

To examine the robustness of adaptive control, we compare the present scheme with the previous counterpart. The numerical values of the control and adaptation gains for both schemes are as follows.

(1) Previous scheme:

$\underline{K} = 20I$; K_1=diag(400,150); $K_2 = 0$;

$P_f = 20I$; $P_1 = 100I$; $P_2 = 0$; $P_3 = 0$; $P_4 = 0.5I$; $K_3 = 400I$; $\rho = 15$.

(2) Present scheme:

$\underline{K} = 20I$; K_1=diag(400,150); $K_2 = 0$;

$P_f = 20I$; $P_1 = 800I$; $P_2 = .005I$; $P_3 = 0$; $P_4 = 0.5I$; $K_3 = 400I$; $\rho = 15$.

'I' denotes the identity matrix with appropriate dimension.

The initial values of the parameters of the dynamics for both schemes are the same (around 1/4 - 1/2 of the true values). The manipulator is assumed to be initially motionless.

Figures 4.4 and 4.5 show the tracking errors of joints 1 and 2 respectively for the previous scheme. Figure 4.6 explains the parameter estimation of the previous scheme for parameters x_2, x_4, x_6, x_8, and x_{10}. One of the parameters (x_4) drifts. When this parameter reaches a certain value, instability occurs and then all the parameters grow rapidly. Since instability is caused by the parameter drift, larger gains cause earlier instability. We have found that faster sinusoids (satisfying the condition of persistent excitation) suppress the parameter drift, and that slower sinusoids help the parameter drift.

Figures 4.7 and 4.8 show the tracking errors of the present scheme for joints 1 and 2 respectively. The parameter estimation is shown in Figure 4.9. Modification of the adaptation law prevents the parameter drift. The scheme maintains stability in the presence of disturbances, sensor noises, and unmodelled dynamics due to the feedback delays. The adaptation law (4.6.4), a simpler form of (4.4.13), by nature, causes nonzero tracking errors. See (4.A.20) and (4.A.26). We may have better results if we use the new adaptation laws (4.4.19) and (4.4.20). However, the tracking errors are within practical tolerances.

Through extensive simulations, we have found that instability occurs when any of initial errors, disturbances, sensor noises, sampling periods, desired trajectories and their time-derivatives, and control and adaptation gains is larger than its certain upper bound. This supports the stability analysis.

In spite of nonlinearities such as a step change of mass 2 which is not included in the derivation of the control law, the performance of the control law such as guarantee of stability and fast transient response is shown to be essentially unchanged. This is another favorable feature of the control law. This is because the sufficient condition for stability of the proposed scheme is too strong.

4.7 Conclusion

In this chapter, we have shown that the previous scheme may become unstable due to parameter drift. We have proposed some modified adaptation laws for the scheme proposed in Chapter 3 to prevent the parameter drift. Moreover, for the scheme redesigned with the modified adaptation laws, we have obtained stability bounds for disturbances, control and adaptation gains, and desired trajectories and their time-derivatives, in the presence of unmodelled dynamics due to feedback delays in the digital control systems. In contrast, no stability bounds have been provided in the literature of adaptive control of robots.

The results of the realistic simulations support the stability analysis and lead to the conclusion that the present scheme is robust (i.e., causes no parameter drift), in the presence of sensor noises, disturbances, and unmodelled dynamics due to feedback delays.

The dynamics of industrial manipulators having usually 6 degrees of freedom are complicated. Hence, implementation of the proposed scheme to these manipulators may not be so simple. Most of these manipulators use a gear-reduction mechanism in power transmission for larger torque with smaller actuators. As a consequence, the coupled dynamics are much suppressed. In this case, we may try a decentralized (jointwise) control scheme. In the next chapter, we will examine this in detail.

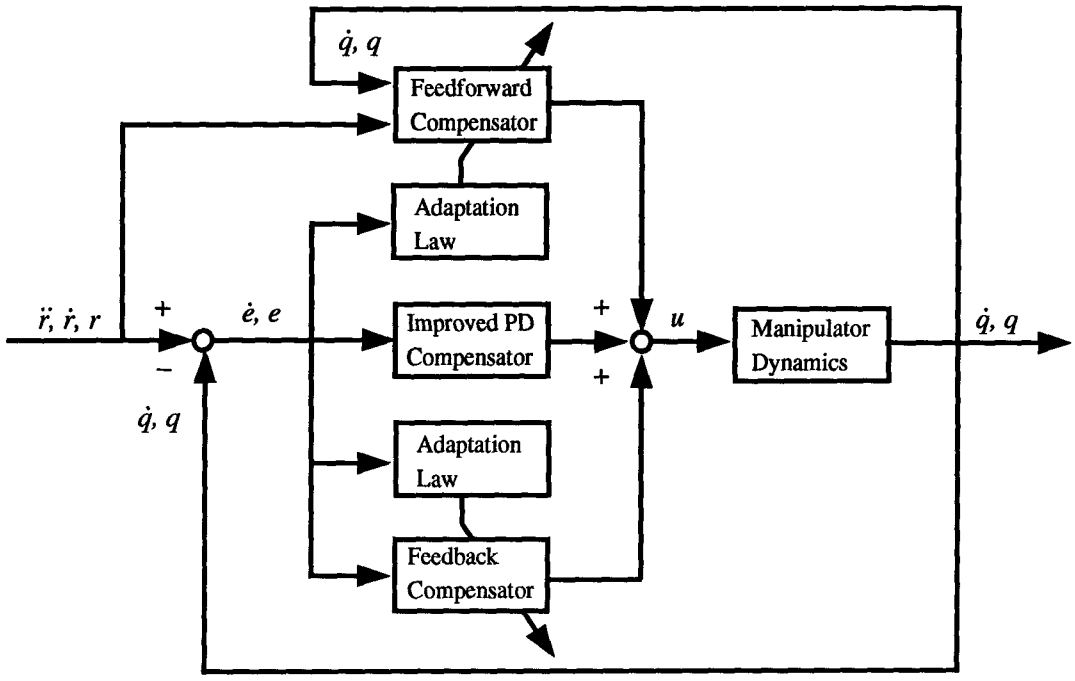

Figure 4.1 Schematic diagram of the proposed control law

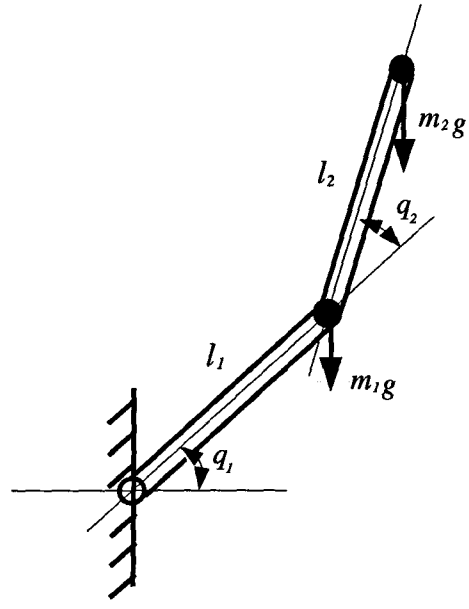

Figure 4.2 Modelling of links

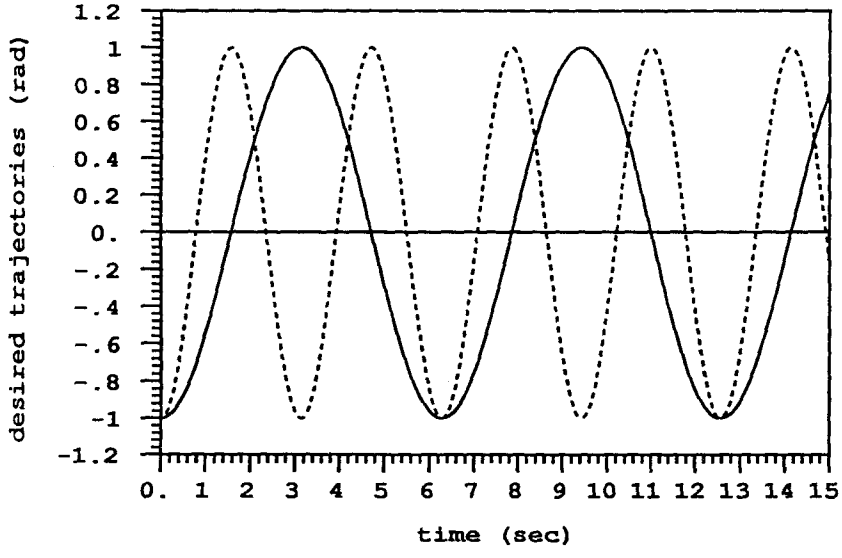

Figure 4.3 Desired trajectories: solid line for joint 1 and dotted line for joint 2

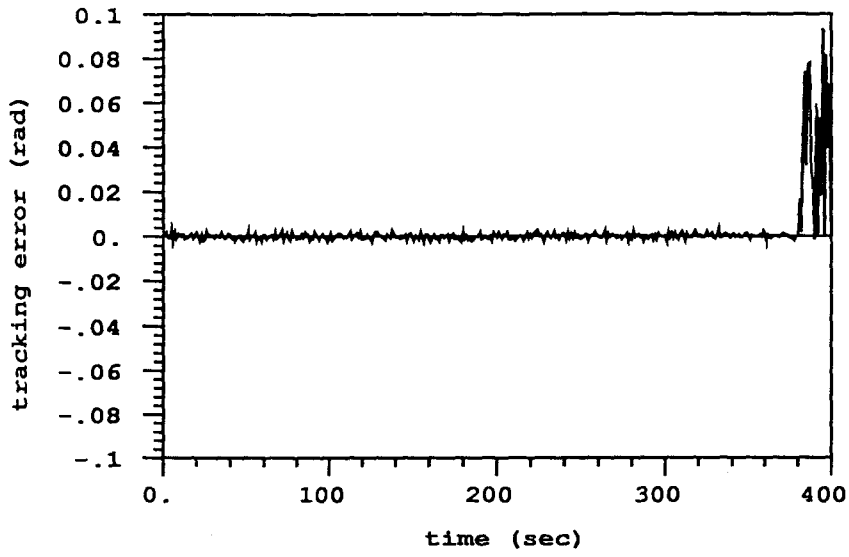

Figure 4.4 Tracking error of the previous scheme (joint 1): instability due to sensor noise

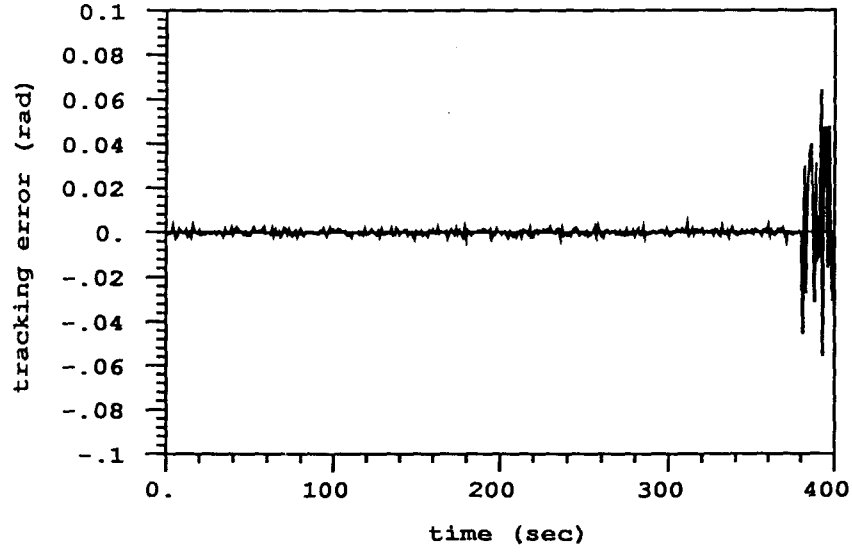

Figure 4.5 Tracking error of the previous scheme (joint 2): instability due to sensor noise

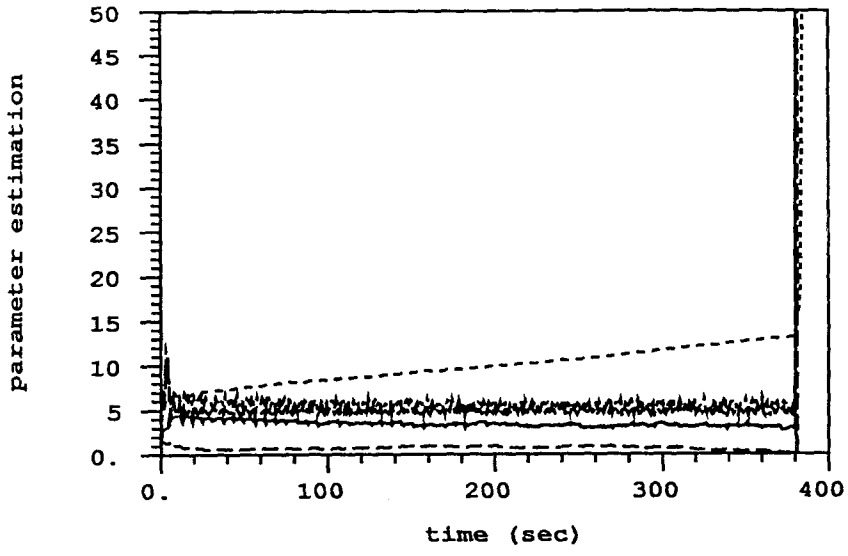

Figure 4.6 Parameter drift of the previous scheme due to sensor noise

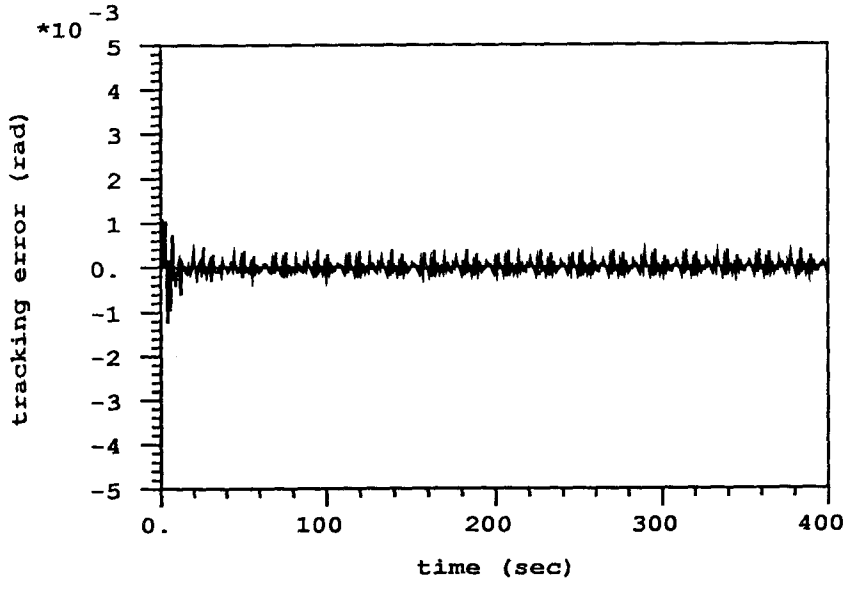

Figure 4.7 Tracking error of the present scheme (joint 1)

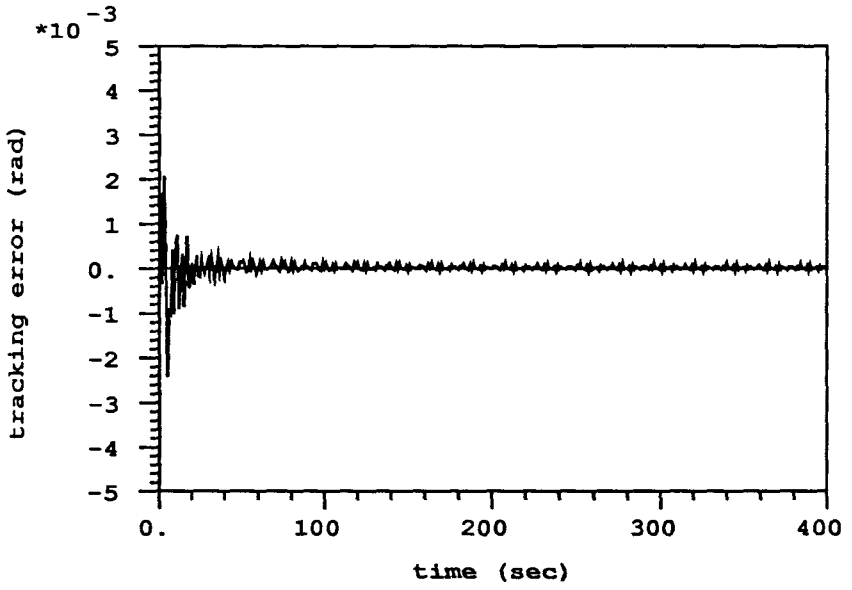

Figure 4.8 Tracking error of the present scheme (joint 2)

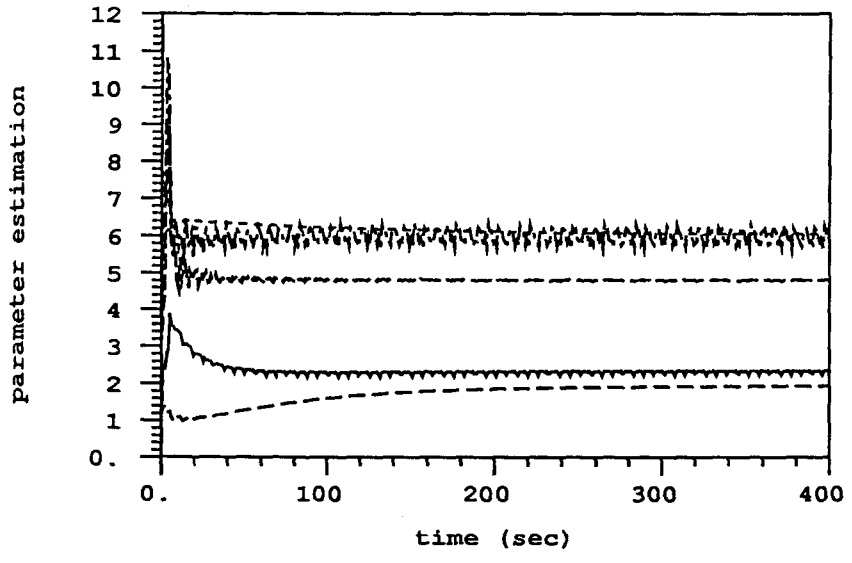

Figure 4.9 Parameter estimation of the present scheme

References

[4.1] Rohrs, C. E., Valavani, L., Atheans, M. and Stein, G., *Robustness of Adaptive Control Algorithms in the Presence of Unmodelled Dynamics,* IEEE Conf. on Decision and Control, Proc., pp. 3-11, 1982.

[4.2] Peterson, B. B. and Narendra, K. S., *Bounded Error Adaptive Control,* IEEE Trans. on Auto. Contr., Vol. AC-27, pp. 1161-1168, Dec. 1982.

[4.3] Samson, C., *Stability Analysis of Adaptively Controlled Systems Subject to Bounded Disturbances,* Automatica, Vol. 19, pp. 81-86, 1983.

[4.4] Kreisselmeier, G. and Narendra, K. S., *Stable Model Reference Adaptive Control in the Presence of Bounded Disturbances,* IEEE Trans. on Auto. Contr., Vol. AC-27, No. 6, pp. 1169-1175, Dec. 1982.

[4.5] Ioannou, P. A. and Tsakalis, K. S., *A Robust Direct Adaptive Controller,* IEEE Trans. on Auto. Contr., Vol. AC-31, No. 11, pp. 1033-1043, Nov. 1986.

[4.6] Ioannou, P. A., *Robust Adaptive Control with Zero Residual Tracking Errors,* IEEE Trans. on Auto. Contr., Vol. AC-31, No. 8, pp. 773-776, Aug. 1986.

[4.7] Ioannou, P. A. and Kokotovic, P. V., *Instability Analysis and Improvement of Robustness of Adaptive Control,* Automatica, Vol. 20, No. 5, pp. 583-594, 1984.

[4.8] Ioannou, P. A. and Kokotovic, P. V., *Robust Redesign of Adaptive Control,* IEEE Trans. on Auto. Contr., Vol. AC-29, No. 3, pp. 202-211, March 1984.

[4.9] Narendra, K. S. and Annaswamy, A. M., *A New Adaptive Law for Robust Adaptation Without Persistent Excitation,* IEEE Trans. on Auto. Contr., Vol. AC-32, No. 2, pp. 134-145, Feb. 1987.

[4.10] Dubowsky, S. and DesForges, D. F., *The Application of Model-Reference Adaptive Control to Robotic Manipulators,* ASME J. of DSMC, Vol. 101, pp. 193-200, 1979.

[4.11] Dubowsky, S. and Kornbluh, R., *On the Development of High Performance Adaptive Control Algorithms for Robotic Manipulators,* Robotics Research

edited by Inoue Hanafusa, pp. 119-126, 1984.

[4.12] Koivo, A. J. and Guo, T. M., *Adaptive Linear Controller for Robotic Manipulators,* IEEE Trans. on Aut. Contr., Vol. AC-28, No. 2, pp. 162-172, 1983.

[4.13] Koivo, A. J., Lewczyk, R. and Chiu, T. H., *Adaptive Path Control of a Manipulator with Visual Information,* IEEE Conference on Robotics, Atlanta, March 1984.

[4.14] Koivo, A. J., *Adaptive Position-Velocity-Force Control of Two Manipulators,* 24th IEEE Conf. on Decision and Control, Fort Lauderdale, Fla., 1985.

[4.15] Koivo, A. J., *Force-Velocity Control with Self-Tuning for Robotic Manipulators,* IEEE Conference on Robotics and Automation, San Francisco, April 1986.

[4.16] Walters, R. G. and Bayoumi, M. M., *Application of a Self-Tuning Pole Placement Regulator to an Industrial Manipulator,* IEEE, Conference on Decision and Control, pp. 323-329, 1982.

[4.17] Leininger, G. G. and Wang , S., *Pole Placement Self-Tuning Control of Manipulators,* IFAC Symposium on Computer Aided Design of Multivariable Technological Systems, West Lafayette, Ind., September 15-17, 1982.

[4.18] Leininger, G. G., *Self-Tuning Control of Manipulators,* International Symposium on Advanced Software in Robotics, Liege, Belgium, May 1983.

[4.19] Leininger, G. G., *Adaptive Control of Manipulators Using Self-Tuning Methods,* Robotics Research, Chap.9 edited by M. Brady and R. Pall, 1984.

[4.20] Backes, P., *Real Time Control with Adaptive Manipulator Control Schemes,* M.S. Thesis, Purdue University, School of Mechanical Engineering, West Lafayette, Ind., December 1984.

[4.21] Backes, P., Leininger, G. G., *Real Time Cartesian Coordinate Hybrid Control of a Puma 560 Manipulator,* IEEE Conference on Robotics and Automation, St. Louis, March 1985.

[4.22] Sundareshan, M. K. and Koenig, M. A., *Decentralized Model Reference Adaptive Control of Robotic Manipulators,* Proceedings, Automatic Control

Conference, pp. 44-49, 1985.

[4.23] Takegaki, M. and Arimoto, S., *An Adaptive Trajectory Control of Manipulators,* Int. J. of Control, Vol. 34, No. 2, pp. 219-230, 1981.

[4.24] Seraji, H., *Direct Adaptive Control of Manipulators in Cartesian Space,* J. of Robotic Systems, Vol. 4, No. 1, pp. 157-178, 1987.

[4.25] Seraji, H., *Decentralized Adaptive Control of Manipulators: Theory, Simulation, and Experimentation,* IEEE Trans. on Robotics and Automation, Vol. 5, No. 2, pp. 183-201, April 1989.

[4.26] Oh, B. J., Jamshidi, M. and Seraji, H., *Decentralized Adaptive Control,* Proc. of IEEE Int. Conf. on Robotics and Automation, pp. 1016-1021, 1988.

[4.27] Gavel, D. T. and Hsia, T. C., *Decentralized Adaptive Control of Robotic Manipulators,* Proc. of IEEE Int. Conf. on Robotics and Automation, pp. 1230-1235, April 1987.

[4.28] Gavel, D. T. and Hsia, T. C., *Decentralized Adaptive Control Experiments with the PUMA Robot Arm,* Proc. of IEEE Int. Conf. on Robotics and Automation, pp. 1022-1027, 1988.

[4.29] Lim, K. Y. and Eslami, M., *New Controller Design for Robot Manipulator Systems,* Proc., Amer. Contr. Conf., pp. 38-43, June 1985.

[4.30] Lim, K. Y. and Eslami, M., *Adaptive Controller Designs for Robot Manipulator Systems Yielding Reduced Cartesian Error,* IEEE Trans. on Automatic Control., Vol. AC-32, No. 2, pp. 184-187, Feb. 1987.

[4.31] Lim, K. Y. and Eslami, M., *Robust Adaptive Controller Designs for Robot Manipulator Systems,* IEEE J. of Robotics and Automation, Vol. RA-3, No. 1, pp. 54-66, Feb. 1987.

[4.32] Nicosia, S. and Tomei, P., *Model Reference Adaptive Control Algorithms for Industrial Robots,* Automatica, Vol. 20, No. 5, pp. 635-644, 1984.

[4.33] Balestrino, A., De Maria, G. and Sciavicco, L., *An Adaptive Model Following Control for Robotic Manipulators,* ASME J. of DSMC, Vol. 105, pp. 143-151, 1983.

[4.34] Ozguner, U., Yurkovich, S. and Al-Abbass, F, *Decentralized Variable Structure Control of Two-Arm Robotic System,* Proc. of IEEE Int. Conf. on Robotics and Automation, pp. 1248-1254, 1987.

[4.35] Pandian, S. R., Hanmandlu, M. and Gopal, M., *A Decentralized Variable Structure Model Following Controller for Robot Manipulators,* Proc. of IEEE Int. Conf. on Robotics and Automation, pp. 1324-1328, 1988.

[4.36] Craig, J. J., *Adaptive Control of Mechanical Manipulators,* Ph.D. thesis, Stanford University, Department of Electrical Engineering, Stanford, CA 94305, June 1986; Also published by Addison-Wesley

[4.37] Craig, J. J., Hsu, P. and Sastry, S. S., *Adaptive Control of Mechanical Manipulators,* Proc. IEEE Conf. on Robotics and Automation, pp. 190-195, 1986.

[4.38] Slotine, J. J. E. and Li, W., *On the Adaptive Control of Robot Manipulators,* Proc. ASME Winter Annual Meeting, 1986.

[4.39] Slotine, J. J. E. and Li, W., *Adaptive Manipulator Control: Parameter Convergence and Task-Space Strategies,* Proc. of the 1987 American Control Conference, pp. 828-835, 1987.

[4.40] Slotine, J. J. E. and Li, W., *Adaptive Manipulator Control: A Case Study,* Proc. of the 1987 Int. Conf. on Robotics and Automation, pp. 1392-1400, 1987.

[4.41] Reed, J. S. and Ioannou, P. A., *Instability Analysis and Robust Adaptive Control of Robotic Manipulators,* Conf. on Decision and Control, Proc., pp. 1607-1612, Dec. 1988.

[4.42] Schwartz, H. M., Warshaw. G. and Janabi, T., *Issues in Adaptive Robot Control,* American Control Conf., Vol. 3, pp. 2797-2805, 1990.

[4.43] Arimoto, A. and Miyazaki, F., *Stability and Robustness of PID Feedback Controller for Robot Manipulators of Sensory Capability,* Robotics Research: The First International Symposium edited by Brady, M. and Paul, R., pp. 783-799, 1984.

[4.44] Press, W. H., Flannery, B. P., Teukolsky, S. A. and Vetterting, W. T., *Numerical Recipes: The Art of Scientific Computing,* Cambridge, 1986.

[4.45] Franklin, G. F. and Powell, J. D., *Digital Control of Dynamic Systems,* Addison-Wesley, Reading, 1980.

Appendix 4.A: Proof of Theorem

To prove the Theorem, we first insert the designed control and adaptation laws into J. Secondly, we derive a lower-bounded function $V(t)$ and its time-derivative ($\dot{V}(t)$) along the trajectory of the given system. Finally, we limit the bounds of disturbances, control and adaptation gains, and desired trajectories and their time-derivatives in order to guarantee $\dot{V}(t) \leq 0$.

(I) For simplicity, we define first-order operators $\mathcal{F}_{1j}$, $\mathcal{F}_2$, and $\mathcal{F}_{3j}$ in relation to the adaptation law (4.4.13) such that

$$\begin{aligned} \dot{\bar{x}}_j &= \mathcal{F}_{1j}[P_{1j}W^T y]; \\ f &= \mathcal{F}_2[K_2 y]; \\ h_j &= \mathcal{F}_{3j}[K_j Y_f y]. \end{aligned} \tag{4.A.1}$$

Then, we have some elementary relationships, which will be shown using the following scalar differential equation and corresponding operator $\mathcal{F}$:

$$\dot{v} + bv = az, \qquad b \geq 0, \quad a > 0, \tag{4.A.2}$$

$$\Longrightarrow \qquad v = \mathcal{F}[az] \equiv ae^{-h(t)}\Big(\int_0^t ze^{h(\tau)}d\tau + \frac{v(0)}{a}\Big), \tag{4.A.3}$$

where

$$h(t) \equiv \int_0^t b(\tau)d\tau. \tag{4.A.4}$$

Then, we have the following relationship:

$$\begin{aligned} \int_0^{t_1} z(t)dt =& \frac{1}{a}\Big\{\mathcal{F}[az(t_1)] + \int_0^{t_1} b\mathcal{F}[az(t)]dt - v(0)\Big\}, \\ & \forall\, a > 0,\ b(t) \geq 0,\ |\dot{b}(t)| < \infty,\ z(t),\ \text{at } [0, t_1]; \end{aligned} \tag{4.A.5}$$

and

$$\int_0^{t_1} z(t)\mathcal{F}[az(t)]dt = \frac{1}{a}\Big(\frac{1}{2}\Big[\mathcal{F}[az(t_1)]\Big]^2 + \int_0^{t_1} b\Big[\mathcal{F}[az(t)]\Big]^2 dt - \frac{v^2(0)}{2}\Big),$$
$$\forall\, a>0,\ b(t)\geq 0,\ |\dot{b}(t)|<\infty,\ z(t),\ \text{at } [0,t_1]. \qquad (4.A.6)$$

(II) We insert the chosen control and adaptation laws (4.4.12) and (4.4.13) into equation (4.4.9):

$$\begin{aligned}
&\int_0^t y^T(\rho M+D)y d\tau + \frac{1}{2}\Big(y^T My - y(0)^T M(0)y(0)\Big)\\
&\quad = \int_0^t y^T\Big[W\Big(x-\sum_{j=1}^{k_1}\bar{x}_j\Big) + \Big(\underline{d}-u_e-K_1 y\Big) - K_2 f - \sum_{j=3}^{k_2} K_j Y_f h_j\Big]d\tau\\
&\quad = x^T P_{11}^{-1}\Big(\bar{x}_1 + \int_0^t P_{21}\bar{x}_1 d\tau - x_o\Big)\\
&\qquad - \int_0^t y^T\Big[W\sum_{j=1}^{k_1}\bar{x}_j - \Big(\underline{d}-u_e-K_1 y\Big) + K_2 f + \sum_{j=3}^{k_2} K_j Y_f h_j\Big]d\tau, \quad (4.A.7)
\end{aligned}$$

where we have applied (4.A.5) with (4.A.1).

Using (4.A.6) and (4.A.1), we have

$$\begin{aligned}
&\int_0^t y^T(\rho M+D)y d\tau + \frac{1}{2}\Big(y^T My - y(0)^T M(0)y(0)\Big)\\
&\quad = x^T P_{11}^{-1}\Big(\bar{x}_1 + \int_0^t P_{21}\bar{x}_1 d\tau - x_o\Big)\\
&\qquad - \frac{1}{2}\Big(\bar{x}_1^T P_{11}^{-1}\bar{x}_1 + 2\int_0^t \bar{x}_1^T P_{11}^{-1}P_{21}\bar{x}_1 d\tau - x_o^T P_{11}^{-1}x_o\Big)\\
&\qquad - \frac{1}{2}\sum_{j=2}^{k_1}\Big(\bar{x}_j^T P_{1j}^{-1}\bar{x}_j + 2\int_0^t \bar{x}_j^T P_{1j}^{-1}P_{2j}\bar{x}_j d\tau\Big) + \int_0^T y^T\Big(\underline{d}-u_e-K_1 y\Big)d\tau\\
&\qquad - \Big(\frac{1}{2}f^T f + \int_0^t f^T P_3 f d\tau\Big) - \sum_{j=3}^{k_2}\Big[\frac{1}{2}h_j^T h_j + \int_0^t h_j^T P_{4j} h_j d\tau\Big]\\
&\quad = \Big[\Big(x^T P_{11}^{-1}\bar{x}_1 - \frac{1}{2}\bar{x}_1^T P_{11}^{-1}\bar{x}_1\Big) - \Big(x^T P_{11}^{-1}x_o - \frac{1}{2}x_o^T P_{11}^{-1}x_o\Big)\Big]
\end{aligned}$$

$$
\begin{aligned}
&+\int_0^t \Big(x^T P_{11}^{-1} P_{21}\bar{x}_1 - \bar{x}_1^T P_{11}^{-1} P_{21}\bar{x}_1\Big)d\tau \\
&-\frac{1}{2}\sum_{j=2}^{k_1}\Big(\bar{x}_j^T P_{1j}^{-1}\bar{x}_j + 2\int_0^t \bar{x}_j^T P_{1j}^{-1} P_{2j}\bar{x}_j d\tau\Big) + \int_0^T y^T\Big(\underline{\mathrm{d}} - u_e - K_1 y\Big)d\tau \\
&-\Big(\frac{1}{2}f^T f + \int_0^t f^T P_3 f d\tau\Big) - \sum_{j=3}^{k_2}\Big[\frac{1}{2}h_j^T h_j + \int_0^t h_j^T P_{4j} h_j d\tau\Big] \\
=&\frac{1}{2}\Big[(x-x_o)^T P_{11}^{-1}(x-x_o) - (x-\bar{x}_1)^T P_{11}^{-1}(x-\bar{x}_1)\Big] \\
&-\frac{1}{2}\int_0^t \Big((x-\bar{x}_1)^T P_{11}^{-1} P_{21}(x-\bar{x}_1) + (\bar{x}_1^T P_{11}^{-1} P_{21}\bar{x}_1 - x^T P_{11}^{-1} P_{21} x)\Big)d\tau \\
&-\frac{1}{2}\sum_{j=2}^{k_1}\Big(\bar{x}_j^T P_{1j}^{-1}\bar{x}_j + 2\int_0^t \bar{x}_j^T P_{1j}^{-1} P_{2j}\bar{x}_j d\tau\Big) + \int_0^T y^T\Big(\underline{\mathrm{d}} - u_e - K_1 y\Big)d\tau \\
&-\Big(\frac{1}{2}f^T f + \int_0^t f^T P_3 f d\tau\Big) - \sum_{j=3}^{k_2}\Big[\frac{1}{2}h_j^T h_j + \int_0^t h_j^T P_{4j} h_j d\tau\Big], \qquad (4.A.8)
\end{aligned}
$$

where it is assumed that x is the $m\times 1$ unknown but constant vector.

We rewrite equation (4.A.8) as

$$
\begin{aligned}
J \equiv& \int_0^t y^T(\rho M + D)y d\tau \\
=&\frac{1}{2}\Big(y(0)^T M(0) y(0) + (x-x_o)^T P_{11}^{-1} P_{21}(x-x_o)\Big) - V(t) \\
&-\frac{1}{2}\int_0^t \Big((x-\bar{x}_1)^T P_{11}^{-1} P_{21}(x-\bar{x}_1) + (\bar{x}_1^T P_{11}^{-1} P_{21}\bar{x}_1 - x^T P_{11}^{-1} P_{21} x)\Big)d\tau \\
&-\sum_{j=2}^{k_1}\int_0^t \bar{x}_j^T P_{1j}^{-1} P_{2j}\bar{x}_j d\tau + \int_0^T y^T\Big(\underline{\mathrm{d}} - u_e - K_1 y\Big)d\tau \\
&-\int_0^t f^T P_3 f d\tau - \sum_{j=3}^{k_2}\int_0^t h_j^T P_{4j} h_j d\tau, \qquad (4.A.9)
\end{aligned}
$$

where the non-negative function $V(t)$ is defined as

$$V(t) \equiv \frac{1}{2}\Big[y^T M y + (x-\bar{x}_1)^T P_{11}^{-1}(x-\bar{x}_1) + \sum_{j=2}^{k_1} \bar{x}_j^T P_{1j}^{-1} \bar{x}_j + f^T f + \sum_{j=3}^{k_3} h_j^T h_j\Big] \geq 0. \tag{4.A.10}$$

Then, it is obvious that the $\bar{x}_j$ $(j = 2, 3, \cdots)$, f, and h_j $(j = 3, 4, \cdots)$ terms reduce the performance index J. Hence, these terms reduce the maximum magnitude of y, the filtered tracking error. Accordingly, these terms improve the transient behavior of the system.

We can also rewrite equation (4.A.8) as

$$\begin{aligned} V(t) =& \frac{1}{2}\Big(y(0)^T M(0) y(0) + (x-x_o)^T P_{11}^{-1} P_{21}(x-x_o)\Big) \\ & - \int_0^t \Big(y^T(\rho M + D + K_1)y - y^T \underline{d} + y^T(\delta_1 u - t_s \dot{u})\Big) d\tau \\ & - \frac{1}{2}\int_0^t \Big((x-\bar{x}_1)^T P_{11}^{-1} P_{21}(x-\bar{x}_1) + (\bar{x}_1^T P_{11}^{-1} P_{21} \bar{x}_1 - x^T P_{11}^{-1} P_{21} x)\Big) d\tau \\ & - \sum_{j=2}^{k_1} \int_0^t \bar{x}_j^T P_{1j}^{-1} P_{2j} \bar{x}_j d\tau - \int_0^t f^T P_3 f d\tau - \sum_{j=3}^{k_2} \int_0^t h_j^T P_{4j} h_j d\tau. \end{aligned} \tag{4.A.11}$$

From this, we obtain the time-derivative of $V(t)$ along the trajectory of the given system:

$$\begin{aligned} \dot{V}(t) =& -\Big(y^T(\rho M + D + K_1)y - y^T \underline{d} + y^T(\delta_1 u - t_s \dot{u})\Big) \\ & - \frac{1}{2}\Big((x-\bar{x}_1)^T P_{11}^{-1} P_{21}(x-\bar{x}_1) + (\bar{x}_1^T P_{11}^{-1} P_{21} \bar{x}_1 - x^T P_{11}^{-1} P_{21} x)\Big) \\ & - \sum_{j=2}^{k_1} \bar{x}_j^T P_{1j}^{-1} P_{2j} \bar{x}_j - f^T P_3 f - \sum_{j=3}^{k_2} h_j^T P_{4j} h_j. \end{aligned} \tag{4.A.12}$$

The true parameter x is bounded and the disturbance vector $\underline{d}$ is assumed to be bounded. Therefore, when δ_1=t_s=0, any initial $V(t)$ converges into a bounded set $\mathcal{S}_1 = \{(y, \bar{x}_j, f, h_j)\}$ which is a function of x, $\underline{d}$, control and adaptation gains,

etc. This means that $V(t)$ is bounded for all time $t \geq 0$. Then, from the definition of $V(t)$ in (4.A.10), y, $\bar{x}_j$, f, and h_j are all bounded for all time $t \geq 0$.

However, when $\delta_1 \neq 0$ or $t_s \neq 0$, $\dot{u}$ may grow unbounded coupled with the control and adaptation laws.

(III) To stabilize the system (i.e., to enforce $\dot{V}(t) \leq 0$ outside B_1), we make the sign-indefinite $\dot{u}$ term in (4.A.12) much smaller than the other terms. Since $t_s \ll 1$, the following constraints stabilize the system:

$$\begin{aligned} &\mathcal{O}(\delta_1 u) \ll \mathcal{O}(K_1 y); \\ &\mathcal{O}(t_s^{\frac{1}{2}} \dot{u}) \leq \mathcal{O}(K_1 y). \end{aligned} \tag{4.A.13}$$

To find the orders of u, $\dot{u}$, K_1, and y, we restrict our analysis inside a set $\mathcal{S}_2$ ($\supset \mathcal{S}_1$):

$$\mathcal{S}_2 = \{(y, \bar{x}_j, f, h_j) \mid V \leq \mu^2\}, \tag{4.A.14}$$

with

$$\mu \equiv \frac{a}{t_s}, \tag{4.A.15}$$

for some finite positive scalar a to be determined later. Note that the size of the set has not been determined yet.

Without loss of generality, we assume that the upper bounds of k_1 and k_2 are limited so that they do not affect our order analysis. Then, inside the set $\mathcal{S}_2$, $\mathcal{O}(y) \leq \mu$, $\mathcal{O}(Y) \leq \mu$, $\mathcal{O}(f) \leq \mu$, and $\mathcal{O}(h_j) \leq \mu$. For simplicity, we limit the orders of P_{11} and P_{1j} to μ^0, where μ^0 denotes unity consistent with the other orders of μ. Then $\mathcal{O}(x - \bar{x}_1) \leq \mu$ and $\mathcal{O}(\bar{x}_j) \leq \mu$. We can readily include the orders of P_{11} and P_{1j} in this analysis when we set them far from $\mathcal{O}(\mu^0)$.

Equations (4.4.4) and (4.4.14) are stable first-order differential equations. Hence, inside the set $\mathcal{S}_2$, $\mathcal{O}(\dot{e}) \leq \mu$, $\mathcal{O}(e) \leq \mu$, and $\mathcal{O}(Y_f) \leq \mu$ under the constraints of $\mathcal{O}(\dot{e}(0)) \leq \mu$, $\mathcal{O}(e(0)) \leq \mu$, $\mathcal{O}(Y_f(0)) \leq \mu$, and $\mathcal{O}(\underline{K}) = \mu^0$. We assume for all time $t \geq 0$ that the desired trajectory satisfies $\mathcal{O}(r) \leq \mu$ and $\mathcal{O}(\dot{r}) \leq \mu$. Then the orders of $\dot{q}$ and q can be obtained as $\mathcal{O}(\dot{q}) \leq \mu$ and $\mathcal{O}(q) \leq \mu$. We also assume that $\mathcal{O}(x) = \mu^0$, which results in $\mathcal{O}(\bar{x}_1) \leq \mu$.

Then, under the constraint of (4.4.16), we can obtain the following bounds:

$$u \leq \mathcal{O}(\mu^3)\underline{u}_1;$$
$$\dot{u} \leq \mathcal{O}(\mu^5)\underline{u}_2, \qquad (4.A.16)$$

for some $n\times 1$ vectors $\underline{u}_1(t)$ and $\underline{u}_2(t)$ of order μ^0. See Appendix 4.B for detailed derivations.

The bounds (4.A.16) are derived for revolute-joint robots. The corresponding bounds for prismatic-joint or prismatic-revolute-joint robots are similar to those in (4.A.16) and they can be readily derived. In this case, the stability analysis (proof) is basically the same as that described below.

(IV) The first constraint in (4.A.13) is already satisfied. See (4.A.16) and (4.B.5). To stabilize the system, we satisfy the second constraint in (4.A.13) by limiting the upper bound of a in (4.A.15):

$$(4.A.13) \quad \Longrightarrow \quad \mu^5 \cdot t_s^{\frac{1}{2}} \leq \mu^3 \quad \Longrightarrow \quad a^2 \leq t_s^{\frac{3}{2}}$$
$$\Longrightarrow \quad a \leq t_s^{\frac{3}{4}} \quad \Longrightarrow \quad \mu \leq t_s^{-\frac{1}{4}}. \qquad (4.A.17)$$

Then, from (4.A.16), there exist $n\times 1$ vectors $\underline{u}_o(t)$ and $\underline{u}_*(t)$ such that $\underline{u}_o \leq \mathcal{O}(\mu^3)$, $\underline{u}_* \leq \mathcal{O}(\mu^3)$,

$$t_s y^T \dot{u} \leq t_s \|\dot{u}\| \|y\| \leq t_s^{\frac{1}{2}} \|\underline{u}_o\| \|y\|,$$
$$\delta_1 y^T u \leq \delta_1 \|u\| \|y\| \leq \delta_1 \|\underline{u}_*\| \|y\|. \qquad (4.A.18)$$

Then, (4.A.12) becomes

$$\dot{V}(t) \leq -\Big(y^T(\rho M + D + K_1)y - \|y\|\|\underline{d}\| - \delta_1\|\underline{u}_*\|\|y\| - t_s^{\frac{1}{2}}\|\underline{u}_o\|\|y\|\Big)$$
$$-\frac{1}{2}\Big((x-\bar{x}_1)^T P_{11}^{-1} P_{21}(x-\bar{x}_1) - x^T P_{11}^{-1} P_{21} x\Big)$$
$$-\sum_{j=2}^{k_1} \bar{x}_j^T P_{1j}^{-1} P_{2j} \bar{x}_j - f^T P_3 f - \sum_{j=3}^{k_2} h_j^T P_{4j} h_j$$

$$\leq - y^T(\rho M + D + \frac{1}{2}K_1)y - \alpha_1\|y\|^2 + \alpha_2\|y\| + \alpha_3$$
$$- \frac{1}{2}(x - \bar{x}_1)^T P_{11}^{-1} P_{21}(x - \bar{x}_1)$$
$$- \sum_{j=2}^{k_1} \bar{x}_j^T P_{1j}^{-1} P_{2j} \bar{x}_j - f^T P_3 f - \sum_{j=3}^{k_2} h_j^T P_{4j} h_j, \qquad (4.A.19)$$

where

$$\alpha_1 = \lambda_{\min}(\frac{1}{2}K_1)$$
$$\alpha_2 = \max(\|\underline{d}\| + \delta_1\|\underline{u}_*\| + t_s^{\frac{1}{2}}\|\underline{u}_o\|)$$
$$\alpha_3 = \frac{1}{2}x^T P_{11}^{-1} P_{21} x. \qquad (4.A.20)$$

When sensor resolutions are sufficiently small, we can safely assume that $\delta_1 \leq t_s^{\frac{1}{2}}$. See (4.3.2). Consequently, from (4.4.16), (4.A.17), and (4.A.18), we obtain $\mathcal{O}(\alpha_1) \leq \mu^2$, $\mathcal{O}(\alpha_2) \leq \mu$, and $\mathcal{O}(\alpha_3) = \mathcal{O}(P_{21}) \leq \mu^2$.

We complete the square to remove the α_2 term:

$$\dot{V}(t) \leq - y^T(\rho M + D + \frac{1}{2}K_1)y - \frac{1}{2}(x - \bar{x}_1)^T P_{11}^{-1} P_{21}(x - \bar{x}_1)$$
$$- \sum_{j=2}^{k_1} \bar{x}_j^T P_{1j}^{-1} P_{2j} \bar{x}_j - f^T P_3 f - \sum_{j=3}^{k_2} h_j^T P_{4j} h_j + \alpha_3 + \alpha_4, \quad (4.A.21)$$

where

$$\alpha_4 = \frac{\alpha_2^2}{4\alpha_1} \qquad \left[\leq \mathcal{O}(\mu) \quad \text{if } \mathcal{O}(\alpha_1) \geq \mu \right]. \qquad (4.A.22)$$

We can rewrite (4.A.21) using $V(t)$ in (4.A.10):

$$\dot{V}(t) + \beta V(t) \leq \alpha_3 + \alpha_4 - \alpha_5(t) \qquad (4.A.23)$$

with

$$\alpha_5(t) = \left[y^T(\rho M + D + \frac{1}{2}K_1)y - \frac{\beta}{2}y^T M y \right]$$

$$+\frac{1}{2}\Big[(x-\bar{x}_1)^T P_{11}^{-1} P_{21}(x-\bar{x}_1) - \beta(x-\bar{x}_1)^T P_{11}^{-1}(x-\bar{x}_1)\Big]$$

$$+\sum_{j=2}^{k_1}\Big[\bar{x}_j^T P_{1j}^{-1} P_{2j}\bar{x}_j - \frac{\beta}{2}\bar{x}_j^T P_{1j}^{-1}\bar{x}_j\Big] + \Big[f^T P_3 f - \frac{\beta}{2} f^T f\Big]$$

$$+\sum_{j=3}^{k_2}\Big[h_j^T P_{4j} h_j - \frac{\beta}{2} h_j^T h_j\Big] \geq 0, \qquad (4.A.24)$$

where the positive constant β is chosen to be the maximum value which makes the expressions in all the brackets ($[\cdots]$) non-negative. Then, $\mathcal{O}(\beta) \leq \mu^2$. See (4.4.16) and (4.A.24).

The solution of (4.A.23) is given by

$$V(t) \leq \exp[-\beta t]\Big(V(0) + \int_0^t \{\alpha_3 + \alpha_4 - \alpha_5(\tau)\}\exp[\beta\tau]d\tau\Big). \qquad (4.A.25)$$

Consequently, we conclude that any initial $V(t)$ belonging to the set $\mathcal{S}_2$ converges into the following residual set:

$$\mathcal{S}_3 = \Big\{(y, \bar{x}_j, f, h_j) \mid V(t) \leq \exp[-\beta t]\int_0^t \{\alpha_3 + \alpha_4 - \alpha_5(\tau)\}\exp[\beta\tau]d\tau$$
$$\leq \frac{1}{\beta}(\alpha_3 + \alpha_4)\Big\} \qquad (4.A.26)$$

at a rate of at least exp[-βt]. Since $\mathcal{O}(\beta) \leq \mu^2$, $\mathcal{O}(\alpha_3) = \mathcal{O}(P_{21}) \leq \mu^2$, and $\mathcal{O}(\alpha_4) \leq \mu$, the size of $\mathcal{S}_3$ is given by $\mu^0 \leq \mathcal{O}(\{\alpha_3 + \alpha_4\}/\beta) < \mu^2$ under the constraints that

$$\mu \leq \mathcal{O}(K_1) \leq \mu^2, \quad \mu^{-1} < \mathcal{O}(P_{21}) \leq \mathcal{O}(P_{2j}) \leq \mu^2,$$
$$\mu^{-1} < \mathcal{O}(P_{21}) \leq \mathcal{O}(P_3) \leq \mu^2, \quad \mu^{-1} < \mathcal{O}(P_{21}) \leq \mathcal{O}(P_{4j}) \leq \mu^2. \qquad (4.A.27)$$

In this case, $\mathcal{O}(\beta) = \min[\mathcal{O}(K_1), \mathcal{O}(P_{21})]$. The constraints in (4.A.27) satisfy the condition $\mathcal{O}(\alpha_1) \geq \mu$ in (4.A.22). See (4.A.20), (4.A.22), and (4.A.24) with (4.4.16).

Note that $\alpha_5(t)$ accelerates the convergence rate and reduces the size of the set $\mathcal{S}_3$ even further. Note also that $\mathcal{S}_3 \subset \mathcal{S}_2$. Hence, from the definition of $V(t)$ in (4.A.10), boundedness of y, $\bar{x}_j$, f, and h_j follows for all time $t \geq 0$. As mentioned in Section 4.5, the region of attraction is finite (inside $\mathcal{S}_2$) for nonzero t_s. Hence, all the initial conditions (tracking errors and parameter errors) must belong to $\mathcal{S}_2$ for stability.

Appendix 4.B: Estimation of $\dot{u}$ and $\ddot{u}$

For simplicity of our analysis, we set $k_1 = 1$ and $k_2 = 3$ so that we omit the subscript j in our analysis. The rest of the terms of the summations can be readily included. Inside the set $\mathcal{S}_2$, we derive the orders of variables related to $\dot{u}$. We keep only important high-order terms of μ since μ is assumed to be much larger than unity. We assume that the sampling period (t_s) is sufficiently small so that the order of the true parameter x is much smaller than that of $\frac{1}{t_s}$. That is,

$$\mathcal{O}(x_i) \ll \mathcal{O}(\frac{1}{t_s}), \qquad \forall\, i = 1, 2, \cdots, m. \tag{4.B.1}$$

According to the control and adaptation laws (4.4.12) and (4.4.13), u, $\dot{u}$, and hence $u_e (= \delta_1 u - t_s \dot{u})$ are functions of the desired trajectories (r, $\dot{r}$, and r^{III}), disturbances ($\underline{d}$), and control and adaptation gains (ρ, K_j, P_{1j}, P_{2j}, P_3, and P_{4j} for $j = 1, 2, 3, \cdots$). Since u_e contains very small constants δ_1 and t_s, we can make the sign-indefinite u_e term in (4.A.12) much smaller than the other terms by limiting the upper bound of a in μ $(=\frac{a}{t_s})$.

If the order of any one of the desired trajectories, disturbances, or control and adaptation gains is significantly larger than the others, it will dominate the orders of u and $\dot{u}$, and hence the size of the stabilizing $\mathcal{S}_2$. Accordingly, we set the upper bounds of the desired trajectories, disturbances, and control and adaptation gains in such a way that we equalize their influences on the other variables including u, $\dot{u}$, and $\ddot{q}$.

For convenience, the dynamics of revolute-joint manipulators will be used in this order analysis. In this case, the inertia matrix is bounded. The order

analysis for prismatic-joint or prismatic-revolute-joint robots can be as readily performed as that for revolute-joint robots described below since the structure of the dynamics is the same regardless of the type of joint.

In this analysis, we begin with variables of known order. Then, we obtain the orders of their time-derivatives using the dynamics (4.3.3), control law (4.4.12), adaptation law (4.4.13), and time-derivatives of these.

From the definition of $W(\rho, \ddot{r}, \dot{r}, r, \dot{q}, q)$ in (4.4.10) or (4.4.17), we have

$$W = \Big[\mathcal{O}(\mu^2) + \mathcal{O}(\ddot{r}) + \mathcal{O}(\rho\mu)\Big]\underline{\mathrm{W}}_1 \tag{4.B.2}$$

for some $n \times m$ matrix $\underline{\mathrm{W}}_1(t)$ such that $\mathcal{O}(\underline{\mathrm{W}}_1) = \mu^0 \ \ (= 1)$. We choose the upper bounds of $\ddot{r}$ and ρ such that they do not increase the order of W more than $\mathcal{O}(\mu^2)$, the contribution from the other variables of the dynamics. That is, we set

$$\mathcal{O}(\ddot{r}) \leq \mu^2 \quad \text{and} \quad \mathcal{O}(\rho) \leq \mu. \tag{4.B.3}$$

From the control law (4.4.12), we can derive

$$u = \Big[\mathcal{O}(\mu^3) + \mathcal{O}(K_1\mu) + \mathcal{O}(K_2\mu) + \mathcal{O}(K_3\mu^2)\Big]\underline{\mathrm{u}}_1 \tag{4.B.4}$$

for some $n \times 1$ vector $\underline{\mathrm{u}}_1(t)$ such that $\mathcal{O}(\underline{\mathrm{u}}_1) = \mu^0$. We select K_1, K_2, and K_3 such that they do not cause the order of u to be higher than $\mathcal{O}(\mu^3)$, the contribution from $W\bar{x}$:

$$\mathcal{O}(K_1) \leq \mu^2, \quad \mathcal{O}(K_2) \leq \mu^2, \quad \text{and} \quad \mathcal{O}(K_3) \leq \mu. \tag{4.B.5}$$

From the adaptation law (4.4.13), we can obtain

$$\begin{aligned}
\dot{\bar{x}} &= \Big[\mathcal{O}(P_2\mu) + \mathcal{O}(\mu^3)\Big]\underline{\mathrm{x}}_1; \\
\dot{f} &= \Big[\mathcal{O}(P_3\mu) + \mathcal{O}(\mu^3)\Big]\underline{\mathrm{f}}_1; \\
\dot{h} &= \Big[\mathcal{O}(P_4\mu) + \mathcal{O}(\mu^3)\Big]\underline{\mathrm{h}}_1,
\end{aligned} \tag{4.B.6}$$

for some $m\times 1$ vector $\underline{x}_1(t)$ and $n\times 1$ vectors $\underline{f}_1(t)$ and $\underline{h}_1(t)$ such that $\mathcal{O}(\underline{x}_1) = \mu^0$, $\mathcal{O}(\underline{f}_1) = \mu^0$, and $\mathcal{O}(\underline{h}_1) = \mu^0$. We select P_2, P_3, and P_4 by limiting the upper bounds of $\dot{\tilde{x}}$, $\dot{f}$, and $\dot{h}$ to $\mathcal{O}(\mu^3)$. That is,

$$\mathcal{O}(P_2) \leq \mu^2, \quad \mathcal{O}(P_3) \leq \mu^2, \quad \text{and} \quad \mathcal{O}(P_4) \leq \mu^2. \tag{4.B.7}$$

From (4.4.14), we have

$$\dot{Y}_f = \mathcal{O}(P_f\mu)\underline{Y}_{f1} \tag{4.B.8}$$

for some $n\times n$ matrix $\underline{Y}_{f1}(t)$ such that $\mathcal{O}(\underline{Y}_{f1}) = \mu^0$.

From the dynamics (4.3.3),

$$\ddot{q} = M^{-1}[u + \delta_1 u - t_s\dot{u} - C\dot{q} - D\dot{q} - g - \underline{d}]. \tag{4.B.9}$$

Then, using the structure of the dynamics ($M(q)$, $C(\dot{q},q)$, and $g(q)$), we can derive

$$\ddot{q} = -M^{-1}[\mathcal{O}(\underline{d}) + \mathcal{O}(u) + \mathcal{O}(\delta_1 u) + \mathcal{O}(t_s\dot{u})]\underline{q}_1 \tag{4.B.10}$$

for some $n\times 1$ vector $\underline{q}_1(t)$ such that $\mathcal{O}(\underline{q}_1) = \mu^0$. We set

$$\mathcal{O}(\underline{d}) \leq \mathcal{O}(u) \leq \mu^3. \tag{4.B.11}$$

Since $\delta_1 \ll 1$, $\mathcal{O}(\delta_1 u) \ll \mathcal{O}(u)$. Hence

$$\ddot{q} = -M^{-1}[\mathcal{O}(\mu^3) + \mathcal{O}(t_s\dot{u})]\underline{q}_1. \tag{4.B.12}$$

By differentiating W in (4.4.10) or (4.4.17) with respect to time, we can obtain $\dot{W}(r^{III}, \ddot{r}, \dot{r}, r, \ddot{q}, \dot{q}, q)$. Using the structure of $\dot{W}$, we can derive

$$\dot{W} = \left[\mathcal{O}(\mu^3) + \mu\mathcal{O}(\ddot{q}) + \mu\mathcal{O}(\dot{y}) + \mathcal{O}(r^{III})\right]\underline{W}_2 \tag{4.B.13}$$

for some $n \times m$ matrix $\underline{\mathrm{W}}_2(t)$ such that $\mathcal{O}(\underline{\mathrm{W}}_2) = \mu^0$. From (4.B.12), $\mathcal{O}(\ddot{q})$ can be greater than μ^3. Hence we set

$$\mathcal{O}(r^{III}) \leq \mu^4. \tag{4.B.14}$$

Taking time-derivative of u yields

$$\dot{u} = W\dot{\bar{x}} + \dot{W}\bar{x} + K_1\dot{y} + K_2\dot{f} + K_3\dot{Y}_f h + K_3 Y_f \dot{h}. \tag{4.B.15}$$

From (4.B.6) and (4.B.7), we can get

$$\dot{u} = \Big[\mathcal{O}(\mu^5) + \mathcal{O}(\dot{W}\bar{x}) + \mathcal{O}(K_1\dot{y}) + \mathcal{O}(P_f\mu^3)\Big]\underline{\mathrm{u}}_2 \tag{4.B.16}$$

for some $n \times 1$ vector $\underline{\mathrm{u}}_2(t)$ such that $\mathcal{O}(\underline{\mathrm{u}}_2) = \mu^0$. We set

$$\mathcal{O}(P_f) \leq \mu^2. \tag{4.B.17}$$

From (4.B.5), (4.B.13), and (4.B.14), $\mathcal{O}(\dot{W}\bar{x}) = \mu^2\mathcal{O}(\ddot{q}) + \mu^2\mathcal{O}(\dot{y}) + \mathcal{O}(\mu^5)$ and $\mathcal{O}(K_1\dot{y}) = \mu^2\mathcal{O}(\dot{y})$. $\mathcal{O}(\dot{y}) = \max[\mathcal{O}(\ddot{q}), \mathcal{O}(\ddot{r})]$ since $\dot{y} = \ddot{r} - \ddot{q} + \underline{\mathrm{K}}\dot{e}$. Note that $\mathcal{O}(\ddot{r}) \leq \mu^2$. Hence

$$\dot{u} = \Big[\mathcal{O}(\mu^5) + \mu^2\mathcal{O}(\ddot{q})\Big]\underline{\mathrm{u}}_2. \tag{4.B.18}$$

Then, from (4.B.12),

$$\ddot{q} = -M^{-1}[\mathcal{O}(\mu^3) + \mathcal{O}(\mu^5 t_s)]\underline{\mathrm{q}}_1 + \mathcal{O}(t_s\mu^2)\ddot{q}. \tag{4.B.19}$$

Under the constraint of

$$t_s^{\frac{1}{2}} \leq \mu^{-2} \tag{4.B.20}$$

with $t_s \ll 1$, $\mathcal{O}(\ddot{q}) \leq \mathcal{O}(\mu^3)$. Then

$$\dot{u} \leq \Big[\mathcal{O}(\mu^5)\Big]\underline{\mathrm{u}}_2. \tag{4.B.21}$$

Chapter 5

A ROBUST DECOUPLED ADAPTIVE CONTROL OF ROBOTS

5.1 Introduction

In the previous chapter, we have discussed the stability and robustness of the proposed adaptive scheme in the presence of bounded disturbances, sensor noises, and unmodelled dynamics due to feedback delays in the digital control systems. We have also derived a sufficient condition for the proposed scheme under which the scheme stabilizes the system.

As mentioned in the previous chapter, application of the proposed scheme to industrial manipulators may not be trivial since their dynamics are usually complicated. Most of them are classified as a gear-reduction arm. Then, the coupled dynamics are considerably suppressed. Accordingly, a decentralized (decoupled) control scheme may be sufficient to control these manipulators for most practical applications. The decentralized control is very attractive since this approach allows fast parallel implementations. In this chapter, we design a robust decentralized adaptive control scheme for manipulators, and examine its performance. The robustness in adaptive control is a measure of insensitiveness of an adaptive scheme not to parameter uncertainty but to parameter drift in the parameter adaptation.

Several decoupled adaptive schemes[5.1,5.2] have been derived under the assumption that the coupled dynamics is bounded and slowly time-varying. This assumption may not be valid for fast trajectories. A model-following adaptive scheme[5.3,5.4] removes the assumption. The output of this scheme is driven to track not the desired trajectories but the state of a reference model — another source of tracking errors. This scheme contains no feedforward compensation,

which may be effective for gear-reduction manipulators. Some variable structure schemes[5.5,5.6] adopt a signum function for compensators. As a result, these schemes generate chattering control inputs which may excite high-frequency unmodelled dynamics.

Self-tuning schemes[5.7-5.10] are also in the category of the decentralized adaptive control. In these schemes, the nonlinear coupled dynamics are linearized around operating points. Consequently, the parameters of the linearized system are time-varying. Then, the estimators for constant parameters may not catch up with the fast time-varying parameters. Furthermore, desired trajectories need to satisfy the condition of persistent excitation.

In this chapter, we propose a robust decentralized adaptive scheme, which is a subset of the scheme proposed in the previous chapter: the scheme in this chapter contains only the decoupled compensators of that in the previous chapter with appropriate changes in the adaptation laws. The scheme in this chapter consists of feedforward adaptive compensators, feedback adaptive compensators, and an improved PD feedback law. To show the stability of the proposed scheme, we follow the same procedures as those in the previous chapter.

The decentralized scheme in this chapter is different from those reviewed above in the following respects. The stability proof of the scheme here does not require the assumption of boundedness and quasi-time-invariance of the coupled dynamics. Nevertheless, the scheme contains feedforward adaptive compensators. Furthermore, the proposed scheme provides stability bounds for disturbances, control and adaptation gains, and desired trajectories and their time-derivatives, in the presence of unmodelled dynamics due to feedback delays in the digital control systems. To prevent the parameter drift[5.11], we use new adaptation laws proposed in the previous chapter.

In Section 2, we model feedback delays and quantization errors in signal conversions from the result of Section 3 of Chapter 4. In Section 3, we define an appropriate quadratic performance index, which is the same as that in Section 4 of Chapter 4. Then, we search for decoupled compensators which reduce the

performance index as much as possible to improve the tracking performance. In the search, we select only the decoupled compensators from the Theorem in Chapter 4. Then, in the Appendix, we analyze the stability of the selected decoupled adaptive scheme for the coupled system of a manipulator. As a result, we find a sufficient condition under which the proposed decoupled adaptive scheme stabilizes the nonlinear coupled system of a manipulator. The region of attraction of the proposed scheme is local due to unmodelled dynamics, but it is large enough for most of applications.

5.2 Modelling A System to Control

From the result of Section 3 of Chapter 4, we represent the dynamics of a robot in the digital control systems as follows:

$$M\ddot{q} + C\dot{q} + D\dot{q} + g + \underline{\mathrm{d}} = u + u_e, \tag{5.2.1}$$

where

$$\underline{\mathrm{d}} = \hat{d} - u_q - \mathcal{O}(t_s^2);$$

$$u_e = \delta_1 u - t_s \dot{u}. \tag{5.2.2}$$

The definitions of the variables and the parameters of the dynamics are the same as those in Section 3 of Chapter 4.

5.3 Design of A Robust Decentralized Adaptive Control Law

As mentioned at the beginning, the robustness in adaptive control is a measure of insensitiveness of an adaptive scheme not to the parameter uncertainty but to the parameter drift in parameter adaptation.

We cannot obtain asymptotic stability with any decoupled control scheme since the decoupled scheme cannot completely compensate for the coupled dynamics, disturbances, and unmodelled dynamics. Accordingly, our control objective is to find a stable and robust adaptive control law which

(1) guarantees for some finite non-negative constants $\tilde{\delta}_1$ and $\tilde{\delta}_2$ that

$$|\dot{e}(t)| \leq \tilde{\delta}_1 \quad \text{and} \quad |e(t)| \leq \tilde{\delta}_2, \qquad \forall\, t \geq 0, \tag{5.3.1}$$

where

$$e = r - q, \tag{5.3.2}$$

r is the $n \times 1$ desired trajectory vector; and

(2) reduces the maximum tracking error (e) as much as possible with bounded control inputs.

5.3.1 Defining A Quadratic Performance Index

To minimize both tracking error (e) and the derivative of the tracking error ($\dot{e}$), we minimize the following quadratic performance index in relation to the system dynamics:

$$J \equiv \int_0^t y^T(\rho M + D) y d\tau, \tag{5.3.3}$$

where we define the filtered tracking error y as

$$y \equiv \dot{e} + \underline{\mathrm{K}} e; \tag{5.3.4}$$

$\underline{\mathrm{K}} = \mathrm{diag}(\kappa_1, \kappa_2, \cdots, \kappa_n) > 0$; ρ is some non-negative scalar to be selected.

To connect J to the system to control, we modify the system equation (5.2.1) and integrate from 0 to t:

$$\int_0^t y^T(\rho M + D) y d\tau = \int_0^t y^T \Big[M(\ddot{q} + \rho y) + C\dot{q} + D\dot{\sigma} + g + \underline{\mathrm{d}} - u - u_e \Big] d\tau, \tag{5.3.5}$$

where σ is defined as

$$\dot{\sigma} \equiv \dot{r} + \underline{\mathrm{K}} e. \tag{5.3.6}$$

Note that σ is a desired trajectory corrected with tracking error.

We replace $\ddot{q}$ in (5.3.5) with $(\ddot{\sigma} - \dot{y})$ to circumvent the requirement of measuring angular accelerations. Then, we can rewrite equation (5.3.5) as

$$J = \int_0^t y^T(\rho M + D) y d\tau$$

$$= -\frac{1}{2}y^T My\Big|_0^t + \int_0^t y^T\Big(M(\ddot{\sigma}+\rho y) + C\dot{\sigma} + D\dot{\sigma} + g + \underline{\mathrm{d}} - u - u_e\Big)d\tau, \tag{5.3.7}$$

where we have used the fact that

$$\int_0^t y^T M\dot{y}d\tau = \frac{1}{2}y^T My\Big|_0^t - \frac{1}{2}\int_0^t y^T \dot{M}yd\tau; \tag{5.3.8}$$

and that $(\dot{M}-2C)$ is skew-symmetric ($y^T(\dot{M}-2C)y = 0$) if the non-unique matrix C is chosen properly[5.12].

We can rewrite (5.3.7) as

$$J = -\frac{1}{2}y^T My\Big|_0^t + \int_0^t y^T\Big(M_d(\ddot{\sigma}+\rho y) + D_s\dot{\sigma}_s + d_u + \underline{\mathrm{d}} - u - u_e\Big)d\tau, \tag{5.3.9}$$

where

$$\begin{aligned}
\dot{\sigma}_s &= K_s\sigma; \\
D_s &= DK_s^{-1}; \\
d_u &= (M - M_d)(\ddot{\sigma}+\rho y) + C\dot{\sigma} + g;
\end{aligned} \tag{5.3.10}$$

M_d is the $n\times n$ positive-definite diagonal matrix containing only the constant diagonal components of M; K_s is the $n\times n$ positive-definite diagonal matrix. Note that d_u can be considered as unmodelled dynamics due to omission of the nonlinear coupled dynamics for the decentralized scheme.

For simplicity, we define the $m\times 1$ true parameter vector x and the $n\times m$ function matrix W as

$$Wx \equiv M_d(\ddot{\sigma}+\rho y) + D_s\dot{\sigma}_s. \tag{5.3.11}$$

Note that Wx is decoupled.

Then, (5.3.9) becomes

$$J = \frac{1}{2}y(0)^T M(0)y(0) - \frac{1}{2}y^T My + \int_0^t y^T\Big(Wx + d_u + \underline{\mathrm{d}} - u - u_e\Big)d\tau. \tag{5.3.12}$$

5.3.2 Design of A Robust Decentralized Adaptive Control Law

As in Section 4.4 of Chapter 4, we design a control law using the performance index J in (5.3.12). The design procedure involves search for compensators in the direction of minimizing J. In this chapter we extract the decoupled compensators from the Theorem of Chapter 4. Then, we show that the decoupled scheme (the decoupled compensators) stabilizes the coupled system, and derive the corresponding stabilizing constraints for the decoupled scheme. We have already proven that the coupled adaptive control law in the Theorem of Chapter 4 stabilizes the system under some moderate constraints.

With the decoupled compensators from the Theorem of Chapter 4, we form the following Theorem:

Theorem : Consider the following control law

$$u = \sum_{j=1}^{k_1} W\bar{x}_j + K_1 y + K_2 f + \sum_{j=3}^{k_2} K_j Y_f h_j, \tag{5.3.13}$$

with an adaptation law

$$\begin{aligned}
&\dot{\bar{x}}_j + P_{2j}\bar{x}_j = P_{1j}W^T y, \qquad \bar{x}_1(0) = x_o, \quad \bar{x}_j(0) = 0,\ j = 2,3,\cdots;\\
&\dot{f} + P_3 f = K_2 y, \qquad f(0) = 0;\\
&\dot{h}_j + P_{4j}h_j = K_j Y_f y, \qquad h_j(0) = 0,\ j = 3,4,\cdots;
\end{aligned} \tag{5.3.14}$$

where

$$\begin{aligned}
&\dot{Y}_f + P_f Y_f = P_f Y,\\
&Y = \mathrm{diag}(y_1, y_2, \cdots, y_n).
\end{aligned} \tag{5.3.15}$$

Then, these control and adaptation laws guarantee that

$$\begin{aligned}
&|\dot{e}_i(t)| < \infty, \quad |e_i(t)| < \infty, \quad \text{and} \quad |\bar{x}_j| < \infty,\\
&\forall\, t \geq 0, \quad \forall\, i = 1,2,\cdots,n, \quad \forall\, j = 1,2,\cdots,m,
\end{aligned} \tag{5.3.16}$$

if desired trajectories, disturbances, and control and adaptation gains satisfy the following constraints:

$$
\begin{aligned}
&(i)\quad \mathcal{O}(r) \le \mathcal{O}(\mu),\ \ \mathcal{O}(\dot{r}) \le \mathcal{O}(\mu),\ \ \mathcal{O}(\ddot{r}) \le \mathcal{O}(\mu^2),\ \ \mathcal{O}(r^{III}) \le \mathcal{O}(\mu^5),\\
&(ii)\quad \mathcal{O}(\underline{\mathrm{d}}) \le \mu^2,\\
&(iii)\quad \mathcal{O}(\rho) \le \mu,\ \ \mu^2 \le \mathcal{O}(K_1) \le \mu^3,\ \ \mathcal{O}(K_2) \le \mu^3,\ \ \mathcal{O}(K_s) \le \mu,\\
&\qquad \mathcal{O}(K_j) \le \mu^2\ (j \ge 3),\ \ \mu \le \mathcal{O}(P_{1j}) \le \mu^2,\ \ \mu^0 < \mathcal{O}(P_{2j}) \le \mu^3,\\
&\qquad \mu^0 < \mathcal{O}(P_3) \le \mu^3,\ \ \mu^0 < \mathcal{O}(P_{4j}) \le \mu^3,\ \ \mathcal{O}(P_f) \le \mu^3, \qquad (5.3.17)
\end{aligned}
$$

where $\mu = t_s^{-\frac{1}{4}}$ with $t_s \ll 1$ and μ^0 denotes unity consistent with the other orders of μ.

Note that the bounds (5.3.17) are derived for revolute-joint robots. The structure of the dynamics of robots is the same regardless of the type of joint. Hence, the corresponding bounds for prismatic-joint or prismatic-revolute-joint robots are similar to those in (5.3.17) and they can be readily derived.

The various symbols appearing in the Theorem are given as follows:

K_1 is the $n\times n$ positive-definite diagonal matrix; K_2 and K_j $(j = 3, 4, \cdots)$ are the $n\times n$ positive-semi-definite diagonal matrices; P_{11} and P_{21} are the $m\times m$ positive-definite diagonal matrices; P_{1j} and P_{2j} $(j = 2, 3, \cdots)$ are the $m\times m$ positive-semi-definite and positive-definite diagonal matrices respectively; P_3 and P_{4j} $(j = 3, 4, \cdots)$ are the $n\times n$ positive-semi-definite and positive-definite diagonal matrices respectively; P_f is the $n\times n$ positive-definite diagonal matrix; k_1 and k_2 are some positive integers such that $k_1 \ge 1$ and $k_2 \ge 3$; $\mathcal{O}(\cdot)$ denotes the order of the argument.

The memory component $\bar{x}$ is the $m\times 1$ estimated parameter vector such that

$$W\bar{x} \equiv \bar{M}_d(\ddot{\sigma} + \rho y) + \bar{D}_s\dot{\sigma}_s, \qquad (5.3.18)$$

where $\bar{M}_d$ and $\bar{D}_s$ correspond to the unbarred variables computed with the estimated parameters.

Proof of this Theorem is given in Appendix 5.A.

The block diagram of this Theorem is shown in Figure 5.1.

5.3.3 Improved Adaptation Laws

To improve the control performance, we proposed two new adaptation laws (4.4.19) and (4.4.20) in Chapter 4, based on the bounds of the parameters of the dynamics. Those adaptation laws can be also used for the decoupled adaptive scheme in this chapter with the same constraints and the same improvements in control performance. In this case, we have the constraint of $\mu^0 < \mathcal{O}(P_5) \leq \mu$ when we go through the stability analysis.

5.4 Remarks

In the Remarks of Chapter 4, we have commented on the stability proof, stabilizing constraints, adaptation laws, and an improved PD feedback law. Those comments are equally valid in this chapter. In addition, we have the following new results.

1. When $W\bar{x}_j$, the dynamics compensator, is removed from the control and adaptation laws (5.3.13) and (5.3.14), a new d_u which includes Wx in (5.3.11) can be defined. In this case, the $\bar{x}_j$ terms are excluded from $V(t)$, $\dot{V}(t)$, $\mathcal{S}_2$, and $\mathcal{S}_3$. Inside the set $\mathcal{S}_2$, $\mathcal{O}(Wx) \leq \mu^2 (= \mathcal{O}(d_u))$, whereas $\mathcal{O}(K_1 y) = \mathcal{O}(W\bar{x}) \leq \mu^4$. See (5.B.6) and (5.B.7). Hence, α_2 in (5.A.14) is still in the order μ^2. Then, inside the set $\mathcal{S}_2$, any initial $V(t)$ converges exponentially into the residual set $\mathcal{S}_3$ in (5.A.20). Hence, from the definition of $V(t)$ in (5.A.4), boundedness of y, f, and h_j follows for all time $t \geq 0$.

2. When the f and h_j terms are removed in addition to $W\bar{x}_j$ from the control and adaptation laws (5.3.13) and (5.3.14), the $\bar{x}_j$, f, and h_j terms are excluded from $V(t)$, $\dot{V}(t)$, $\mathcal{S}_2$, and $\mathcal{S}_3$. In this case, we can readily show that any initial $V(t)$ inside the set $\mathcal{S}_2$ converges exponentially into the residual set $\mathcal{S}_3$. Hence, $K_1 y$ $(= K_1(\dot{e} + \underline{K}e))$, a PD feedback law, is sufficient to guarantee the stability of the system. Consequently, we have proven the stability of PD or PID (when $P_3 = 0$

and $K_2 \neq 0$) feedback laws for trajectory control of robots. When we use $W\bar{x}_j$, $K_2 f$, and $K_j Y_f h_j$ in addition to $K_1 y$, the performance index J becomes smaller, and hence the maximum magnitude of the tracking error becomes smaller.

5.5 Computer Simulation

As an example, one of the schemes developed here has been applied to a two-link direct-drive manipulator shown in Figure 5.2. Simulation of the scheme is performed on a Sun Microsystems Sparkstation 1. We used a 4^{th}-order Runge-Kutta method[5.13] with adaptive step size to guarantee accuracy in the solution of the manipulator dynamics. The dynamics of the manipulator and the numerical values of its parameters are given in (3.6.1) - (3.6.3) in Section 3.6 of Chapter 3. As a bounded disturbance, the mass 2 is doubled between 2 and 4 seconds.

In this simulation, we use only the first terms of the summations in the control and adaptation laws:

$$u = K_1 y + K_2 f + K_3 Y_f h, \tag{5.5.1}$$

where

$$\dot{Y}_f + P_f Y_f = P_f Y; \tag{5.5.2}$$

$$Y = \mathrm{diag}(y_1, y_2, \cdots, y_n). \tag{5.5.3}$$

One of the adaptation laws is given by

$$\begin{aligned} \dot{\bar{x}} + P_2 \bar{x} &= P_1 W^T y; \\ \dot{f} + P_3 f &= K_2 y; \\ \dot{h} + P_4 h &= K_3 Y_f y. \end{aligned} \tag{5.5.4}$$

In this simulation, we do not use $W\bar{x}$, the feedforward compensator, since it is not effective for trajectory control of a direct-drive manipulator, considering required computation time. See the Remarks for stability proof in this case. The

decoupled feedforward compensator $W\bar{x}$ may be very effective for gear-reduction manipulators whose coupled dynamics are much suppressed.

As in the previous chapters, we have computed the filterings associated with y in the control law by using the following trapezoid rule (Tustin's rule)[5.14]:

$$s \simeq \frac{2}{t_s}\frac{z-1}{z+1}, \tag{5.5.5}$$

where t_s denotes sampling period.

To make our simulations realistic, we include a delay of one sampling period (2 msec) in our control inputs for measurements, computations, and DA and AD conversions.

The desired trajectories for the simulation are chosen as

$$\begin{aligned} r_1 &= \cos 2t, \\ r_2 &= -\cos 5t, \end{aligned} \tag{5.5.6}$$

which are shown in Figure 5.3.

We compare the performance of the present scheme with that of the PD feedback law. For fair comparison, we use the maximum stabilizing gains for the PD feedback law. Since the desired trajectories are sinusoidal, the I (integral) feedback compensator is not effective for reducing the tracking errors. Hence, in both schemes, we do not use the I feedback law ($K_2 = 0$ for the present scheme). In the figures, the dotted and solid lines will denote the PD feedback law and the present scheme respectively.

The numerical values of the control gains for the PD feedback law and the present scheme are as follows.

(1) PD feedback law:

$\underline{K}$=diag(20,20); K_1=diag(600,225).

(2) Present scheme:

$\underline{K}$=diag(20,20); K_1=diag(400,150); $K_2 = 0$;

P_f=diag(20,20); P_1=0; $P_2 = 0$; $P_3 = 0$; P_4=diag(0.5,0.5); K_3=diag(400,400).

The manipulator is assumed to be initially motionless.

Figures 5.4 and 5.5 show the tracking errors of both schemes for joints 1 and 2 respectively. Improvement by the present scheme is substantial. Notice the responses to the step changes of the mass 2 at time 2 and 4 seconds. Both schemes guarantee stability. The present scheme maintains almost the same magnitudes of the tracking errors even when the mass 2 is doubled (from 11.36 kg to 22.72 kg).

Figures 5.6 and 5.7 show the control inputs of both schemes for joints 1 and 2 respectively. The required inputs are almost identical except the transient periods. Nevertheless, the tracking performance of the two schemes are considerably different.

The second simulation is performed with sensor noises added to angular velocities and positions of the links. The desired trajectories and the numerical values of the control gains are the same. To simulate sensor noises, we use "drand48()," the random number generator in the Sparkstation 1. The maximum magnitude of the noises is 5×10^{-4}.

Figures 5.8 and 5.9 show the tracking errors of both schemes for joints 1 and 2 respectively in the presence of sensor noises. The tracking errors contain sensor noises. The tracking performances of both schemes remain almost the same. Figures 5.10 and 5.11 show the control inputs of both schemes for joints 1 and 2 respectively. The required control input for the PD control law contains periodic spikes. This means that the gains for the PD law are too large to tolerate the sensor noises. When the gains of the PD law are reduced, the spikes disappear, but the tracking errors increase. The present scheme generates almost the same control inputs as those without sensor noises. Note that the feedback adaptive compensator (the h term) filters out high-frequency sensor noises. The present scheme guarantees stability in the presence of the sensor noises.

With extensive simulations, we have found that instability occurs when any of initial errors, disturbances, sensor noises, desired trajectories and their time-derivatives, or control and adaptation gains is larger than its certain upper bound.

This supports our stability analysis.

In spite of disturbances such as a step change of mass 2 which is not included in the derivation of the control law, the performance of the control law such as guarantee of stability and fast transient response is shown to be essentially unchanged. This is because the sufficient condition for the stability of our scheme is too strong.

5.6 Conclusion

In this chapter, we have shown that the proposed decentralized adaptive scheme, a subset of the scheme proposed in Chapter 4, stabilizes the nonlinear coupled system of manipulators. In addition, we have proven the stability of PD and PID feedback laws, and have derived the stability bounds for their gains.

In contrast to existing literature of decentralized adaptive control of manipulators, the scheme proposed in this chapter has the following features. The stability proof of the proposed scheme does not require the assumption of boundedness and quasi-time-invariance of the coupled dynamics. The proposed scheme includes feedforward compensators in addition to feedback adaptive compensators and an improved PD feedback law. Moreover, the scheme provides stability bounds for disturbances, control and adaptation gains, and desired trajectories and their time-derivatives, in the presence of unmodelled dynamics due to feedback delays in the digital control systems.

The results of the realistic simulations support our stability analysis and lead to the conclusion that the control law developed here outperforms the PD (or PID) feedback laws. The present scheme guarantees stability in the presence of disturbances, sensor noises, and unmodelled dynamics due to feedback delays in the digital control systems. Since the present scheme allows fast parallel implementations, the scheme is one of the practical solutions for precise control of robots.

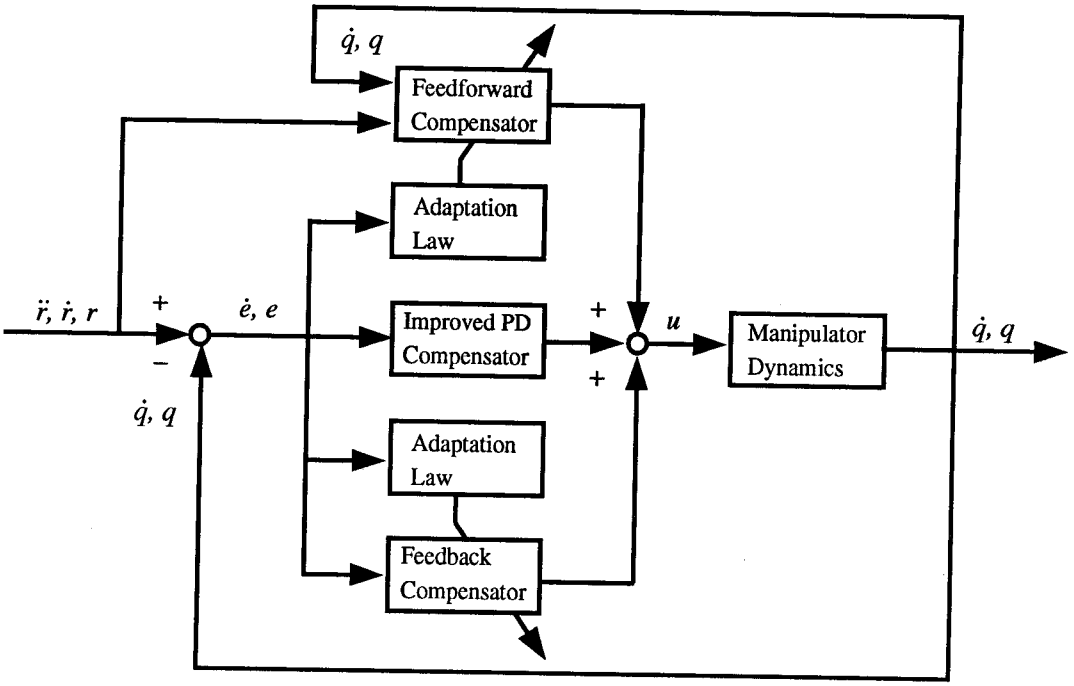

Figure 5.1 Schematic diagram of the proposed control law

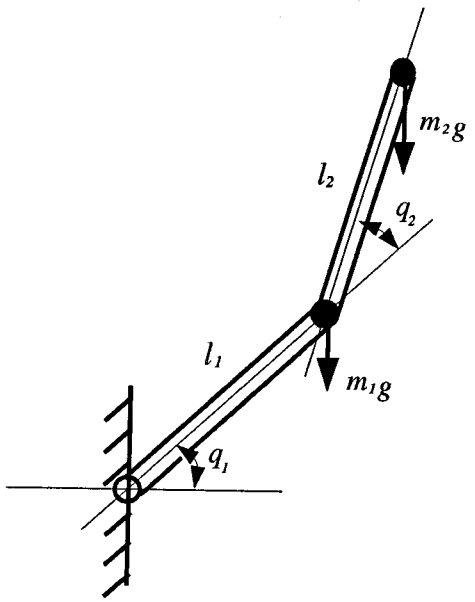

Figure 5.2 Modelling of links

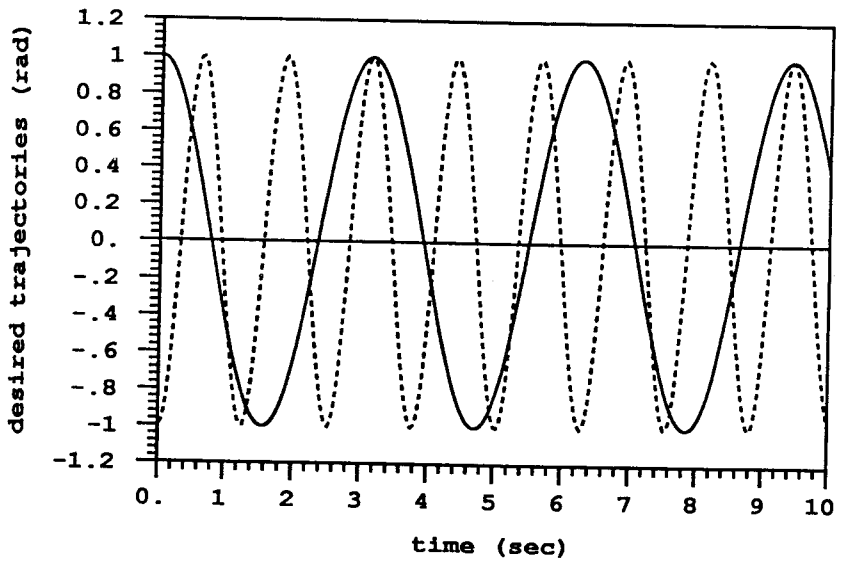

Figure 5.3 Desired trajectories: solid line for joint 1 and dotted line for joint 2

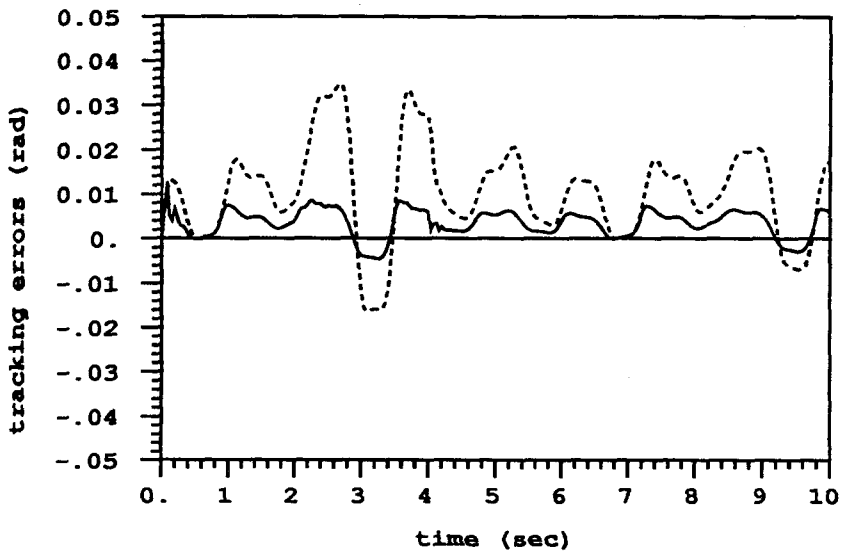

Figure 5.4 Tracking errors of joint 1: dotted line for PD feedback law and solid line for the present scheme

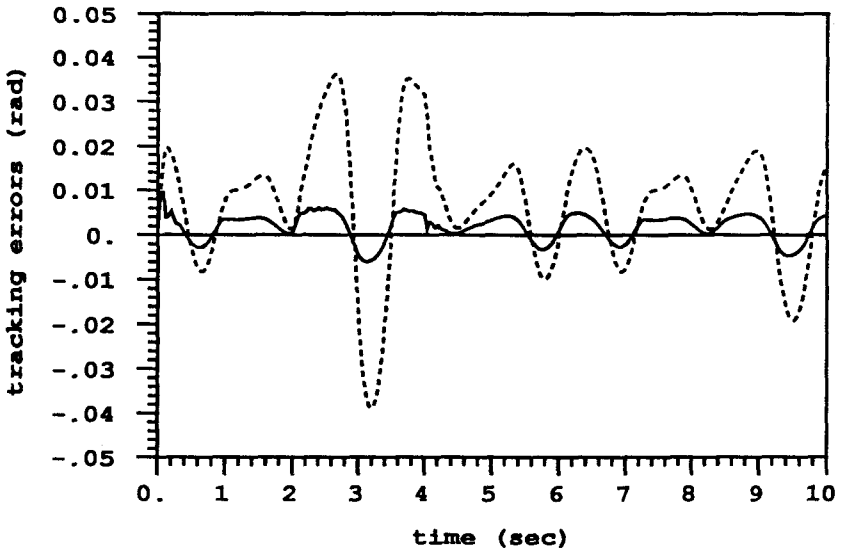

Figure 5.5 Tracking errors of joint 2: dotted line for PD feedback law and solid line for the present scheme

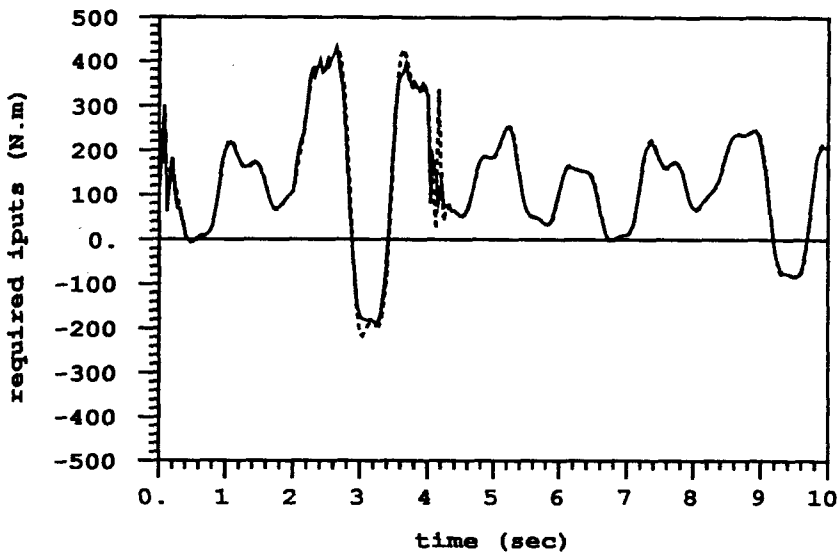

Figure 5.6 Control inputs of joint 1: dotted line for PD feedback law and solid line for the present scheme

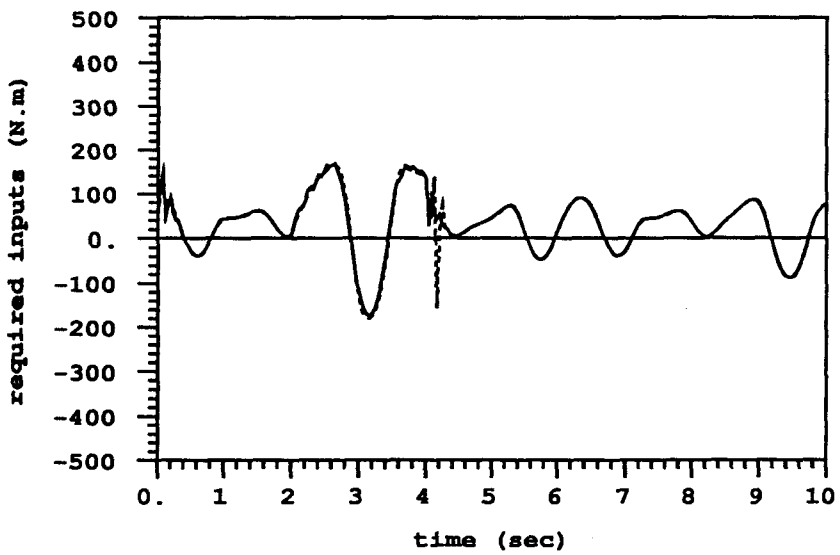

Figure 5.7 Control inputs of joint 2: dotted line for PD feedback law and solid line for the present scheme

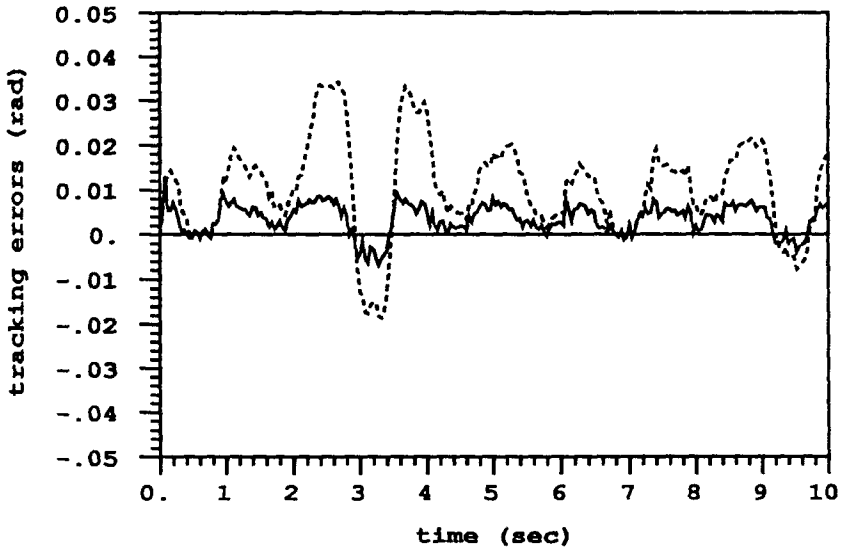

Figure 5.8 Tracking errors of joint 1 in the presence of sensor noises: dotted line for PD feedback law and solid line for the present scheme

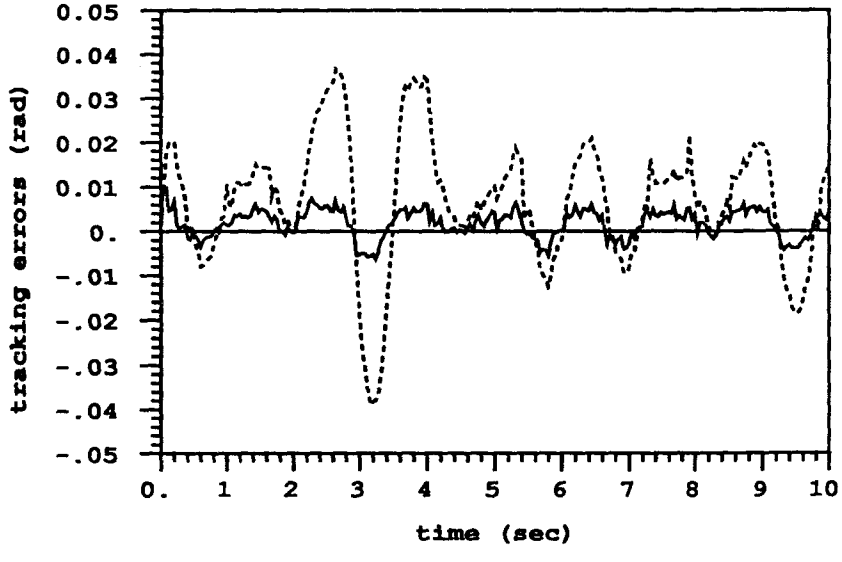

Figure 5.9 Tracking errors of joint 2 in the presence of sensor noises: dotted line for PD feedback law and solid line for the present scheme

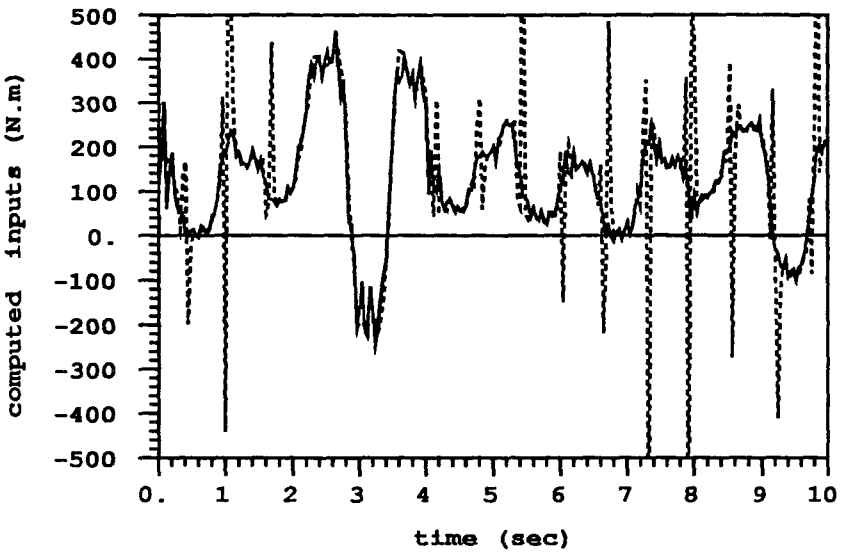

Figure 5.10 Control inputs of joint 1 in the presence of sensor noises: dotted line for PD feedback law and solid line for the present scheme

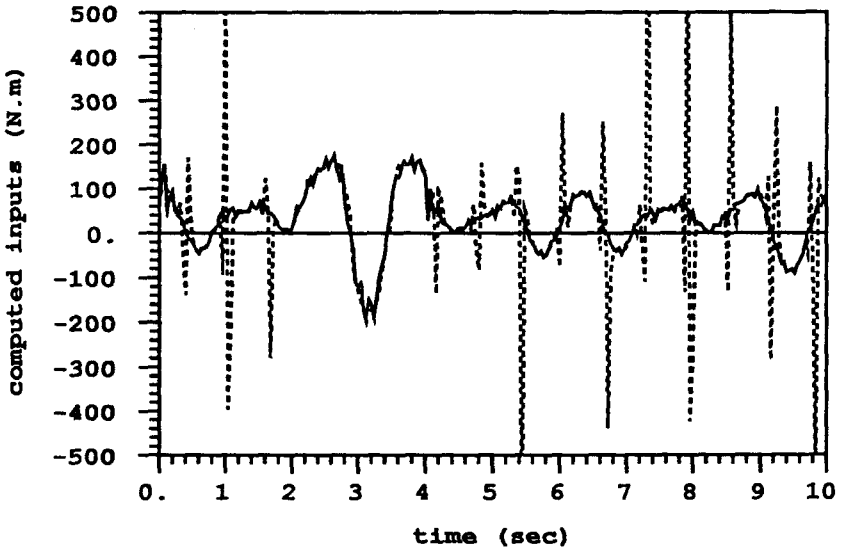

Figure 5.11 Control inputs of joint 2 in the presence of sensor noises: dotted line for PD feedback law and solid line for the present scheme

References

[5.1] Seraji, H., *Decentralized Adaptive Control of Manipulators: Theory, Simulation, and Experimentation,* IEEE Trans. on Robotics and Automation, Vol. 5, No. 2, pp. 183-201, April 1989.

[5.2] Oh, B. J., Jamshidi, M. and Seraji, H., *Decentralized Adaptive Control,* Proc. of IEEE Int. Conf. on Robotics and Automation, pp. 1016-1021, 1988.

[5.3] Gavel, D. T. and Hsia, T. C., *Decentralized Adaptive Control of Robotic Manipulators,* Proc. of IEEE Int. Conf. on Robotics and Automation, pp. 1230-1235, April 1987.

[5.4] Gavel, D. T. and Hsia, T. C., *Decentralized Adaptive Control Experiments with the PUMA Robot Arm,* Proc. of IEEE Int. Conf. on Robotics and Automation, pp. 1022-1027, 1988.

[5.5] Ozguner, U., Yurkovich, S. and Al-Abbass, F, *Decentralized Variable Structure Control of Two-Arm Robotic System,* Proc. of IEEE Int. Conf. on Robotics and Automation, pp. 1248-1254, 1987.

[5.6] Pandian, S. R., Hanmandlu, M. and Gopal, M., *A Decentralized Variable Structure Model Following Controller for Robot Manipulators,* Proc. of IEEE Int. Conf. on Robotics and Automation, pp. 1324-1328, 1988.

[5.7] Koivo, A. J. and Guo, T. M., *Adaptive Linear Controller for Robotic Manipulators,* IEEE Trans. on Aut. Contr., Vol. AC-28, No. 2, pp. 162-172, 1983.

[5.8] Walters, R. G. and Bayoumi, M. M., *Application of a Self-Tuning Pole Placement Regulator to an Industrial Manipulator,* IEEE, Conference on Decision and Control, pp. 323-329, 1982.

[5.9] Leininger, G. G., *Adaptive Control of Manipulators Using Self-Tuning Methods,* Robotics Research, Chap.9 edited by M. Brady and R. Pall, 1984.

[5.10] Sundareshan, M. K. and Koenig, M. A., *Decentralized Model Reference Adaptive Control of Robotic Manipulators,* Proceedings, Automatic Control Conference, pp. 44-49, 1985.

[5.11] Ioannou, P. A. and Kokotovic, P. V., *Robust Redesign of Adaptive Control,* IEEE Trans. on Auto. Contr., Vol. AC-29, No. 3, pp. 202-211, March 1984.

[5.12] Arimoto, A. and Miyazaki, F., *Stability and Robustness of PID Feedback Controller for Robot Manipulators of Sensory Capability,* Robotics Research: The First International Symposium edited by Brady, M. and Paul, R., pp. 783-799, 1984.

[5.13] Press, W. H., Flannery, B. P., Teukolsky, S. A. and Vetterting, W. T., *Numerical Recipes: The Art of Scientific Computing,* Cambridge, 1986.

[5.14] Franklin, G. F. and Powell, J. D., *Digital Control of Dynamic Systems,* Addison-Wesley, Reading, 1980.

Appendix 5.A: Proof of Theorem

The stability proof of the decoupled scheme in this chapter is basically the same as that of the coupled scheme in Chapter 4. Hence we follow the same steps in this proof.

(I) We insert the chosen control and adaptation laws (5.3.13) and (5.3.14) into equation (5.3.12):

$$\begin{aligned}\int_0^t y^T(\rho M + D)y d\tau + \frac{1}{2}\Big(y^T My - y(0)^T M(0)y(0)\Big) \\ =x^T P_{11}^{-1}\Big(\bar{x}_1 + \int_0^t P_{21}\bar{x}_1 d\tau - x_o\Big) \\ - \int_0^t y^T\Big[W\sum_{j=1}^{k_1}\bar{x}_j - \Big(d_u + \underline{\mathrm{d}} - u_e - K_1 y\Big) + K_2 f + \sum_{j=3}^{k_2} K_j Y_f h_j\Big]d\tau,\end{aligned} \tag{5.A.1}$$

where we have applied (4.A.5) with (4.A.1) in Chapter 4. Note that we obtained a similar relationship in the stability proof in Chapter 4.

Using (4.A.6) and (4.A.1) in Chapter 4, we have

$$\int_0^t y^T(\rho M + D)y d\tau + \frac{1}{2}\Big(y^T My - y(0)^T M(0)y(0)\Big)$$

$$
\begin{aligned}
=&\frac{1}{2}\Big[(x-x_o)^T P_{11}^{-1}(x-x_o)-(x-\bar{x}_1)^T P_{11}^{-1}(x-\bar{x}_1)\Big] \\
&-\frac{1}{2}\int_0^t \Big((x-\bar{x}_1)^T P_{11}^{-1}P_{21}(x-\bar{x}_1)+(\bar{x}_1^T P_{11}^{-1}P_{21}\bar{x}_1-x^T P_{11}^{-1}P_{21}x)\Big)d\tau \\
&-\frac{1}{2}\sum_{j=2}^{k_1}\Big(\bar{x}_j^T P_{1j}^{-1}\bar{x}_j+2\int_0^t \bar{x}_j^T P_{1j}^{-1}P_{2j}\bar{x}_j d\tau\Big)+\int_0^T y^T\Big(d_u+\underline{d}-u_e-K_1 y\Big)d\tau \\
&-\Big(\frac{1}{2}f^T f+\int_0^t f^T P_3 f d\tau\Big)-\sum_{j=3}^{k_2}\Big[\frac{1}{2}h_j^T h_j+\int_0^t h_j^T P_{4j}h_j d\tau\Big], \qquad (5.A.2)
\end{aligned}
$$

where it is assumed that x is the $m\times 1$ unknown but constant vector. See Appendix 4.A of Chapter 4 for details.

We rewrite equation (5.A.2) as

$$
\begin{aligned}
J\equiv&\int_0^t y^T(\rho M+D)y d\tau \\
=&\frac{1}{2}\Big(y(0)^T M(0)y(0)+(x-x_o)^T P_{11}^{-1}P_{21}(x-x_o)\Big)-V(t) \\
&-\frac{1}{2}\int_0^t \Big((x-\bar{x}_1)^T P_{11}^{-1}P_{21}(x-\bar{x}_1)+(\bar{x}_1^T P_{11}^{-1}P_{21}\bar{x}_1-x^T P_{11}^{-1}P_{21}x)\Big)d\tau \\
&-\sum_{j=2}^{k_1}\int_0^t \bar{x}_j^T P_{1j}^{-1}P_{2j}\bar{x}_j d\tau+\int_0^T y^T\Big(d_u+\underline{d}-u_e-K_1 y\Big)d\tau \\
&-\int_0^t f^T P_3 f d\tau-\sum_{j=3}^{k_2}\int_0^t h_j^T P_{4j}h_j d\tau, \qquad (5.A.3)
\end{aligned}
$$

where the non-negative function $V(t)$ is defined as

$$
V(t)\equiv\frac{1}{2}\Big[y^T My+(x-\bar{x}_1)^T P_{11}^{-1}(x-\bar{x}_1)+\sum_{j=2}^{k_1}\bar{x}_j^T P_{1j}^{-1}\bar{x}_j+f^T f+\sum_{j=3}^{k_3}h_j^T h_j\Big]\geq 0. \qquad (5.A.4)
$$

Then, it is obvious that the $\bar{x}_j$ $(j=2,3,\cdots)$, f, and h_j $(j=3,4,\cdots)$ terms reduce the performance index J. Hence, these terms reduce the maximum magnitude of y, the filtered tracking error. Accordingly, these terms improve the transient

behavior of the system.

We can also rewrite equation (5.A.2) as

$$\begin{aligned} V(t) =& \frac{1}{2}\Big(y(0)^T M(0) y(0) + (x - x_o)^T P_{11}^{-1} P_{21}(x - x_o)\Big) \\ & - \int_0^t \Big(y^T(\rho M + D + K_1)y - y^T d_u - y^T \underline{d} + y^T(\delta_1 u - t_s \dot{u})\Big) d\tau \\ & - \frac{1}{2}\int_0^t \Big((x - \bar{x}_1)^T P_{11}^{-1} P_{21}(x - \bar{x}_1) + (\bar{x}_1^T P_{11}^{-1} P_{21} \bar{x}_1 - x^T P_{11}^{-1} P_{21} x)\Big) d\tau \\ & - \sum_{j=2}^{k_1} \int_0^t \bar{x}_j^T P_{1j}^{-1} P_{2j} \bar{x}_j d\tau - \int_0^t f^T P_3 f d\tau - \sum_{j=3}^{k_2} \int_0^t h_j^T P_{4j} h_j d\tau. \end{aligned} \tag{5.A.5}$$

From this, we obtain the time-derivative of $V(t)$ along the trajectory of the given system:

$$\begin{aligned} \dot{V}(t) =& - \Big(y^T(\rho M + D + K_1)y - y^T d_u - y^T \underline{d} + y^T(\delta_1 u - t_s \dot{u})\Big) \\ & - \frac{1}{2}\Big((x - \bar{x}_1)^T P_{11}^{-1} P_{21}(x - \bar{x}_1) + (\bar{x}_1^T P_{11}^{-1} P_{21} \bar{x}_1 - x^T P_{11}^{-1} P_{21} x)\Big) \\ & - \sum_{j=2}^{k_1} \bar{x}_j^T P_{1j}^{-1} P_{2j} \bar{x}_j - f^T P_3 f - \sum_{j=3}^{k_2} h_j^T P_{4j} h_j. \end{aligned} \tag{5.A.6}$$

The true parameter x is bounded and the disturbance vector $\underline{d}$ is assumed to be bounded. Therefore, when δ_1=t_s=0, any initial $V(t)$ converges into a bounded set $\mathcal{S}_1 = \{(y, \bar{x}_j, f, h_j)\}$ which is a function of x, $\underline{d}$, d_u, control and adaptation gains, etc. This means that $V(t)$ is bounded for all time $t \geq 0$. Then, from the definition of $V(t)$ in (5.A.4), y, $\bar{x}_j$, f, and h_j are all bounded for all time $t \geq 0$.

However, when $\delta_1 \neq 0$ or $t_s \neq 0$, d_u and $\dot{u}$ may grow unbounded coupled with the control and adaptation laws.

(II) To stabilize the system (i.e., to enforce $\dot{V}(t) \leq 0$ outside $\mathcal{S}_1$), we make the sign-indefinite d_u and $\dot{u}$ terms in (5.A.6) much smaller than the other terms. Since $t_s \ll 1$, the following constraints stabilize the system:

$$\mathcal{O}(\delta_1 u) \ll \mathcal{O}(K_1 y);$$

$$\mathcal{O}(d_u) \ll \mathcal{O}(K_1 y);$$

$$\mathcal{O}(t_s^{\frac{1}{2}} \dot{u}) \leq \mathcal{O}(K_1 y). \tag{5.A.7}$$

To find the orders of u, $\dot{u}$, K_1, and y, we restrict our analysis inside a certain set $\mathcal{S}_2$ ($\supset \mathcal{S}_1$):

$$\mathcal{S}_2 = \{(y, \bar{x}_j, f, h_j) \mid V \leq \mu^2\}, \tag{5.A.8}$$

with

$$\mu \equiv \frac{a}{t_s}, \tag{5.A.9}$$

for some finite positive scalar a to be determined later. Note that the size of the set has not been determined yet.

Without loss of generality, we assume that the upper bounds of k_1 and k_2 are limited so that they do not affect our order analysis. Then, inside the set $\mathcal{S}_2$, $\mathcal{O}(y) \leq \mu$, $\mathcal{O}(Y) \leq \mu$, $\mathcal{O}(f) \leq \mu$, and $\mathcal{O}(h_j) \leq \mu$. In this analysis, we limit the orders of P_{11} and P_{1j} such that $\mu \leq \mathcal{O}(P_{11}) \leq \mu^2$ and $\mu \leq \mathcal{O}(P_{1j}) \leq \mu^2$. Then $\mathcal{O}(x - \bar{x}_1) \leq \mu^2$ and $\mathcal{O}(\bar{x}_j) \leq \mu^2$.

Equations (5.3.4) and (5.3.15) are stable first-order differential equations. Hence, inside the set $\mathcal{S}_2$, $\mathcal{O}(\dot{e}) \leq \mu$, $\mathcal{O}(e) \leq \mu$, and $\mathcal{O}(Y_f) \leq \mu$ under the constraints of $\mathcal{O}(\dot{e}(0)) \leq \mu$, $\mathcal{O}(e(0)) \leq \mu$, $\mathcal{O}(Y_f(0)) \leq \mu$, and $\mathcal{O}(\underline{\mathrm{K}}) = \mu^0$, where μ^0 denotes unity consistent with the other orders of μ. We assume for all time $t \geq 0$ that the desired trajectory satisfies $\mathcal{O}(r) \leq \mu$ and $\mathcal{O}(\dot{r}) \leq \mu$. Then, the orders of $\dot{q}$ and q can be obtained as $\mathcal{O}(\dot{q}) \leq \mu$ and $\mathcal{O}(q) \leq \mu$. We also assume that $\mathcal{O}(x) = \mu^0$, which results in $\mathcal{O}(\bar{x}_1) \leq \mu^2$.

Then, under the constraints of (5.3.17) and (5.B.22), we can obtain the following bounds:

$$u \leq \mathcal{O}(\mu^4)\underline{\mathrm{u}}_1;$$

$$\dot{u} \leq \mathcal{O}(\mu^7)\underline{\mathrm{u}}_2;$$

$$d_u \leq \mathcal{O}(\mu^2)\underline{\mathrm{u}}_3, \tag{5.A.10}$$

for some $n\times 1$ vectors $\underline{u}_1(t)$, $\underline{u}_2(t)$, and $\underline{u}_3(t)$ of order μ^0. See Appendix 5.B for detailed derivations.

The bounds (5.A.10) are derived for revolute-joint robots. The corresponding bounds for prismatic-joint or prismatic-revolute-joint robots are similar to those in (5.A.10) and they can be readily derived. In this case, the stability analysis (proof) is basically the same as that described below.

(III) The first two constraints of (5.A.7) are already satisfied. See (5.A.10) and (5.B.7). To stabilize the system, we satisfy the last constraint in (5.A.7) by limiting the upper bound of a in (5.A.9):

$$(5.A.7) \quad \Longrightarrow \quad \mu^7 \cdot t_s^{\frac{3}{5}} \leq \mu^4 \quad \Longrightarrow \quad a^3 \leq t_s^{\frac{12}{5}}$$

$$\Longrightarrow \quad a \leq t_s^{\frac{4}{5}} \quad \Longrightarrow \quad \mu \leq t_s^{-\frac{1}{5}}. \qquad (5.A.11)$$

Note that this satisfies the constraint (5.B.22). When sensor resolutions are sufficiently small, we can safely assume that $\delta_1 \leq t_s^{\frac{2}{5}}$. See (4.3.2) and (5.2.2). Then, from (5.A.10), there exist $n\times 1$ vectors $\underline{u}_o(t)$ and $\underline{u}_*(t)$ such that $\underline{u}_o \leq \mathcal{O}(\mu^2)$, $\underline{u}_* \leq \mathcal{O}(\mu^2)$,

$$\begin{aligned} t_s y^T \dot{u} &\leq t_s \|\dot{u}\| \|y\| \leq \|\underline{u}_o\| \|y\|, \\ \delta_1 y^T u &\leq \delta_1 \|u\| \|y\| \leq \|\underline{u}_*\| \|y\|. \end{aligned} \qquad (5.A.12)$$

Then, (5.A.6) becomes

$$\begin{aligned} \dot{V}(t) \leq & - y^T(\rho M + D + \frac{1}{2}K_1)y - \alpha_1\|y\|^2 + \alpha_2\|y\| + \alpha_3 \\ & - \frac{1}{2}(x-\bar{x}_1)^T P_{11}^{-1} P_{21}(x-\bar{x}_1) \\ & - \sum_{j=2}^{k_1} \bar{x}_j^T P_{1j}^{-1} P_{2j} \bar{x}_j - f^T P_3 f - \sum_{j=3}^{k_2} h_j^T P_{4j} h_j, \end{aligned} \qquad (5.A.13)$$

where

$$\alpha_1 = \lambda_{\min}(\frac{1}{2}K_1) \leq \mathcal{O}(\mu^3)$$

$$\alpha_2 = \max(\|d_u\| + \|\underline{d}\| + \|\underline{u}_*\| + \|\underline{u}_o\|) \le \mathcal{O}(\mu^2)$$

$$\alpha_3 = \frac{1}{2} x^T P_{11}^{-1} P_{21} x = \mathcal{O}(P_{11}^{-1} P_{21}) \le \mathcal{O}(\mu^2). \tag{5.A.14}$$

See (5.3.17), (5.A.11), (5.A.12), and (5.B.3).

We complete the square to remove the α_2 term:

$$\dot{V}(t) \le -y^T(\rho M + D + \frac{1}{2}K_1)y - \frac{1}{2}(x - \bar{x}_1)^T P_{11}^{-1} P_{21}(x - \bar{x}_1)$$
$$- \sum_{j=2}^{k_1} \bar{x}_j^T P_{1j}^{-1} P_{2j} \bar{x}_j - f^T P_3 f - \sum_{j=3}^{k_2} h_j^T P_{4j} h_j + \alpha_3 + \alpha_4, \tag{5.A.15}$$

where

$$\alpha_4 = \frac{\alpha_2^2}{4\alpha_1} \qquad \left[\le \mathcal{O}(\mu^2) \quad \text{if } \mu^2 \le \mathcal{O}(\alpha_1) \le \mu^3 \right]. \tag{5.A.16}$$

We can rewrite (5.A.15) using $V(t)$ in (5.A.4):

$$\dot{V}(t) + \beta V(t) \le \alpha_3 + \alpha_4 - \alpha_5(t) \tag{5.A.17}$$

with

$$\alpha_5(t) = \left[y^T(\rho M + D + \frac{1}{2}K_1)y - \frac{\beta}{2} y^T M y \right]$$
$$+ \frac{1}{2}\left[(x - \bar{x}_1)^T P_{11}^{-1} P_{21}(x - \bar{x}_1) - \beta(x - \bar{x}_1)^T P_{11}^{-1}(x - \bar{x}_1) \right]$$
$$+ \sum_{j=2}^{k_1} \left[\bar{x}_j^T P_{1j}^{-1} P_{2j} \bar{x}_j - \frac{\beta}{2} \bar{x}_j^T P_{1j}^{-1} \bar{x}_j \right] + \left[f^T P_3 f - \frac{\beta}{2} f^T f \right]$$
$$+ \sum_{j=3}^{k_2} \left[h_j^T P_{4j} h_j - \frac{\beta}{2} h_j^T h_j \right] \ge 0, \tag{5.A.18}$$

where the positive constant β is chosen to be the maximum value which makes the expressions in all the brackets ($[\cdots]$) non-negative. Then, $\mathcal{O}(\beta) \le \mu^3$. See (5.3.17) and (5.A.18).

The solution of (5.A.17) is given by

$$V(t) \leq \exp[-\beta t]\Big(V(0) + \int_0^t \{\alpha_3 + \alpha_4 - \alpha_5(\tau)\}\exp[\beta\tau]d\tau\Big). \qquad (5.A.19)$$

Consequently, we conclude that any initial $V(t)$ belonging to the set $\mathcal{S}_2$ converges into the following residual set:

$$\mathcal{S}_3 = \Big\{(y, \bar{x}_j, f, h_j) \mid V(t) \leq \exp[-\beta t]\int_0^t \{\alpha_3 + \alpha_4 - \alpha_5(\tau)\}\exp[\beta\tau]d\tau \leq \frac{1}{\beta}(\alpha_3 + \alpha_4)\Big\} \qquad (5.A.20)$$

at a rate of at least exp[-βt]. Since $\mathcal{O}(\beta) \leq \mu^3$, $\mathcal{O}(\alpha_3) \leq \mu^2$, and $\mathcal{O}(\alpha_4) \leq \mu^2$, the size of the set $\mathcal{S}_3$ is given by $\mu^{-1} \leq \mathcal{O}(\{\alpha_3 + \alpha_4\}/\beta) < \mu^2$ under the constraints of $\mathcal{O}(\beta) > \mu^0$ and $\mu^2 \leq \mathcal{O}(\alpha_1) \leq \mu^3$, from which we have

$$\mu^2 \leq \mathcal{O}(K_1) \leq \mu^3, \quad \mu^0 < \mathcal{O}(P_{2j}) \leq \mu^3,$$
$$\mu^0 < \mathcal{O}(P_3) \leq \mu^3, \quad \mu^0 < \mathcal{O}(P_{4j}) \leq \mu^3. \qquad (5.A.21)$$

See (5.A.14), (5.A.16), and (5.A.18) with (5.3.17).

Note that $\alpha_5(t)$ accelerates the convergence rate and reduces the size of the residual set $\mathcal{S}_3$ even further. Note also that $\mathcal{S}_3 \subset \mathcal{S}_2$. Hence, from the definition of $V(t)$ in (5.A.4), boundedness of y, $\bar{x}_j$, f, and h_j follows for all time $t \geq 0$. The region of attraction is finite (inside $\mathcal{S}_2$) for nonzero t_s. Hence all the initial conditions (tracking errors and parameter errors) must belong to $\mathcal{S}_2$ for stability.

Appendix 5.B: Estimation of $\dot{u}$ and $\ddot{u}$

For simplicity of our analysis, we set $k_1 = 1$ and $k_2 = 3$ so that we omit the subscript j in our analysis. The rest of the terms of the summations can be readily included. Inside the set $\mathcal{S}_2$, we derive the orders of variables related to $\dot{u}$. We keep only important high-order terms of μ since μ is assumed to be much larger than unity. We assume that the sampling period (t_s) is sufficiently small so

that the order of the true parameter x is much smaller than that of $\frac{1}{t_s}$. That is,

$$\mathcal{O}(x_i) \ll \mathcal{O}(\frac{1}{t_s}), \qquad \forall\, i = 1, 2, \cdots, m. \tag{5.B.1}$$

According to the control and adaptation laws (5.3.13) and (5.3.14), u, $\dot{u}$, and hence $u_e (= \delta_1 u - t_s \dot{u})$ are functions of the desired trajectories (r, $\dot{r}$, and r^{III}), disturbances ($\underline{d}$), and control and adaptation gains (ρ, K_j, P_{1j}, P_{2j}, P_3, and P_{4j} for $j = 1, 2, 3, \cdots$). Since u_e contains very small constants δ_1 and t_s, we can make the sign-indefinite u_e term in (5.A.6) much smaller than the other terms by limiting the upper bound of a in μ $(= \frac{a}{t_s})$.

If the order of any one of the desired trajectories, disturbances, or control and adaptation gains is significantly larger than the others, it will dominate the orders of u and $\dot{u}$, and hence the size of the stabilizing $\mathcal{S}_2$. Accordingly, we set the upper bounds of the desired trajectories, disturbances, and control and adaptation gains in such a way that we equalize their influences on the other variables including u, $\dot{u}$, and $\ddot{q}$.

For convenience, the dynamics of revolute-joint manipulators will be used in this order analysis. In this case, the inertia matrix is bounded. The order analysis for prismatic-joint or prismatic-revolute-joint robots can be as readily performed as that for revolute-joint robots described below since the structure of the dynamics is the same regardless of the type of joint.

In this analysis, we begin with variables of known order. Then, we obtain the orders of their time-derivatives using the dynamics (5.2.1), control law (5.3.13), adaptation law (5.3.14), and time-derivatives of these.

The unmodelled dynamics d_u is a function of $(\ddot{\sigma} + \rho y)$, $\dot{\sigma}$, $\dot{q}$, and q. The second constraint in (5.A.7) requires the upper bound of the sign-indefinite d_u term to be limited. The upper bound of $C\dot{\sigma}$ in d_u is $\mathcal{O}(\mu^2)$. Hence, we set the upper bounds of ρ and $\ddot{r}$ contained in $\ddot{\sigma}$ such that their orders are not larger than the order of $C\dot{\sigma}$:

$$\mathcal{O}(\ddot{r}) \leq \mu^2 \quad \text{and} \quad \mathcal{O}(\rho) \leq \mu, \tag{5.B.2}$$

which leads to

$$\mathcal{O}(d_u) \leq \mu^2. \tag{5.B.3}$$

From the definition of $W(\rho, \ddot{r}, \dot{r}, r, \dot{q}, q)$ in (5.3.11) or (5.3.18), we have

$$W = \Big[\mathcal{O}(\ddot{r}) + \mathcal{O}(\rho\mu) + \mathcal{O}(\mu K_s)\Big]\underline{\mathrm{W}}_1 \tag{5.B.4}$$

for some $n \times m$ matrix $\underline{\mathrm{W}}_1(t)$ such that $\mathcal{O}(\underline{\mathrm{W}}_1) = \mu^0$ $(= 1)$. We choose the upper bound of K_s such that they increase the order of W not more than $\mathcal{O}(\mu^2)$, the contribution from $\ddot{\sigma}$ and ρy:

$$\mathcal{O}(K_s) \leq \mu. \tag{5.B.5}$$

From the control law (5.3.13), we can derive

$$u = \Big[\mathcal{O}(\mu^4) + \mathcal{O}(K_1\mu) + \mathcal{O}(K_2\mu) + \mathcal{O}(K_3\mu^2)\Big]\underline{\mathrm{u}}_1 \tag{5.B.6}$$

for some $n \times 1$ vector $\underline{\mathrm{u}}_1(t)$ such that $\mathcal{O}(\underline{\mathrm{u}}_1) = \mu^0$. We select K_1, K_2, and K_3 such that they do not cause the order of u to be higher than $\mathcal{O}(\mu^4)$, the contribution from $W\bar{x}$:

$$\mathcal{O}(K_1) \leq \mu^3, \quad \mathcal{O}(K_2) \leq \mu^3, \quad \text{and} \quad \mathcal{O}(K_3) \leq \mu^2. \tag{5.B.7}$$

Note that the upper bound of K_1 satisfies the first two constraint in (5.A.7). See (5.B.3) and (5.B.6).

From the adaptation law (5.3.14), we can obtain

$$\begin{aligned}
\dot{\bar{x}} &= \Big[\mathcal{O}(P_2\mu^2) + \mathcal{O}(\mu^5)\Big]\underline{\mathrm{x}}_1; \\
\dot{f} &= \Big[\mathcal{O}(P_3\mu) + \mathcal{O}(\mu^4)\Big]\underline{\mathrm{f}}_1; \\
\dot{h} &= \Big[\mathcal{O}(P_4\mu) + \mathcal{O}(\mu^4)\Big]\underline{\mathrm{h}}_1
\end{aligned} \tag{5.B.8}$$

for some $m \times 1$ vector $\underline{\mathrm{x}}_1(t)$ and $n \times 1$ vectors $\underline{\mathrm{f}}_1(t)$ and $\underline{\mathrm{h}}_1(t)$ such that $\mathcal{O}(\underline{\mathrm{x}}_1) = \mu^0$, $\mathcal{O}(\underline{\mathrm{f}}_1) = \mu^0$, and $\mathcal{O}(\underline{\mathrm{h}}_1) = \mu^0$. We select P_2 by limiting the upper bound of $\dot{\bar{x}}$ to $\mathcal{O}(\mu^5)$, and P_3 and P_4 by limiting the upper bounds of $\dot{f}$ and $\dot{h}$ to $\mathcal{O}(\mu^4)$. That is,

$$\mathcal{O}(P_2) \leq \mu^3, \quad \mathcal{O}(P_3) \leq \mu^3, \quad \text{and} \quad \mathcal{O}(P_4) \leq \mu^3. \tag{5.B.9}$$

From (5.3.15), we have

$$\dot{Y}_f = \mathcal{O}(P_f\mu)\underline{Y}_{f1} \tag{5.B.10}$$

for some $n\times n$ matrix $\underline{Y}_{f1}(t)$ such that $\mathcal{O}(\underline{Y}_{f1}) = \mu^0$.

From the dynamics (5.2.1),

$$\ddot{q} = M^{-1}[u + \delta_1 u - t_s\dot{u} - C\dot{q} - D\dot{q} - g - \underline{d}]. \tag{5.B.11}$$

Then, using the structure of the dynamics ($M(q)$, $C(\dot{q},q)$, and $g(q)$), we can derive

$$\ddot{q} = -M^{-1}[\mathcal{O}(\underline{d}) + \mathcal{O}(u) + \mathcal{O}(\delta_1 u) + \mathcal{O}(t_s\dot{u})]\underline{q}_1 \tag{5.B.12}$$

for some $n\times 1$ vector $\underline{q}_1(t)$ such that $\mathcal{O}(\underline{q}_1) = \mu^0$. We set

$$\mathcal{O}(\underline{d}) \le \mathcal{O}(u) \le \mu^4. \tag{5.B.13}$$

Since $\delta_1 \ll 1$, $\mathcal{O}(\delta_1 u) \ll \mathcal{O}(u)$. Hence

$$\ddot{q} = -M^{-1}[\mathcal{O}(\mu^4) + \mathcal{O}(t_s\dot{u})]\underline{q}_1. \tag{5.B.14}$$

By differentiating W in (5.3.11) or (5.3.18) with respect to time, we can obtain $\dot{W}(r^{III}, \ddot{r}, \dot{r}, r, \ddot{q}, \dot{q}, q)$. Using the structure of $\dot{W}$, we can derive

$$\dot{W} = \left[\mathcal{O}(\mu^3) + \mu\mathcal{O}(\ddot{q}) + \mu\mathcal{O}(\dot{y}) + \mathcal{O}(r^{III})\right]\underline{W}_2 \tag{5.B.15}$$

for some $n\times m$ matrix $\underline{W}_2(t)$ such that $\mathcal{O}(\underline{W}_2) = \mu^0$. From (5.B.14), $\mathcal{O}(\ddot{q})$ can be greater than μ^4. Hence we set

$$\mathcal{O}(r^{III}) \le \mu^5. \tag{5.B.16}$$

Taking time-derivative of u yields

$$\dot{u} = W\ddot{\bar{x}} + \dot{W}\dot{\bar{x}} + K_1\dot{y} + K_2\dot{f} + K_3\dot{Y}_f h + K_3 Y_f \dot{h}. \tag{5.B.17}$$

From (5.B.8) and (5.B.9), we can get

$$\dot{u} = \Big[\mathcal{O}(\mu^7) + \mathcal{O}(\dot{W}\bar{x}) + \mathcal{O}(K_1\dot{y}) + \mathcal{O}(P_f\mu^4)\Big]\underline{u}_2 \qquad (5.B.18)$$

for some $n\times 1$ vector $\underline{u}_2(t)$ such that $\mathcal{O}(\underline{u}_2) = \mu^0$. We set

$$\mathcal{O}(P_f) \leq \mu^3. \qquad (5.B.19)$$

From (5.B.7), (5.B.15), and (5.B.16), $\mathcal{O}(\dot{W}\bar{x}) = \mu^3\mathcal{O}(\ddot{q}) + \mu^3\mathcal{O}(\dot{y}) + \mathcal{O}(\mu^7)$ and $\mathcal{O}(K_1\dot{y}) = \mu^3\mathcal{O}(\dot{y})$. $\mathcal{O}(\dot{y}) = \max[\mathcal{O}(\ddot{q}), \mathcal{O}(\ddot{r})]$ since $\dot{y} = \ddot{r} - \ddot{q} + \underline{K}\dot{e}$. Note that $\mathcal{O}(\ddot{r}) \leq \mu^2$. Hence

$$\dot{u} = \Big[\mathcal{O}(\mu^7) + \mu^3\mathcal{O}(\ddot{q})\Big]\underline{u}_2. \qquad (5.B.20)$$

Then, from (5.B.14),

$$\ddot{q} = -M^{-1}[\mathcal{O}(\mu^4) + \mathcal{O}(\mu^7 t_s)]\underline{q}_1 + \mathcal{O}(t_s\mu^3)\ddot{q}. \qquad (5.B.21)$$

Under the constraint of

$$t_s^{\frac{3}{5}} \leq \mu^{-3} \qquad (5.B.22)$$

with $t_s \ll 1$, $\mathcal{O}(\ddot{q}) \leq \mathcal{O}(\mu^4)$. Then,

$$\dot{u} \leq \Big[\mathcal{O}(\mu^7)\Big]\underline{u}_2. \qquad (5.B.23)$$

Chapter 6

ADAPTIVE CONTROL OF FLEXIBLE-JOINT ROBOTS

6.1 Introduction

In the previous three chapters, we have discussed the design of robust adaptive control laws for manipulators in the presence of bounded disturbances, sensor noises, and unmodelled dynamics. The underlying assumption for this is that the structures of manipulators are rigid. In reality, there exist no such manipulators. The links and joint couplings exhibit a certain degree of flexibility. For most commercial manipulators, the links are well approximated by rigid bodies[6.1]. Accordingly, in this chapter, we focus on the flexibility of the joint couplings due to the flexibility of belts, cables, drive shafts, harmonic drives, and so on, for power transmission from actuators to links.

The compliance of the joint couplings may be positively used for force control and protection of mechanical components from collisions. There are, however, some accompanying problems of control. Experimental results[6.2,6.3] have shown that the flexibility between the links and actuators affects the manipulator dynamics, degrading the performance and possibly causing instabilities.

The idea of feedback linearization[6.4-6.7], the concept of integral manifolds [6.8-6.10], and gain scheduling[6.11-6.14] have been applied to treat the aforementioned problems. As we reviewed in Section 1.2.2 of Chapter 1, all these approaches have problems of signal measurements and/or lack of robustness (i.e., uncertainty in the parameters dominates stability). A singular perturbation approach[6-15] seems to avoid the problems for some applications. However, the stability of this scheme is not proven.

The control law proposed here is intended to avoid those problems. It is rel-

atively insensitive to parametric uncertainties necessarily accompanied in models of link and actuator dynamics, stiffnesses of joint couplings, and external disturbances. The computational burden of the present scheme is almost the same as that of the corresponding scheme for robots having rigid joints. Moreover, measurement problems are minimized because the proposed scheme requires measurements of only angular positions and velocities. Hence, the present scheme is one of the applicable practical solutions to the control of manipulators having flexible joint couplings.

In our approach, we consider the actuators and joint couplings as second-order low-pass prefilters for the link dynamics, since the torque inputs pass through the actuator and joint dynamics. We design an appropriate flexibility compensator for joint flexibility so that we transform the systems of flexible-joint manipulators to those of the corresponding rigid-joint manipulators with a certain degree of high-frequency unmodelled dynamics. In other words, we make the flexible joint couplings artificially rigid using the flexibility compensator. As a consequence, control of flexible-joint manipulators is converted to that of the corresponding rigid-joint manipulators, which has been already discussed in the previous chapters. We derive an adaptive control scheme for the transformed rigid-joint manipulators, which is a simpler form of the scheme developed in Chapter 4. Then, we derive a sufficient condition for the robust stability of the scheme with the flexibility compensator, for the system of the original flexible-joint manipulators.

As a mathematical tool, we use standard Lyapunov's second method reviewed in Chapter 2, even though we can apply the design approach we have followed in Chapters 4 and 5.

In Section 2, using an appropriate flexibility compensator, we change the unwanted characteristics of the prefilters by placing the poles of the prefilters in more desirable locations. Then, we transform the system of a flexible-joint manipulator to that of the corresponding rigid-joint manipulator with the high-frequency prefilter dynamics as unmodelled dynamics to the new system.

In Section 3, neglecting the unmodelled dynamics, we design an adaptive

control scheme, which is called a reduced-order adaptive control law. The resulting control scheme is a simpler form of the adaptive control law proposed in Chapter 4. Via additional stability analysis, we derive a sufficient condition for the reduced-order adaptive control law, which guarantees robust stability in the presence of the unmodelled dynamics we neglected.

In Section 5, we discuss attenuation of sensor noises associated with the flexibility compensation since high gain of the flexibility compensation loop may magnify high-frequency sensor noises. We also explain why our scheme is almost insensitive to disturbances inside the flexibility loop.

6.2 Transformation to A System of Manipulators Having Rigid Joints

6.2.1 Preliminaries

The dynamics of manipulators with flexible joint couplings can be modelled as[6.8]:

$$M(q_l)\ddot{q}_l + C(\dot{q}_l, q_l)\dot{q}_l + D\dot{q}_l + g(q_l) + \underline{d} = K_c(N^{-1}q_a - q_l), \tag{6.2.1}$$

$$J_a\ddot{q}_a + B_a\dot{q}_a + N^{-1}K_c(N^{-1}q_a - q_l) = u_a, \tag{6.2.2}$$

where

$q_l, \dot{q}_l, \ddot{q}_l$: $n\times 1$ joint displacement, velocity, and acceleration vector for the links;

$q_a, \dot{q}_a, \ddot{q}_a$: $n\times 1$ joint displacement, velocity, and acceleration vector for the actuators;

$M(q_l)$: $n\times n$ effective coupling inertia matrix for the links including payloads;

J_a : $n\times n$ diagonal matrix of the actuator inertia;

$C(\dot{q}_l, q_l)\dot{q}_l$: $n\times 1$ centrifugal and Coriolis force vector;

D : $n\times n$ matrix for viscous damping coefficients of the links;

B_a : $n\times n$ diagonal matrix for viscous damping coefficients of the actuators;

$g(q_l)$: $n\times 1$ gravitational loading vector;

$\underline{d}$: $n\times 1$ bounded disturbance vector;

N : $n\times n$ diagonal matrix for the gear ratio between the links and the actuators;

K_c : $n \times n$ diagonal matrix for the stiffness of the joint couplings;

u_a : $n \times 1$ actuator input vector;

n : number of joints.

Note that the two equations are coupled through $K_c(N^{-1}q_a - q_l)$, which is generated by the actuator dynamics (6.2.2) from the input u_a and transmitted to the link dynamics (6.2.1) through reduction gears.

As a background for compensation of joint flexibility, we examine the role of the joint flexibility. We rewrite the link dynamics (6.2.1) and actuator dynamics (6.2.2) as

$$M(q_l)\ddot{q}_l + C(\dot{q}_l, q_l)\dot{q}_l + D\dot{q}_l + g(q_l) = K_c v, \tag{6.2.3}$$

$$NJ_a\ddot{v} + NB_a\dot{v} + N^{-1}K_c v = N^{-1}(Nu_a - N^2 J_a\ddot{q}_l - N^2 B_a\dot{q}_l), \tag{6.2.4}$$

where v is defined as

$$v = N^{-1}q_a - q_l. \tag{6.2.5}$$

Now, for convenience, let us define u_l as

$$u_l = Nu_a - N^2 J_a\ddot{q}_l - N^2 B_a\dot{q}_l. \tag{6.2.6}$$

Then, the actuator dynamics (6.2.4) becomes

$$NJ_a\ddot{v} + NB_a\dot{v} + N^{-1}K_c v = N^{-1}u_l. \tag{6.2.7}$$

According to equations (6.2.3) and (6.2.7), the actuator dynamics acts as a second-order low-pass prefilter for the link dynamics. In other words, u_l is filtered through the actuator dynamics, and $K_c v$, the output of the actuator, is fed into the link dynamics (6.2.3), which can be interpreted as a second-order low-pass filter. Note that the output of the link dynamics for a sinusoidal input is no longer sinusoidal since the system is nonlinear and coupled. The degree of distortion of the sinusoidal signal depends on the degree of coupling and nonlinearity.

By definition, any low-pass filter has low gain in the high-frequency region. Hence, regardless of the control laws used, large magnitudes of control inputs are

required to control a trajectory whose spectral range covers the high-frequency low-gain region of the link dynamics and/or the prefilter (6.2.7). Consequently, regardless of the control laws, the control bandwidth (the spectral content of the reference inputs) must be limited for a given manipulator since its actuators or amplifiers with limited capacities can not generate control inputs larger than a certain bound.

When the bandwidth of the prefilter (6.2.7) is sufficiently larger than the spectral range of the inputs, we may assume that the behavior of the prefilter (6.2.7) is approximated by

$$K_c v = u_l. \tag{6.2.8}$$

If the relationship above is to be valid for all signals u_l, the prefilter must be an all-pass filter. Then, the undamped natural frequency of the prefilter, $N^{-1}\sqrt{J_a^{-1}K_c}$, must be infinitely large, implying that $K_c \to \infty$, the limiting case of rigid joints. In this limit, the link dynamics (6.2.3) and the actuator dynamics (6.2.8) with (6.2.6) become the following model for a manipulator having rigid joints:

$$(M(q_l) + N^2 J_a)\ddot{q}_l + C(\dot{q}_l, q_l)\dot{q}_l + (D + N^2 B_a)\dot{q}_l + g(q_l) + \underline{d} = u_t, \tag{6.2.9}$$

where

$$u_t = N u_a. \tag{6.2.10}$$

When the bandwidth of the prefilter is smaller than the control bandwidth, u_l is distorted while passing through the prefilter. The bandwidth of the prefilter is inversely proportional to N. See the dynamics of the prefilter (6.2.7). Hence, the bandwidth of the prefilter decreases as N increases, increasing the distortion of u_l. The distortion of u_l also depends on the damping ratio of the prefilter. If the damping of the prefilter is too small, instability may be caused by magnification of even apparently negligible torque inputs near the resonance frequency. If the damping is too large, most of the torque inputs may be filtered out. Larger distortion of the input signals causes larger magnitudes of the tracking errors,

even though the exact inverse dynamic models of the links and actuators are used in control laws.

For commercial manipulators, the gear ratio N is normally large and the damping ratio of the prefilter is small. As a consequence, the distortion of the signal u_l is significant. Hence, gear reduction with flexibility increases the magnitudes of the tracking errors even to the point of instability, depending on various factors such as the gear ratio, joint stiffness, and inertia and damping of actuators. In practical applications, the actuator angles, rather than the link angles, are controlled. This avoids the instability but induces vibration and additional tracking errors.

6.2.2 Compensation of Joint Flexibility

Based on the discussion and equation (6.2.10) in the preliminaries, we select the control input (actuator input) for a manipulator with flexible joints as

$$u_a = K_{nt}N^{-1}u_{ta} + u_c, \tag{6.2.11}$$

where K_{nt} is the $n\times n$ positive-definite diagonal matrix to be determined later; u_{ta} and u_c are the $n\times 1$ vectors for the joint torque and for the joint flexibility compensation respectively which will be determined later.

Then, equation (6.2.2) for the actuator dynamics becomes

$$NJ_a\ddot{v} + NB_a\dot{v} + N^{-1}K_cv = K_{nt}N^{-1}(u_{ta} - K_{nt}^{-1}N^2J_a\ddot{q}_l - K_{nt}^{-1}N^2B_a\dot{q}_l) + u_c. \tag{6.2.12}$$

Similar to the case for rigid joints, we redefine u_l as

$$u_l = u_{ta} - K_{nt}^{-1}N^2J_a\ddot{q}_l - K_{nt}^{-1}N^2B_a\dot{q}_l. \tag{6.2.13}$$

We move the poles of the prefilter (6.2.12) to more desirable locations by choosing

$$u_c = -K_{cv}\dot{v} - K_{cp}v, \tag{6.2.14}$$

where K_{cp} and K_{cv} are the $n \times n$ positive-definite diagonal matrices to be selected. Note that v is proportional to the torque transmitted to the link dynamics. Therefore, this can be readily measured by using simple torque sensors with strain gauges. The time-derivative of v can be attained by differentiating v after passing through low-pass filters. Alternatively, this can be obtained by measuring the rotational velocities of the links and actuators.

Then the prefilter (6.2.12) becomes

$$NJ_a\ddot{v} + (NB_a + K_{cv})\dot{v} + (N^{-1}K_c + K_{cp})v = K_{nt}N^{-1}u_l. \tag{6.2.15}$$

Since we have two free parameters K_{cv} and K_{cp}, we can increase the bandwidth of the prefilter as much as we wish, while maintaining the appropriate damping ratio (approximately 0.707). In reality, the upper bound of the bandwidth of the prefilter is limited by some constraints such as sensor noises, unmodelled inductance of actuators, and sampling rates in the digital control systems. Consequently, the reference inputs (or desired trajectories) contained in input u_l are filtered while passing through the prefilter. Especially, a signal in the spectral range higher than the bandwidth of the compensated prefilter is seriously distorted and can not be tracked with any control law for robots having rigid joints. However, as discussed in the preliminaries, the control bandwidth must be limited due to the low-gain characteristics of the uncompensated prefilter (6.2.7) and link dynamics in the high-frequency region. Therefore, the bandwidth of the prefilter need not necessarily be infinite.

Static (or low-frequency) gain of the compensated prefilter (6.2.15) becomes smaller when $K_{cp}v$ is added to the prefilter. The torque input is transmitted to the link dynamics through $K_c v$. Hence, the design problem would be simpler if we select the static (or low-frequency) gain of the compensated prefilter (6.2.15) to be equal to that of the uncompensated prefilter (6.2.7), which means that we modify only the damping ratio and the bandwidth of the prefilter. However, there

always exist uncertainties with K_c. Therefore, we select K_{nt} as

$$K_{nt} = (N^{-1}K_{nc} + K_{cp})K_{nc}^{-1}N = P_u K_t, \tag{6.2.16}$$

where

$$K_t \equiv (N^{-1}K_c + K_{cp})K_c^{-1}N; \tag{6.2.17}$$

K_{nc} is the nominal value of K_c; P_u is the $n \times n$ positive-definite diagonal matrix reflecting the uncertainties associated with the parameter K_c, the joint stiffness. P_u is unity if $K_{nc} = K_c$ (i.e., if there exists no uncertainty in K_c).

Then, the prefilter becomes

$$J_c\ddot{v} + C_c\dot{v} + K_c v = P_u u_l, \tag{6.2.18}$$

where

$$\begin{aligned} J_c &= N^2 K_t^{-1} J_a, \\ C_c &= N K_t^{-1}(N B_a + K_{cv}). \end{aligned} \tag{6.2.19}$$

6.2.3 Deriving A Model of A Rigid-Joint Robot

For an input applied to the prefilter (6.2.18), the corresponding output is the passing-through signal (the input itself magnified by the static gain of the prefilter) with a filtered-out signal (representing distortion of the input by the prefilter) subtracted. That is, we represent the prefilter (6.2.18) as

$$\eta + K_c v = P_u u_l, \tag{6.2.20}$$

where η is the $n \times 1$ vector representing distortion of high-frequency content of the input signal.

Then, the distortion η can be obtained by inserting (6.2.20) into (6.2.18):

$$J_c\ddot{\eta} + C_c\dot{\eta} + K_c\eta = P_u(J_c\ddot{u}_l + C_c\dot{u}_l). \tag{6.2.21}$$

Then, the link dynamics (6.2.3) and the actuator dynamics (6.2.20) with (6.2.13) become the following model:

$$(M(q_l) + K_t^{-1}N^2J_a)\ddot{q}_l + C(\dot{q}_l, q_l)\dot{q}_l + (D + K_t^{-1}N^2B_a)\dot{q}_l + g(q_l) + \underline{d} + \eta = P_u u_{ta}; \tag{6.2.22}$$

$$\mathcal{E}^2\ddot{\eta} + 2\mathcal{Z}\mathcal{E}\dot{\eta} + \eta = P_u(\mathcal{E}^2\ddot{u}_l + 2\mathcal{Z}\mathcal{E}\dot{u}_l), \tag{6.2.23}$$

where

$$\mathcal{E}^2 = K_c^{-1}J_c \qquad \text{and} \qquad 2\mathcal{Z}\mathcal{E} = K_c^{-1}C_c; \tag{6.2.24}$$

$\mathcal{E}$ is the $n\times n$ positive-definite diagonal matrix of order ϵ which is assumed to be much smaller than unity. $\mathcal{Z}$ is the $n\times n$ positive-definite diagonal matrix representing the damping ratio of the compensated prefilter. Note that uncertainties with J_a and B_a are included in $\mathcal{E}$ and $\mathcal{Z}$.

The structure of equation (6.2.22) is the same as that of the rigid-joint model (6.2.9). In other words, using the concept of prefilter, we have transformed a system of a flexible-joint manipulator to that of the corresponding rigid-joint manipulator (6.2.22) with η representing unmodelled dynamics to the new system.

6.3 Design of A Control Law

From (6.2.22), (6.2.23), and (6.2.24), we have the following system to control:

$$M_e\ddot{q}_l + C(\dot{q}_l, q_l)\dot{q}_l + D_e\dot{q}_l + g(q_l) + \underline{d} + \eta = P_u u_{ta}; \tag{6.3.1}$$

$$\mathcal{E}^2\ddot{\eta} + 2\mathcal{Z}\mathcal{E}\dot{\eta} + \eta = 2P_u\mathcal{Z}\mathcal{E}\dot{u}_l + P_u\mathcal{E}^2\ddot{u}_l, \tag{6.3.2}$$

where, from (6.2.13) and (6.2.16),

$$u_l = u_{ta} - P_u^{-1}B_e\dot{q}_l - P_u^{-1}J_e\ddot{q}_l; \tag{6.3.3}$$

$$M_e \equiv (M(q_l) + J_e) \quad \text{and} \quad D_e \equiv (D + B_e); \tag{6.3.4}$$

$$J_e \equiv K_t^{-1}N^2J_a \quad \text{and} \quad B_e \equiv K_t^{-1}N^2B_a. \tag{6.3.5}$$

Note that we lose some useful characteristics of the link dynamics such as positive definiteness of the mass matrix if we premultiply equation (6.3.1) by the inverse of the uncertainty P_u, unless all the diagonal components of P_u are the same.

6.3.1 Design of A Control Law Based on the Reduced-Order System

The behavior of the system (6.3.1) is very complicated due to η. In this section, we temporarily neglect the distortion η from the system (6.3.1) to circumvent the complexity in the design procedure. The system without η is called a reduced-order system. In this case, η represents unmodelled dynamics for the reduced-order system. We design an adaptive control law based on the reduced-order system, which is called a reduced-order adaptive control law. In the next section, we will impose some restrictions on the reduced-order adaptive control law so that this stabilizes the original full-order system (containing η).

In this chapter we will follow the design procedure reviewed in Section 2.3.2.1 of Chapter 2.

Consider the following lower-bounded Lyapunov function:

$$V_1 = \frac{c_1}{2}\Big[y^T M_e y + (x - P_m\bar{x})^T (P_m P_1)^{-1}(x - P_m\bar{x}) + f^T P_u f + h^T P_u h\Big], \quad (6.3.6)$$

where

$$\begin{aligned} y &= \dot{e} + \underline{\mathrm{K}} e; \\ e &= r - q_l; \end{aligned} \quad (6.3.7)$$

the positive scalar c_1 is chosen such that $\mathcal{O}(c_1 M_e) = 1$; x and $\bar{x}$ are the $m\times 1$ true and estimated parameter vectors respectively; m is the number of parameters; f and h are the $n\times 1$ vectors to be determined later; $\underline{\mathrm{K}}$ is the $n\times n$ positive-definite diagonal matrix; P_1 is the $m\times m$ positive-definite diagonal matrix; P_m is the $m\times m$ positive-definite diagonal matrix to be determined later. P_m is used to compensate the uncertainty P_u.

The time-derivative of the Lyapunov function along the trajectory (6.3.1) is given by

$$\begin{aligned}\dot{V}_1 =& c_1\Big[y^T M_e\dot{y} + \frac{1}{2}y^T\dot{M}_e y - \dot{\bar{x}}^T P_1^{-1}(x - P_m\bar{x}) + \dot{f}^T P_u f + \dot{h}^T P_u h\Big] \\ =& c_1 y^T\Big[M_e(\ddot{\sigma} + \rho y) + C\dot{\sigma} + D_e\dot{\sigma} + g + \underline{d} + \eta \\ & + P_u K_1 y + P_u K_2 f + P_u K_3 Y_f h - P_u u_{ta}\Big] \\ & - c_1 y^T(\rho M_e + D_e + P_u K_1)y - c_1\dot{\bar{x}}^T P_1^{-1}(x - P_m\bar{x}) \\ & - c_1(y^T P_u K_2 f - \dot{f}^T P_u f) - c_1(y^T P_u K_3 Y_f h - \dot{h}^T P_u h), \end{aligned} \tag{6.3.8}$$

where

$$\dot{\sigma} = \dot{r} + \underline{K}e;$$

$$\dot{Y}_f + P_f Y_f = P_f Y; \tag{6.3.9}$$

$$Y = \mathrm{diag}(y_1, y_2, \cdots, y_n); \tag{6.3.10}$$

$\rho \geq 0$; K_1 is the $n\times n$ positive-definite diagonal matrix; K_2 and K_3 are $n\times n$ positive-semi-definite diagonal matrices; P_f is the $n\times n$ positive-definite diagonal matrix representing the break frequencies of the low-pass filter (6.3.9); from the link dynamics, $y^T(\dot{M}_e - 2C)y = 0$ if the non-unique matrix C is chosen properly[6.16].

Now, let us define an $n\times m$ function matrix W and parameter vector x such that

$$Wx = M_e(\ddot{\sigma} + \rho y) + C\dot{\sigma} + D_e\dot{\sigma} + g. \tag{6.3.11}$$

Then,

$$\begin{aligned}\dot{V}_1 =& c_1 y^T\Big[Wx + \underline{d} + \eta + P_u K_1 y + P_u K_2 f + P_u K_3 Y_f h - P_u u_{ta}\Big] \\ & - c_1 y^T(\rho M_e + D_e + P_u K_1)y - c_1\dot{\bar{x}}^T P_1^{-1}(x - P_m\bar{x}) \\ & - c_1(y^T P_u K_2 f - \dot{f}^T P_u f) - c_1(y^T P_u K_3 Y_f h - \dot{h}^T P_u h).\end{aligned}$$

(6.3.12)

Let us choose a control law as

$$u_{ta} = W\bar{x} + K_1 y + K_2 f + K_3 Y_f h, \tag{6.3.13}$$

where

$$W\bar{x} = \bar{M}_e(\ddot{\sigma} + \rho y) + \bar{C}\dot{\sigma} + \bar{D}_e\dot{\sigma} + \bar{g}. \tag{6.3.14}$$

The over-barred variables denote the corresponding unbarred counterparts computed with estimated values.

We define W, x, and $\bar{x}$ joint by joint. Then, we have the following relationship between P_m and P_u:

$$P_u W\bar{x} = WP_m\bar{x}. \tag{6.3.15}$$

The matrix P_m is of the following form:

$$P_m = \mathrm{diag}\Big(p_{u1}I_1, p_{u2}I_2, \cdots, p_{un}I_n\Big), \tag{6.3.16}$$

where p_{ui} is the i^{th} diagonal component of P_u and I_i is the identity matrix whose dimension is the same as the number of parameters belonging to the joint i.

Then,

$$\begin{aligned}
\dot{V}_1 =& c_1\Big[W^T y - P_1^{-1}\dot{\bar{x}}\Big]^T(x - P_m\bar{x}) - c_1(y^T P_u K_2 f - \dot{f}^T P_u f) \\
& - c_1(y^T P_u K_3 Y_f h - \dot{h}^T P_u h) - c_1 y^T(\rho M_e + D_e + P_u K_1)y + c_1 y^T(\underline{\mathrm{d}} + \eta) \\
=& c_1\Big[W^T y - P_1^{-1}\dot{\bar{x}} - P_1^{-1}P_2\bar{x}\Big]^T(x - P_m\bar{x}) \\
& - c_1(x - P_m\bar{x})^T(P_mP_1)^{-1}P_2(x - P_m\bar{x}) + c_1 x^T(P_mP_1)^{-1}P_2(x - P_m\bar{x}) \\
& - c_1 f^T\Big[P_u K_2 y - P_u\dot{f} - P_u P_3 f\Big] - c_1 f^T P_u P_3 f \\
& - c_1 h^T\Big[P_u K_3 Y_f y - P_u\dot{h} - P_u P_4 h\Big] - c_1 h^T P_u P_4 h \\
& - c_1 y^T(\rho M_e + D_e + P_u K_1)y + c_1 y^T(\underline{\mathrm{d}} + \eta),
\end{aligned} \tag{6.3.17}$$

where P_2 is the $m \times m$ positive-definite diagonal matrix; P_3 and P_4 are the $n \times n$ positive-semi-definite and positive-definite diagonal matrices respectively.

To stabilize the system ($\dot{V}_1 \leq 0$), we need to remove the sign-indefinite terms in (6.3.17). Hence, we select the following adaptation law:

$$\begin{aligned} \dot{\bar{x}} + P_2 \bar{x} &= P_1 W^T y; \\ \dot{f} + P_3 f &= K_2 y; \\ \dot{h} + P_4 h &= K_3 Y_f y. \end{aligned} \tag{6.3.18}$$

Then,

$$\begin{aligned} \dot{V}_1 = & -\frac{c_1}{2}(x - P_m\bar{x})^T (P_m P_1)^{-1} P_2 (x - P_m \bar{x}) \\ & - \frac{c_1}{2}\bar{x}^T P_1^{-1} P_m P_2 \bar{x} + \frac{c_1}{2} x^T (P_m P_1)^{-1} P_2 x - c_1 f^T P_u P_3 f \\ & - c_1 h^T P_u P_4 h - c_1 y^T (\rho M_e + D_e + P_u K_1) y + c_1 y^T (\underline{\mathrm{d}} + \eta) \\ \leq & - c_1(\rho\gamma_1 + \gamma_2 + \gamma_3)\|y\|^2 - c_1\gamma_4\|f\|^2 - c_1\gamma_5\|h\|^2 \\ & - \frac{c_1\gamma_6}{2}\|(x - P_m\bar{x})\|^2 + c_1\|y\|(\|\underline{\mathrm{d}}\| + \|\eta\|) + \frac{c_1\gamma_7}{2}\|x\|^2, \end{aligned} \tag{6.3.19}$$

where

$$\begin{aligned} \gamma_1 &= \lambda_{\min}(M_e); & \gamma_2 &= \lambda_{\min}(D_e); \\ \gamma_3 &= \lambda_{\min}(P_u K_1); & \gamma_4 &= \lambda_{\min}(P_u P_3); \\ \gamma_5 &= \lambda_{\min}(P_u P_4); & \gamma_6 &= \lambda_{\min}(P_m^{-1} P_1^{-1} P_2); \\ \gamma_7 &= \lambda_{\max}(P_m^{-1} P_1^{-1} P_2). \end{aligned} \tag{6.3.20}$$

Hereafter, $\|\cdot\|$ denotes Euclidean norm of the argument vector, and $\lambda_{\min}(\cdot)$ and $\lambda_{\max}(\cdot)$ denote the minimum and maximum eigenvalues respectively.

Suppose $\eta = 0$. Then, $\dot{V}_1$ in (6.3.19) becomes negative when $\|y\|$ grows larger than a certain upper bound since the true parameter vector x is bounded

and the disturbance $\underline{d}$ is assumed to be bounded. Hence, we can conclude that the reduced-order adaptive control law, the chosen control law (6.3.13) and adaptation law (6.3.18), stabilizes the reduced-order system (with $\eta = 0$). However, we can not conclude anything when we include η since η may grow unbounded coupled with the reduced-order adaptive control law. Hence, in the next section, we impose some constraints on the reduced-order control law so that η is bounded.

The block diagram of the proposed control scheme is shown in Figure 6.1.

6.3.2 Stability Analysis in the Presence of Unmodelled Dynamics

In this section, we obtain certain conditions for the chosen control law (6.3.13) and adaptation law (6.3.18) under which η is bounded. To achieve this, we construct the following additional lower-bounded Lyapunov function:

$$V_2 = \frac{1}{2}\Big[\xi^T\mathcal{E}\xi + \eta^T(6\mathcal{Z}^2 - I)\mathcal{E}\eta\Big], \tag{6.3.21}$$

where

$$\xi \equiv 2\mathcal{Z}\mathcal{E}\dot{\eta} + \eta. \tag{6.3.22}$$

We choose $\sqrt{\frac{1}{2}}I \leq \mathcal{Z} \leq I$ for the reasonable transient response of the system. Hereafter, I denotes the $n\times n$ identity matrix.

The time-derivative of V_2 along the trajectory (6.3.2) is given by

$$\begin{aligned}
\dot{V}_2 =& \Big[-\frac{1}{2}\mathcal{Z}\xi - (3\mathcal{Z}^2 - I)\mathcal{E}\dot{\eta} - \frac{3}{2}\mathcal{Z}\eta + 2\mathcal{Z}P_u(2\mathcal{Z}\mathcal{E}\dot{u}_l + \mathcal{E}^2\ddot{u}_l)\Big]^T\xi + \dot{\eta}^T(6\mathcal{Z}^2 - I)\mathcal{E}\eta \\
=& -\frac{1}{2}\xi^T\mathcal{Z}\xi - \frac{3}{2}\eta^T\mathcal{Z}\eta - 2\dot{\eta}^T\mathcal{Z}(3\mathcal{Z}^2 - I)\mathcal{E}^2\dot{\eta} + 2(2\mathcal{Z}\mathcal{E}\dot{u}_l + \mathcal{E}^2\ddot{u}_l)^T\mathcal{Z}P_u\xi \\
\leq& -\frac{1}{2}\gamma_8\|\xi\|^2 - \frac{3}{2}\gamma_8\|\eta\|^2 - \epsilon^2\gamma_9\|\dot{\eta}\|^2 + 2(2\mathcal{Z}\mathcal{E}\dot{u}_l + \mathcal{E}^2\ddot{u}_l)^T\mathcal{Z}P_u\xi,
\end{aligned} \tag{6.3.23}$$

where

$$\gamma_8 = \lambda_{\min}(\mathcal{Z}) \qquad \text{and} \qquad \gamma_9 = \lambda_{\min}\Big(2(3\mathcal{Z}^2 - I)\mathcal{E}^2/\epsilon^2\Big). \tag{6.3.24}$$

Note that $\dot{V}_1$ and $\dot{V}_2$, the time-derivatives of Lyapunov functions, are coupled through $\|\eta\|\|y\|$ in $\dot{V}_1$ and $(2\mathcal{Z}\mathcal{E}\dot{u}_l + \mathcal{E}^2\ddot{u}_l)^T\mathcal{Z}\xi$ in $\dot{V}_2$. Hence, we define a combined

Lyapunov function V_o for the system (6.3.1) and (6.3.2) as

$$\begin{aligned} V_o =& V_1 + V_2 \\ =& \frac{c_1}{2}\Big[y^T M_e y + (x - P_m\bar{x})^T (P_m P_1)^{-1}(x - P_m\bar{x}) + f^T P_u f + h^T P_u h\Big] \\ &+ \frac{1}{2}\Big[\xi^T \mathcal{E}\xi + \eta^T (6\mathcal{Z}^2 - I)\mathcal{E}\eta\Big]. \end{aligned} \tag{6.3.25}$$

Then, from (6.3.19) and (6.3.23),

$$\begin{aligned} \dot{V}_o =& \dot{V}_1 + \dot{V}_2 \\ \leq& - c_1(\rho\gamma_1 + \gamma_2 + \gamma_3)\|y\|^2 - c_1\gamma_4\|f\|^2 - c_1\gamma_5\|h\|^2 \\ &- \frac{c_1\gamma_6}{2}\|(x - P_m\bar{x})\|^2 + c_1\|y\|(\|\underline{d}\| + \|\eta\|) + \frac{c_1\gamma_7}{2}\|x\|^2 \\ &- \frac{1}{2}\gamma_8\|\xi\|^2 - \frac{3}{2}\gamma_8\|\eta\|^2 - \epsilon^2\gamma_9\|\dot{\eta}\|^2 + 2(2\mathcal{Z}\mathcal{E}\dot{u}_l + \mathcal{E}^2\ddot{u}_l)^T \mathcal{Z} P_u \xi. \end{aligned} \tag{6.3.26}$$

To guarantee stability ($\dot{V}_o \leq 0$), we make $c_1\|\eta\|\|y\|$ and the sign-indefinite term $(2\mathcal{Z}\mathcal{E}\dot{u}_l + \mathcal{E}^2\ddot{u}_l)^T\mathcal{Z}\xi$ in (6.3.26) cancelled out, or much smaller than the other terms in $\dot{V}_o$. Here, we restrict our analysis inside a certain set, as in the previous two chapters:

$$\mathcal{S}_1 = \{(y, \bar{x}, f, h, \eta, \xi) \mid V_o \leq \mu^2\}, \tag{6.3.27}$$

where

$$\mu \equiv \frac{a}{\epsilon}, \tag{6.3.28}$$

for some finite positive scalar a to be determined later. Note that the size of the set $\mathcal{S}_1$ has not been determined yet.

For simplicity, we assume that $\mathcal{O}(c_1) = \mu^0$ and $\mathcal{O}(P_u) = \mathcal{O}(P_m) = \mu^0$. Note that μ^0 denotes unity consistent with the other orders of μ. Then, inside the set $\mathcal{S}_1$, $\mathcal{O}(y) \leq \mu$, $\mathcal{O}(Y) \leq \mu$, $\mathcal{O}(\xi) \leq \mu\epsilon^{-\frac{1}{2}}$, $\mathcal{O}(\eta) \leq \mu\epsilon^{-\frac{1}{2}}$, $\mathcal{O}(\dot{\eta}) \leq \mu\epsilon^{-\frac{3}{2}}$, $\mathcal{O}(f) \leq \mu$, and $\mathcal{O}(h) \leq \mu$. For simplicity, we limit the order of P_1 to μ^0. Then $\mathcal{O}(x - P_m\bar{x}) \leq \mu$. We can readily include the orders of c_1, P_u, and P_1 in this analysis if they are far from $\mathcal{O}(\mu^0)$.

Equations (6.3.7) and (6.3.9) are stable first-order differential equations. Hence, inside the set $\mathcal{S}_1$, $\mathcal{O}(\dot{e}) \leq \mu$, $\mathcal{O}(e) \leq \mu$, and $\mathcal{O}(Y_f) \leq \mu$ under the constraints of $\mathcal{O}(\dot{e}(0)) \leq \mu$, $\mathcal{O}(e(0)) \leq \mu$, $\mathcal{O}(Y_f(0)) \leq \mu$, and $\mathcal{O}(\underline{\mathrm{K}}) = \mu^0$. We assume for all time $t \geq 0$ that the desired trajectory satisfies $\mathcal{O}(r) \leq \mu$ and $\mathcal{O}(\dot{r}) \leq \mu$. Then, the orders of $\dot{q}_l$ and q_l can be obtained as $\mathcal{O}(\dot{q}_l) \leq \mu$ and $\mathcal{O}(q_l) \leq \mu$. We also assume that $\mathcal{O}(x) = \mu^0$, which results in $\mathcal{O}(\bar{x}) \leq \mu$.

Then, inside the set $\mathcal{S}_1$, we can obtain the following bounds:

$$
\begin{aligned}
\dot{u}_{ta} &= \Big[\mathcal{O}(\mu^5) + \mathcal{O}(\mu^3 \epsilon^{-\frac{1}{2}})\Big] \underline{\mathrm{u}}_2, \\
\ddot{u}_{ta} &= \Big[\mathcal{O}(\mu^7) + \mathcal{O}(\mu^5 \epsilon^{-\frac{1}{2}}) + \mathcal{O}(\mu^3 \epsilon^{-\frac{3}{2}})\Big] \underline{\mathrm{u}}_3, \\
q_l^{III} &= -M_e^{-1} \dot{\eta} + \mathcal{O}(\dot{u}_{ta}), \\
q_l^{IV} &= M_e^{-1} \Big[\mathcal{E}^{-2} \xi + \Big(\mathcal{O}(\mathcal{E}^{-1} \dot{u}_{ta}) + \mathcal{O}(\ddot{u}_{ta}) + \mathcal{O}(\mu^7)\Big) \underline{\mathrm{q}}_3\Big],
\end{aligned}
\tag{6.3.29}
$$

for some $n \times 1$ vectors $\underline{\mathrm{u}}_2(t)$, $\underline{\mathrm{u}}_3(t)$, and $\underline{\mathrm{q}}_3(t)$ of order μ^0. See Appendix 6.A for detail. These bounds are derived under the following constraints:

$$
\begin{aligned}
(i) \quad & \mathcal{O}(r) \leq \mathcal{O}(\mu), \quad \mathcal{O}(\dot{r}) \leq \mathcal{O}(\mu), \quad \mathcal{O}(\ddot{r}) \leq \mathcal{O}(\mu^2), \\
& \mathcal{O}(r^{III}) \leq \mathcal{O}(\mu^4), \quad \mathcal{O}(r^{IV}) \leq \mathcal{O}(\mu^6); \\
(ii) \quad & \mathcal{O}(\underline{\mathrm{d}}) \leq \mu, \quad \mathcal{O}(\dot{\underline{\mathrm{d}}}) \leq \mu^5, \quad \mathcal{O}(\ddot{\underline{\mathrm{d}}}) \leq \mu^7; \\
(iii) \quad & \mathcal{O}(\rho) \leq \mu, \quad \mathcal{O}(K_1) \leq \mu^2, \quad \mathcal{O}(K_2) \leq \mu^2, \\
& \mathcal{O}(K_3) \leq \mu, \quad \mathcal{O}(P_1) \leq \mu^0, \quad \mathcal{O}(P_2) \leq \mu^2, \\
& \mathcal{O}(P_3) \leq \mu^2, \quad \mathcal{O}(P_4) \leq \mu^2, \quad \mathcal{O}(P_f) \leq \mu^2.
\end{aligned}
\tag{6.3.30}
$$

The bounds (6.3.29) and (6.3.30) are derived for revolute-joint robots. The structure of the dynamics of robots is the same regardless of the type of joint. Hence, the corresponding bounds for prismatic-joint or prismatic-revolute-joint robots are similar to those in (6.3.29) and (6.3.30) and can be readily derived. In this case, the stability analysis is basically the same as that described below.

With (6.3.3), (6.3.29), and the constraints of

$$\bar{\sigma}_{\max}(B_e M_e^{-1}) \leq \mu^0 \quad \text{and} \quad \bar{\sigma}_{\max}(J_e M_e^{-1}) \leq \mu^0, \tag{6.3.31}$$

we have the following relationship:

$$\begin{aligned} 2(2\mathcal{Z}\mathcal{E}\dot{u}_l + \mathcal{E}^2\ddot{u}_l)^T \mathcal{Z} P_u \xi \\ &= 2\Big[\mathcal{O}(\mu^5\epsilon) + \mathcal{O}(\mu^3\epsilon^{\frac{1}{2}}) + \mathcal{O}(\mu^7\epsilon^2)\Big]\xi_o^T \mathcal{Z}\xi \\ &\quad + 2(2\mathcal{E}\mathcal{Z}B_e M_e^{-1}\dot{\eta} - \mathcal{E}^2 J_e M_e^{-1}\mathcal{E}^{-2}\xi)^T \mathcal{Z}\xi \end{aligned} \tag{6.3.32}$$

for some $n\times 1$ vector $\xi_o(t)$ such that $\mathcal{O}(\xi_o) = \mu^0$.

Hereafter, $\bar{\sigma}_{\min}(\cdot)$ and $\bar{\sigma}_{\max}(\cdot)$ denote the minimum and maximum singular values respectively. Note that J_e and B_e are functions of the free design parameter K_{cp}. See (6.2.17) and (6.3.5).

To guarantee $\dot{V}_2 \leq 0$ inside the set $\mathcal{S}_1$, the sign-indefinite term $(2\mathcal{Z}\mathcal{E}\dot{u}_l + \mathcal{E}^2\ddot{u}_l)^T \mathcal{Z} P_u \xi$ in (6.3.32) must be much smaller than the other terms in $\dot{V}_2$ in (6.3.23). Accordingly, based on the assumption of $\epsilon \ll 1$, we set

$$2\Big[\mathcal{O}(\mu^5\epsilon) + \mathcal{O}(\mu^3\epsilon^{\frac{1}{2}}) + \mathcal{O}(\mu^7\epsilon^2)\Big] < \epsilon^{\frac{3}{5}}\mathcal{O}(\xi). \tag{6.3.33}$$

This leads to

$$0 < a < \epsilon^{\frac{4}{5}} \qquad (\implies \qquad \mu < \epsilon^{-\frac{1}{5}} \quad). \tag{6.3.34}$$

Let $\tilde{\xi}$ be the maximum value of ξ inside the set $\mathcal{S}_1$. Then, from (6.3.33), there exists an $n\times 1$ vector $\bar{\xi}(t)$ such that $\mathcal{O}(\bar{\xi}_{\max}) < \mathcal{O}(\tilde{\xi})$ and

$$2\Big[\mathcal{O}(\mu^5\epsilon) + \mathcal{O}(\mu^3\epsilon^{\frac{1}{2}}) + \mathcal{O}(\mu^7\epsilon^2)\Big]\xi_o \leq \epsilon^{\frac{3}{5}}\bar{\xi}. \tag{6.3.35}$$

Then, (6.3.32) with (6.3.22) becomes

$$\begin{aligned} 2(2\mathcal{Z}\mathcal{E}\dot{u}_l + \mathcal{E}^2\ddot{u}_l)^T \mathcal{Z} P_u \xi \leq &\epsilon^{\frac{3}{5}}\bar{\xi}^T \mathcal{Z}\xi + 4\eta^T \mathcal{E}\mathcal{Z}^2 B_e M_e^{-1}\dot{\eta} + 8\dot{\eta}^T \mathcal{E}^2 \mathcal{Z}^3 B_e M_e^{-1}\dot{\eta} \\ &- 2\xi^T \mathcal{E}^2 \mathcal{Z} J_e M_e^{-1}\mathcal{E}^{-2}\xi. \end{aligned} \tag{6.3.36}$$

Then, (6.3.23) with (6.3.36) yields

$$\begin{aligned}\dot{V}_2 \le & -\frac{1}{2}\gamma_8\|\xi\|^2 - \frac{3}{2}\gamma_8\|\eta\|^2 - \epsilon^2\gamma_9\|\dot{\eta}\|^2 + \epsilon^{\frac{3}{5}}\bar{\xi}^T\mathcal{Z}\xi + 4\eta^T\mathcal{E}\mathcal{Z}^2B_eM_e^{-1}\dot{\eta} \\ & + 8\dot{\eta}^T\mathcal{E}^2\mathcal{Z}^3B_eM_e^{-1}\dot{\eta} - 2\xi^T\mathcal{E}^2\mathcal{Z}J_eM_e^{-1}\mathcal{E}^{-2}\xi \\ \le & -\frac{1}{2}\gamma_8\|\xi\|^2 - \frac{3}{2}\gamma_8\|\eta\|^2 - \epsilon^2\gamma_9\|\dot{\eta}\|^2 + \epsilon\gamma_{10}\|\eta\|\|\dot{\eta}\| + \epsilon^2\gamma_{11}\|\dot{\eta}\|^2 \\ & + \gamma_{12}\|\xi\|^2 + \epsilon^{\frac{3}{5}}\gamma_{13}\|\bar{\xi}\|\|\xi\|, \end{aligned} \tag{6.3.37}$$

where

$$\begin{aligned}\gamma_{10} &= \bar{\sigma}_{\max}\Big(4\mathcal{E}\mathcal{Z}^2B_eM_e^{-1}/\epsilon\Big); \\ \gamma_{11} &= \bar{\sigma}_{\max}\Big(8\mathcal{E}^2\mathcal{Z}^3B_eM_e^{-1}/\epsilon^2\Big); \\ \gamma_{12} &= \bar{\sigma}_{\max}\Big(2\mathcal{E}^2\mathcal{Z}J_eM_e^{-1}\mathcal{E}^{-2}\Big); \\ \gamma_{13} &= \bar{\sigma}_{\max}(\mathcal{Z}). \end{aligned} \tag{6.3.38}$$

If we choose J_e and B_e such that

$$\begin{aligned}\gamma_{12} \le \frac{\gamma_8}{8} \quad \Big(\quad \Longleftrightarrow \quad \bar{\sigma}_{\max}\Big(2\mathcal{E}^2\mathcal{Z}J_eM_e^{-1}\mathcal{E}^{-2}\Big) \le \frac{1}{8}\bar{\sigma}_{\min}(\mathcal{Z}) \quad \Big); \\ \gamma_{11} \le \frac{\gamma_9}{2} \quad \Big(\quad \Longleftrightarrow \quad \bar{\sigma}_{\max}\Big(8\mathcal{E}^2\mathcal{Z}^3B_eM_e^{-1}\Big) \le \frac{1}{2}\bar{\sigma}_{\min}(2(3\mathcal{Z}^2 - I)\mathcal{E}^2) \quad \Big), \end{aligned} \tag{6.3.39}$$

then, we can remove the positive terms $\epsilon^2\gamma_{11}\|\dot{\eta}\|^2$ and $\gamma_{12}\|\xi\|^2$ from $\dot{V}_2$:

$$\begin{aligned}\dot{V}_2 \le & -\gamma_8\|\eta\|^2 - \frac{1}{2}(\gamma_8\|\eta\|^2 - 2\epsilon\gamma_{10}\|\eta\|\|\dot{\eta}\| + \epsilon^2\gamma_9\|\dot{\eta}\|^2) - \frac{\gamma_8}{4}\|\xi\|^2 \\ & - \frac{1}{8}(\gamma_8\|\xi\|^2 - 8\epsilon^{\frac{3}{5}}\gamma_{13}\|\bar{\xi}\|\|\xi\| + 16\epsilon^{\frac{6}{5}}\gamma_{14}\|\bar{\xi}\|^2) + 2\epsilon^{\frac{6}{5}}\gamma_{14}\|\bar{\xi}\|^2. \end{aligned} \tag{6.3.40}$$

If we set γ_{14} and B_e such that

$$\gamma_{14} \ge \frac{\gamma_{13}^2}{\gamma_8} = \frac{\lambda_{\max}^2(\mathcal{Z})}{\lambda_{\min}(\mathcal{Z})}; \tag{6.3.41}$$

$$\gamma_{10} \le \sqrt{\gamma_8\gamma_9} \quad \Big(\iff \bar{\sigma}_{\max}(4\mathcal{E}\mathcal{Z}^2 B_e M_e^{-1}) \le \sqrt{\lambda_{\min}(\mathcal{Z})\lambda_{\min}(2(3\mathcal{Z}^2 - I)\mathcal{E}^2)} \Big), \tag{6.3.42}$$

then, $\frac{1}{2}(\cdots)$ and $\frac{1}{8}(\cdots)$ in (6.3.40) become positive (squared) so that we can delete them from $\dot{V}_2$:

$$\dot{V}_2 \le -\gamma_8\|\eta\|^2 - \frac{\gamma_8}{4}\|\xi\|^2 + 2\epsilon^{\frac{6}{5}}\gamma_{14}\|\bar{\xi}\|^2. \tag{6.3.43}$$

We combine (6.3.19) and (6.3.43):

$$\begin{aligned}
\dot{V}_o =& \dot{V}_1 + \dot{V}_2 \\
\le& - c_1(\rho\gamma_1 + \gamma_2 + \gamma_3)\|y\|^2 - c_1\gamma_4\|f\|^2 - c_1\gamma_5\|h\|^2 - \frac{c_1\gamma_6}{2}\|(x - P_m\bar{x})\|^2 \\
&+ c_1\|y\|(\|\hat{d}\| + \|\eta\|) + \frac{c_1\gamma_7}{2}\|x\|^2 - \gamma_8\|\eta\|^2 - \frac{\gamma_8}{4}\|\xi\|^2 + 2\gamma_{14}\epsilon^{\frac{6}{5}}\|\bar{\xi}\|^2 \\
\le& - c_1(\rho\gamma_1 + \gamma_2 + \gamma_{15})\|y\|^2 - c_1\gamma_4\|f\|^2 - c_1\gamma_5\|h\|^2 - \frac{c_1\gamma_6}{2}\|(x - P_m\bar{x})\|^2 \\
&- \frac{\gamma_8}{4}\|\xi\|^2 - \frac{\gamma_8}{2}\|\eta\|^2 + \frac{c_1}{\gamma_3}\|\hat{d}\|^2 + \frac{c_1\gamma_7}{2}\|x\|^2 + 2\gamma_{14}\epsilon^{\frac{6}{5}}\|\hat{\xi}\|^2,
\end{aligned} \tag{6.3.44}$$

where we have removed η terms by completing the square with

$$\|\hat{d}\| \equiv \|\underline{d}\|_{\max} \quad \text{and} \quad \hat{\xi} \equiv \|\bar{\xi}\|_{\max}, \quad \forall\, t \ge 0; \tag{6.3.45}$$

$$\gamma_{15} = \frac{3}{4}\gamma_3 - \frac{c_1^2}{2\gamma_8}. \tag{6.3.46}$$

From (6.3.20), (6.3.24), (6.3.30), (6.3.34), (6.3.41), and (6.3.46), we obtain the following bounds:

$$\begin{aligned}
&\mathcal{O}(\gamma_3) \le \mu^2, \;\; \mathcal{O}(\gamma_4) \le \mu^2, \;\; \mathcal{O}(\gamma_5) \le \mu^2, \\
&\mathcal{O}(\gamma_6) \le \mu^2, \;\; \mathcal{O}(\gamma_7) \le \mu^2, \;\; \mathcal{O}(\gamma_8) \le \mu^0, \\
&\mathcal{O}(\gamma_{14}) \le \mu^0, \;\; \mathcal{O}(\gamma_{15}) \le \mu^2, \;\; \mathcal{O}(\hat{\xi}) \le \epsilon^{-\frac{1}{2}}\mu, \\
&\mathcal{O}(\hat{d}) \le \mu.
\end{aligned} \tag{6.3.47}$$

Then, we rewrite (6.3.44) using V_o in (6.3.25):

$$\dot{V}(t) + \beta V(t) \le \alpha_1 - \alpha_2(t) \tag{6.3.48}$$

with

$$\alpha_1 = \frac{c_1}{\gamma_3}\|\hat{d}\|^2 + \frac{c_1\gamma_7}{2}\|x\|^2 + 2\gamma_{14}\epsilon^{\frac{6}{5}}\|\hat{\xi}\|^2 \qquad \Big[\ \leq \max[\mathcal{O}(\mu), \mathcal{O}(\gamma_7)] \quad \text{if } \mathcal{O}(\gamma_3) \geq \mu\ \Big],$$

$$\begin{aligned}\alpha_2 =& c_1\Big[(\rho\gamma_1 + \gamma_2 + \gamma_{15})\|y\|^2 - \frac{\beta}{2}y^T M_e y\Big] \\ &+ c_1\Big[\gamma_4\|f\|^2 - \frac{\beta}{2}f^T P_u f\Big] + c_1\Big[\gamma_5\|h\|^2 - \frac{\beta}{2}h^T P_u h\Big] \\ &+ c_1\Big[\frac{\gamma_6}{2}\|(x - P_m\bar{x})\|^2 - \frac{\beta}{2}(x - P_m\bar{x})^T(P_m P_1)^{-1}(x - P_m\bar{x})\Big] \\ &+ \Big[\frac{\gamma_8}{4}\|\xi\|^2 - \frac{\beta}{2}\xi^T\mathcal{E}\xi\Big] + \Big[\frac{\gamma_8}{2}\|\eta\|^2 - \frac{\beta}{2}\eta^T(6\mathcal{Z}^2 - I)\mathcal{E}\eta\Big] \geq 0, \end{aligned} \tag{6.3.49}$$

where the positive constant β is chosen to be the maximum value which makes the expressions in all the brackets ($[\cdots]$) non-negative. Then, $\mathcal{O}(\beta) \leq \mu^2$. See (6.3.34), (6.3.47), and (6.3.49).

The solution of (6.3.48) is given by

$$V(t) \leq \exp[-\beta t]\Big(V(0) + \int_0^t \{\alpha_1 - \alpha_2(\tau)\}\exp[\beta\tau]d\tau\Big). \tag{6.3.50}$$

Consequently, we conclude that any initial $V(t)$ belonging to the set $\mathcal{S}_1$ converges into the following residual set:

$$\mathcal{S}_2 = \Big\{(y, \bar{x}_j, f, h, \eta, \xi) \mid V(t) \leq \exp[-\beta t]\int_0^t \{\alpha_1 - \alpha_2(\tau)\}\exp[\beta\tau]d\tau \leq \frac{\alpha_1}{\beta}\Big\} \tag{6.3.51}$$

at a rate of at least exp[-βt]. Since $\mathcal{O}(\beta) \leq \mu^2$ and $\alpha_1 \leq \max[\mathcal{O}(\mu), \mathcal{O}(\gamma_7)]$, the size of $\mathcal{S}_2$ is given by $\mu^0 \leq \mathcal{O}(\alpha_1/\beta) < \mu^2$ under the constraints that

$$\begin{aligned}&\mu \leq \mathcal{O}(K_1) \leq \mu^2, \quad \mu^{-1} < \mathcal{O}(P_2) \leq \mu^2, \\ &\mu^{-1} < \mathcal{O}(P_2) \leq \mathcal{O}(P_3) \leq \mu^2, \quad \mu^{-1} < \mathcal{O}(P_2) \leq \mathcal{O}(P_4) \leq \mu^2, \end{aligned} \tag{6.3.52}$$

which satisfy the condition $\mathcal{O}(\gamma_3) \geq \mu$ in (6.3.49). Note that $\mathcal{O}(\gamma_7) = \mathcal{O}(P_2) \leq \mu^2$ and $\mathcal{O}(\beta) = \min[\mathcal{O}(K_1), \mathcal{O}(P_2)]$. See (6.3.30) and (6.3.49) with the definitions of

γ_j's.

Note that $\alpha_2(t)$ accelerates the convergence rate and reduces the size of the set $\mathcal{S}_2$ even further. Note also that $\mathcal{S}_2 \subset \mathcal{S}_1$. As a consequence, under the assumption of $\epsilon \ll 1$, any initial $V_o(t)$ belonging to $\mathcal{S}_1$ converges exponentially into the residual set $\mathcal{S}_2$. Hence, from the definition of $V_o(t)$ in (6.3.25), boundedness of y, $\bar{x}$, f, h, η, and ξ follows for all time $t \geq 0$. Note that the region of attraction is finite (inside $\mathcal{S}_1$) for nonzero ϵ. Hence, all the initial conditions (tracking errors and parameter errors) must belong to $\mathcal{S}_1$ for stability.

6.3.3 An Improved Adaptation Law

To improve the control performance, we proposed two new adaptation laws (4.4.19) and (4.4.20) in Chapter 4, based on the bounds of the parameters of the dynamics. We apply one of these in this chapter to improve the transient response of the system.

We use integrators for the adaptation law when the magnitude of $\bar{x}$ is smaller than the preset value (or the nominal value), and otherwise, we use first-order filters with variable break frequencies, as follows:

$$\dot{\bar{x}} + P_2\bar{x} = P_1 W^T y \tag{6.3.53}$$

with

$$p_{2i} = \begin{cases} 0, & \text{for } |\bar{x}_i| < x_i^*, \quad i = 1, 2 \cdots, n; \\ p_{5i}(|\bar{x}_i| - x_i^*), & \text{for } |\bar{x}_i| \geq x_i^*, \quad i = 1, 2, \cdots, n, \end{cases} \tag{6.3.54}$$

where p_{5i} and x_i^* are selected such that $p_{5i} > 0$ and $x_i^* > |x_i|/p_{mi}$; the subscript i denotes the i^{th} component of the corresponding vectors (x, $\bar{x}$ and x^*) or the i^{th} diagonal component of the corresponding matrices (P_2, P_5, and P_m).

Then, in equation (6.3.19)

$$\frac{c_1}{2}\bar{x}^T P_1^{-1} P_m P_2 \bar{x} \geq \frac{c_1}{2} x^T (P_m P_1)^{-1} P_2 x, \quad \forall\, \bar{x}. \tag{6.3.55}$$

Hence, $\dot{V}_1$ and hence $\dot{V}_o$ exclude the $\|x\|$ term so that the error bounds become smaller. In this case, we have the constraint of $\mu^{-1} < \mathcal{O}(P_5) \leq \mu$ when we go through the stability analysis.

6.4 Remarks

We can summarize our stability analysis with the adaptive control law (6.2.11), (6.2.14), (6.2.16), (6.3.13), and (6.3.18) as follows.

1. When we allow uncertainties in the torque constants of actuators, the dynamics of manipulators are also represented by (6.3.1): $\eta = 0$ for rigid-joint robots and $\eta \neq 0$ for flexible-joint robots. Consequently, the design method in Section 6.3.1 also treats those uncertainties.

2. According to (6.3.6), $\bar{x}$ converges to $P_m^{-1}x$ in an ideal situation ($\eta = 0$ and $\underline{d} = 0$ with persistently excited reference inputs). This means that the parameter $\bar{x}_j$ belonging to the joint i converges to x_j/p_{ui}. Consequently, the uncertainty P_u can be considered to be included in those of the parameter x. Hence, the proposed control law (6.3.13) and (6.3.18) is robust to uncertainties in the stiffness of the joint couplings. Even though the proposed control law is robust to uncertainties with K_c, the nominal value of K_c is to be used in computation of K_{nt} in (6.2.16) for the best transient response of the dynamic system.

3. Constraints in (6.3.30) require that the reference inputs and disturbances have limited spectral ranges so that they must not excite the high-frequency prefilter dynamics, and that the magnitudes of control and adaptation gains be also limited to avoid excitation of the high-frequency prefilter dynamics.

4. Constraints (6.3.31), (6.3.39), and (6.3.42) require that $\bar{\sigma}_{\max}(J_e M_e^{-1})$ and $\bar{\sigma}_{\max}(B_e M_e^{-1})$ be small. This may require that $\lambda_{\max}(J_e)$ be smaller than $\lambda_{\min}(M(q_l))$ since $M_e = M(q_l) + J_e$ with $J_e = K_t^{-1}N^2 J_a$. Smaller $\bar{\sigma}_{\max}(B_e M_e^{-1})$ requires smaller B_e ($= K_t^{-1}N^2 B_a$). Accordingly, larger $M(q_l)$ and K_{nt} and smaller N, J_a and B_a cause a larger stability margin. If $M(q_l)$ is too small or N is too large, we may have instability since K_{nt} can not be increased infinitely due to other unmodelled dynamics such as inductance of electrical actuators and feedback delays in the digital control systems.

5. Constraint (6.3.42) requires that the damping ratio ($\mathcal{Z}$) be greater than $1/\sqrt{3}$. This numerical value may be adjusted more or less depending on the choice

of Lyapunov function V_2 in (6.3.21) and its time-derivative $\dot{V}_2$ in (6.3.23).

6. Constraint (6.3.27) with (6.3.34) means that S_1, the region of attraction, is finite (local) for nonzero ϵ, and that all the initial conditions (tracking errors and parameter errors) must belong to S_1 for stability.

7. When the adaptation law (6.3.18) is used, larger P_2 causes larger tracking errors. See the $\|x\|$ term in (6.3.49) and (6.3.51) with the definition of γ_7 in (6.3.20). However, smaller P_2 causes smaller robustness (higher possibility of parameter drift). The new adaptation law (6.3.54) solves these contradictory problems.

8. When we set $P_3 = 0$, $K_2 f$ becomes a PI feedback compensator. $K_1 y$ is a PD feedback compensator. Therefore, we may select the gains K_1 and K_2 using a linearized model of robot dynamics.

6.5 Attenuation of Sensor Noise in Flexibility Compensation

We converted control of flexible-joint manipulators to that of the rigid-joint counterparts by adding an appropriate flexibility compensator. Then, we designed a robust adaptive control law subject to some moderate constraints. In this section, we focus on only the flexibility compensation loop since serious problems may arise from high gains K_{cv} and K_{cp} for larger bandwidth of the flexibility compensation loop. Small measurement noises may be so magnified as to degrade the performance of the proposed scheme. Discretization of analogue signals always contains a certain degree of high-frequency noises, which depends mainly on sensor resolution and sampling interval. The objective in this section is to minimize the effects of high-frequency sensor noises.

To examine the effect of high-frequency sensor noises, we need to separate the measured signals from the states of the system (the actual signals). In flexibility compensation, u_c is the measured signal. Since the flexibility loop is a linear decoupled time-invariant system, we take Laplace transformations of (6.2.12) and (6.2.14):

$$NJ_aVs^2 + NB_aVs + N^{-1}K_cV = K_tN^{-1}U_l + U_c, \tag{6.5.1}$$

$$U_c = -(K_{cv}s + K_{cp})V, \tag{6.5.2}$$

where V, U_l, and U_c are the Laplace transformations of v, u_l, and u_c respectively. From (6.2.13),

$$U_l = U_{ta} - K_{nt}^{-1} N^2 D_a, \tag{6.5.3}$$

with

$$D_a = (J_a s^2 + B_a s) Q_l, \tag{6.5.4}$$

where Q_l is the Laplace transform of q_l.

Since the system is decoupled, hereafter we will consider each joint separately. Figure 6.2 shows the block diagram of the original flexibility compensator for the i^{th} joint, based on (6.5.1), (6.5.2), and (6.5.3), where $\bar{N}_i$ represents the sensor noises in the Laplace domain; D_{bi} is the disturbances to the flexibility loop in the Laplace domain. The transfer functions associated with the closed loop system are defined as follows:

$$\begin{aligned}
&\frac{V_i}{U_{tai}} = K_{nti} N^{-1} \frac{G_i}{1 + L_i}, \\
&\frac{V_i}{D_{ai}} = N_i \frac{G_i}{1 + L_i}, \\
&\frac{V_i}{D_{bi}} = \frac{G_i}{1 + L_i}, \\
&\frac{V_i}{\bar{N}_i} = \frac{L_i}{1 + L_i} = N_i K_{nti}^{-1} (K_{cpi} + K_{cvi} s) \cdot \frac{V_i}{U_{tai}}, \\
&T_i = K_{ci} V_i,
\end{aligned} \tag{6.5.5}$$

with

$$\begin{aligned}
&G_i = \frac{1}{N_i J_{ai} s^2 + N_i B_{ai} s + N_i^{-1} K_{ci}}, \\
&L_i = (K_{cvi} s + K_{cpi}) G_i,
\end{aligned} \tag{6.5.6}$$

where the subscript i indicates the i^{th} joint, i.e., the i^{th} component of the corresponding vector and the i^{th} diagonal component of the corresponding matrix. Effects of the actuator dynamics (i.e., V_i due to D_{ai}) are compensated by the

adaptive control law U_{tai}. See the model of the system (6.3.1) to control. According to V_i/D_{bi} in (6.5.5) with L_i in (6.5.6), large gains K_{cvi} and K_{cpi} substantially suppress the effects of disturbances. Hence, we do not try to suppress the effects of disturbances inside the flexibility loop.

Since $V_i/\bar{N}_i$ in (6.5.5) has a surplus zero $(K_{cpi} + K_{cvi}s)$ over V_i/U_{tai}, the closed loop system is more sensitive to unavoidable high-frequency sensor noises than to the high-frequency input U_{tai}. Therefore we need to reduce the gain of $V_i/\bar{N}_i$ in the high-frequency region. One of the possible solutions is to add to the feedback loop (next to H_{1i}) a low-pass filter H_{2i} of the following form:

$$H_{2i} = \frac{P_{6i}}{s + P_{6i}}. \tag{6.5.7}$$

See Figure 6.3. The break frequency $P_{6i}(\geq 0)$ must be chosen to be moderately larger than the crossover frequency of the open loop transfer function L_i so as to minimize the reduction of the phase margin (i.e., stability of the closed loop system) caused by addition of the pole. Note that in the continuous time domain the open loop transfer function L_i in (6.5.6) has approximately 90 degrees of phase margin almost independent of the crossover frequency. However, in the discrete time domain, the phase margin of L_i decreases as the crossover frequency increases because L_i includes an additional phase lag due to the delay of one sampling interval in the feedback loop for computations, measurements, and conversion of signals. The additional phase lag at a certain frequency due to the delay is proportional to the frequency and the sampling interval. See Section 3 in Chapter 3.

The block diagram of the new flexibility compensation is shown in Figure 6.3. The corresponding transfer functions now become

$$\frac{V_i}{U_{tai}} = N_i K_{nti}^{-1} \frac{G_i}{1 + H_{2i}L_i},$$
$$\frac{V_i}{U_{ai}} = N_i \frac{G_i}{1 + H_{2i}L_i},$$

$$\frac{V_i}{D_{bi}} = \frac{G_i}{1 + H_{2i}L_i},$$

$$\frac{V_i}{\bar{N}_i} = \frac{H_{2i}L_i}{1 + H_{2i}L_i} = \frac{P_{6i}}{P_{6i} + s} \cdot N_i K_{nti}^{-1}(K_{cvi}s + K_{cpi}) \cdot \frac{V_i}{U_{tai}}. \qquad (6.5.8)$$

Note that H_{2i} affects the closed loop only in the high-frequency region (where L_i is much smaller than 1). Consequently, $(1+L_i)$ and $(1+H_{2i}L_i)$, the denominators of the old and new closed loop transfer functions, are almost the same. Hence, addition of H_{2i} hardly changes the closed loop transfer functions V/U_{tai}, V_i/U_{ai}, and V_i/U_{bi}. However, H_{2i} filters out high-frequency sensor noises since H_{2i} provides the new $V_i/\bar{N}_i$ in (6.5.8) with an additional pole $(P_{6i} + s)$. In this case, the flexibility compensator and the actuator input become

$$U_{ai} = K_{nt}N^{-1}U_{tai} + U_{ci},$$

$$U_{ci} = -H_{2i}(K_{cvi}s + K_{cpi})V_i, \qquad (6.5.9)$$

where U_{ai}, U_{tai} and U_{ci} are the Laplace transformations of u_a u_{ta}, and u_c for the i^{th} joint respectively. In fact, we can add any kind and/or number of low-pass filters so long as addition of these filters does not reduce the phase margin much.

6.6 Computer Simulation

As an example, we apply one of the schemes developed here to a two-link gear-reduction arm shown in Figure 6.4. We use a 4^{th}-order Runge-Kutta method[6.26] with adaptive step size to guarantee accuracy in the solution of the manipulator dynamics. The dynamic equations of motion of the manipulator are given by

$$M\ddot{q}_l + C\dot{q}_l + D\dot{q}_l + g = K_c v, \qquad (6.6.1)$$

$$J_a\ddot{q}_a + B_a\dot{q}_a + N^{-1}K_c v + 50\tanh(50 * \dot{q}_a) = u_a, \qquad (6.6.2)$$

where

$$M = \begin{bmatrix} \chi_1 + 2\chi_2\cos(q_{l2}) + \chi_3 & \chi_1 + \chi_2\cos(q_{l2}) \\ \chi_1 + \chi_2\cos(q_{l2}) & \chi_1 \end{bmatrix},$$

$$C = \begin{bmatrix} -\chi_2 \sin(q_{l2})\dot{q}_{l2} & -\chi_2 \sin(q_{l2})\dot{q}_{l1} - \chi_2 \sin(q_{l2})\dot{q}_{l2} \\ +\chi_2 \sin(q_{l2})\dot{q}_{l1} & 0 \end{bmatrix},$$

$$D = \begin{bmatrix} \chi_4 & 0 \\ 0 & \chi_5 \end{bmatrix},$$

$$g = \begin{pmatrix} \chi_6 \cos(q_{l1} + q_{l2}) + \chi_7 \cos(q_{l1}) \\ \chi_6 \cos(q_{l1} + q_{l2}) \end{pmatrix}, \tag{6.6.3}$$

with

$$\chi_1 = l_2^2 m_2,$$

$$\chi_2 = l_1 l_2 m_2,$$

$$\chi_3 = l_1^2 (m_1 + m_2),$$

$$\chi_6 = m_2 l_2 g,$$

$$\chi_7 = (m_1 + m_2) l_1 g. \tag{6.6.4}$$

Matrix D (χ_4 and χ_5) represents the damping coefficients of the links.

The numerical values for the parameters of the manipulator are as follows: $m_1 = 15.91$ kg, $m_2 = 11.36$ kg, and $l_1 = l_2 = 0.432$ m. These values represent links 2 and 3 of the Unimation Puma 560 arm. We set $\chi_4 = 10.8$ Nm/sec, $\chi_5 = 3.2$ Nm/sec; N=diag(100,100); J_a=diag(0.005, 0.005) N.m/sec^2; B_a=diag(0.02, 0.02) N.m/sec.

As a bounded disturbance, the mass 2 undergoes step increase and decrease of 5 Kg at time 2 and 5 seconds respectively. This violates the assumption in the derivation of the control and adaptation laws that the parameters of the dynamics are constant. To simulate the friction damping we used "tanh($50\dot{q}_a$)" for "sgn($\dot{q}_a$)" in the actuator dynamics. The sgn function causes some problems with accuracy of the simulations via the Runge-Kutta method with adaptive step size. Notice that the friction damping coefficient is much larger (2500 times) than the viscous damping coefficient (B_a).

From (6.5.7) and (6.5.9), the improved flexibility compensator is given by

$$U_{ai} = K_{nt}N^{-1}U_{tai} + U_{ci},$$

$$U_{ci} = -H_{2i}(K_{cvi}s + K_{cpi})V_i, \qquad i = 1,2, \tag{6.6.5}$$

with

$$H_{2i} = \frac{P_{6i}}{s + P_{6i}}, \qquad i = 1,2. \tag{6.6.6}$$

The required torque u_{ta} is computed by

$$u_{ta} = W\bar{x} + K_1 y + K_2 f + K_3 Y_f h, \tag{6.6.7}$$

where

$$\dot{Y}_f + P_f Y_f = P_f Y; \tag{6.6.8}$$

$$Y = \text{diag}(y_1, y_2). \tag{6.6.9}$$

One of the adaptation laws for u_{ta} is given by

$$\dot{\bar{x}} + P_2\bar{x} = P_1 W^T y;$$

$$\dot{f} + P_3 f = K_2 y;$$

$$\dot{h} + P_4 h = K_3 Y_f y. \tag{6.6.10}$$

W and x are defined as follows:

$$x = (x_1\ x_2\ \cdots x_{11})^T,$$

$$W = \begin{bmatrix} w_1 & w_2 & w_3 & w_4 & w_5 & w_6 & 0 & 0 & 0 & 0 & 0 \\ 0 & 0 & 0 & 0 & 0 & 0 & w_7 & w_8 & w_9 & w_{10} & w_{11} \end{bmatrix}, \tag{6.6.11}$$

with

$$w_1 = w_7 = (\ddot{\sigma}_1 + \rho y_1) + (\ddot{\sigma}_2 + \rho y_2),$$

$$w_2 = [2(\ddot{\sigma}_1 + \rho y_1) + (\ddot{\sigma}_2 + \rho y_2)]\cos(q_{l2}) - [\dot{q}_{l2}\dot{\sigma}_1 + \dot{q}_{l1}\dot{\sigma}_2 + \dot{q}_{l2}\dot{\sigma}_2]\sin(q_{l2}),$$

$$w_3 = \ddot{\sigma}_1 + \rho y_1,$$

$$w_4 = \dot{q}_{l1},$$

$$w_5 = w_{11} = 10\cos(q_{l1} + q_{l2}),$$

$$w_6 = 20\cos(q_{l1}),$$

$$w_8 = (\ddot{\sigma}_1 + \rho y_1)\cos(q_{l2}) + \dot{q}_{l1}\dot{\sigma}_1 \sin(q_{l2}),$$

$$w_9 = \ddot{\sigma}_2 + \rho y_2,$$

$$w_{10} = \dot{q}_{l2}. \tag{6.6.12}$$

As in the previous chapters, we have computed the filterings in the control and adaptation laws using the following trapezoid rule (Tustin's rule)[6.27]:

$$s \simeq \frac{2}{t_s}\frac{z-1}{z+1}, \tag{6.6.13}$$

where t_s denotes the sampling time.

To reduce the computational burden, we used a triple-time update rule: 1 msec for the flexibility compensator (u_c), 2 msec for the feedback compensators ($K_1 y + K_2 f + K_3 Y_f h$), and 10 msec for the feedforward compensator ($W\bar{x}$). To make our simulations realistic, we include delays of one sampling period in our control inputs for measurements, computations, and DA and AD conversions. Since we used a triple-time update technique, there are three different delays in our control inputs.

The desired trajectories for the simulation are chosen as

$$r_1 = -\cos 3t,$$

$$r_2 = -\cos 2.5t, \tag{6.6.14}$$

which are shown in Figure 6.5.

In the figures, the solid and dotted lines will denote joints 1 and 2 respectively.

The numerical values of the control and adaptation gains for the first simulation (K_c=100I N.m/rad) are as follows.

$\underline{K} = 20I$; K_1=diag(720,840); $K_2 = 0$; $K_3 = 150I$;

$P_f = 20I$; $P_1 = 500I$; $P_2 = 0.005I$; $P_3 = 0$; $P_4 = 0.5I$; $P_6 = 300I$;

$\rho = 15$; $K_{cv} = 5. * K_c$, $K_{cp} = 150. * K_c$, K_{nt}=diag$(12. * 10^3, 6. * 10^3)$.

'I' denotes the identity matrix with appropriate dimension.

K_t and the uncertainty matrix P_u for K_{nc} are computed with (6.2.16) and (6.2.17): K_t=$15. * 10^3 I$ and P_u=diag$(0.8, 0.4)$.

The initial values for the parameters of the dynamics in this simulation are around 1/4 - 1/2 of the true values. The manipulator is assumed to be initially motionless. The initial angular positions of the actuators are computed using gravitational force and gear-reduction ratios.

Figure 6.6 shows the tracking errors of joints 1 and 2. Figure 6.7 shows the actuator inputs. Notice the responses to the step changes of the mass 2 at time 2 and 5 seconds. The maximum tracking error is about 1 degree. The actuator inputs have periodic spikes. Their magnitudes for joint 2 are much larger than those for joint 1. These are caused by the large-magnitude disturbance 50tanh$(50\dot{q}_a)$ in the actuator dynamics. The ratio of the disturbance to the actuator input for joint 2 is much larger than that for joint 1. When the disturbance is removed, the actuator inputs become smooth. The initial actuator inputs from the control law are about 5 times the steady state inputs. However, the actuator inputs are limited to the range of [-700A,700A] to simulate actuator saturation. The magnitudes of the transient inputs depend on various factors such as the desired trajectories, the initial tracking and parameter errors, the sampling rate of the flexibility compensator u_c, and the damping ratio and the undamped natural frequency of the prefilter.

The second simulation was performed with more flexible joint couplings. The stiffness of the joint couplings is given by K_c=diag$(10, 10)$ Nm/rad. We used the same desired trajectories, control and adaptation laws, and triple-time update rule. The following numerical values for the control gains are different from those

for the first simulation: $K_{cv} = 30 * K_c$, $K_{cp} = 900 * K_c$, K_{nt}=diag$(8. * 10^4, 4. * 10^4)$. Accordingly, K_t and the uncertainty matrix P_u are computed as K_t=$9. * 10^4 I$ and P_u=diag$(\frac{8}{9}, \frac{4}{9})$. Different gains are used for the flexibility compensator to compensate for the change of the stiffness of the joint couplings.

The joint errors and the actuator inputs are shown in Figures 6.8 and 6.9 respectively. Stability is guaranteed in the presence of the step changes of the mass 2 at time 2 and 5 seconds. The tracking performance of the control scheme remains the same even though the stiffnesses of the joints become 10 times as flexible as those for the first simulation. In the second simulation, the effects of the disturbance $50\tanh(50\dot{q}_a)$ are almost negligible since the ratio of the disturbance to the actuator input is very small. The actuator inputs are also limited to the range of [-6500A,6500A] in order to simulate the actuator saturation.

Figure 6.10 shows a long time behavior of parameters ($\bar{x}_1$, $\bar{x}_3$, $\bar{x}_5$, $\bar{x}_7$, $\bar{x}_9$, and $\bar{x}_{11}$) estimated by the adaptation law (6.6.10) for the second simulation. Almost the same results are obtained for the first simulation. No parameter drift is observed due to the characteristics of the first-order filters in the adaptation law.

The steady state tracking errors do not approach zero. This is because (i) the prefilter (6.2.18) is not an all-pass filter, (ii) we include delays of one sampling period (1, 2, 10 msec), (iii) we include the large disturbance ($50\tanh 50\dot{q}_a$) in the actuator dynamics, and (iv) the adaptation law (6.6.10), by nature, causes nonzero tracking errors. We may have better results if we use the new adaptation law (6.3.54).

In both simulations, the magnitudes of the tracking errors of joint 2 are larger than those of joint 1. This is because the uncertainty with K_{nc} is larger for joint 2. See the uncertainty matrix P_u. We may reduce the maximum tracking errors for joint 2 down to the level of those for joint 1 by increasing the control and adaptation gains for joint 2.

In both simulations, the tracking errors are within practical tolerances, and stability is guaranteed for control of heavy links 2 and 3 of a PUMA 560 with extremely flexible joint stiffnesses (10 and 100 N.m/rad) and high gear ratio

(100). Note that the chosen numerical values of the joint stiffnesses do not make sense. The joints are too flexible. The purpose of this simulation is to show that the proposed control law guarantees stability almost independent of the joint stiffness. The proposed flexibility compensator may work for some other stable control schemes for rigid-joint manipulators.

Due to small joint stiffnesses and high gear ratios, the resonance frequencies of the uncompensated prefilter ($\sqrt{0.2}$ for $K_c = 10I$ and $\sqrt{2}$ for $K_c = 100I$) are smaller than the frequencies of the desired trajectories (2.5 and 3). Accordingly, the magnitudes of the control inputs are very large. We might aggravate this by using unity torque constants for actuators. The control inputs for $K_c = 10I$ are almost 10 times as large as those for $K_c = 100I$. This is in good agreement with the arguments in the preliminaries: regardless of the control laws, larger control inputs are required when the spectral range of the desired trajectories covers high-frequency low-gain region of the link and/or actuator dynamics.

In spite of nonlinearities such as, step changes of mass 2, input saturation, and friction damping of the actuators, which are not included in the derivation of the control law, the performance of the control law such as guarantee of stability and fast transient response is shown to be essentially unchanged. This is because the sufficient condition for the stability of our scheme is too strong.

6.7 Conclusion

In this work, we have interpreted the dynamics of actuators and flexible joint couplings as prefilters for the link dynamics. This concept of prefilter leads to the design of a flexibility compensator. With flexibility compensation, we have transformed a system of a flexible-joint manipulator to that of the corresponding rigid-joint manipulator with the high-frequency prefilter dynamics as unmodelled dynamics. As a consequence, we could design an adaptive control scheme based on the model of the transformed rigid-joint manipulator so that we could avoid the complexity of the flexible-joint system in the design procedure.

With additional stability analysis, we have shown that the proposed adap-

tive scheme for the transformed rigid-joint manipulator stabilizes the system of the original flexible-joint manipulator under some moderate constraints on disturbances, control and adaptation gains, and desired trajectories and their time-derivatives. The stability analysis also provides some interesting stability conditions on gear ratios, damping coefficients of actuators, and mass moment of inertias of links and actuators. This is the main result of this chapter.

The proposed adaptive scheme is unique in the following respects. The scheme is almost insensitive to the gear ratios, joint stiffness, and disturbances. The scheme here is practical since its implementation requires measurements only of angular positions and velocities of the links and actuators. The proposed scheme provides stability bounds for disturbances, control and adaptation gains, desired trajectories and their time-derivatives. The computational burden of the proposed scheme is almost the same as that of the corresponding scheme for robots having rigid joints.

The results of realistic simulations support the stability analysis, and also lead to the conclusion that the control law developed here will work for commercial manipulators. The approach proposed in this work seems to provide a widely applicable practical solution to the control of manipulators having flexible joint couplings.

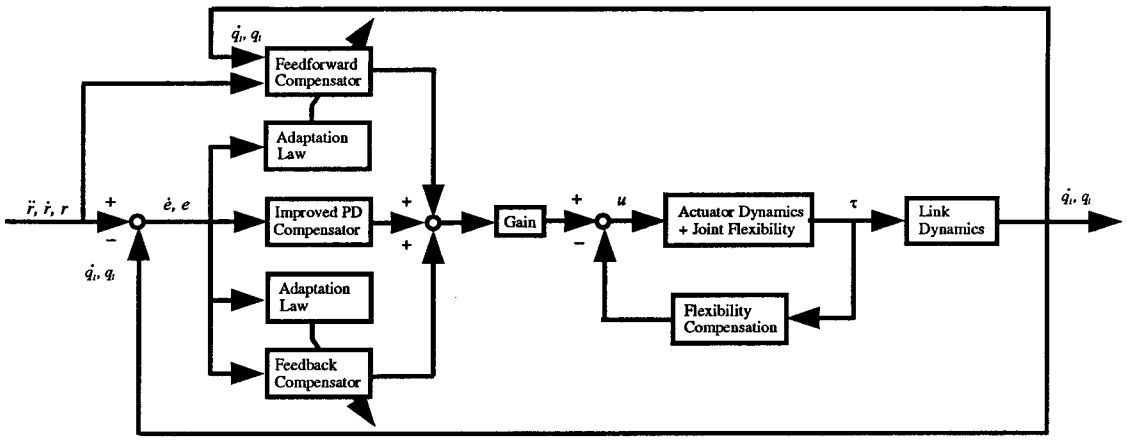

Figure 6.1 Schematic diagram of the proposed control law

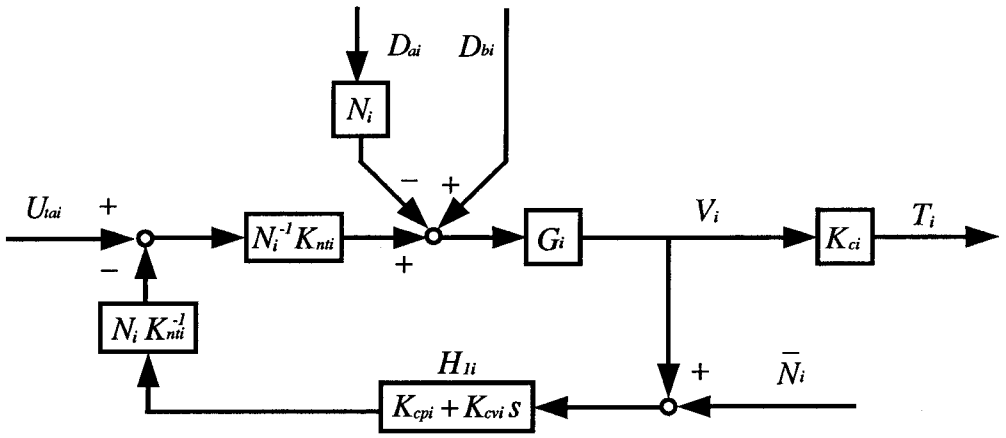

Figure 6.2 The original flexibility compensation

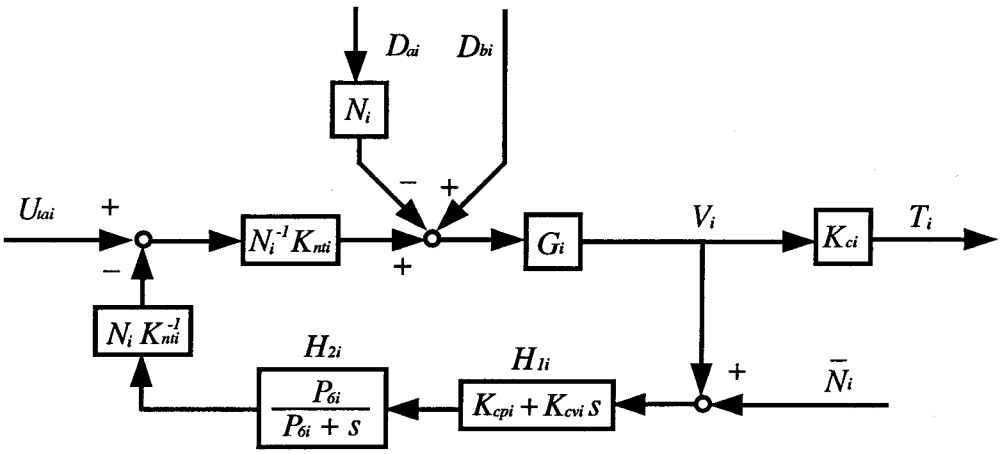

Figure 6.3 An improved flexibility compensation

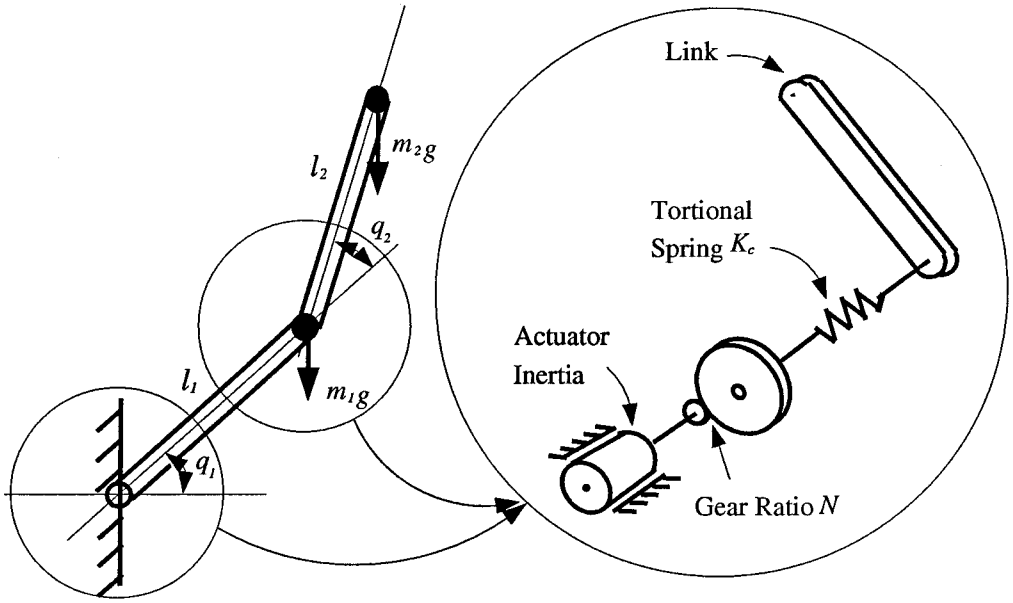

Figure 6.4 Modelling of links and joints

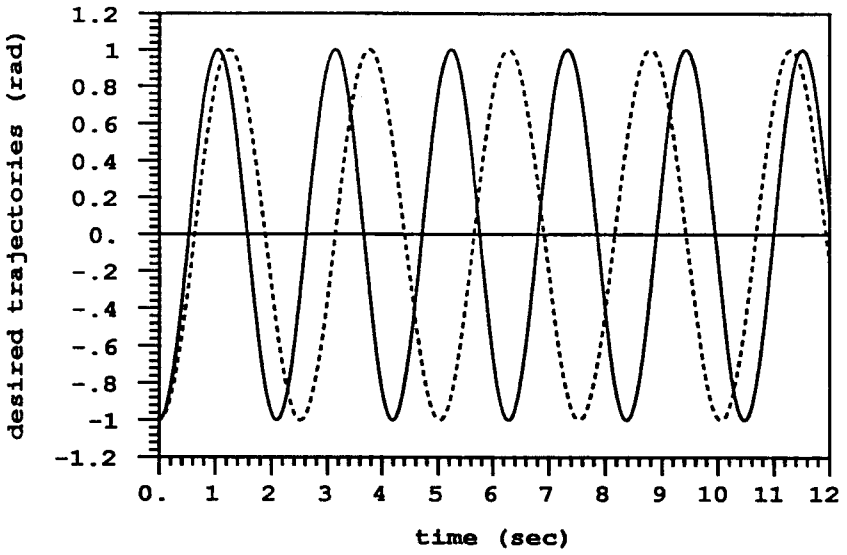

Figure 6.5 Desired trajectories: solid line for joint 1 and dotted line for joint 2

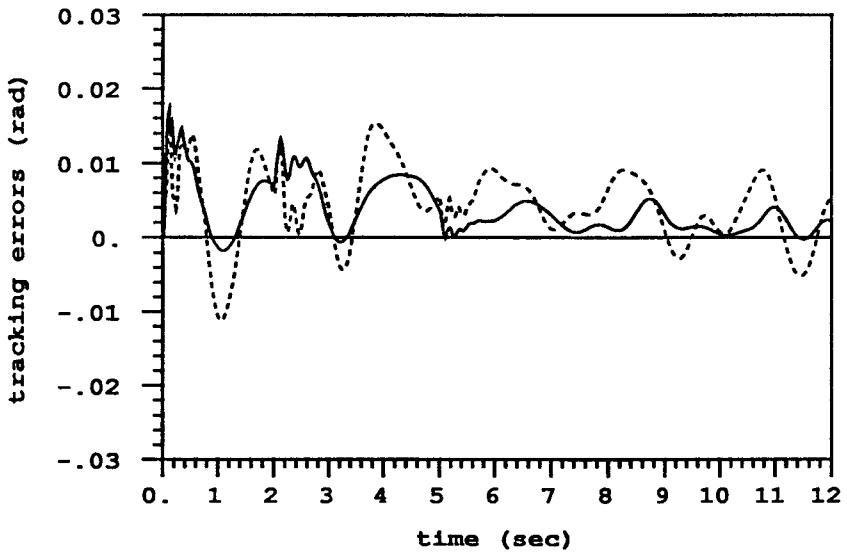

Figure 6.6 Tracking errors associated with K_c=diag(100,100) (N.m/rad): solid line for joint 1 and dotted line for joint 2

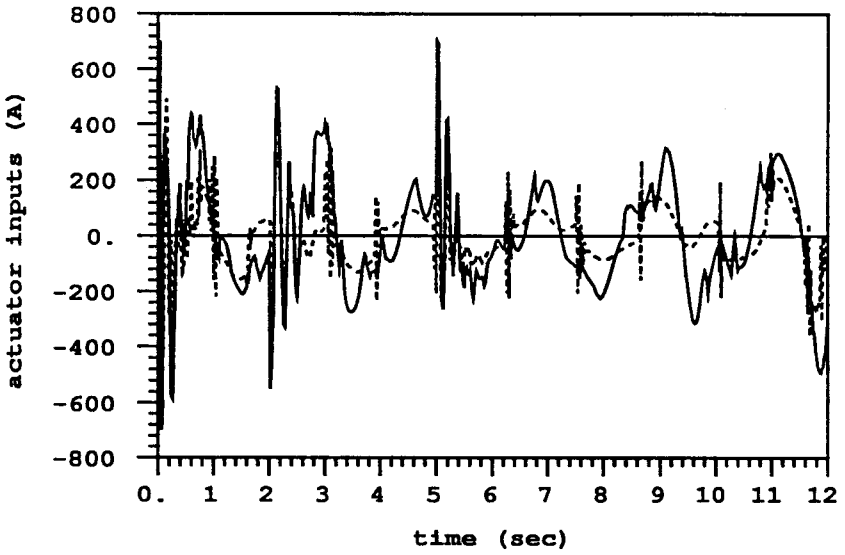

Figure 6.7 Actuator inputs associated with K_c=diag(100,100) (N.m/rad): solid line for joint 1 and dotted line for joint 2

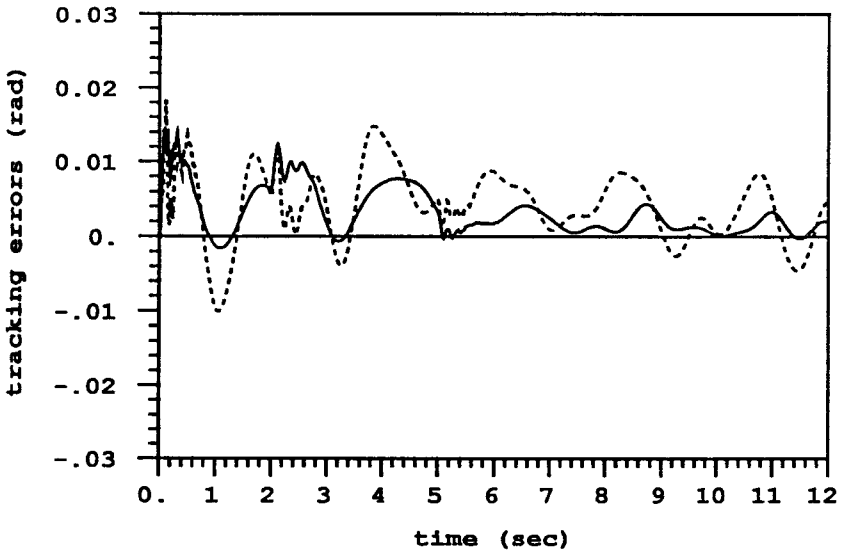

Figure 6.8 Tracking errors associated with K_c=diag(10,10) (N.m/rad): solid line for joint 1 and dotted line for joint 2

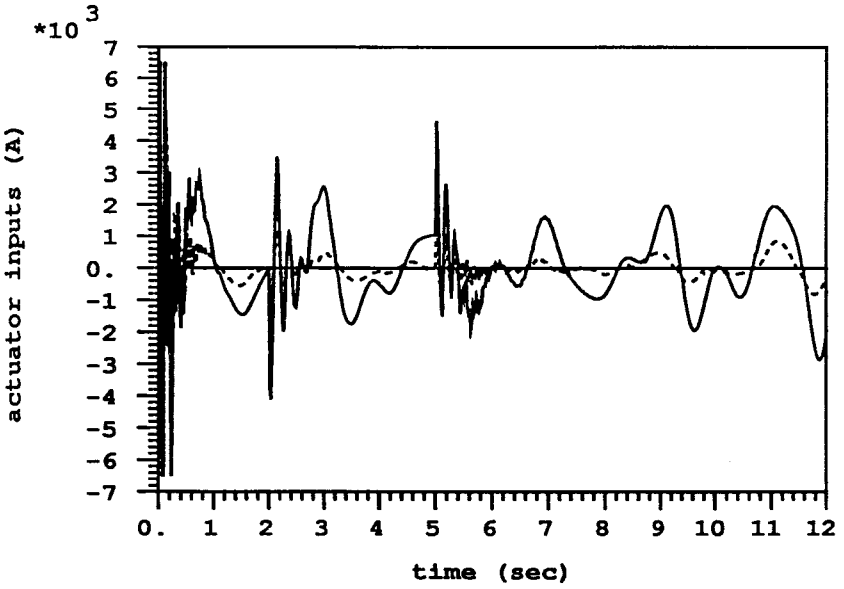

Figure 6.9 Actuator inputs associated with K_c=diag(10,10) (N.m/rad): solid line for joint 1 and dotted line for joint 2

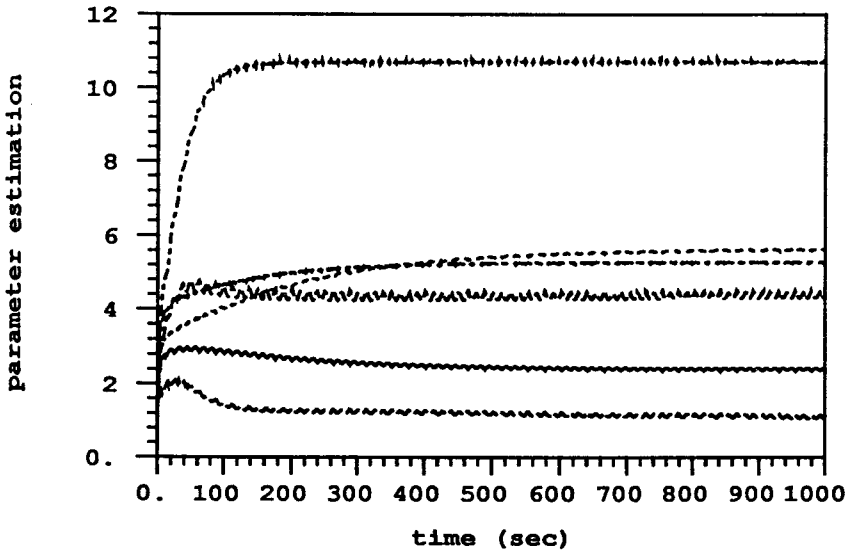

Figure 6.10 Parameter estimation associated with K_c=diag(10,10) (N.m/rad)

References

[6.1] Rivin, E. R., *Effective Rigidity of Robot Structures: Analysis and Enhancement,* Proc. American Control Conf., pp. 381-382, Boston, June 1985.

[6.2] Sweet, L. M. and Good, M. C., *Redefinition of the Robot Motion Control Problem: Effects of Plant Dynamics, Drive System Constraints, and User Requirements,* Proc. 23^{rd} IEEE CDC, Las Vegas, NV, 1984.

[6.3] Stepien, T. M., Sweet, L. M., Good, M. C. and Tomizuka, M., *Control of Tool/Working Piece Contact Force with Application to Robotic Deburring,* IEEE J. of Robotics and Automation, Vol. RA-3, pp. 7-18, 1987.

[6.4] De Luca, A., *Control Properties of Robot Arms with Joint Elasticities,* Proc. MTNS, Phoenix, AZ, June, 1987.

[6.5] De Luca, A., Isadori, A. and Nicolo, F., *An Application of Nonlinear Model Matching to the Control of Robot Arms with Elastic Joints,* 1^{st} IFAC Symp. Robot Control, Barcelona, 1985.

[6.6] Spong, M. W., *Modelling and Control of Elastic Joint Manipulators,* J. of Dyn. Sys. Meas. and Control, Vol. 109, pp. 310-319, 1987.

[6.7] Chen, K. and Fu, L., *Nonlinear Adaptive Motion Control for a Manipulator with Flexible Joints*, Proc. of IEEE Int. Conf. on Robotics and Automation, pp. 1201-1206, 1989.

[6.8] Khorasani, K. and Spong, M. W., *Invariant Manifolds and Their Application to Robot Manipulators with Flexible Joints,* Proc. IEEE Int'l Conf. on Robotics and Automation, St. Louis, Mar. 1985.

[6.9] Spong, M. W., Khorasani, K. and Kokotovic, P. V., *An Integral Manifold Approach to the Feedback Control of Flexible Joint Robots,* IEEE J. of Robotics and Automation, Vol. RA-3, No. 4, pp. 291-300, Aug. 1987.

[6.10] Khorasani, K., *Robust Adaptive Stabilization of Flexible Joint Manipulators,* Proc. of IEEE Int. Conf. on Robotics and Automation, pp. 1194-1199, 1989.

[6.11] Hollars, M. G. and Cannon, Jr. R. H., *Initial Experiments on End-Point*

Control of a Two-Link Manipulator with Flexible Tendons, Prec. of ASME Winter Annual Meeting, Fl., November 1985.

[6.12] Hollars, M. G. and Cannon, Jr., R. H., *Experiments on End-Point Control of a Two-Link Robot with Elastic Drive,* Proc of AIAA Guidance, Navigation and Control Conf., pp. 19-27, August 1986.

[6.13] Hollars, M. G., *Experiments in End-Point Control of Manipulators with Elastic Drive,* Ph.D. thesis, Stanford University, Department of Aeronautics and Astronautics, Stanford, CA 94305, May 1988.

[6.14] Uhlik, C. R., *Experiments in High-Performance Nonlinear and Adaptive Control of a Two-Link, Flexible-Drive-Train Manipulator,* Ph.D. thesis, Stanford University, Department of Aeronautics and Astronautics, Stanford, CA 94305, May 1990.

[6.15] Ghorbel, F., Hung, J. Y. and Spong, M. W., *Adaptive Control of Flexible Joint Manipulators,* IEEE Conf. on Robotics and Automation, pp. 1188-1193, 1989.

[6.16] Arimoto, A. and Miyazaki, F., *Stability and Robustness of PID Feedback Controller for Robot Manipulators of Sensory Capability,* Robotics Research: The First International Symposium edited by Brady, M. and Paul, R., pp. 783-799, 1984.

[6.17] Rohrs, C. E., Valavani, L., Atheans, M. and Stein, G., *Robustness of Adaptive Control Algorithms in the Presence of Unmodelled Dynamics,* IEEE Conf. on Decision and Control, Proc., pp. 3-11, 1982.

[6.18] Peterson, B. B. and Narendra, K. S., *Bounded Error Adaptive Control,* IEEE Trans. on Auto. Contr., Vol. AC-27, pp. 1161-1168, Dec. 1982.

[6.19] Samson, C., *Stability Analysis of Adaptively Controlled Systems Subject to Bounded Disturbances,* Automatica, Vol. 19, pp. 81-86, 1983.

[6.20] Kreisselmeier, G. and Narendra, K. S., *Stable Model Reference Adaptive Control in the Presence of Bounded Disturbances,* IEEE Trans. on Auto. Contr., Vol. AC-27, No. 6, pp. 1169-1175, Dec. 1982.

[6.21] Ioannou, P. A. and Tsakalis, K. S., *A Robust Direct Adaptive Controller,*

IEEE Trans. on Auto. Contr., Vol. AC-31, No. 11, pp. 1033-1043, Nov. 1986.

[6.22] Ioannou, P. A., *Robust Adaptive Control with Zero Residual Tracking Errors,* IEEE Trans. on Auto. Contr., Vol. AC-31, No. 8, pp. 773-776, Aug. 1986.

[6.23] Ioannou, P. A. and Kokotovic, P. V., *Instability Analysis and Improvement of Robustness of Adaptive Control,* Automatica, Vol. 20, No. 5, pp. 583-594, 1984.

[6.24] Ioannou, P. A. and Kokotovic, P. V., *Robust Redesign of Adaptive Control,* IEEE Trans. on Auto. Contr., Vol. AC-29, No. 3, pp. 202-211, March 1984.

[6.25] Narendra, K. S. and Annaswamy, A. M., *A New Adaptive Law for Robust Adaptation Without Persistent Excitation,* IEEE Trans. on Auto. Contr., Vol. AC-32, No. 2, pp. 134-145, Feb. 1987.

[6.26] Press, W. H., Flannery, B. P., Teukolsky, S. A. and Vetterting, W. T., *Numerical Recipes: The Art of Scientific Computing,* Cambridge, 1986.

[6.27] Franklin, G. F. and Powell, J. D., *Digital Control of Dynamic Systems,* Addison-Wesley, Reading, 1980.

Appendix 6.A: Estimation of $\dot{u}_l$ and $\ddot{u}_l$

Inside the set $\mathcal{S}_1$, we express the orders of variables using $\mu(=\frac{a}{\epsilon})$. We keep only important high-order terms of μ since μ is assumed to be much larger than unity.

According to the control and adaptation laws (6.3.13) and (6.3.18), u_l, $\dot{u}_l$, $\ddot{u}_l$, and hence $(2\mathcal{Z}\mathcal{E}\dot{u}_l + \mathcal{E}^2\ddot{u}_l)^T\mathcal{Z}P_u\xi$ are functions of the desired trajectories (r, $\dot{r}$, $\ddot{r}$, r^{III}, and r^{IV}), disturbances ($\underline{d}$, $\dot{\underline{d}}$, and $\ddot{\underline{d}}$), and control and adaptation gains (ρ, P_j, and K_i for $j = 1,2,3,4$ and $i = 1,2,3$). Since $(2\mathcal{Z}\mathcal{E}\dot{u}_l + \mathcal{E}^2\ddot{u}_l)^T\mathcal{Z}P_u\xi$ is sign-indefinite, to guarantee $\dot{V}_o \leq 0$ inside $\mathcal{S}_1$, we set the order of this term smaller than those of the other terms in $\dot{V}_2$ in (6.3.23) by limiting the upper bound of a in μ. It is possible since the sign-indefinite term $(2\mathcal{Z}\mathcal{E}\dot{u}_l + \mathcal{E}^2\ddot{u}_l)^T\mathcal{Z}P_u\xi$ contains small constants $\mathcal{E}$ (of order $\epsilon \ll 1$) and $\mathcal{E}^2$. The size of the stabilizing $\mathcal{S}_1$ is given by a in μ. When $\epsilon = 0$ (representing rigid-joint manipulator), the size of $\mathcal{S}_1$ is

infinitely large.

If the order of any one of the desired trajectories, disturbances, or control and adaptation gains is significantly larger than the others, it will dominate the orders of u_l, $\dot{u}_l$, and $\ddot{u}_l$, and hence the size of the stabilizing $\mathcal{S}_1$. Accordingly, we set the upper bounds of the desired trajectories, disturbances, and control and adaptation gains in such a way that we equalize their influences on the other variables including u_{ta}, $\dot{u}_{ta}$, $\ddot{u}_{ta}$, q_l^{III}, and q_l^{IV}.

For convenience, the dynamics of revolute-joint manipulators will be used in this order analysis. In this case, the inertia matrix is bounded. The order analysis for prismatic-joint or prismatic-revolute-joint robots can be as readily performed as that for revolute-joint robots described below since the structure of the dynamics is the same regardless of the type of joint.

In this analysis, we begin with variables of known order. Then, we obtain the orders of their time-derivatives using the dynamics (6.3.1), control law (6.3.13), adaptation law (6.3.18), and time-derivatives of these.

From the definition of $W(\rho, \ddot{r}, \dot{r}, r, \dot{q}_l, q_l)$ in (6.3.14), we can derive

$$W = \Big[\mathcal{O}(\mu^2) + \mathcal{O}(\ddot{r}) + \mathcal{O}(\rho\mu)\Big]\underline{\mathrm{W}}_1 \tag{6.A.1}$$

for some $n \times m$ matrix $\underline{\mathrm{W}}_1(t)$ such that $\mathcal{O}(\underline{\mathrm{W}}_1) = \mu^0$ $(= 1)$. See the orders of related variables inside $\mathcal{S}_1$ in (6.3.27). We choose the upper bounds of $\ddot{r}$ and ρ such that they do not increase the order of W more than $\mathcal{O}(\mu^2)$, the contribution from the other variables of the dynamics (6.3.1). That is, we set

$$\mathcal{O}(\ddot{r}) \leq \mu^2 \quad \text{and} \quad \mathcal{O}(\rho) \leq \mu. \tag{6.A.2}$$

From the control law u_{ta} in (6.3.13), we can obtain

$$u_{ta} = \Big[\mathcal{O}(\mu^3) + \mathcal{O}(K_1\mu) + \mathcal{O}(K_2\mu) + \mathcal{O}(K_3\mu^2)\Big]\underline{\mathrm{u}}_1 \tag{6.A.3}$$

for some $n \times 1$ vector $\underline{\mathrm{u}}_1(t)$ such that $\mathcal{O}(\underline{\mathrm{u}}_1) = \mu^0$. We select K_1, K_2, and K_3 such

that $\mathcal{O}(u_{ta}) \leq \mu^3$:

$$\mathcal{O}(K_1) \leq \mu^2, \quad \mathcal{O}(K_2) \leq \mu^2, \quad \text{and} \quad \mathcal{O}(K_3) \leq \mu. \tag{6.A.4}$$

From the adaptation law (6.3.18), we can get

$$\begin{aligned} \dot{\hat{x}} &= \Big[\mathcal{O}(P_2\mu) + \mathcal{O}(\mu^3)\Big]\underline{x}_1; \\ \dot{f} &= \Big[\mathcal{O}(P_3\mu) + \mathcal{O}(\mu^3)\Big]\underline{f}_1; \\ \dot{h} &= \Big[\mathcal{O}(P_4\mu) + \mathcal{O}(\mu^3)\Big]\underline{h}_1 \end{aligned} \tag{6.A.5}$$

for some $m\times 1$ vector $\underline{x}_1(t)$ and $n\times 1$ vectors $\underline{f}_1(t)$ and $\underline{h}_1(t)$ such that $\mathcal{O}(\underline{x}_1) = \mu^0$, $\mathcal{O}(\underline{f}_1) = \mu^0$, and $\mathcal{O}(\underline{h}_1) = \mu^0$. We limit the orders of $\dot{\hat{x}}$, $\dot{f}$, and $\dot{h}$ to μ^3. Then, we have

$$\mathcal{O}(P_2) \leq \mu^2, \quad \mathcal{O}(P_3) \leq \mu^2, \quad \text{and} \quad \mathcal{O}(P_4) \leq \mu^2. \tag{6.A.6}$$

From the definition of Y_f in (6.3.9), we can obtain

$$\dot{Y}_f = \mathcal{O}(P_f\mu)\underline{Y}_{f1} \tag{6.A.7}$$

for some $n\times n$ matrix $\underline{Y}_{f1}(t)$ such that $\mathcal{O}(\underline{Y}_{f1}) = \mu^0$.

From the dynamics (6.3.1), we have

$$\ddot{q}_l = M_e^{-1}[u_{ta} - C\dot{q}_l - D_e\dot{q}_l - g - \underline{d} - \eta]. \tag{6.A.8}$$

Then, using the structure of the dynamics ($M_l(q_l)$, $C(\dot{q}_l, \dot{q}_l)$, and $g(\dot{q}_l)$), we can derive

$$\ddot{q}_l = -M_e^{-1}\Big[\eta + \Big(\mathcal{O}(\underline{d}) + \mathcal{O}(u_{ta})\Big)\underline{q}_1\Big] \tag{6.A.9}$$

for some $n\times 1$ vector $\underline{q}_1(t)$ such that $\mathcal{O}(\underline{q}_1) = \mu^0$. Hence, we can impose a constraint on $\underline{d}$ as

$$\mathcal{O}(\underline{d}) \leq \mu^3. \tag{6.A.10}$$

Note that $\mathcal{O}(u_{ta}) \leq \mu^3$. We will impose $\mathcal{O}(\eta) \leq \mathcal{O}(u_{ta})$ when we determine the size of the set $\mathcal{S}_1$ (the magnitude of a contained in μ).

Using the structure of $\dot{W}(r^{III}, \ddot{r}, \dot{r}, r, \ddot{q}_l, \dot{q}_l, q_l)$, the time-derivative of W in (6.3.14), we can obtain

$$\dot{W} = \Big[\mathcal{O}(\eta\mu) + \mathcal{O}(\mu^4) + \mathcal{O}(r^{III})\Big]\underline{\mathrm{W}}_2 \tag{6.A.11}$$

for some $n \times m$ matrix $\underline{\mathrm{W}}_2(t)$ such that $\mathcal{O}(\underline{\mathrm{W}}_2) = \mu^0$. We set

$$\mathcal{O}(r^{III}) \leq \mu^4. \tag{6.A.12}$$

The time-derivative of u_{ta} in (6.3.13) is given by

$$\dot{u}_{ta} = W\ddot{\bar{x}} + \dot{W}\dot{\bar{x}} + K_1\ddot{y} + K_2\ddot{f} + K_3\dot{Y}_f h + K_3 Y_f \dot{h}. \tag{6.A.13}$$

Since we have obtained the orders of all the variables related to $\dot{u}_{ta}$, we readily get the order of $\dot{u}_{ta}$:

$$\dot{u}_{ta} = \Big[\mathcal{O}(\mu^5) + \mathcal{O}(\eta\mu^2) + \mathcal{O}(P_f\mu^3)\Big]\underline{\mathrm{u}}_2 \tag{6.A.14}$$

for some $n \times 1$ vector $\underline{\mathrm{u}}_2(t)$ such that $\mathcal{O}(\underline{\mathrm{u}}_2) = \mu^0$. Here, we set

$$\mathcal{O}(P_f) \leq \mu^2. \tag{6.A.15}$$

Taking time-derivative on the dynamics (6.3.1) yields

$$q_l^{III} = M_e^{-1}[\dot{u}_{ta} - (\dot{M}_e + C + D_e)\ddot{q}_l - \dot{C}\dot{q}_l - \dot{g} - \dot{\underline{\mathrm{d}}} - \dot{\eta}]. \tag{6.A.16}$$

Then, using the structure of the dynamics ($\dot{M}_l(\dot{q}_l, q_l)$, $\dot{C}(\ddot{q}_l, \dot{q}_l, q_l)$, and $\dot{g}(\dot{q}_l, q_l)$), we have

$$q_l^{III} = -M_e^{-1}\Big[\dot{\eta} + \Big(\mathcal{O}(\dot{\underline{\mathrm{d}}}) + \mathcal{O}(\dot{u}_{ta})\Big)\underline{\mathrm{q}}_2\Big] \tag{6.A.17}$$

for some $n \times 1$ vector $\underline{\mathrm{q}}_2(t)$ such that $\mathcal{O}(\underline{\mathrm{q}}_2) = \mu^0$. This gives the upper bound of $\dot{\underline{\mathrm{d}}}$ as

$$\mathcal{O}(\dot{\underline{\mathrm{d}}}) \leq \mu^5. \tag{6.A.18}$$

Using the structure of $\ddot{W}(r^{IV}, r^{III}, \ddot{r}, \dot{r}, r, q_l^{III}, \ddot{q}_l, \dot{q}_l, q_l)$, the second time-derivative of W in (6.3.14), we can obtain

$$\ddot{W} = \Big[\mathcal{O}(\dot{\eta}\mu) + \mathcal{O}(\eta^2) + \mathcal{O}(\mu^6) + \mathcal{O}(\eta\mu^3) + \mathcal{O}(r^{IV})\Big]\underline{\mathrm{W}}_3 \qquad (6.A.19)$$

for some $n\times m$ matrix $\underline{\mathrm{W}}_3(t)$ such that $\mathcal{O}(\underline{\mathrm{W}}_3) = \mu^0$. Therefore, we set

$$\mathcal{O}(r^{IV}) \leq \mu^6. \qquad (6.A.20)$$

The time-derivatives of the adaptation laws in (6.3.18) are given by

$$\begin{aligned}
\ddot{\bar{x}} &= P_2^2\bar{x} - P_2P_1(W^Ty) + P_1\dot{W}^Ty + P_1W^T\dot{y};\\
\ddot{f} &= P_3^2 f - P_3K_2y + K_2\dot{y};\\
\ddot{h} &= P_4^2 h - P_4K_3Y_f y + K_3\dot{Y}_f y + K_3Y_f\dot{y}.
\end{aligned} \qquad (6.A.21)$$

Then, using the orders of the related variables, we have

$$\begin{aligned}
\ddot{\bar{x}} &= \Big[\mathcal{O}(\mu^5) + \mathcal{O}(\eta\mu^2)\Big]\underline{\mathrm{x}}_2;\\
\ddot{f} &= \Big[\mathcal{O}(\mu^5) + \mathcal{O}(\eta\mu^2)\Big]\underline{\mathrm{f}}_2;\\
\ddot{h} &= \Big[\mathcal{O}(\mu^5) + \mathcal{O}(\eta\mu^2)\Big]\underline{\mathrm{h}}_2,
\end{aligned} \qquad (6.A.22)$$

for some $m\times 1$ vector $\underline{\mathrm{x}}_2(t)$ and $n\times 1$ vectors $\underline{\mathrm{f}}_2(t)$ and $\underline{\mathrm{h}}_2(t)$ such that $\mathcal{O}(\underline{\mathrm{x}}_2) = \mu^0$, $\mathcal{O}(\underline{\mathrm{f}}_2) = \mu^0$, and $\mathcal{O}(\underline{\mathrm{h}}_2) = \mu^0$.

Taking time-derivative on Y_f in (6.3.9) yields

$$\ddot{Y}_f = P_f^2Y_f - P_f^2Y + P_f\dot{Y}. \qquad (6.A.23)$$

Hence,

$$\ddot{Y}_f = \Big[\mathcal{O}(\mu^5) + \mathcal{O}(\eta\mu^2)\Big]\underline{\mathrm{Y}}_{f2} \qquad (6.A.24)$$

for some $n\times n$ matrix $\underline{\mathrm{Y}}_{f2}(t)$ such that $\mathcal{O}(\underline{\mathrm{Y}}_{f2}) = \mu^0$.

The time-derivative of $\dot{u}_{ta}$ in (6.A.13) is given by

$$\ddot{u}_{ta} = W\ddot{\bar{x}} + 2\dot{W}\dot{\bar{x}} + \ddot{W}\bar{x} + K_1\ddot{y} + K_2\ddot{f} + K_3(\ddot{Y}_f h + 2\dot{Y}_f\dot{h} + Y_f\ddot{h}). \qquad (6.A.25)$$

We have already obtained the orders of all the related variables. Hence, we can readily get

$$\ddot{u}_{ta} = \Big[\mathcal{O}(\mu^7) + \mathcal{O}(\dot{\eta}\mu^2) + \mathcal{O}(\eta^2\mu) + \mathcal{O}(\eta\mu^4)\Big]\underline{u}_3 \qquad (6.A.26)$$

for some $n\times 1$ vector $\underline{u}_3(t)$ such that $\mathcal{O}(\underline{u}_3) = \mu^0$.

Taking the time-derivative on the dynamics (6.3.1) twice gives

$$\begin{aligned} q_l^{IV} =& M_e^{-1}[(I - P_u)\ddot{u}_{ta} - 2\mathcal{Z}P_u\mathcal{E}^{-1}\dot{u}_{ta} + \mathcal{E}^{-2}\xi - (2\dot{M}_e + C + D_e)q_l^{III} \\ & - (\ddot{M}_e + 2\dot{C})\ddot{q}_l - \ddot{C}\dot{q}_l - \ddot{g} - \ddot{\underline{d}}]. \end{aligned} \qquad (6.A.27)$$

Hence, using the structure of the dynamics ($\ddot{M}_l(\ddot{q}_l, \dot{q}_l, q_l)$, $\ddot{C}(q_l^{III}, \ddot{q}_l, \dot{q}_l, q_l)$, and $\ddot{g}(\ddot{q}_l, \dot{q}_l, q_l)$), we can estimate q_l^{IV} as

$$q_l^{IV} = M_e^{-1}\Big[\mathcal{E}^{-2}\xi + \Big(\mathcal{O}(\mathcal{E}^{-1}\dot{u}_{ta}) + \mathcal{O}(\ddot{u}_{ta}) + \mathcal{O}(\ddot{\underline{d}})\Big)\underline{q}_3\Big] \qquad (6.A.28)$$

for some $n\times 1$ vector $\underline{q}_3(t)$ such that $\mathcal{O}(\underline{q}_3) = \mu^0$. Accordingly, we have

$$\mathcal{O}(\ddot{\underline{d}}) \le \mu^7. \qquad (6.A.29)$$

Chapter 7

SUMMARY AND FUTURE WORK

7.1 Summary

This thesis has discussed adaptive trajectory control of rigid-joint manipulators and extended to adaptive control of flexible-joint manipulators. Each chapter can be summarized as follows.

In Chapter 1, this thesis covered the overview of robotics as an introduction, and then described the background and motivation of the study.

In Chapter 2, the essence of adaptive control was reviewed with applications to a spring-mass-damper system having one degree of freedom. This thesis discussed the design procedures of the self-tuning method. With the summary of Lyapunov's second method and Popov's hyperstability theory, this thesis also explained how these stability theories could be applied to the design of model reference adaptive control laws.

In Chapter 3, this thesis emphasized the importance of the transient behavior of adaptive control schemes and took it into account in controller design. The loop shaping method was combined with adaptive control strategy and concept of optimal control in harmony to extract the maximum benefits from each method. Compensators were searched in the direction of minimizing a certain performance index so as to improve the transient response. Then, to guarantee asymptotic stability of the system, those compensators were shown to satisfy a new stability criterion which was derived based on the characteristics of a weighted 2-norm of a differentiable signal.

In Chapter 4, it was shown that the integration adaptation law in Chapter 3 might cause instability due to parameter drift in the presence of sensor noises

or bounded disturbances. The scheme proposed in Chapter 3 was redesigned by replacing the integration adaptation law with the σ-modification to prevent parameter drift. New adaptation laws were also proposed based on the bounds of parameters. Moreover, in the presence of feedback delays in the digital control systems, stability bounds for disturbances, control and adaptation gains, and trajectories and their time-derivatives were obtained for the scheme redesigned with the new adaptation laws.

In Chapter 5, a robust decentralized adaptive scheme was proposed, which is a subset of the scheme proposed in Chapter 4. The scheme in this chapter contains only the decoupled compensators of that in Chapter 4 with appropriate changes in the adaptation laws. Under some moderate constraints, the proposed decentralized adaptive scheme was shown to stabilize the nonlinear coupled systems of manipulators. The stability proof of the proposed scheme does not require the assumption of boundedness and quasi-time-invariance of the coupled dynamics. Furthermore, the scheme provides stability bounds for disturbances, control and adaptation gains, and desired trajectories and their time-derivatives, in the presence of unmodelled dynamics due to feedback delays in the digital systems. In addition, the stabilities of PD and PID feedback laws were proven, and their regions of attraction and stability bounds for their gains were also derived.

In Chapter 6, an appropriate flexibility compensator was designed for joint flexibility. With this compensator, systems of flexible-joint manipulators were transformed to those of the corresponding rigid-joint manipulators with a certain degree of high-frequency unmodelled dynamics. As a consequence, control of flexible-joint manipulators is converted to that of the corresponding rigid-joint manipulators, which has been already discussed in the previous chapters. An adaptive control scheme for the transformed rigid-joint manipulators was proposed, which is a simpler form of the scheme developed in Chapter 4. Then, a sufficient condition for the robust stability of the scheme with the flexibility compensator was derived for the system of the original flexible-joint manipulators.

7.2 Discussion and Future Work

In this thesis, a quadratic performance index is used as a measure of the transient response of adaptive control systems. Compensators are searched in the direction of minimizing the performance index. Criteria for compensator searches are given in (3.4.17), (3.4.19), and (3.4.20). Many different control and adaptation laws can be found which satisfy the criteria. It would be worthwhile to perform further research toward finding the most efficient control and adaptation law in terms of robustness, computation time, and suppression of tracking errors, based on the criteria. The proposed method may be applied to the controller design for any system whose dynamics is linear in the parameters of the system, with appropriate modifications based on the order of the system.

In Chapter 4, this thesis discussed how to find bounds on control gains, adaptation gains, disturbances, desired trajectories, and the time-derivatives of the trajectories. These bounds are sufficient conditions for stability in the presence of unmodelled dynamics due to feedback delays in the digital control systems. The same concept was applied to the control of flexible-joint robots in Chapter 6 where similar results were obtained. The bounds constitute a sufficient condition for stability, but they are not unique. In this research, the effects of two different unmodelled dynamics (feedback delays and joint flexibility) were examined independently. It would be interesting to investigate the combined effects of those unmodelled dynamics on the stability of a given system.

In Chapter 5, it is shown that a PD (or PID) feedback law is sufficient to control a manipulator. It is also demonstrated that additional adaptive compensators reduce a performance index and hence the maximum tracking error. The dynamics of commercial robots (usually having 6 degree of freedom) are very complicated. To save computation time, components with smaller contributions to the total behavior of the system may be safely removed from control and adaptation laws without significant deterioration in tracking performance as long as a PD feedback law is included in the control and adaptation laws for stability. Accord-

ingly, further efforts are required to determine experimentally (or by simulations) which compensators can be removed from the centralized control and adaptation laws in Chapter 4.

In Chapters 4 and 5, the effects of feedback delays in the digital control systems on the stability of a given system were considered. The robot dynamics are continuous in time even though control inputs are computed discretely using digital systems. Hence, we treated the problem in the continuous time domain. It may be worthwhile to treat the problem in a discrete form, and compare the results.

The approach in Chapters 4 and 5 has features of both the hyperstability approach and Lyapunov's method. As a consequence, the difficulty of selecting an appropriate Lyapunov's function is relaxed. Compensators are searched toward minimizing a certain performance index — a feature of the hyperstability approach. Then, the selected compensators with the system dynamics are shown to results in a lower-bounded function whose time-derivative is non-positive outside a certain ball to prove the stability — a characteristic of Lyapunov's approach.

In Chapter 6, a flexibility compensator was designed to treat the problem of joint flexibility. The flexibility compensator allows use of a reduced-order model for controller design. Consequently, the proposed scheme avoids the need for certain difficult measurements (angular accelerations and jerks) and relieves computational burden. This flexibility compensator may be applied in conjunction with any stable control scheme for rigid-joint robots. A simpler form of the centralized adaptive scheme proposed in Chapter 4 was worked out. It would be useful to try the simpler centralized scheme after removing the compensators which make relatively small contributions to the control input, to save additional computation time. In this case, the stability and robustness may be proven as in Chapter 6.

In this thesis, the discussion was limited to trajectory control. Extension to hybrid trajectory/force control may have great potential for practical applications.